The University Of Sheffield.

The Influence of Antibiotics, Hypoxia and Neutrophil Proteins on the Evolution of Antibiotic Resistance in *Staphylococcus aureus*

Rebecca Clare Hull

Submitted for the degree of Doctor of Philosophy

The University of Sheffield,

Faculty of Medicine, Dentistry, and Health,

Department of Infection, Immunity and Cardiovascular Disease

September 2022

Acknowledgements

Most importantly, I would like to thank my supervisors, Professor Alison Condliffe, Professor Michael Brockhurst and Professor Simon Foster. Your guidance, support, time and patience have been invaluable, I couldn't have asked for better supervisors. Professor Alison Condliffe thank you for your dedication to your students, consistent encouragement, and freedom to explore ideas and opportunities.

This PhD would not have been the same without the opportunities I was given in the COVID-19 pandemic. Thank you, Professor James Chalmers, for taking me on placement in Dundee in the middle of a pandemic, and your brilliant supervision during placement and afterwards. Thanks to Dr Merete Long, Dr Holly Keir and all the Chalmers group for being so welcoming during my placements in Dundee and making me feel instantly part of the team.

Thank you to all the ALLI group and all the unofficial members for always having time to enjoy a coffee or pub trip and being there to discuss new ideas. I am also grateful for all the support I have received from the technicians and members of IICD.

My PhD experience has been massively enriched through being part of the MRFs national PhD training programme in AMR. Thank you to the MRF for funding this programme and everyone who have organised events in person and online over the 4 years. I am so grateful for the friendships I have built in the "Green Dots" cohort and for taking me out of the lab.

Thanks to my incredible friends in Sheffield, who I have shared food, wine, gin, coffee and lockdown walks with. You are the people who have made my time in Sheffield so much fun and always bring perspective to my work. Jane, you have been the best friend and housemate, and have been brilliant at cheering me up on the hard days, making me laugh, and allowing lockdowns to be a time with so many great memories.

Finally thank you to my family Mum, Dad, Matt and Beth for being so supportive. Emily, it has been brilliant to have you as a twin and best friend in Sheffield over the last four years.

This PhD was not as I had expected, but you have all made it a truly enjoyable experience.

Abstract

Invading bacterial pathogens are confronted by numerous challenges including harsh environmental conditions at the site of infection, host immune responses and exposure to antibiotic treatments. Herein, I have studied the interactions between antibiotics, hypoxia and neutrophil-derived proteins in driving the development of antibiotic resistance in *Staphylococcus aureus,* using an in vitro system. Spontaneous mutations (no antibiotic selection) conferred bacterial clarithromycin, flucloxacillin and tobramycin resistance, but doxycycline and linezolid resistance did not emerge spontaneously. *S. aureus* evolved in each antibiotic developed mutations associated with resistance, including 50S ribosomal proteins, following *S. aureus* evolution in clarithromycin, tobramycin and linezolid. Doxycycline selection conferred low level cross-resistance to tobramycin even in the absence of doxycycline resistance. Acquiring the tetracycline-specific efflux pump *tetL* reduced competitive growth against the isogenic strain without *tetL* for *S. aureus* in hypoxia, but not in normoxia. Treatment of *S. aureus* carrying *tetL* with tetracycline or doxycycline drove enhanced resistance through mutations in an RluD-like protein and duplications of *tetL*, suggesting that horizontal acquisition of a resistance mechanism may accelerate the emergence of higher level resistance under antibiotic selection. By contrast, exposure of *S. aureus* to hypoxic conditions without antibiotics drove adaptive mutations including those in *gyrB*, and this was prevented by antibiotic treatment. Extensive neutrophilic inflammation was revealed by sputum proteomics from patients with chronic lung diseases, with specific neutrophil proteins upregulated in samples from participants with *Pseudomonas aeruginosa* infections. Sensitivity to killing by the neutrophil antimicrobial peptide LL-37 was decreased in *S. aureus* that had evolved clarithromycin, linezolid and tobramycin resistance but not organisms evolved in doxycycline or flucloxacillin. Together these data suggest that interactions between antibiotic treatment and environmental selective forces such as hypoxia and antimicrobial peptides, may alter pathogen adaptation and survival and the evolution of antimicrobial resistance. These important interactions remain to be tested in vivo.

Declaration

I declare the work in this thesis is my own, with any work carried out in collaboration identified in the text. All sources of information are acknowledged as references. This thesis is based on work carried out under the supervision of Professor Alison Condliffe (University of Sheffield, Department of Infection, Immunity and Cardiovascular Disease), Professor Michael Brockhurst (University of Manchester, Division of Evolution, Infection and Genomic Sciences) and Professor Simon Foster (University of Sheffield, School of Biosciences).

The following publications are associated with this thesis:

- Hull RC, Wright RCT, Sayers JR, et al. Antibiotics Limit Adaptation of Drug-Resistant Staphylococcus aureus to Hypoxia. *Antimicrob Agents Chemother.* 2022
- Hajdamowicz NH, Hull RC, Foster SJ, Condliffe AM. The Impact of Hypoxia on the Host-Pathogen Interaction between Neutrophils and Staphylococcus aureus. *Int J Mol Sci.* 2019.
- Hull RC, Huang JT, Barton AK, et al. Sputum Proteomics in non-Tuberculous Mycobacterial Lung Disease. *Chest.* 2021.
- Keir HR, Long MB, Abo-Leyah H, et al. Dipeptidyl peptidase-1 inhibition in patients hospitalised with COVID-19: a multicentre, double-blind, randomised, parallel-group, placebo-controlled trial. *The Lancet Respiratory Medicine.* 2022.
- The following publication is available on medRxiv (26/09/2022): Long MB, Howden AJM, Keir HR, et al. Neutrophil proteomics identifies temporal changes and hallmarks of delayed recovery in COVID19. *medRxiv.* 2022:2022.2008.2021.22279031.

Some work presented in Chapters five, six and seven were previously published in Hull RC et al. 2022 or Hull RC et al. 2021. All authors contributed substantially to the study design, data generation and analysis. I carried out the data analysis and interpretation in Hull RC et al. 2021 with Dr Jeffrey Huang and Professor James Chalmers.

Table of Contents

List of Figures

Chapter 1

List of Tables

Chapter 1

Abbreviations

ACME	Arginine catabolic mobile element
Agr	Accessory gene regulator
AIP	Auto-inducing peptide
AMR	Antimicrobial resistance
ANOVA	Analysis of variance
ARDS	Acute respiratory distress syndrome
AUC	Area under the curve
BE	Bronchiectasis
BHI	Brain heart infusion
BPI	Bactericidal permeability increasing protein
BSA	Bovine serum albumin
CA	Community acquired
CAP	Community-acquired pneumonia
CF	Cystic fibrosis
CFTR	Cystic fibrosis transmembrane conductance regulator
CFU	Colony forming units
CG	Cathepsin G
CGD	Chronic granulomatous disease
CHIPs	Chemotaxis inhibitory protein
ClfA	Clumping factor A
COPD	Chronic obstructive pulmonary disease
DMSO	Dimethyl sulfoxide
DOX	Doxycycline
DPP-1	Dipeptidyl peptidase-1
Eap	Extracellular adherence protein
EDTA	Ethylenediaminetetraacetic acid
EUCAST	European Committee on Antimicrobial Susceptibility Testing
FBS	Fetal Bovine Serum
FIH	Factor inhibiting HIF

GPA	Granulomatosis with polyangiitis
HBSS	Hanks balanced salt solution
HCAP	Health care-associated pneumonia
HEPES	4-(2-hydroxyethyl)-1-piperazineethanesulfonic acid
HIF	Hypoxia inducible factor
HNP	Human neutrophil peptides
HREs	Hypoxia response elements
IGV	Integrative Genomics Viewer
IPA	isopropanol
ISARIC	International Severe Acute Respiratory and Emerging Infections Consortium
LB	Luria Broth
LL-37	Cathelicidin
LPS	Lipopolysaccharides
MGE	Mobile genetic elements
MIC	Minimum inhibitory concentration
MMP9	Matrix metallopeptidase 9
MOI	Multiplicity of infection
MPO	Myeloperoxidase
MprF	Multiple peptide resistance factor
MRSA	Methicillin-resistant *S. aureus*
NE	Neutrophil elastase
NETs	Neutrophil extracellular traps
NGAL	Neutrophil gelatinase-associated lipocalin
NICE	The National Institute for Health and Care Excellence
NSP4	Serine protease 4
NSPs	Neutrophil serine proteases
NTM	Non-tuberculous mycobacteria
PAMPs	Pathogen associated molecular patterns
PBMCs	Peripheral blood mononuclear cells
PBPs	Penicillin binding proteins

PBS	Phosphate Buffered Saline
PCA	Principal component analysis
PE	R-Phycoerythrin
PEP	Phosphoenolpyruvate
PFA	Paraformaldehyde
PHDs	Prolyl hydroxylase domain-containing enzymes
PI3K	Phosphoinositide 3-kinase
PPP	Platelet poor plasma
PR3	Proteinase 3
PRP	Platelet rich plasma
PRRs	Pattern recognition receptors
PSMs	Phenol soluble modulins
PVL	Panton-Valentine leukocidin
RBCs	Red blood cells
RNAP	RNA polymerase
ROS	Reactive oxygen species
rRNA	Ribosomal RNA
S protein	Spike protein
SCIN	Staphylococcal complement inhibitor
SCVs	Small colony variants
SDS	Sodium Dodecyl Sulfate
SNPs	Single nucleotide polymorphisms
SpA	Protein A
SSLs	Staphylococcal superantigen like
STOP-COVID19	Superiority Trial of Protease inhibition in COVID-19
TCS	Two-component system
TEMED	N,N,N',N'-Tetramethylethylenediamine
TET	Tetracycline
TNFα	Tumour necrosis factor-alpha
tRNA	Transfer RNA
WBCs	White blood cells

1 Introduction

1.1 Staphylococcus aureus

Staphylococcus aureus is a Gram-positive commensal bacterium capable of causing a range of opportunistic infections[1]. Although naturally highly susceptible to antibiotics, *S. aureus* has proven adept at acquiring resistance mechanisms, and its consequently increased level of antibiotic resistance poses a serious challenge for the effective treatment of infections[2,3]. There is a large health and economic burden from antimicrobial resistant (AMR) infections. In 2019 one report found 178,000 deaths attributable to *S. aureus* resistant to at least 1 antibiotic. It was the second highest pathogen responsible for AMR associated deaths behind *Escherichia coli*[4]. This is mirrored by the U.S. Centres for Disease Control and Prevention reporting 119,247 bloodstream infections with 19,832 associated deaths in 2017[5]. During infections *S. aureus* is exposed to harsh conditions, including antibiotics (section 1.3), low oxygen tensions (hypoxia) (section 1.1.4.2) and immune products (section 1.2) to which it must survive and adapt to establish infections. In this thesis I will be looking at how *S. aureus* evolves to survive these conditions as found at infections sites and their influence on antibiotic resistance.

1.1.1 Infections

S. aureus can exist in the human body both as a pathogen causing infections, or as a commensal organism. Around 20- 30% of the population are healthy carriers of *S. aureus,* with it forming part of their nasal or skin microbiome[6-9]. In most cases, carriage of *S. aureus* seems to have no detrimental effects, however in certain circumstances adverse consequences do result. A study of 1,497 patients in Germany between 1993-1999 found carriers were more likely to develop staphylococcal bacteraemia, with strain genotypes commonly originating from nasal colonies[10]. Carriage of *S. aureus* is approximately three times commoner in patients suffering from granulomatosis with polyangiitis (GPA, formerly known as Wegener's granulomatosis) than in healthy individuals[11] and carriage is associated with increased risk of disease relapse by an unknown mechanism. However, most adverse consequences of nasal *S. aureus* carriage relate to direct infection.

Commensal *S. aureus* occasionally becomes pathogenic. It can cause infections at a number of sites, including bacteraemia (bacteria detected in the blood), skin infections (section 1.4.2), pneumonia, cellulitis, abscesses (section 1.1.4.1), osteomyelitis (section 1.4.2) and endocarditis[12]. Environmental influences and exposures as well as host factors also contribute to susceptibility to invasive staphylococcal infection. In one study in the USA[13], patients with community-acquired pneumonia (CAP) were infected with *S. aureus* in 25.5% of cases rising to 46.7% cases of health care-associated pneumonia (HCAP), with HCAP patients displaying lower levels of *Streptococcus pneumoniae and Haemophilus sp.* Of the *S. aureus* infections, methicillin-resistant *S. aureus* (MRSA) accounted for 34.8% of CAP *S. aureus* cases compared to 56.8% in HCAP[13]. This is likely influenced by the exposure of these patients to different pathogens during their hospital stay, and the treatments they are experiencing, with HCAP patients also having more comorbidities. Due to these differences between hospital and community settings, different preventative measures (e.g. screening and decolonisation regimens for MRSA in hospital patients) may be appropriate - these measures have proven highly effective at reducing MRSA infections in the UK[14].

1.1.2 Virulence factors

Virulence factors are molecules which are produced to enable bacteria to establish and maintain an infection within its host[15]. *S. aureus* has an arsenal of virulence factors, which enable it to persist within host niches and cause disease when defences are breached, with those facilitating resistance to hypoxia and neutrophil killing summarised in Table 1-1. The expression of virulence factors is regulated by a range of two-component systems (TCSs) which comprise an environmental sensor (usually a histidine kinase) coupled to a response regulator (usually a transcription factor). Host phagocytes are essential in *S. aureus* clearance, and patients with defective phagocytes in diseases such as chronic granulomatous disease (defects in NADPH oxidase components leading to impaired respiratory burst) are at greatly increased risk of life-threatening *S. aureus* infections (section 1.1.4). Many virulence determinants allow *S. aureus* to resist phagocyte clearance through: preventing phagocyte recognition; preventing immune cell chemotaxis; evading phagocyte killing; persisting or escaping from phagocytes; causing phagocyte and cellular damage; and regulating the expression of adhesins and exoproteins[16] (Table 1-1).

The majority of *S. aureus* strains infections humans (75-80%) produce capsular polysaccharide type 5 or 8[17]. These capsules contain trisaccharide repeating units of N-acetyl mannosaminuronic acid, N-acetyl l-fucosamine, and N-acetyl d-fucosamine. The repeating nature of this capsule helps to prevent the recognition of *S. aureus* by phagocytes, facilitating immune evasion. It is not expressed in the logarithmic growth phase (see below) indicating it enables immune evasion and pathogenesis in combination with other virulence factors[18]. Additionally, the transcriptional regulator SarZ can sense environmental cues such as oxidative stress to regulate capsule production in a context-dependent fashion[19].

Expression of virulence factors is energetically costly and so is tightly controlled by a range of TCSs, of which the best studied is the accessory gene regulator (*agr*). *agr* and a range of other systems regulate *S. aureus* virulence factors, interacting to adapt the organism to its environment in a flexible and responsive manner (summarised by Jenul and Horswill[20]).The *agr* operon controls many virulence factors (for example the phenol soluble modulins PSMs and alpha-toxin) which are only expressed when the bacteria reaches a critical mass in late-exponential to stationary growth phase[21]. The *agr* operon produces an auto-inducing peptide (AIP) which is secreted to the extracellular space. This coordinates communication with other bacteria in the environment through quorum sensing. At a threshold level, AIP binds to the AgrC receptor on *S. aureus'* surface to activate the *agr* operon[21,22]. The result is increased expression of RNAIII, a small regulatory RNA that regulates gene expression by promoting expression of genes such as alpha-toxin by causing a conformational change, increasing access to the ribosomes initiation site although, in an alternative conformation, translation can be blocked through antisense RNA, mRNA complex formation[23].

Phagocytic cells such as neutrophils engulf bacteria within a phagosomal membrane. This membrane is thought to prevent the AIP from diffusing away so the *agr* operon is activated as the 'critical mass' threshold is reached in the small enclosed space[24]. This threshold likely needs to be met by a high enough number of *S. aureus* phagocytosed within one phagosome without replication, as there is some evidence to suggest *S. aureus* does not replicate within the neutrophil phagosome, unlike the macrophage phagosome[25,26]. Of note, some neutrophils ingest very large numbers of *S. aureus* while others do not, and this may relate to properties intrinsic to the neutrophil and to the local oxygen tension[27]. Bacterial clumping

may also encourage the ingestion of multiple prey particles within a single phagosome. The AIP threshold being reached is consistent with increased RNAIII inside neutrophils activating the *agr* operon, however this increased expression does not correlate with increased intracellular *S. aureus* survival[24]. Phenol-soluble modulin α (PSMα) is regulated by the *agr* operon and is associated with escape from the phagosome by cell lysis in tandem with other factors[26]. Phagosomal escape is associated with an increase in *S. aureus* survival [25].

Table 1-1: Summary of some virulence factors facilitating S. aureus resistance to hypoxia and neutrophil killing

Group	Virulence factor	Mechanism	Refs.
Prevent phagocyte recognition from opsonisation	Protein A (SpA)	Cross links Fab domain of IgM and binds Fcγ domain of immunoglobulin	[28,29]
	Clumping factor A (ClfA)	Fibrinogen-binding surface protein causing platelet aggregation. Antiphagocytic effect with or without presence of fibrinogen.	[30,31]
	Staphylococcal complement inhibitor (SCIN)	Inhibits C3 complement convertase.	[32]
	Aureolysin	Blocks C3 complement activity through cleaving C3 blocking C3a activation of neutrophils.	[33]
Phagocyte and cellular damage	Panton-Valentine leukocidin (PVL)	Triggers apoptosis and necrosis of cells dependent on concentration, initiated by pore formation.	[34]
	Phenol-soluble modulins (PSMs)	Cause lysis of blood cells, assists in the structuring and dispersal of biofilms.	[1,35]
	Alpha-hemolysin (alpha toxin)	Forms pores in cells through its interaction with the ADAM10 receptor resulting in cell lysis.	[1]

Prevent Immune Cell Chemotaxis	Chemotaxsis inhibitory protein (CHIPs)	Blocks chemotaxis towards C5a and formylated peptides by binding to neutrophil C5a receptors formyl peptide receptors.	[36,37]
	Extracellular adherence protein (Eap)	Block classical and lectin pathways needed to convert C3 into its active form C3a and C3b.	[38]
	Staphylococcal superantigen like (SSLs)	A group of structurally similar antigens with functions including binding IgA (SSL7), preventing neutrophil adherence through binding to trisaccharide sialyllactosamine (SSL5, SSL11)	[39]
Evade phagocyte killing	Lysozyme Resistance	Resistance to lysozyme degradation due to genes including OatA which catalyses the O-acetylation of peptidoglycan.	[40]
	Superoxide dismutase	A group of enzymes which provide resistance to reactive oxygen species (ROS) including superoxide and hydrogen peroxide.	[41,42]
	Staphyloxanthin	A carotenoid which provides protection against oxidative stress and ROS	[43]
	Phenol-soluble modulins (PSMs)	Cause cell lysis, aid in biofilm development and stimulate inflammation.	[35]

Adaptation to hypoxia	Anaerobic metabolism	Gene required to maintain anaerobic metabolism, *oflAB*, *adhE* and *nrdDG* are expressed in anaerobic conditions under the regulation of the *SrrAB* two component system.	[44]
	Biofilm production	Increased expression genes under the control of the intercellular adhesion (*ica*) operon in hypoxic conditions including β-1,6- linked glucosaminyl glycan leading to enhanced biofilm formation.	[45]
Regulation of virulence factors	*agr*	Regulation of virulence factors including PVL, alpha-toxin and PSMs through quorum sensing.	[21,22]
	sasX	Activates *agr* promoter and *cap8*.	[1,28]
	srrAB	Two component system controlling the expression of genes required for anaerobic metabolism, iron-sulfur cluster repair, $NO^{\cdot}$ detoxification and cytochrome biosynthesis and assembly.	[44]
Mobile genetic element	Arginine catabolic mobile element (ACME)	Associated with the success of strain USA-300. *speG* within the locus provides resistance against polyamines proving advantageous in skin infections.	[1]

1.1.3 *S. aureus* virulence factors and immune evasion

Many of *S. aureus'* virulence factors as described in Table 1-1 contribute to its ability to resist the innate immune response. Bacterial phagocytosis is expedited by opsonins (chiefly immunoglobulins/antibodies and activated complement factors) which bind the target and are also recognised by receptors on the phagocyte surface. Staphylococcal protein A binds to opsonic immunoglobulin to limit phagocytosis[28,29]. Opsonisation is also prevented by the inhibition of C3 convertase by proteins including staphylococcal complement inhibitor (SCIN)[32]. C3 can also be cleaved by the metalloprotease aureolysin to a C3a and C3b component. C3b is then proteolytically degraded within the hosts serum, and C3a-mediated activation of neutrophils is blocked in the presence of aureolysin and serum, being converted into a smaller fragment[33]. The ability of some strains of *S. aureus* to evade neutrophil phagocytosis highlights the importance of alternative extracellular killing mechanisms such as NETosis[46] and perhaps extracellular degranulation.

Neutrophil lysis can be induced by secretion of phenol soluble modulins (PSMs)[1,35]. Another form of neutrophil evasion is demonstrated by the highly virulent *S. aureus* strains MW2, MnCop, and LAC, isolated from patients with community acquired (CA) MRSA. These strains express Panton-Valentine leukocidin (PVL), a toxin which forms pores in host cell membranes, compromising their integrity and leading to cell lysis[47]. PVL can lyse neutrophils from within, post-phagocytosis[25].

As well as evading killing by neutrophils, *S. aureus* has been found to manipulate these cells to enhance intracellular survival. Although most *S. aureus* live extracellularly, in some circumstances it has been found to persist intracellularly, with the host cell acting as a "Trojan horse" to spread the bacteria to other parts of the body[48]. The bacteria are usually phagocytosed by neutrophils into small, 'tight' phagosomes. *S. aureus* mutants without the *sar* regulatory locus associated with virulence factors and thus with decreased propensity for intracellular survival have been associated with these tight phagosomes, which appear to fuse readily with azurophil granules leading to bacterial death (Table 1-1)[49]. In contrast, the bacteria can be engulfed into large ('spacious') phagosomes, which resemble macropinosomes. These large vacuoles are not thought to fuse effectively with azurophil

granules. Therefore, the bacteria within are allowed time to lyse the phagosome, initiate survival and replication within the cell cytoplasm. In a zebrafish model, inhibition of the neutrophil NADPH oxidase modified host autophagy responses and promoted the formation of spacious phagosomes[50]. This phenomenon has also been seen in human neutrophils ingesting *S. aureus*, both with chemical inhibition of the neutrophil NADPH oxidase and also in association with hypoxia, which limits the neutrophil oxidative burst (Dr Natalia Hajdamowicz, personal communication and PhD thesis[51]). However, the staphylococcal virulence factors catalase and superoxide dismutase (which break down the products of the oxidative burst) did not promote spacious phagosome formation, suggesting activation of the NADPH oxidase is sufficient for this process. The virulence factor *sar* (a global regulatory element which, like *agr*, controls the expression of a range of staphylococcal virulence factors including cell wall components[52]) is linked to intracellular survival of *S. aureus,* with loss of function mutants having decreased survival rates due to enhanced killing by neutrophils and the mutants lacking *sar* segregating almost entirely within tight phagosomes[49]. Survival within or escape from phagosomes thus enables *S. aureus* to persist within highly mobile host phagocytes. Intracellular bacteria are then able to be transported by neutrophils in the circulation to additional sites within the body, resulting in disseminated infection[28]. In combination, with these and other mechanisms, *S. aureus* is, at times, able to overcome the host innate defences to establish an infection.

1.1.4 *S. aureus* in the infection environment

1.1.4.1 Infection and abscess formation

During infections, *S. aureus* encounters many barriers which it must adapt to or overcome, summarised at a cellular level in Figure 1-2. The interaction with the immune environment is a major challenge, hence many of its virulence factors (Table 1-1) as noted are associated with immune evasion. Of the immune cells involved in *S. aureus* clearance, neutrophils play an essential role, evident by the increase in *S. aureus* infections in patients with chronic granulomatous disease (CGD). In CGD one of the five NADPH oxidase subunits in neutrophils is deficient in expression or function, inhibiting respiratory burst production (section

1.2.2.1)[53]. This leads to patients with elevated infection levels including *S. aureus* associated pneumonia, subcutaneous abscesses and liver abscesses[54].

The majority of *S. aureus* infections manifest as abscesses, with 85% of infections classified as such in one study[55]. These can form at a range of sites, mostly skin and soft tissue, but also occasionally deeper muscle tissue and almost any internal organ[56]. Due to their consistent structure, independent of the site, abscesses provide a good model to study the host-pathogen interaction. Abscesses start to form around an infection as governed by the resulting inflammatory response. The centre of an abscess is composed of live bacteria, neutrophils (alive or necrotic), cell debris and fibrin. Bacteria are thus exposed to neutrophil cytoplasmic, granule and nuclear contents in the central abscess. A mature abscess becomes surrounded by a fibrous capsule formed due to fibroblastic proliferation and tissue repair at the edge of the abscess (Figure 1-1)[56]. This capsule contains the pathogen, limiting its ability to invade other tissues, but also limits the ability of immune cells to enter the abscess. In addition to the structural features of abscesses, there are compounding physical properties the bacteria encounter such as hypoxia, especially in large abscesses[57]. Being in a hypoxic environment alters the behaviour of *S. aureus,* including the secretion of leukocidins, and increasing neutrophil degranulation (section 1.2.2.3)[16]. Thus the host-pathogen interaction is profoundly influenced by these infection-associated environmental cues.

Other types of staphylococcal infections occur, many having features in common with the classic ‘abscess’. These include infections of the bones (osteomyelitis), joints (septic arthritis) and heart valves (endocarditis). *S. aureus* can also establish a superficial spreading infection in the subcutaneous tissues (cellulitis) and aided by its ability to form biofilms it has a propensity to infect the artificial surfaces of medical devices such as indwelling cannulae[1]. All these infection sites are characterised by low ambient oxygen tensions.

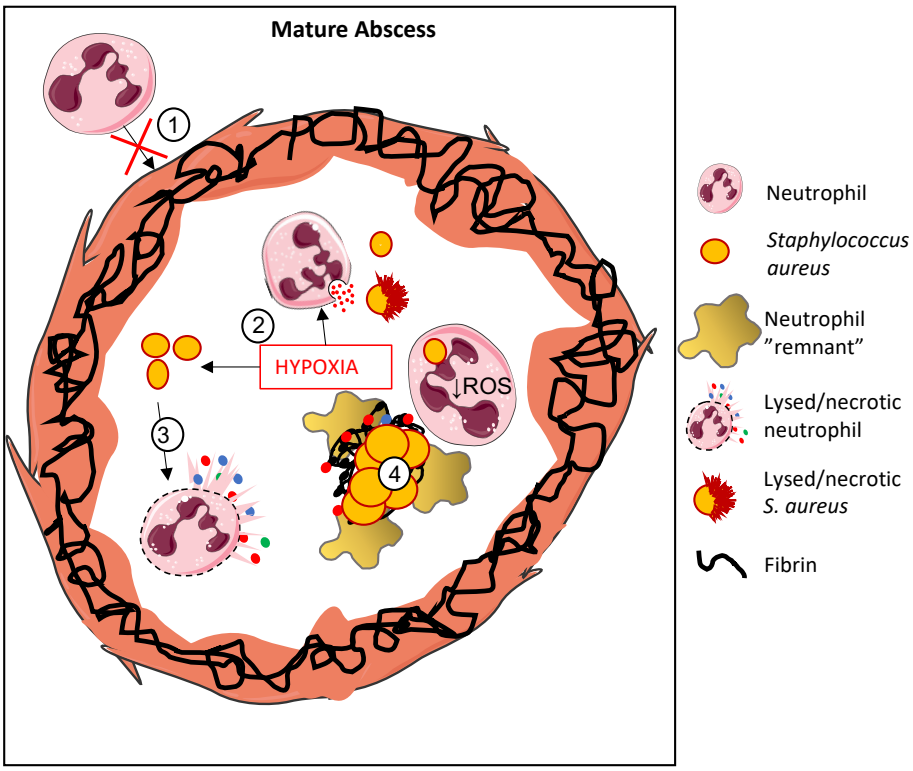

Figure 1-1: Neutrophils and hypoxia contribute to abscess formation and development.

The fully formed mature abscess fibrin capsule prevents further neutrophil infiltration (1). The highly hypoxic conditions alter neutrophil processes by enhancing degranulation (2) and enhanced S. aureus *secretion of leukocidins (3) to induce neutrophil lysis. The mature abscess contains products from necrotic and degranulated neutrophils, multiplying* S. aureus *and persisting intracellular* S. aureus *within neutrophils (4). This figure was created using Servier Medical Art templates, which are licensed under a Creative Commons Attribution 3.0 Unported License; https://smart.servier.com. Adapted from*[16]

1.1.4.2 Hypoxia

The atmospheric oxygen concentration is 160 mmHg or 21 kPa. Cells and bacteria alike are standardly studied in experimental cell culture conditions, usually around 152 mmHg or 20.3 kPa O_2 in a 5% CO_2 environment. In contrast, recorded healthy tissue oxygen tensions include 42.8 mmHg = 5.6 kPa in lung tissue, 29.2 mmHg = 3.9 kPa in muscle, 8 mmHg = 1 kPa in the superficial skin region and 48.9 mmHg = 6.5 kPa in the bone marrow[58]. Therefore, in standard conditions bacteria and immune cells are operating in conditions that are hypoxic relative to those within the typical cell culture environment (see section 1.2.2.3).

This 'physiological' hypoxia is further enhanced during infections from increased oxygen consumption or decreased availability. Oxygen availability may be limited by blood supply being compromised e.g. from low blood pressure in sepsis or a build-up of phagocytes and platelets in blood vessels with development of microthrombi limiting blood flow[59,60]. Oxygen within tissues is decreased further by the high metabolic demands of phagocytes migrating to the site of infection, and respiration of pathogens. Oxygen is also consumed by neutrophils to produce respiratory bursts through in their NADPH oxidation complex[61]. Hypoxic conditions are sensed by host cell prolyl hydroxylase domain-containing enzymes (PHDs), which then prevent HIF (hypoxia inducible factor) degradation. HIF is a transcription factor which causes neutrophils to switch to an adaptive hypoxic phenotype (section 1.2.2.3). 'Pathological' hypoxia is a common feature of *S. aureus* infections: for example, the archetypal *S. aureus* abscess can prevent oxygen exchange (and antibiotic penetration) through its fibrous capsule, exacerbated by poor blood supply to the necrotic centre[62,63]. Models of biofilm formation by *S. aureus* suggests such environments have little or no detectable oxygen (anoxia)[64]. *S. aureus* is exposed to hypoxia (or even anoxia) in the setting of many chronic infections including the cystic fibrosis airway[65], chronic osteomyelitis[66] and diabetic foot ulcers[67]. Therefore, to understand *S. aureus* infections the impact of hypoxia on *S. aureus*, immune cells and on their interactions needs to be considered.

1.2 Immune responses to infection

The immune system has a plethora of defences, orchestrated to kill invading bacteria including *S. aureus* (Figure 1-2). The innate immune system (particularly the phagocytic

macrophages and neutrophils) is rapidly responsive but lack specificity and memory. Lymphocytes are the effectors of the adaptive immune system and co-ordinate and enhance innate responses but respond less rapidly (although 'memory' cells enact more rapid responses on repeat exposure). There are a huge number of lymphocyte subsets, but broadly they are divided into T lymphocytes (particularly T helper cells which secreted cytokines to regulate many aspects of immune responses, and T cytotoxic cells which kill infected host cells) and B lymphocytes (which produce antibodies/immunoglobulins). This coordinated system results in an effective defence mechanism which is usually successful in preventing bacterial infections from establishing or eliminates them effectively. However, at times this is unsuccessful, and infections become established. For *S. aureus* these can have a range of manifestations as discussed in section 1.1.1. Whilst many cell types contribute clearance of staphylococcal infections (Figure 1-2), I have focused on neutrophils due to their abundance and the pivotal role the play in infection clearance, exemplified by recurrent staphylococcal infections in individuals with neutrophil dysfunction.

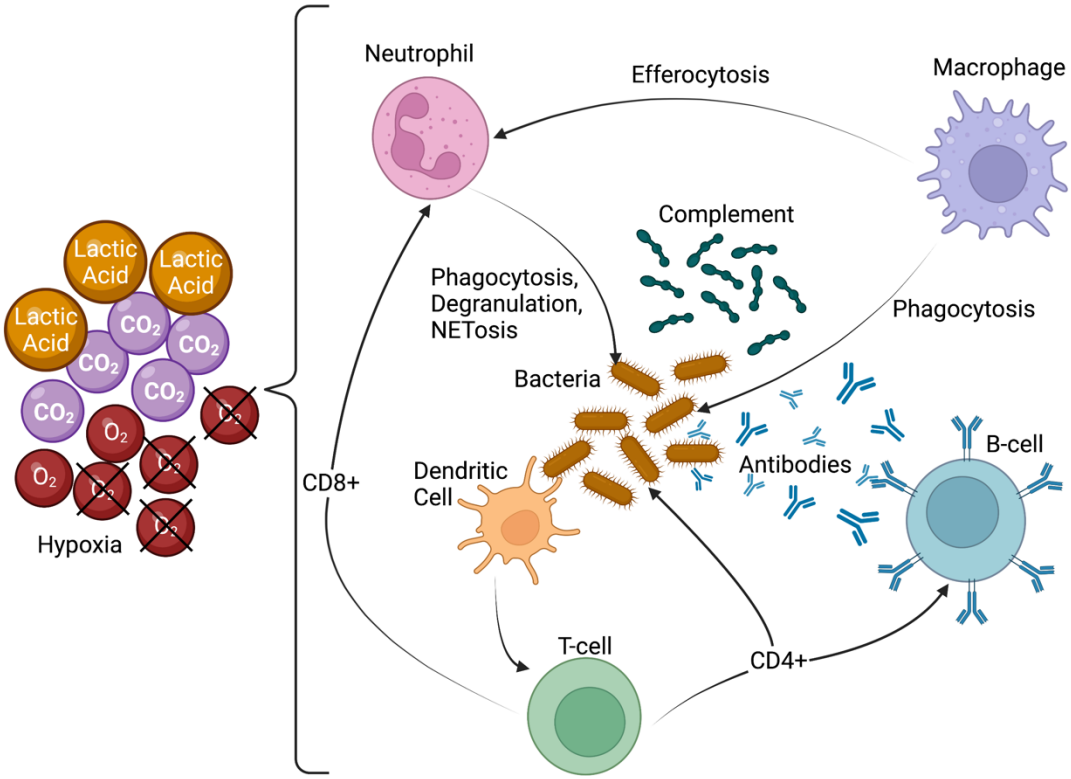

***Figure 1-2: Overview of the innate and adaptive immune response to* S. aureus**

Both the innate and adaptive immune system contribute to defence against S. aureus *infections. Neutrophils (innate immunity) kill* S. aureus *via phagocytosis, degranulation and releasing neutrophil extracellular traps (NETosis). Macrophages phagocytose both bacteria and also neutrophils which have died by apoptosis. Complement enhances phagocytosis of* S. aureus *through opsonisation. Dendritic cells recognise* S. aureus *through pattern recognition receptors (PRRs) before priming naïve T cells, bridging innate and adaptive immunity. Lymphocytes are the effectors of the adaptive immune system. T lymphocytes aid* S. aureus *clearance by recruitment of additional phagocytes, increasing macrophage bactericidal activity, killing infected host cells through cytotoxic T cells, and by enhancing B lymphocyte responses. B lymphocytes generate opsonic antibodies to cells enhance innate immune cell phagocytosis* S. aureus *phagocytosis through opsonisation. Respiration of immune cells and* S. aureus *is associated with a decrease in oxygen concentrations (hypoxia) and increased carbon dioxide and lactic acid concentrations. These environmental conditions may influence host immune cells such as neutrophils. Created with BioRender.com. Source of information* [68-71]

1.2.1 Antimicrobial components of plasma or serum

Plasma is a complex solution which displays antimicrobial properties against a multitude of organisms[72]. Plasma consists of water, fibrinogen (lacking in serum), inorganic salts, organic compounds, and proteins[73]. Within this, plasma also carries proteins with antimicrobial properties, including many secreted from immune cells including neutrophils (section 1.2.2.1). Additionally, platelets can release granules upon activation due to tissue injury or microbial infection. Within α-granules antimicrobial proteins include chemokines (CXCL4, CXCL7), defensins, and antimicrobial peptides[74]. Complement is carried in plasma in a predominantly inactive form in health. Upon activation by inflammatory stimuli (including immune complexes and pathogen associated molecular patterns or PAMPs), a series of proteolytic cleavage act on substrate molecules to generate the anaphylatoxins (such as C3a and C5a) which can induce activation and degranulation of neutrophils, and the complement activation cascade ultimately results in the formation of the membrane attack complex. This is a ring structure, which is bacteriocidal against Gram-negative bacteria. In the presence of immune cells and antibodies, complement opsonisation by factors such as C3a also enhances recognition by phagocytes[75].

1.2.2 Neutrophils

Neutrophils are the most abundant leukocyte in the human body with a daily turnover averaging 10^{11} per day in adults[76]. They develop and mature in the bone marrow, from pluripotent hematopoietic stem cells, passing through a number of maturation stages before being stored or released into the blood[47]. Within the circulation neutrophils have a limited lifespan of less than one day[77], unless they leave the circulation to enter tissues. This process of extravasation is initiated at inflamed sites (reviewed[78]) allowing neutrophils to migrate from the blood stream to a site of infection or tissue damage. Once within the tissue, neutrophils precisely locate and access the site of infections by following chemotactic gradients, including H_2O_2 produced by damaged cells[79], bacterial products such as N-formylated peptides and chemokines such as CXCL8, produced at the site of infection[80,81]. Upon reaching the site of infection they have an arsenal of weapons which are deployed to kill bacteria (Figure 1-3). These neutrophil products need to be controlled as neutrophil

products, and cells recruited by secreted pro-inflammatory mediators, can themselves cause damage and contribute to inflammatory diseases such as rheumatoid arthritis[82].

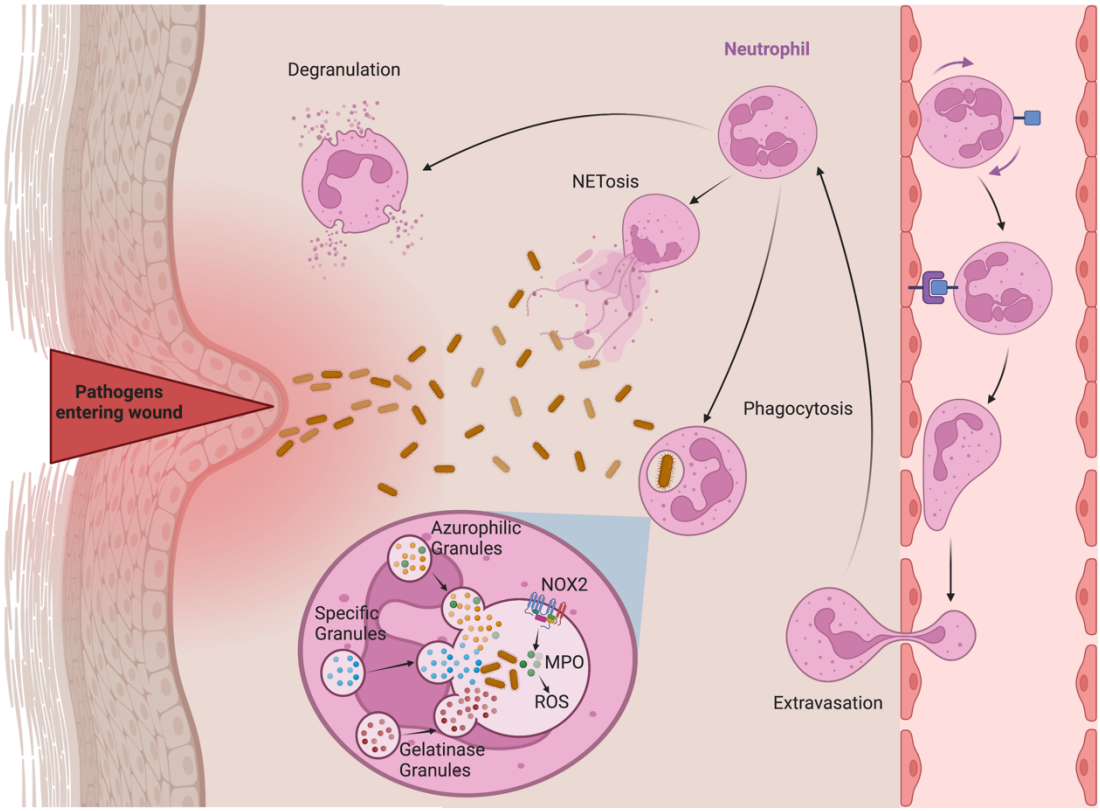

Figure 1-3: Neutrophil antimicrobial mechanisms.

Neutrophils phagocytose and kill S. aureus *by generation of reactive oxygen species (ROS) and fusion of azurophilic, specific and gelatinase granules with the phagosomal membrane. Extracellular release of neutrophil granules can kill extracellular bacteria. Neutrophil extracellular traps (NETs), composed of DNA with histones and proteases attached may be expelled, trapping and killing surrounding bacteria. Created with BioRender.com.*

1.2.2.1 Neutrophil weapons

Neutrophils have numerous mechanisms which combine to form an effective defence against bacterial infections (Figure 1-3). The primary mechanism of bacterial killing is initiated by the recognition of PAMPs by pattern recognition receptors (PRRs) on the neutrophil surface. As the markers are non-specific but widely distributed bacterial products, such as lipopolysaccharide (Gram-negative bacteria) and peptidoglycan (Gram-positive bacteria), this allows a rapid and generalised innate response, in contrast to the highly specific adaptive immunity. Once recognised, neutrophils phagocytose the bacteria through cytoskeletal rearrangement (mainly actin polymerisation). This produces a phagosome, which becomes bactericidal as it matures by vesicles and neutrophil granule compartments fusing with its membrane (and hence membrane proteins) and releasing their contents into the maturing phagosome[47].

There are three types of neutrophil granules which contain proteases and antimicrobial agents (section 1.2.2.3), namely primary or azurophilic granules, secondary or specific granules and tertiary (or gelatinase) granules, all with different membrane markers and protein content. Primary (or azurophilic) granules appear early in granulopoiesis and contain numerous components including: myeloperoxidase (MPO); neutrophil elastase (NE); antimicrobial and cytotoxic peptides α-defensins and antimicrobicidal serine proteases including serpocidins such as azurocidin[83]. Secondary (specific) granules appear later in development, have a high lactoferrin content and include proteins such as collagenase, flavo-cytochrome b558 and receptors for extracellular matrix proteins, cytokines, opsonins, chemotactic peptides and adhesion proteins[47]. Tertiary or gelatinase granules are smaller than secondary granules, containing fewer antimicrobial components, incorporating gelatinase (matrix metallopeptidase 9 or MMP9), leukolysin, lysozyme, acetyltransferase and diacylglycerol deacetylating enzyme[83]. Defective granule formation or fusion with the phagosome leads to immune deficiencies such as the neutrophil specific granule deficiency[84,85], Grey Platelet syndrome[86] and the Chediak Higashi syndrome[87], with defective neutrophil function (and other cellular defects) and increased susceptibility to *S. aureus* infection.

In addition to directed fusion with the phagosomal membrane, neutrophil granules can also fuse with the plasma membrane leading to the release of their contents to the extracellular milieu (exocytosis). This can be initiated by a range of stimuli, e.g. formylated bacterial peptides and activated complement, with granule release greatly increase by priming agents, e.g. tumour necrosis factor-alpha (TNFα)[88], and also by hypoxia[89]. Since granule constituents are highly bactericidal by a variety of mechanisms, e.g. direct protease activity or iron sequestration, their liberation may kill or damage extracellular bacteria and potentially exert selective pressure to promote bacterial adaptation and ultimately evolution. However, this is a risky strategy, and augmented exocytosis increases bystander tissue damage[89].

Neutrophils have mechanisms which act alongside granule production to kill bacteria. Reactive oxygen species (ROS) are produced by the multi-component neutrophil NADPH oxidase, initially forming superoxide (O^-_2). This is then processed by the heme enzyme, MPO (present in neutrophil azurophilic granules) to produce hydrogen peroxide (H_2O_2) and other reactive oxygen species including hypochlorous acid (HOCl)[90]. This has been shown to be an important mechanism of killing for *S. aureus* but not *Escherichia coli*[91]. Like the degranulation function, ROS can also be generated extracellularly, with potential bactericidal but also tissue-damaging effects. Another means of extracellular bacterial killing is the release of neutrophil extracellular traps (NETs) from active neutrophils. NETs contain fibres of DNA beaded with granule-derived antimicrobials such as elastase and histones; NETs are extruded following ROS generation and can trap or kill extracellular bacteria, as well as degrading virulence factors. This expands the neutrophils range of action preventing the spread of bacteria[46].

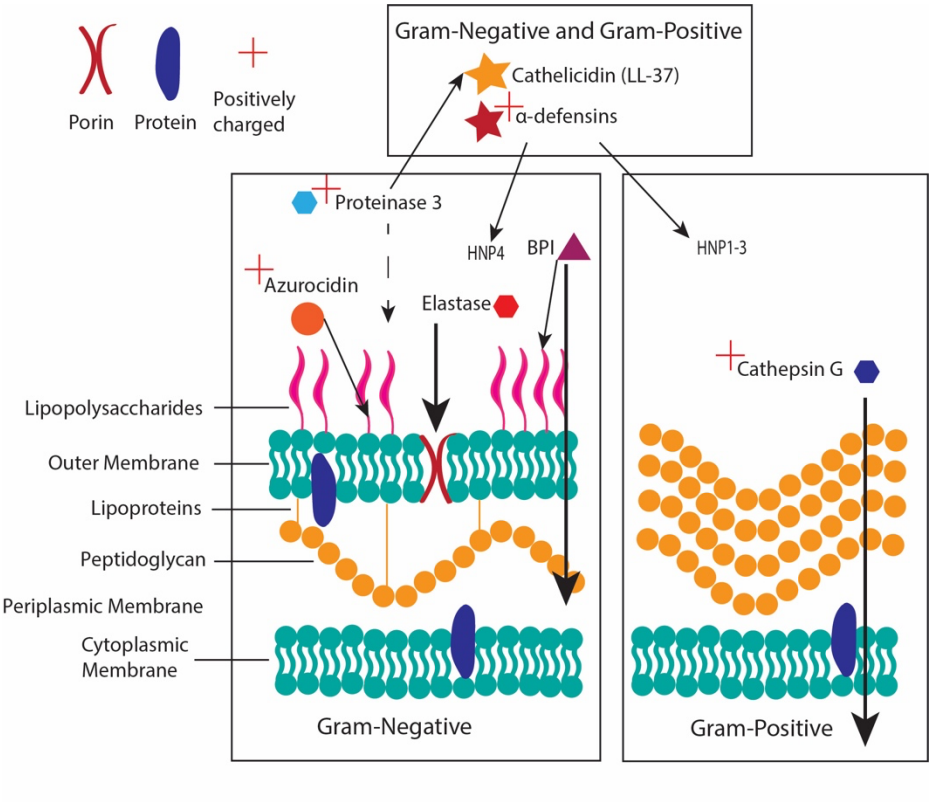

Figure 1-4: Neutrophil antimicrobial proteins/peptides bacterial targets

Neutrophil antimicrobial proteins/peptides targets in Gram-negative and Gram-positive bacteria, for antimicrobial peptides (stars, cathelicidin and α-defensins), neutrophil serine proteases (hexagon, proteinase 3, elastase, cathepsin G), azurocidin (circle) and BPI (triangle). Plus (+) beside protein/peptide represents an overall positive charge. In Gram-negative bacteria, azurocidin targets lipid A, BPI targets LPS and the cytoplasmic membrane, proteinase 3 cleaves cathelicidin precursor hCAP-18 to its active form (LL-37) but also has low level interactions with LPS. In Gram-positive bacteria cathepsin G kills bacteria by inhibiting protein synthesis. α-defensins have both Gram-negative (HNP-4) and Gram-positive (HNP-1/2/3) targets, which kill by forming pores in the bacterial membrane.

1.2.2.2 Neutrophil antimicrobial proteins and peptides

Many neutrophil proteins and peptides have direct or indirect bacteriocidal and bacteriostatic mechanisms, facilitating the control of bacterial infections (Figure 1-4). These can be classified by whether they are active against Gram-positive or Gram-negative bacteria (Figure 1-4) but there is considerable overlap, so I will discuss them according to their mode of action.

Neutrophils produce 4 α-defensins (Human neutrophil peptides HNP-1 to HNP-4), which comprise around 30% of the azurophilic granule protein content[92]. HNPs cause bacterial cell lysis as the cationic defensin inserts into the anionic outer bacterial membrane, permeabilising the membrane leading to lysis[93]. hCAP-18 is a cathelicidin antimicrobial precursor peptide which is cleaved by proteinase-3 into the active form LL-37. LL-37 is an amphipathic α-helical peptide thought to exert its antimicrobial effect through insertion into bacterial membranes[94]. Both LL-37 and HNPs can target Gram-positive and Gram-negative bacteria.

Bactericidal permeability increasing protein (BPI) is the most potent bactericidal agent within azurophilic granules against *E. coli* [95] but not Gram-positive organisms. Bacterial killing by BPI occurs in two stages. BPI binding to lipopolysaccharides (LPS) in the outer membrane initiates an early bacteriostatic phase when phospholipids and peptidoglycans are degraded, increasing cell permeability[96]. During the second stage, lesions in the inner cytoplasmic membrane, result in cell death, as energy generation and biochemical processes are disrupted[97].

Sequestration of nutrients is a bacteriostatic mode of action attributed to some innate immune proteins. Calprotectin contributes to 40% of neutrophil cytoplasmic protein content. Calprotectin is released in large quantities at sites of infection resulting in tissue concentrations around 1mg/ml within abscesses[98]. Calprotectin is predominantly released during cell death in necrosis or NETosis[98,99]. At the infection site calprotectin has a bacteriostatic impact through the sequestration of Zn^{2+} and Mn^{2+}. It has also been shown to augment the activity of the *S. aureus* SaeRS TCS and increase mortality in a mouse infection model, hence not all antimicrobial compounds are beneficial to the host[100]. Lactoferrin is found in most mammalian exocrine secretions, including milk and saliva and is also stored

within neutrophil specific granules, before release into the phagolysosome or extracellularly where it can be bound to NETs. Tissue concentrations of lactoferrin increase from 1 mg/ml to 200 mg/ml during inflammation[101]. Lactoferrin's sequestration of iron confers modest bacteriostatic properties towards mostly Gram-negative bacteria including *E. coli* and *Salmonella enterica* serovar Typhimurium[102,103]. Lactoferrin is also able to bind and cause the release of LPS which is proposed to be lactoferrins main bactericidal mechanism[103].

Neutrophils produce 4 serine proteases (NSPs): neutrophil elastase (NE), cathepsin G (CG), proteinase 3 (PR3) and serine-protease-4 (NSP4) with His-Asp-Ser catalytic triad essential for activity, in addition to azurocidin which shares NH2-terminal amino acid sequence homology but is enzymatically inactive[104]. NSPs have non-redundant functions in bacterial killing[105]. NE predominantly directly targets Gram-negative bacteria with increased survival of *E. coli* and *Klebsiella spp.* but not *S. aureus* in NE knockout mouse models[106]. In *E. coli* NE targets OmpA, although the exact killing mechanisms is unclear as OmpA's absence does not alter survival in NE wild type or knockout mice. NE alters OmpA positive *E. coli* cell morphology, with cleavage possibly facilitating death by disrupting membrane integrity, either inducing cell lysis or allowing access to an intracellular target of NE[107,108]. Targets in other species include OprF[109] (*Pseudomonas aeruginosa*) and aminopeptidase N[110] (*S. pneumoniae*) although other proteins are also involved in cell death. CG is a positively charged potent antimicrobial protein against Gram-positive bacteria, including *S. aureus,* and has some activity against the Gram-negatives *E. coli* and *P. aeruginosa*. CG maintains activity against *Enterococcus faecalis* after heat inactivation showing killing is independent of protease activity[111]. Cell death is caused by CG through the inhibition of protein synthesis[112]. PR3 has some direct antimicrobial activity against *E. coli* and *E. faecalis* in vitro, however, this activity is rather weak compared to other azurophilic proteins in the conditions tested[95]. NSP4 is the most recently discovered neutrophil serine protease and its biological role and antimicrobial activity have yet to be characterised[113,114]. Azurocidin (also known as CAP37 or heparin-binding protein) is a catalytically inactive serine protease homologue in which serine has been replaced by glycine within the active site[115]. Azurocidin is predominantly active against Gram-negative bacteria through binding to lipid A[116], and it primarily aids in the killing of *S. aureus* through opsonization, rather than direct killing[117]. Azurocidin binds to *S. aureus* increasing

phagocytosis in monocytes, but not granulocytes, and increases ROS production in both monocytes and granulocytes thus likely increasing immune mediated killing of *S. aureus*[117].

In addition to direct antimicrobial activity, serine proteases have a plethora of interactions hindering bacterial virulence factors. Many neutrophil proteins interact and neutralise bacterial virulence factors. CG, and NE to a lesser extent, can degrade flagellin[118]. α-defensins have broad influences beyond direct killing including: neutralisation of *Bacillus anthracis* toxin by HNP-1, HNP-2 and HNP-3[119]; HNP-1 can neutralise Diphtheria toxin and *Pseudomonas aeruginosa's* exotoxin A[120] and HNP-3 can partially inhibit *S. aureus* PVL's pore forming ability by binding LukS-PV and LukF-PV[121]. Low concentrations of LL-37 can reduce biofilm formation in *P. aeruginosa* by promoting twitching and reducing surface attachment[122].

The potent activity of neutrophil proteins is tightly controlled to prevent the by-stander effect. For example, CG's activity is dependent on pH and ionic strength, favoured by acidic environments but active at pH 5-7.5[123]. In contrast PR3 is only active in neutral environments, so not within low pH surroundings[124]. Containment of activity to the desired site can also be achieved through inhibition by commonly occurring biological agents. NaCl, $CaCl_2$ and serum all restrict the activity of azurocidin in a dose dependent manor, limiting its activity extracellularly. Concentrations of NaCl within the phagolysosome could limit its activity in the intracellular environment[104]. Heparin, found in serum, can bind to azurocidin inhibiting its bacterial binding site to restrict its activity[125]. BPI's bacteriocidal activity can also be prevented by the presence of the serum protein albumin before or shortly after BPI binding[126]. Some proteins are stored in an inactive form prior to cleavage for rapid activation. These include cathelicidin (cleaved by PR3 to active LL-37)[127] and HNP-1, which is processed by PR3 and NE[128].

As well as mechanisms directly involved in bacterial killing, NSPs can have more global influences on neutrophil behaviour. Patients with Papillon-Lefèvre syndrome have a mutation in *CTSC*[129], which encodes dipeptidyl peptidase I (DPPI), a proteinase which cleaves NSPs (NE, CatG, PR3 and NSP4) to their active forms, during development in the bone marrow[130]. PR3 is required to cleave LL-37 to its active form. As a result, patients with Papillon-Lefèvre syndrome are unable to produce active NSPs or LL-37. These patients' neutrophils cannot undergo suicidal NETosis which requires active NE. Despite the defect of serine proteases in

patients with Papillon-Lefèvre syndrome, patients are still able to produce a neutrophil antimicrobial response, highlighting the overlapping role of many proteins and effector cells in the clearance of pathogens[129,131,132]. The main clinical features are severe oral inflammation and hyperkeratosis of the skin, with a surprising lack of increased infection frequency[133].

1.2.2.3 Neutrophil adaptations to hypoxia

Neutrophils primarily utilise glycolysis rather than oxidative phosphorylation for respiration[134], indicating they are fundamentally adapted to operate in hypoxic environments. As neutrophils circulate within the body, they encounter different oxygen tensions. Oxygen sensing is achieved through the PHD/HIF pathway. There are three prolyl hydroxylase (PHD) isoforms which sense oxygen at slightly different thresholds to regulate HIF stability[135] and which have slightly different roles in immunity. The heterodimeric transcription factor HIF (Hypoxia Inducible Factor) is the master regulator of hypoxic responses. It has two subunits, α and β. In the presence of oxygen, PHDs target the α subunit for degradation via the proteasome[136]. When PHDs are inactivated in hypoxic conditions, HIF-α can accumulate, dimerise with HIF-β and translocate to the nucleus to regulate the transcription of genes with hypoxia response elements (HREs) in their promoters. Factor inhibiting HIF (FIH) represses HIF by hydroxylation of an asparaginyl residue preventing coactivators binding, repressing transcription[137].

In many cells the HIF/PHD pathway regulates the switch between aerobic and anaerobic respiration. In neutrophils it is pivotal in regulating the energy supply within the cell, since HIF-1α controls glycolytic enzyme expression, so intracellular ATP levels are lower in normoxic conditions compared to hypoxia[138]. Lower ATP levels help to restrain inflammatory response in normoxic conditions[139]. The HIF/PHD pathway regulates other adaptive changes through a series of complex, isoform dependent interactions. HIF-1α has been shown to promote survival in hypoxic conditions, delaying apoptosis; HIF-2α promote neutrophil persistence; PHD2 increase inflammation, migration, glycolysis and survival; PHD3 reduces inflammation and is essential for hypoxic survival[140]. Some neutrophil functionality is maintained or even increased in hypoxic conditions including chemotaxis and receptor recognition. Phagocytosis of bacteria including *S. aureus* is preserved or even increased in hypoxic conditions[91,141].

However, ROS production and killing of *S. aureus* was reduced, in line with reduced availability of the substrate O_2[91].

Hypoxia has been reported to have somewhat variable effect on NETosis. 2 studies have shown no hypoxic increase in NETosis in response to physiological stimuli GM-CSF and fMLP[89] or PAF and fMLP[142]. Branitzki-Heinemann et al.[143] showed no increase in NETosis in hypoxia with a live *S. aureus* stimulus, but heat-inactivated *S. aureus* resulted in lower levels of NETs in hypoxia. The latter study did not pre-incubate media in hypoxia, and neutrophils did not show HIF-1α stabilisation in this setting. Hypoxia intuitively seems likely to be important to NET formation given the known ROS-dependent mechanisms involved in this process[143]. This is an area which requires further study and highlights the importance of using physiological stimuli and oxygen tension.

Hypoxia also influences the expression and degranulation of antimicrobial proteins from neutrophil granules. HIF-1α regulated the expression of granule proteins such as elastase and cathepsin G, and antibacterial peptides such as cathelicidins[139]. In hypoxia degranulation of some proteins is increased, including neutrophil gelatinase-associated lipocalin (NGAL), MPO, neutrophil elastase and cathelicidin. This has been shown to be dependent on phosphoinositide 3-kinase (PI3K)γ signalling through phosphorylating the effector kinase AKT[89,142]. How hypoxic conditions are sensed by this pathway are still unknown.

These studies highlight the different mechanisms of killing for different pathogens, and how they are modulated by the environmental oxygen levels, although our understanding of these complex processes remains incomplete.

1.2.2.4 Contribution of neutrophils to disease progression in COVID-19

The capacity for inappropriate neutrophil activation to induce bystander tissue damage has been highlighted by recent research into the pathogenesis of severe COVID-19. SARS-CoV-2 is a respiratory coronavirus which causes COVID-19, with the primary mechanism of cell entry enacted via the spike (S) protein[144]. The S protein is primed by the cellular serine protease TMPRSS2, or neutrophil serine proteases[145-147], prior to binding to the ACE2 receptor to infect cells in the nasal epithelium, tracheal cells and airway epithelial cells[148,149]. In severe cases,

patients will develop pneumonitis and even acute respiratory distress syndrome (ARDS) typically at around 8-9 days after initial symptoms. ARDS develops due to an overly aggressive immune response following infection. Patient with ARDS are typically hypoxic with a proinflammatory and neutrophil immune signature[150]. Neutrophil activation[151] and NETosis[152,153] within the alveolar space is strongly associated with lung tissue damage and ARDS in patients with COVID-19[154,155]. Additionally, NETs can contribute to the initiation and development of microthrombi by obstructing blood vessels, driving cardiac events and increasing hypoxia[156]. The contribution of inflammation to disease progression in COVID-19 is supported by the success of the anti-inflammatory therapeutics, including dexamethasone reducing general inflammation[157] and tocilizumab the anti-IL-6 antibody[158]. The strong association of neutrophil degranulation products and NETosis with severe manifestations of COVID-19 led to speculation that neutrophils were a potential therapeutic target in this condition[159,160].

1.3 Antibiotics and resistance

In addition to the immune environment, bacteria encounter selective pressures due to human interventions, such as the use of antibiotics. The rapid development of AMR following each antibiotics introduction (Figure 1-5) epitomises the adaptability of bacteria. Sulfonamides were the first antibiotics to be used clinically in 1937. This was rapidly followed by the detection of sulfonamide resistance in the late 1930's[161]. This pattern of resistance detection has been seen for all classes introduced since. The continued evolution of AMR has a large health and economic impact, predicted to be responsible for 4.95 million deaths globally in 2019, of which 1.27 million directly associated were bacterial AMR. The pathogens responsible for deaths in this study were: *E. coli*, followed by *S. aureus*, *Klebsiella pneumoniae*, *S. pneumoniae*, *Acinetobacter baumannii*, and *P. aeruginosa*[4]. The WHO declared AMR a top 10 global public health threat in 2019[162]. AMR is a complex, multifaceted issues with many areas needing to be addressed including: a better understanding of antibiotic mechanisms; development, spread and maintenance of resistance; and interaction at sites of infections.

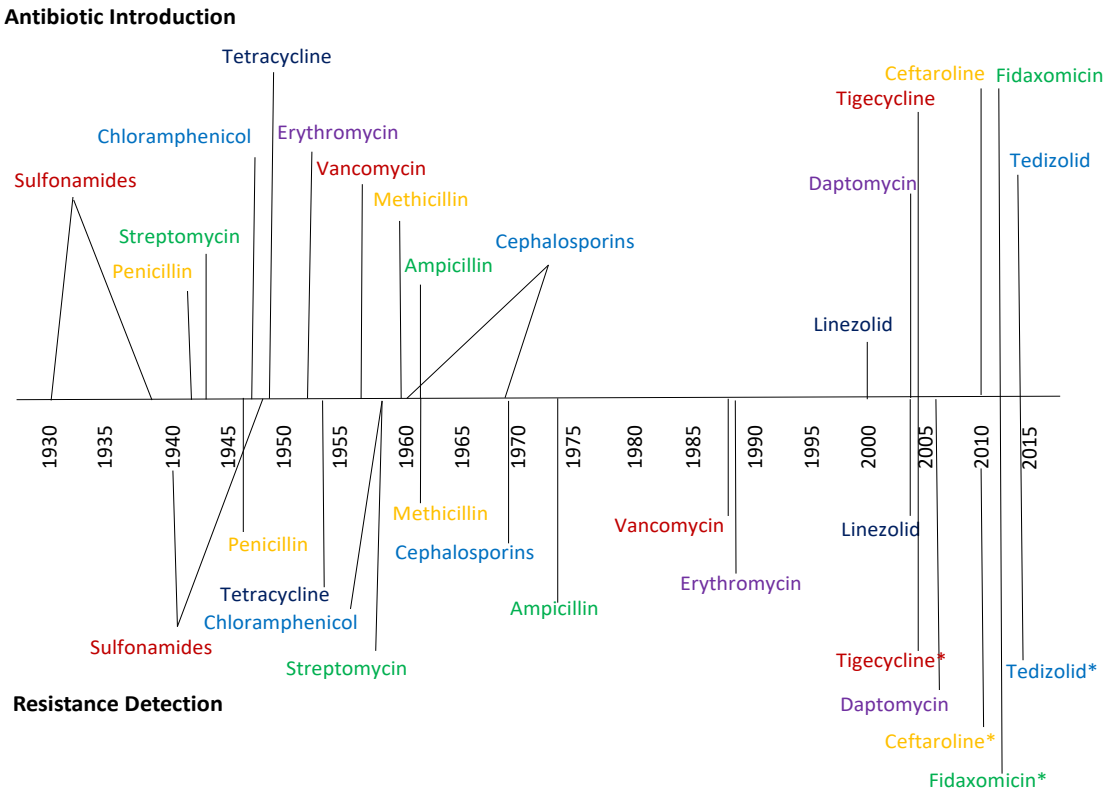

Figure 1-5: Antibiotic resistance timeline

*Timeline showing the year key antibiotics were first clinically introduced compared to discovery of antibiotic resistance. *indicates resistance was reported prior to antibiotic release date. Adapted with permission*[163-167]

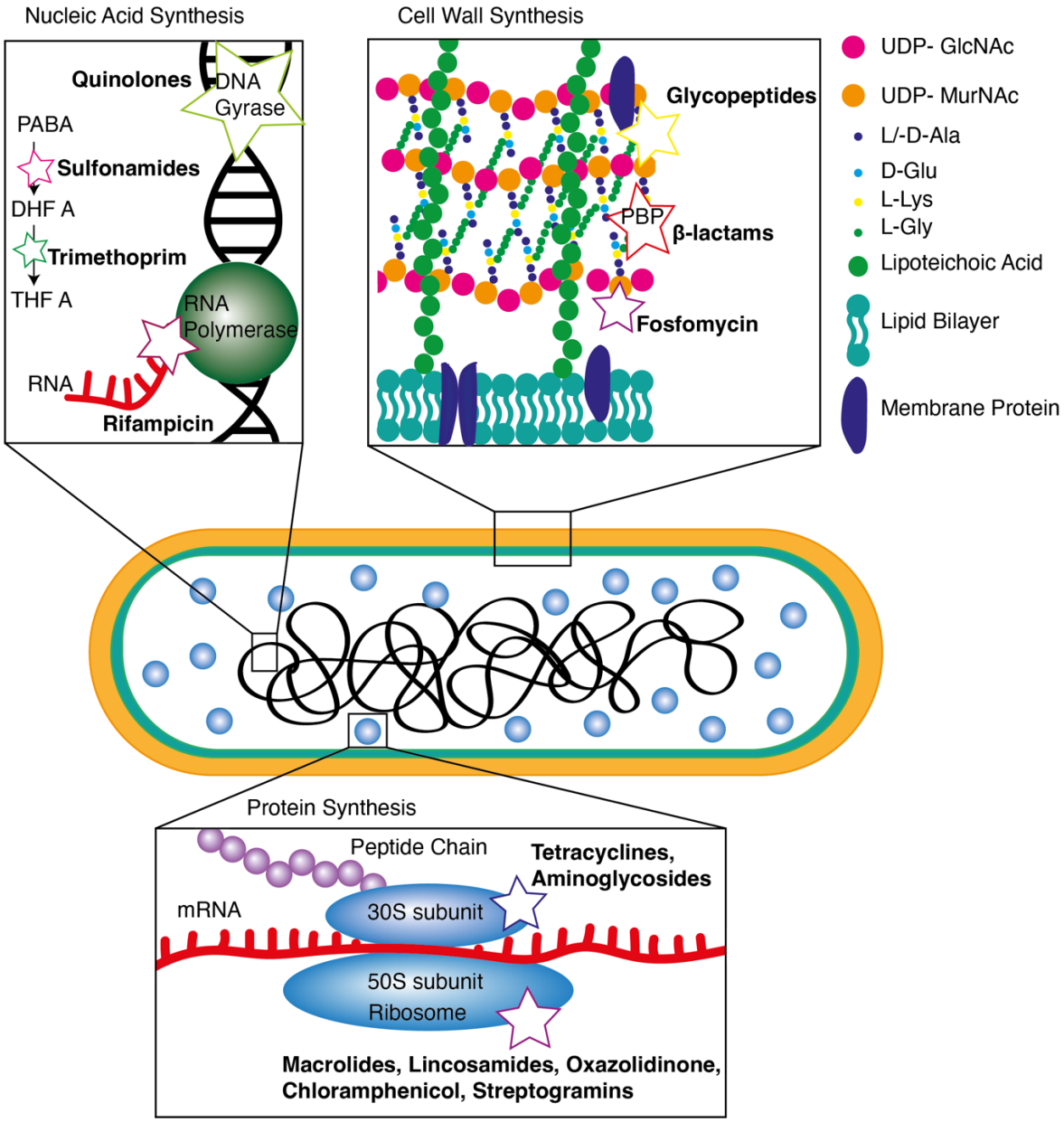

Figure 1-6: Targets of antibiotics.

Major antibiotic targets (stars) include nucleic acid synthesis, cell wall synthesis and stability and protein synthesis. Nucleic acid synthesis is through inhibition of DNA gyrase (quinolones), folic acid synthesis (sulfonamides and trimethoprim) or by blocking RNA polymerase (rifampicin). Gram-positive cell wall synthesis targets include binding the acyl-d-alanyl-d-alanine growing peptidoglycan chain (glycopeptides), penicillin binding proteins preventing cross linking (ß-lactams) and inhibiting phosphoenolpyruvate synthetase (fosfomycin). Protein synthesis is blocked by binding to the 30S ribosomal subunit (tetracyclines and aminoglycosides) or 50S ribosomal subunit (macrolides, lincosamides, oxazolidinone, chloramphenicol, streptogramins). Details of mechanisms in section 1.3.1. Adapted from[168].

1.3.1 Antibiotic targets

Antibiotics are either bacteriocidal (killing the target) or bacteriostatic (preventing growth/replication), with their mechanisms of action predominantly targeting cell wall, nucleic acid or protein synthesis[168] (Figure 1-6, Table 1-2). A range of antibiotics act by modulating cell wall synthesis. β-lactams, including penicillins, cephalosporins, carbapenems and monobactams, interfere with cell wall synthesis by targeting penicillin binding proteins (PBPs). β-lactams mimic the PBPs substrate, the D-alanyl, D-alanine of the peptide chain, thereby prevents crosslinking in the cell wall and hence leading to cell lysis. The β-lactam flucloxacillin is the most commonly used antistaphylococcal antibiotic against MSSA, with the advantage of being resistant to penicillinases unlike earlier generations of β-lactams[169]. Glycopeptides and lipoglycopeptides including vancomycin, prevent cell wall synthesis by directly targeting the D-alanyl, D-alanine of the peptide chain, again preventing crosslinking[168]. Phosphonic acid antibiotics (fosfomycin) target cell wall cross-linking by mimicking phosphoenolpyruvate (PEP), allowing them to bind MurA which is essential in peptidoglycan biosynthesis[170]. Lipopeptides are amphiphilic and can therefore interact with the negative bacteria membrane leading to cell death, and are proposed to cause cell death by either forming pores in the cell membrane and depolarising the cell or by driving the extraction of lipids from the cell membrane which are then released forming water pores[171,172].

Nucleic acid synthesis is another main target of antibiotics. Folic acid is a key precursor in nucleic acid (specifically synthesis of the base thymine) synthesis[173], and the target of some antibiotics. Dihydropyrimidine antibiotics (trimethoprim) inhibit dihydrofolate reductase, hence preventing folate biosynthesis[173]. Sulphonamides target dihydropteroate synthase (DHPS) preventing the formation of 7,8-dihydropteroate, a key intermediate in the folate pathway[174]. Antibiotics also target proteins which directly interact with DNA, for example quinolones such as ciprofloxacin target DNA gyrase. DNA gyrase negatively supercoils DNA through the creation of breaks in double stranded DNA followed by re-ligation. Quinolones inhibit DNA ligation by DNA gyrase, resulting in permanent double stranded breaks which, upon accumulation, are toxic to the cell[175]. Another antibiotic target is RNA polymerase

(RNAP) blocking RNA synthesis. Rifampicin forms a stable complex with RNAP, inactivating it and thus blocking transcription[176].

A third target of antibiotics is protein synthesis, often via inhibition of the ribosomal 30S or 50S subunits. Tetracyclines bind to the 16s rRNA within the 30S subunit, weaking interactions tRNAs[177]. Similarly, aminoglycosides interact with the 16s rRNA through hydrogen bonds binding to the A-site (the Aminoacyl-site, which is the first binding site for tRNAs importing amino acids within the ribosome). Aminoglycosides can inhibit initiation, block protein elongation or cause misreading depending on the chemical structure[178]. The 50S ribosomal subunit is also a major antibiotic target. Macrolides and streptogramin B antibiotics prevent protein synthesis by inhibiting the formation of the peptide bond in the growing peptide chain[179]. Streptogramin A antibiotics prevent the growing peptide chain from binding to A and P sites within the ribosome[180]. Lincosamides also bind within the 50S ribosomal subunit and stop the growth of the nacent peptide chain through binding to the peptidyl transferase loop of 23S rRNA[181]. Similarly, chloramphenicol also interacts with the peptidyl transferase activity preventing translation[182]. Oxazolidinones provide a different ribosomal target for antibiotics, by preventing the formation of the 70S ribosomal subunit, by binding to the 50S subunit interface with the 30S subunit[183].

Most of the above antibiotics have activity against *S. aureus* and may be used therapeutically for staphylococcal infection, but AMR commonly develops on exposure to the relevant antibiotic, leading to challenges in treatment despite the wide range of available agents. Some antibiotics such as flucloxacillin have a very narrow spectrum of activity (largely restricted to *S. aureus*) whilst other are broad-spectrum agents targeting a range of pathogens. Whilst historically referred to as 'methicillin resistant', MRSA are in fact resistant to all ß-lactam agents, including cephalosporins and carbapenems, comprising a major public health challenge[184].

Antibiotic resistance can be acquired by mutations which are transmitted 'vertically' to the offspring, but bacteria can also exchange large amounts of genetic material including antibiotic resistance genes by 'horizontal' transfer. Antibiotic resistance can spread between bacterial strains and species through horizontal gene transfer. Horizontal gene transfer is whereby a mobile genetic element is acquired by the host with the most prominent

mechanisms being conjugation, transduction and transformation. Conjugation is the process by which a plasmid or mobile genetic element is passed from one bacterium to the other via a pilus. Conjugation allows the transfer of large volumes of DNA (medium plasmid size 90kpb), the co-selection of resistance by other genes on the plasmid, and the transfer of DNA which is not self-transmittable. Transduction is where genetic material is passed between bacterium via a bacteriophage during the infection cycle the donors genes are incorporated into the bacteriophage. Transformation is bacteria's uptake of "naked" DNA from the environment[185-187].

Table 1-2: Anti-staphylococcal antibiotics[168,169,188] (section 4.12).

Horizontally acquired resistance mechanisms in bold.

Antibiotics and Class	Antibiotic Target	Main Resistance Mechanisms
Flucloxacillin (β-lactam)	Penicillin-binding protein 2, preventing cell wall cross linking	**PBP-2a** (*SCCmec* cassette, alternative PBP)
Cefoxitin (β-lactam Cephalosporin)	Penicillin-binding protein 2, preventing cell wall cross linking	**β-lactamases, PBP-2a** (*SCCmec* cassette, alternative PBP)
Vancomycin (Glycopeptide)	D-alanyl, D-alanine of growing peptide chain, preventing cell wall cross linking	***vanA*** operon (changes peptidoglycan precursors to D-alanyl-D-lactate)
Teicoplanin (Glycopeptide)	D-alanyl, D-alanine of growing peptide chain, preventing cell wall cross linking	***vanA*** operon
Daptomycin (Cyclic Lipopeptide)	Reduces membrane potential and inhibits cell wall synthesis	Mutations in *mprF* (Modifies charge of phosphatidylglycerol), *yycG* (controls peptidoglycan metabolism), *rpoB/C* (β and β' subunits of RNA polymerase)
Ciprofloxcin (Fluoroquinolone)	DNA gyrase and topoisomerase IV	Mutations in *gyrA* and *gyrB* (DNA gyrase)
Tobramycin (Aminoglycoside)	30S ribosomal protein	***rmt*** genes (methyltransferases), ***aadA*** (aminoglycoside nucleotidyltransferase), mutations in *rpsL* (Ribosomal protein S12), *fusA1* (Elongation factor G), *gyrA* (DNA gyrase A)
Clarithromycin (Macrolide)	50S ribosomal protein	***erm*** genes (methylation of 23S rRNA binding site)

Clindamycin (Lincosamides)	50S ribosomal protein	***erm*** genes (methylation of 23S rRNA binding site)
Linezolid (Oxazolidinones	23rRNA in the 50S ribosomal protein	Mutations in ribosomal proteins L3, L4, L22, ***cfr*** (methylation of 23S rRNA)
Doxycycline (Tetracycline)	30S ribosomal protein	***tetK/L*** (efflux pump), ***tetO/M*** (ribosomal protection)***, nonB*** (efflux pump), mutations in *rpsJ* (30S ribosomal subunit protein S10)

1.3.1.1 Mechanisms of antibiotic resistance

There are multiple mechanisms by which bacteria can resist antibiotics (Table 1-2). These include: modification of the target; preventing antibiotic uptake; removal of the antibiotic through efflux, and changing metabolic pathways (reviewed by[189]). This is an extensive topic and I have provided examples only below. A more extensive description of antibiotic resistance mechanisms relevant to *S. aureus* can be found in section 4.1.2.

In some cases, resistance will develop against the same antibiotics by different mechanisms, as exemplified by tetracycline resistance. Tetracycline binds to the bacterial 16S ribosomal RNA (rRNA) of the 30S ribosomal subunit, preventing the aminoacyl-transfer RNA (tRNA) from docking during elongation, thereby arresting translation. Chromosomal point mutations in 16S rRNA and the ribosomal protein S10 (which binds to 16S rRNA as part of the small subunit) have both been associated with tetracycline resistance[190,191]. At the time of writing there are 63 known horizontally acquired resistance genes and 11 mosaic genes encoding tetracycline resistance (accessed 13/08/22)[192]. Of these the known mechanisms of protection are efflux, ribosomal protection and enzymatic protection. *tetK* encodes a Gram-positive efflux pump which actively exports tetracyclines (other than minocycline) via proton-coupled active transport. *tetK* is common on small plasmids and has been found integrated in 5.14% of *S. aureus* chromosomes on the NCBI database (accessed 13/08/22)[193,194]. TetM, the most commonly reported ribosomal protection protein, has around 45% sequence homology to elongation factor E. Resistance is provided when TetM binds the 70S ribosomal complex, blocking the access of tetracycline by inducing a conformational change at the binding site[195]. Mosaic genes are ribosomal protection proteins which have undergone recombination and therefore function by similar mechanisms[196]. Enzymatic protection is provided by the monooxygenase TetX, a NADP-requiring oxidoreductase inactivating tetracyclines by hydroxylation before they are degraded[197].

In *S. aureus* methicillin resistance (MRSA) is mostly caused by the acquisition of *mecA,* encoding PBP2a, on the *SCCmec* cassette (mobile genetic element). The *SCCmec* cassette has 3 components: the *mec* gene complex; the cassette chromosome recombinase (*ccr*) gene complex and the joining region (J region). The *mec* gene complex consisting of the resistance gene (*mec*A), regulatory genes and the insertion sequence. The *crr* gene complex facilitates

the integration and excision of SCC*mec* into and out of the chromosome[198]. Finally, the J region contains housekeeping genes. There are 13 *SCCmec* elements, classified based on the specific *ccr* and *mec* gene complexes[199]. Importantly, acquisition of a gene by horizontal gene transfer is not an evolutionary endpoint, and chromosomal genes are also required for the development of high-level resistance (recently reviewed[199]). 48 auxiliary genes, which are required for resistance through *mecA* but do not confer resistance themselves, show that *mecA* is working through normal cellular functions not independently. The auxiliary genes contributing to methicillin resistance include: *tarA/B/D/L*[200] (involved in cell wall synthesis); *murA/B/C/D/E/F/Z* (involved in intracellular peptidoglycan synthesis) and *ftsA/W/Z* (contribute to cell division)[199,201]. Mutations in auxiliary genes may increase or decrease methicillin resistance. Potentiators of resistance include: *clpX* involved in protein stability[202]; *relA* in nucleotide signalling and the stringent response[203] and *rpoB/C* in transcription[204]. In a population of methicillin resistant cells, only a small proportion of cells will display high level methicillin resistance, with the potential to form a homogenous population presenting high level resistance on exposure to β-lactams by 'fixing' the potentiator mutations [199,205].

1.3.2 Preserving antibiotic activity

To retain effective antibiotics in the context of AMR there has been a search for new antibiotics, development of 2nd and 3rd generation compounds, combination therapies and combining antibiotics with adjuvants[206,207]. Despite a drive to find new classes of antibiotics, with novel mechanisms of action, there have only been 2 classes introduced since 2000. These are oxazolidinones (linezolid, FDA approval 2000[208]) and cyclic lipopeptides (daptomycin, FDA approval 2003[209]), both active against Gram-positive organisms, with linezolid an oral agent useful in treating MRSA. Recently, there has been the development of oxepanoprolinamides, a synthetic derivative of lincosamide, which appears to have a different binding site within the ribosomal site A. Iboxamycin, an oxepanoprolinamides, is active against strains expressing *erm* and *cfr*, which encode ribosomal RNA methyltransferase enzymes that confer resistance to antibiotics targeting 50S ribosomal subunit, including macrolides, lincosamides, phenicols, oxazolidinones. Despite only recently being developed, resistance against iboxamycin has already been detected[210,211].

Due to the dearth of new classes of antibiotics, existing antibiotics have been developed to maintain or enhance their activity and properties in vivo or overcome resistance mechanisms. Clarithromycin is a second-generation macrolide derivative of erythromycin. Compared to erythromycin, clarithromycin has favourable pharmacokinetic and pharmacodynamic properties with enhanced bioavailability, cellular availability and a longer half-life[212]. Doxycycline is a second-generation tetracycline. It has improved antimicrobial activity and resistance profile compared to tetracycline[213]. *S. aureus* carrying the *tetM* resistance gene are sensitive to doxycycline but not tetracycline[214]. Flucloxacillin is a penicillin G derivative. Resistance to penicillin G is common as β-lactamases hydrolyse the β-lactam ring, preventing covalent bonding to PBPs, rendering them inactive[207]. Flucloxacillin has improved oral absorption compared with penicillin G. It is also resistant to β-lactamases through steric hinderance preventing access to the β-lactam group[215]. Tobramycin is an aminoglycoside antibiotic. It has increased activity and improved interactions in serum compared to other aminoglycosides. However, tobramycin still has poor oral bioavailability[216].

AMR is a key example of bacterial adaptation to environmental conditions, but such adaptations also occur in response to the adverse pressures exerted by the host immune system and factors such as nutritional deprivation, hypoxia and acidosis.

1.4 Bacterial adaptation to host conditions

In biological ecosystems bacteria are required to adapt to the host environment. In harsh conditions (section 1.2) within the environment or host, there is a higher selective pressure for advantageous adaptations or genetic modifications. As noted, the staphylococcal TCSs can lead to wide-ranging adaptions by linking detection of an environmental stress to a transcription factor regulating multiple genes (increasing or decreasing target expression). The 16 (17 in some MRSA strains) staphylococcal TCS systems have been recently reviewed[217]. TCSs engage a flexible response with cessation of the environmental cue leading to reversal of the transcriptional response. However, if the stressor persists, this can create a bottleneck if limited genetic diversity is present. If genetic adaptations are essential for survival, ‘quick fix’ mutations are often selected for[218].

1.4.1 Selective pressures acting on *S. aureus* in the human body

The human body is a hostile environment for colonising bacteria due to low oxygen levels (section 1.2.2.3), host defences (section 1.2) and competition with co-colonising microbes, which drives *S. aureus* evolution[44]. Factors contributing to a successful infection include: overcoming immune attack from the innate and adaptive immune system; surviving adverse host tissue conditions, expressing appropriate adhesins to adhere to cells or the extracellular matrix and resisting external pressures such as antibiotics (section 1.3.1)[219]. This is partially achieved through the expression of virulence factors, discussed in section 1.1.2.

Within the host tissue, *S. aureus* is exposed to hypoxic conditions. *S. aureus* is a facultative anaerobe, able to grow in hypoxic conditions through switching its metabolism to fermentation or using substrates such as nitrate as their terminal electron acceptor[220]. Therefore, in hypoxic conditions *S. aureus* adapts by activating genes required for anaerobic respiration through the SrrAB two component system, which senses oxygen concentration by menaquinone reduction, leading to SrrB-dependent phosphorylation of SrrA[44]. Intracellular adhesion of *S. aureus* increases, through increased expression of β-1,6- linked glucosaminyl glycan, in hypoxic conditions (Table 1-1), enhances biofilm formation and is associated with lower metabolic rates and resistance to antibiotics[45]. Therefore, although *S. aureus* has adaptations to survive in hypoxic conditions, it is limited by its metabolic rate.

In contrast to our knowledge of the SrrAB TCS, little is known about mutational events induced in the *S. aureus* genome by hypoxia that might better enable infection.

The SaeRS TCS is induced by phagocytosis-related signals, with HNP1–3 having the most pronounced effect[221] and calprotectin and β-lactam antibiotics having weaker effects[100,221]. Activation of SaeRS upregulates the transcription of over 20 virulence factors comprising inhibitors of neutrophil chemotaxis, phagocytosis and killing. These include hemolysins, SCIN, CHIPS and leukocidins. Engagement of this TCS in the face of innate immune pressures may be to promote host invasion and biofilm formation[222]. Again, equivalent mutational responses engendered by exposure to host antimicrobial proteins are largely unknown.

1.4.2 Chronic staphylococcal infections

Rather than being rapidly resolved, some infections due to *S. aureus* can persist for weeks or even months, even in the face of antibiotic treatment. Studies monitoring bacterial populations over the course of such chronic infections indicate evolutionary adaptations in response to medical interventions and to the host environment. In one study of *S. aureus* chronic pulmonary infection in 14 patients with CF (cystic fibrosis), phenotypic changes (but not genome sequencing) including *S. aureus spa* type and nuclease activity were observed over a 1-year period with 3-5 visits. This was despite the patients having had chronic *S. aureus* infections for at least 10 years prior to the observational period[223]. During such chronic infections *S. aureus* are exposed to multiple pressures including hypoxia due to mucus plugging the airway, and increased epithelial oxygen consumption[224], neutrophilic inflammation[225], antibiotics and *Pseudomonas* co-infections[223,226].

During infections *S. aureus* can adapt by lifestyle changes. In chronic *S. aureus* osteomyelitis, reduced antibiotic susceptibility has been demonstrated, compared to acute infections. This has been suggested to be due to: decreased antibiotic concentration reaching intracellular populations within osteoblasts; metabolic activity of persisting bacteria not being high enough for efficacy; poorly remodelled bone providing protection from antibiotic, and sub-inhibitory antibiotic concentrations promoting small colony variants (SCVs). In chronic infections, SCVs accumulate, with reduced antibiotic susceptibility in vitro and in vivo. SCVs have reduced metabolic rates and down-regulate virulence factors, forming tiny colonies lacking pigment. SCVs are associated with persistence and host innate immune system evasion which is regulated through phenotype switching. Despite populations with a SCV lifestyle having reducing antibiotic susceptibility, it is unclear if this change in lifestyle was responsible for all of the identified antibiotic resistance, or if this was the first step before evolutionary processes, including genetic changes, resulting in antibiotic resistance[227]. In contrast, *S. aureus* isolates from patients with osteomyelitis have increased levels of non-typeable *S. aureus* compared to acute cases, indicating the loss of the capsule is associated with persistence[228].

In addition to lineages of well adapted strains emerging, genetic diversity developing within a population is common in chronic infections. Bacterial isolates from patients with chronic osteomyelitis are highly heterogeneous compared to homogeneous samples from acute infections suggesting either that heterogeneity aids persistence or that persistence engenders heterogeneity[228]. In a study of patients with diabetic foot disease (chronic foot ulcers which may progress to osteomyelitis) only 25% of patients were infected with the same *S. aureus* lineage for more than 4 weeks[67]. Genetic evolution was observed during this study, however, diversity was far more common due to re-infection. Similarly, in cystic fibrosis infections, *S. aureus* has been shown to have high levels of genetic diversity[65,229] with higher levels of diversity in sputum samples from patients with cystic fibrosis with chronic infections compared to nasal specimen of healthy individuals. Higher diversity correlated with increased bacteria density in the sputum[229]. In a different cohort of patients with cystic fibrosis single lineages have been tracked over 26 months and show genetic diversification[230]. The combination of these studies points genetic diversity increasing within bacterial populations by a combination of genetic evolution and reinfection. Pathogenic *S. aureus* are likely to face a more hostile environment compared to commensal bacteria due to the immune attack, hence the requirement for increased diversity. This is in support of the "insurance hypothesis" where diversity allows buffering against changes within an ecosystem[231]. Diversity increases the likelihood of suitable genes being available for survival. However, in vivo mouse experiments show, in some organs, *S. aureus* infections are established through an individual bacterium[232]. Further study is required to establish how heterogeneity in infections establishes from an initial clonal population.

1.4.3 Evolution of antibiotic resistance in a clinical environment

The development of antibiotic resistance in a clinical environment can be from chromosomal or horizontal factors. This has been seen in human infections in vivo, as exemplified by vancomycin resistance. Vancomycin is commonly used to treat MRSA. In 1997, the first *S. aureus* isolate with reduced vancomycin susceptibility was reported in Japan, with a small increase in the minimum inhibitory concentration (MIC) (since designated as vancomycin intermediate-resistant *S. aureus* or VISA)[233]. Longitudinal data from a patient who received prolonged treatment with vancomycin and other antibiotics while undergoing chemotherapy,

allowed the development of VISA to be tracked, with the MIC of bacterial isolates from the patient increasing from 1µg/ml to 8µg/ml over 12 weeks associated with 35-point mutations between the 1st and last sample[234]. In contrast, vancomycin resistant *S. aureus* (VRSA) (defined as MIC ≥32 µg/ml pre-2006), first identified in 2002 with resistance due to the *vanA* gene which is thought to have been transferred horizontally from vancomycin-resistant *enterococci* possibly via other members of the patients microbiome[235]. Unlike the resistance seen in VISA, VRSA demonstrate a major genetic change via the *vanHAX* gene cluster. This resulted in a change of vancomycin target D-alanyl-D-alanine cell wall precursor to D-alanyl-D-lactate, reducing vancomycin affinity 1000-fold [236].

The long-term evolution of *S. aureus* strains within clonal complex 8 (which included MRSA USA300) has been traced through clinical samples of patients in 2004, 2009 and 2010 followed by whole genome sequencing[237]. During the study, MGEs (mobile genetic elements), which promote movements of genes within genomes or between species, carried by prophages and plasmids accumulated, increasing the diversity of the accessory elements present. For 95% of USA300 isolates, antibiotic resistance was carried on a plasmid highlighting, their importance in antibiotic resistance. As well as increased diversity through MGEs, some MGEs were also lost during the study. This is likely to be through whole gene deletion events. There was also evidence of evolution through vertical gene transfer with increased heterogeneity in the core genome (accumulation of non-synonymous mutations) over time, suggesting a divergence in evolutionary trajectories[237]. The order of these gene accumulation and deletion events is unclear due to the infrequency of sampling. Additionally, the precise drivers and impact of each genomic change is uncertain due to the highly diverse environment which *S. aureus* will have encountered within the human body.

Whilst vancomycin and methicillin resistance are the best studied examples, there are growing concerns that resistance may evolve to linezolid. As noted above, linezolid inhibits ribosome function by blocking the 'A-site' for incoming tRNA docking into the 50S ribosomal subunit. Although linezolid resistance was initially felt to be uncommon, genome sequencing of clinical isolates following longer-term linezolid treatment have revealed linezolid resistance associated with mutations in genes encoding the 23S rRNA, and in the ribosomal proteins L4 and L3 in *S. epidermidis*[238]. Interestingly, mutations in MRSA L3 were re-capitulated using an

in vitro linezolid selection protocol, suggesting that in vitro evolution can reflect in vivo selection.

1.5 In vitro evolution studies

Despite the abundant information derived from in vivo longitudinal studies on the evolution of bacteria, it is challenging to determine the precise drivers and interactions influencing bacterial evolution due to the complexity of infections in the human body. In vitro evolution studies can be highly controlled allowing specific factors influencing bacterial evolution, and the mechanisms of evolution to be interrogated. As noted above, in vitro studies have in some cases re-capitulated mutations seen in vivo.

Antibiotic resistance has been studied through evolution experiments, allowing resistance mechanisms to be determined, as well as mechanisms of cross-antibiotic resistance to be studied (described in more detail, section 4.1.3). An evolution study of *S. aureus* immediately after *mecA* acquisition looked to understand how *S. aureus* transitions from a heterogeneous population with low-level resistance, to a population with high-level resistance[204]. Panchal et al.[204] inserted *mecA* into SH1000, evolved the new strain in oxacillin (β-lactam antibiotic), and then analysed the evolved clones by undertaking whole genome sequencing and analysis of evolved clones, and performing transcriptomic analysis of evolved clones and follow up assays on genes of interest. In this study the low-level resistance was associated with increased expression of genes related to anaerobic metabolism (targets normally down-regulated by the transcriptional repressor Rex) and a reduction in oxygen consumption. In the high level resistant clones mutations were identified in *rpoB/C* (RNA polymerase β/ β'), which increased oxacillin resistance and increased the expression of 11 genes including *mecA*[204], but the genes related to anaerobic metabolism had reverted to basal level (prior to *mecA* insertion). These results suggested acquisition and expression of *mecA* elicits low-level resistance but perturbs cellular redox balance with fitness cost in some settings, resulting in de-repression of Rex-regulated genes. The missense mutations in *rpoB/C* identified here allowed improved cell growth removing the need for the anaerobic shift in addition to the high-level resistance. Importantly, *rpoB/C* mutations have previously been identified in highly resistant clinical isolates of MRSA[239], and intriguingly *rpoB* mutations have also been associated with

rifampicin resistance[240]. Other evolution studies have also allowed for genes facilitating interactions between resistance to different antibiotic to be identified. For example, cross-resistance between vancomycin (glycopeptide) and daptomycin (cyclic lipopeptides) was via *mprF* mutations[241]. MprF (Multiple peptide resistance factor) is bacterial membrane protein which modifies phosphatidylglycerol by adding amino acids; in addition to mediating daptomycin resistance it has been implicated in conferring resistance to a range of cationic antimicrobial peptides including HNPs[242], demonstrating an interplay between antibiotics and host innate immunity in generating selection pressures. In another study, resistance to trimethoprim (target folate synthesis) drove increased sensitivity to ciprofloxacin by mutations in *rsbW* (inhibits the stress-response regulator sigma factor B)[243].

Other in vitro evolution studies have studied the fitness associated with mutations and horizontal elements, questioning the rationale that removing antibiotic treatment will cause resistance genes to be removed from a bacterial population due to the fitness cost associated with the gene. In one study, *E. coli* carrying two antibiotic resistance genes was fitter than strains carrying each gene individually[244]. As noted above, *rpoB/C* mutations generated high level oxacillin resistance and compensated for the fitness cost associated with *mecA* acquisition[242]. In addition, despite horizontally acquired genes (chromosomal or plasmid borne) initially being poorly adapted to their host with associated fitness costs, multiple studies have shown compensatory mutations[245-247] or metabolic changes[248] can rapidly ameliorate these fitness costs.

How some specific in vivo conditions affect bacteria have also been studied through in vitro evolution experiments. Insights were found into how *E. coli* adapt to utilise available nutrients. Analysis of 12 lines of *E. coli* evolved on glucose-limited minimal media for over 40,000 generations identified the rare evolutionary event of citrate utilisation (an abundant component in the media) after 31,000 generations, which became dominant in the population at 33,000 generations. From sequencing and re-sequencing clones in the lineage that developed the citrate utilisation trait the mutation responsible for the adaptation could be identified (amplification of the *rnk* promoter and *citT* gene) and tracked as it was refined the trait became prominent in the populations (four copies of the amplification and SNPs identified)[249]. There are however only limited studies which look at the evolution of bacteria

within an immune cell. The study of the evolution of bacteria in macrophages or macrophage-like cells have found: in *Mycobacterium tuberculosis* the development of a heterogeneous population, through mutations, although this couldn't be associated with any fitness advantage[250]; the development of SCVs in *E. coli* with fitness advantages in macrophages[251]; adaptive mutations in *E. coli* associated with LPS and iron metabolism[252]. These studies are a good start in understanding how factors in the human body are influencing the evolution of bacteria. As more factors are included in these models a more complete picture of the influence of individual factors of bacterial evolution will be possible.

1.6 Conclusion

S. aureus is constantly evolving to resist the stresses of the host and the infection environment (e.g. low oxygen tension, nutrient deprivation), the immune environment and factors generated by a range of immune cells, and antibiotic therapies. This evolution results in strains able to resist the specific stresses, through expression of virulence factors, repression or de-repression of compensatory genes, and mutations or horizontal acquisition of genes conferring antibiotic resistance or resistance to the environmental stressors. Expression of virulence factors are tightly controlled to reduce the cost of adaptations. As the threat of *S. aureus* infections is ever increasing with the rise of antibiotic resistance, a better understanding of how *S. aureus* adapts to host conditions is essential to develop effective future therapeutics. For these to be effective, we need to understand how the host is driving *S. aureus* evolution, to understand the pitfalls of future therapies, and factors less dispensable for *S. aureus* to survival in chronic, difficult to treat infections.

2 Hypotheses and Aims

2.1 Hypothesis:

Staphylococcus aureus is exposed to a multitude of factors during infections, including hypoxia, neutrophil proteins and antibiotics, as exemplified in the staphylococcal abscess. These harsh environmental conditions will drive mutations that promote survival in these settings.

2.1.1 Aims:

My overarching aim is to better understand how hypoxia, neutrophil proteins and antibiotics influence the development of antibiotic resistance in *S. aureus*.

My specific aims are:

- To test the antibiotic sensitivity of *S. aureus* SH1000 at baseline and following evolution in a range of antibiotics
- To explore changes in *S. aureus* growth, antibiotic sensitivity and mutations selected for by prolonged antibiotic exposure
- To investigate the propensity for antibiotic cross-resistance to occur following prolonged antibiotic exposure
- To determine if hypoxia influences the acquisition of resistance genes and their associated fitness cost
- To characterise population behaviour of *S. aureus* during prolonged exposure to hypoxia with or without antibiotic(s)
- To describe the genetic changes in clones that are associated with hypoxia and antibiotic selection, and how mutated genes influence bacterial fitness
- To measure the antimicrobial activity of candidate recombinant antimicrobial proteins against *S. aureus*
- To ascertain if antimicrobial resistance, developed by evolution in the presence of antibiotics, can influence the killing of *S. aureus* by LL-37

3. Materials and Methods

3.1. Materials

Table 3-1: Media and reagents

Media/reagent	Supplier	Preparation	Storage
1x running buffer	Fisher Scientific- Tris Base, Sodium Dodecyl Sulfate (SDS), Glycine	10x solution prepared as 30.3 g/l Tris Base, 190 g/l glycine, 0.01% SDS solution, in H_2O. 10x solution diluted 1-in-10 when used.	Room temperature
4x Laemmli sample buffer	Severn Biotech- Tris-HCl Fisher Scientific- Sodium Dodecyl Sulfate (SDS), glycerol Tocris Bioscience- Dithiothreitol Sigma-Aldrich- Bromophenol blue	100 mM Tris-HCl pH 6.8, 8% w/v SDS, 20% glycerol, 200 mM dithiothreitol (DTT), and 0.2% w/v bromophenol blue	-20°C
30% Acrylamide	Geneflow- AccuGel™ 29:1, 30%(w/v)29:1 Acrylamide: Bis-Acrylamide Solution		Room temperature
20% Ammonium persulfate (APS)	Sigma-Aldrich		Room Temperature
pH 11 alkaline water	Alfa Aesar- 6M NaOH Baxter- Sterile water	Dilute 6M NaOH in sterile water to 666 µM, pH 11. Filter sterilise though 0.22 µm Miller®GP filter unit before use.	Use on the same day
Brain heart infusion (BHI) Agar	Sigma-Aldrich	Mix 52 g/l H_2O before autoclaving.	Room temperature

Brain heart infusion (BHI) Broth	Sigma-Aldrich	Mix 37 g/l H_2O water before autoclaving.	Room temperature
BSA	Sigma-Aldrich- Bovine serum albumin (A6003)		4°C
2% BSA solution	Sigma-Aldrich- Bovine serum albumin (A6003) Gibco- Dulbecco's Phosphate Buffered Saline (PBS)	2% BSA solution made in PBS. Filter sterilise though 0.22 µm Miller®GP filter unit before use.	4°C
Coomassie blue solution	Fisher Scientific- Methanol, Acetic acid (glacial) Amresco- Coomassie blue	0.1% w/v Coomassie blue, 40% v/v MeOH, 10% v/v acetic acid in H_2O	Room temperature
De-staining solution	Fisher Scientific- Acetic acid (glacial)	10% v/v acetic acid in H_2O	Room temperature
Dulbecco's Phosphate Buffered Saline (PBS)	Gibco		Room temperature
Ethylenediaminetetraacetic acid disodium salt solution (EDTA)	Sigma-Aldrich-for molecular biology, pH 8.0, ~0.5 M in H_2O		4°C
EasySep™ Neutrophil Isolation Kit (contains EasySep™ Direct Human Neutrophil Isolation Cocktail and EasySep™ Direct RapidSpheres™	Stemcell- cat no 196666		4°C
Fetal Bovine Serum, Heat inactivated (FBS)	Gibco	Heat inactivate for 30mins in 56°C water bath on arrival. Store in 5 ml aliquots.	-20°C

Gel fixing solution	Fisher Scientific- propan-2-ol, Acetic acid (glacial)	25% v/v propan-2-ol and 10% v/v acetic acid solution diluted in H_2O	Room temperature
Glycerol	Fisher Scientific- glycerol Baxter- sterile water	Dilute to 80% glycerol and filter sterilise though 0.22 μm Miller®GP filter unit before use.	Room temperature
Luria Broth (LB)	Sigma-Aldrich- LB Broth (Miller)	Mix 25 g/l LB with H_2O before autoclaving.	Room temperature
Luria Broth (LB) agar	Sigma-Aldrich- LB Broth (Miller), Agar	Mix 25 g/l LB with 11 g/l agar in H_2O before autoclaving.	Room temperature
Lysostaphin	Sigma-Aldrich- 1 mg/ml Lysostaphin in 20mM sodium acetate pH4.5 (>500U/ mg activity)		-20°C
RNA/DNA SHIELD buffer	Zymo research-R1100-50		Room temperature
RPMI Medium 1640	Gibco		4°C
RPMI 10mM HEPES (4-(2-hydroxyethyl)-1-piperazineethanesulfonic acid)	Gibco- RPMI Medium 1640 ThermoTisher Scientific- HEPES, 0.5 M buffer solution, pH 7,6	Dilute to 10mM HEPES in RPMI in a 50 ml falcon tube.	4°C
R-Phycoerythrin (PE)-CD63 antibody	BD Biosciences	Protect from light at all times.	4°C
N,N,N',N'-Tetramethylethylene diamine (TEMED)	Sigma-Aldrich		Room temperature

pH7 Tris Buffer	Severn Biotech- 0.5 M Tris HCl pH 6.8 EMPROVE®bio-6M HCL	0.5 M Tris HCl pH 6.8 with 0.0102 M HCl achieving a final pH 7. Filter sterilise though 0.22 µm Miller®GP filter unit before use.	Use on the same day
1.5 M Tris buffer pH 8.8	Severn Biotech		Room temperature
0.5 M Tris buffer pH 6.8	Severn Biotech		Room temperature
20% SDS	Fisher Scientific		Room temperature
6% Dextran	Sigma-Aldrich	3 g dextran diluted in 50 ml 0.9% saline at 37°C giving a 6% solution	4°C
3.8% tris-sodium citrate	Ethypharm	3.8% tri-sodium citrate	Room temperature
0.9% Sterile Saline Solution	Baxter		Room temperature
90% Percoll	GE medical systems Ltd		4°C
4% Paraformaldehyde (PFA)	Sigma-Aldrich	Dilute in H_2O	4°C
HBSS (Hanks balanced salt solution 1X without magnesium and calcium)	ThermoFisher Scientific		Room temperature

Table 3-2: Antibiotics preparation and storage.

Following reconstitution, all antibiotics were stored in aliquots at -20℃.

Antibiotic	Supplier	Preparation
Clarithromycin	Sigma-Aldrich- clarithromycin, acetone	Dissolve in acetone to 50 mg/ml.
Daptomycin	Sigma-Aldrich- daptomycin, Dimethyl sulfoxide (DMSO)	Dissolve in DMSO to 1 mg/ml.
Doxycycline	Sigma-Aldrich- Doxycycline hyclate Baxter- Sterile water	Dissolve in sterile water to 5 mg/ml. Filter sterilise though 0.22µm Miller®GP filter unit before use.
Erythromycin	Sigma-Aldrich- Erythromycin Fisher Scientific-Ethanol	Dissolve in ethanol to 5 mg/ml.
Flucloxacillin	Sigma-Aldrich- Flucloxacillin sodium Baxter- Sterile water	Dissolve in sterile water to 5 mg/ml. Filter sterilise though 0.22µm Miller®GP filter unit before use.
Kanamycin	Sigma-Aldrich- Kanamycin A sulfate salt Baxter- Sterile water	Dissolve in sterile water to 50 mg/ml. Filter sterilise though 0.22µm Miller®GP filter unit before use.
Lincomycin	Sigma-Aldrich- Lincomycin hydrochloride Fisher Scientific- Ethanol	Dissolve in ethanol to 25 mg/ml.
Linezolid	Sigma-Aldrich- Linezolid Fisher Scientific- Ethanol	Dissolve in ethanol to 10 mg/ml.
Tetracycline	Sigma-Aldrich- Tetracycline hydrochloride	Dissolve in sterile water to 5 mg/ml. Filter sterilise though 0.22µm Miller®GP filter unit before use.

	Baxter- Sterile water	
Tobramycin	Sigma-Aldrich- Tobramycin Baxter- Sterile water	Dissolve in sterile water to 50 mg/ml. Filter sterilise though 0.22µm Miller®GP filter unit before use.

Table 3-3: Recombinant neutrophil antimicrobial proteins or peptides.

Following reconstitution, all proteins and peptides were stored in aliquots at -20℃.

Recombinant protein or peptide	**Supplier**	**Preparation**
BPI (in 80 mM citrate Phosphate, pH 5.6, with 150 mM NaCL)	Sigma-Aldrich- BPI Gibco- PBS	Dilute to 200 µg/ml in PBS.
Cathepsin G	Sigma-Aldrich- Cathepsin G, CH_3COONa, NaCl EMPROVE®bio-6M HCL	Reconstitute in 150 mM NaCl, 50 mM CH_3COONa buffer, pH 5.5 to 400 µg/ml.
Elastase	Abcam- Native human Neutrophil Elastase protein (Active) Sigma-Aldrich- CH_3COONa, NaCl EMPROVE®bio-6M HCL	Reconstitute in 50 mM CH_3COONa, pH 5.5, 150 mM NaCl to 100 µg/ml.
HNP-1	Sigma-Aldrich- HNP-1 Baxter- Sterile water	Reconstitute in sterile water to 100 µg/ml.
LL-37	Sigma-Aldrich- LL-37 (human) trifluoroacetate salt Baxter- Sterile water	Reconstitute 100 µg/ml in sterile water.

All experiments were carried out using sterile plastic ware vessels, which were sterile on arrival or sterilised by autoclaving. All experiments using standard 96 well plates were carried out in Greiner bio-one cell culture plate, U bottomed, CELLSTAR®.

Deep well (1.2 ml) 96 well plates were used when a higher volume was needed, and plates needed to be mixed (280 rpm). Sterile Abgene™ 96 Well 1.2 ml Polypropylene Deepwell Storage Plates were used covered in a 96 well plate sealing mat (ThermoFisher 96-well Sealing Mats: AB0674). The 96 well plate sealing mat had a slit above each well, to allow gas exchange, made by a scalpel before autoclaving.

Unless stated otherwise, optical density readings were taken with the Biochrom WPACO8000 Cell Density Meter for volumes of 1 ml or the Tecan Sunrise plate reader for 96 well plate readings and cultures were mixed on the grant-bio PSU-10i orbital shaker (280 rpm).

3.2. Methods

All methods used the materials listed in section 3.1 unless otherwise stated. All assays, other than Coomassie staining proteins (section 3.2.12.7), were carried out in a laminar flow Class 2 safety cabinet.

3.2.1. Bacterial strains

All strains used in this study are listed in Table 3-4. Unless stated, *S. aureus* was grown in BHI broth or agar and *E. coli* was grown in LB broth or agar including antibiotic concentrations below.

Table 3-4: Bacterial strains used in this study.

Antibiotic concentration for when grown on selective media.

Bacterial Strain	Characteristics	Antibiotic concentration	Reference
SH1000	Methicillin sensitive derivative of *S. aureus* 8325-4	N/A	[253]
USA300 JE2 LAC	Methicillin resistant. Parent of the Nebraska Library. Plasmids removed from the strain USA300.	N/A	[254]
NewHG	Methicillin sensitive (point mutation in *saeS* repaired from Newman strain)	N/A	[255]
GMSA017 SH1000 TetR	SH1000 with tetracycline resistance inserted by the plasmid *lysA*::pGM070	Tetracycline 5 µg/ml	[232]

GMSA016 SH1000 KanR	SH1000 with kanamycin resistance inserted by the plasmid *lysA*::pGM072	Kanamycin 50 µg/ml	[232]
GMSA015 SH1000 EryR	SH1000 with erythromycin resistance inserted by the plasmid *lysA*::pGM068	Erythromycin 5 µg/ml, Lincomycin 25 µg/ml	[232]
GMSA023 NewHG TetR	NewHG with tetracycline resistance inserted *lysA*::pGM070	Tetracycline 5 µg/ml	[232]
GMSA022 NewHG KanR	NewHG with kanamycin resistance inserted *lysA*::pGM072	Kanamycin 50 µg/ml	[232]
GMSA021 NewHG EryR	NewHG with erythromycin resistance inserted by the plasmid *lysA*::pGM068	Erythromycin 5 µg/ml, Lincomycin 25 µg/ml	[232]
E. coli BL21	*E. coli* kindly donated from Prof. Jon Sayers. This strain is typically used for recombinant protein production	N/A	[256]

3.2.2. *S. aureus* bacterial culture

3.2.2.1. Streaking out bacteria

To produce single bacteria colonies, and to check for contamination, bacteria were streaked out from microbank bead stocks (section 3.2.2.2) or glycerol stocks (section 3.2.2.3) onto BHI agar plates using a sterile inoculation loop. When bacteria contained antibiotic resistant markers, antibiotics were added to the broth or agar at the concentrations specified in Table 3-4. Bacteria were incubated overnight at 37°C without added CO_2.

3.2.2.2. Microbank bead stocks

A single colony was selected from a bacteria streak plate (section 3.2.2.1) using a sterile inoculation loop and transferred to 5 ml BHI broth in a 15 ml falcon tube. Bacteria were grown to log phase ($A_{600\ nm}$=0.6-0.8) in a humidity-controlled incubator (Sanyo CO_2 incubator, MCO-18AIC) shaking at 280 rpm, 37°C, 5% CO_2. 500µl liquid was removed from Microbank™ bead vial and 500 µl bacteria BHI broth was added. The beads were mixed by inversion before excess liquid above the beads was removed. Bead stocks were stored at -80°C.

3.2.2.3. Glycerol stocks

Glycerol was diluted to 80% with sterile water and filter sterilised. Bacterial populations or individual clones from experiments were then mixed with glycerol to achieve a final glycerol concentration of 20% in a 1.5 ml screw top cryovial. Glycerol stocks were stored at -80°C.

3.2.2.4. Bacterial counts by serial dilutions

To estimate population density, samples were serially diluted 1-in-10 in PBS from 10^{-1} to 10^{-6} in 1.5 ml Eppendorf's (competition assay 3.2.8) or in shallow 96 well plates (all other experiments). 10µl of sample was then spotted onto an agar plates. Bacteria were grown overnight at 37°C, no entrained CO_2. Colonies were counted at the highest countable concentration and CFU/ml was calculated as:

3.2.2.5. Bacterial spread plates

S. aureus was diluted through 1-in-10 serial dilutions in PBS. 50µl was then plated onto BHI agar and spread using a sterile L-shaped spreader. Bacteria were grown overnight at 37°C, atmospheric CO_2. Bacteria were diluted so there were approximately 50-500 colonies per plate.

3.2.2.6. S. aureus *frozen stocks (Chapter 7)*

S. aureus mid-log frozen stocks were prepared by: growing *S. aureus* (SH1000) overnight in BHI broth (280rpm, 37°C, 5% CO_2), inoculating into fresh BHI broth so $A_{600\,nm}$=0.05; incubating (280rpm, 37°C, 5% CO_2) for approximately 2h until in mid-log phase ($A_{600\,nm}$=0.6-0.8); aliquoting in 1 ml Eppendorf tubes; freezing at -80°C; removing 2 aliquots and measuring the CFUs by serial dilutions (section 3.2.2.4).

3.2.3. *E. coli* bacterial culture (Chapter 7)

E. coli was cultured identically to *S. aureus* (section 3.2.2), using LB broth or agar. When counting colonies, bacterial spread plates were used due to the large colony size of *E. coli* BL21.

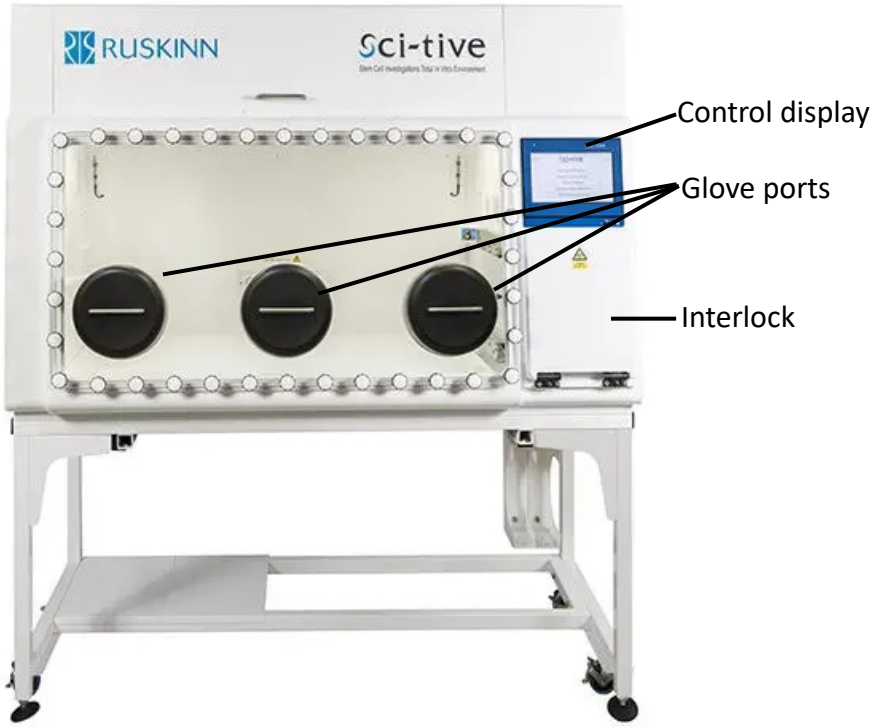

Figure 3-1: Ruskinn Sci-tive hypoxic workstation

Hypoxic chamber with programmable oxygen, carbon dioxide, humidity and temperature (control display panel), three glove ports (to allow access to the inside of the chamber to carry out experiments) and an interlock (allowing items to be taken into and out of the chamber). All glove ports and interlock are flushed with nitrogen to prevent re-oxygenation when adding or removing items. The chamber is equipped with an electrical power socket, which allows the use of devices including a grant-bio PSU-10i orbital shaker, microfuge and vortex mixer inside. https://bakerco.com/products/grow/sci-tive/sci-tive/

3.2.4. Controlling oxygen tensions (Chapter 5 and 6)

In Chapter 5 and 6 the impact of hypoxia on *S. aureus* was studied by comparing assays in hypoxia (0.8% O_2, which gives on oxygen tension of 3KPa in media[91]) to normoxia (i.e. atmospheric oxygen concentration, 21% O_2). For all experiments comparing hypoxia with normoxia, media were equilibrated overnight in the hypoxic chamber (Figure 3-1, Ruskinn Sci-tive hypoxic chamber 0.8% O_2, 5% CO_2, 70% humidity) or the normoxic chamber (Sanyo CO_2 incubator, MCO-18AIC, 5% CO_2, 95% humidity). Media was equilibrated with 10 ml in 50 ml falcon tubes, shaken at 280 rpm overnight. Within the hypoxia treatment, continuous hypoxia was maintained as all experimental procedures were carried out within the hypoxic chamber, with samples removed for quantification mid-experiment where necessary. All experiments were carried out in parallel for normoxia and hypoxia, minimising time between readings in each condition. Overnight cultures were grown in normoxia before use in either oxygen tension apart from neutrophil intracellular survival assays in section 3.2.12.9.

3.2.5. Fluctuation Assay (Chapter 4)

Fluctuation assays were used to characterise the mutation rate of *S. aureus* against a range of antibiotics using a method adapted from Krašovec et al.[257]. 10 experimental lines were established by picking 10 different collonies and inocculating an individual colony into 10 ml BHI broth, 10 times, followed by a 7h incubation at 37°C, 5% CO_2, 280rpm. Bacterial cultures were diluted 1-in-2000 in PBS, then 100µl was added to 10 ml BHI broth and grown overnight at 37°C, 5% CO_2, 280rpm. Overnight cultures were diluted in PBS so $A_{600\,nm}$=0.05 in 5 ml PBS, before 1-in-1000 dilution in BHI broth. 1 ml was added to 6 separate wells (1 well for each of the 5 antibiotics used later, plus an antibiotic free conditions) for each of the bacterial cultures (10 lines, 60 wells) in a deep well 96 well plate avoiding wells on the outside of the plate. A slitted 96 well plate sealing mat was placed on the deep well 96 well plate. The deep well plate was weighed before 24 h incubation at 37°C, 5% CO_2, 280 rpm. A 0h bacterial count was measured by serial dilutions (section 3.2.2.4) for each of the 10 experimental lines. After 24 h, the 96 well plate was weighed, to allow the amount of evaporation to be measured. Spread plates (section 3.2.2.5) were made for each of the 10 experimental lines onto agar containing antibiotics at the minimum inhibitory concentration (MIC) for each antibiotic (measured for

S. aureus as section 3.2.9) (60 plates in total- 5 antibiotics and an antibiotic free agar plate for each of the 10 experimental lines). 50 µl bacteria was added to BHI agar plates containing clarithromycin (1 µg/ml), doxycycline (0.5 µg/ml), linezolid (8 µg/ml) or tobramycin (8 µg/ml). Preliminary experiments found confluent growth when 50µl bacteria were added to flucloxacillin plates, therefore 10µl was added to BHI agar containing flucloxacillin (0.125 µg/ml). Bacterial counts in each of the 10 experimental lines were measured in antibiotic free conditions by serial dilutions (section 3.2.2.4). Preliminary experiments found clones on clarithromycin and tobramycin took 48 h to appear, therefore all agar plates were incubated overnight and bacterial counts were recorded, plates were then placed back into the incubator until a total incubation time of 48 h and any additional colonies were counted where possible (not possible if the colonies were too large and had merged). 1 clone from each fluctuation plate was selected at random to make a glycerol stock for subsequent analysis (section 3.2.2.3). Using 0 h counts, overnight (or 48 h) counts and the weight difference of the 96 well plate, the mutation rate against each of the antibiotics could be calculated.

3.2.5.1. Calculating mutation rates (Chapter 4)

The R package 'flan'[258] was used to calculate the mutation rate from the fluctuation assay (section 3.2.4) against each antibiotic, as well as the mutation number (m), and the probability of mutations occurring. m was divided by the mean number of bacteria which grew in antibiotic free media (Nt), adjusted for evaporation in the experiment, to give the mutation rate of resistance against each antibiotic in the antibiotic free environment of this experiment (m/Nt). This mutation rate was multiplied by the size of the closest available genome (NCTC 8325- 2,803,000bp) to give the mutation rate per genome. The number of mutations (m) were calculated using the "GF-test", which calculates the probability of a mutation occurring using a probability generating function. Other methods were incompatible with the data I obtained: the "ML" (maximum likelihood) method was incompatible with the flucloxacillin data due to the high colony counts obtained, and the "P0" (probability of null counts) method is based on the probability of 0 values, which did not occur for flucloxacillin.

3.2.6. Selection experiments

Selection experiments were carried out to determine how *S. aureus* responded to selective pressure. In each experiment the evolved clones and populations were compared to the ancestor (starting strain) to establish changes in growth, antibiotic sensitivity and genetics. Control populations, which were not exposed to the selective pressure being studied, were established to identify adaptations to laboratory conditions.

3.2.6.1. SH1000_TetR evolution in hypoxia and tetracyclines (Chapters 5 and 6)

To establish experimental lines, 6 independent colonies for both SH1000 controls and for SH1000_TetR were selected from streak plates. Individual colonies were inoculated into 10 ml BHI broth and grown in normoxia overnight (37°C, 5% CO_2, 280 rpm), and were thereafter designated as populations 1-6 for each treatment condition. 1-in-100 dilutions of overnight cultures (populations 1-6) were established in 8 experimental treatment conditions (antibiotic free SH1000_TetR, 30 µg/ml tetracycline SH1000_TetR, 2 µg/ml doxycycline SH1000_TetR) plus controls (antibiotic free SH1000) all in matched in normoxia and hypoxia, see Figure 3-2. All treatment populations (48 in total) were grown in a final volume of 400 µl BHI broth in deep well (1.2 ml) 96 well plates sealed with slitted plate seals to allow gas exchange whilst preventing contamination while shaking at 280 rpm. Every 24 h for 34 days each population underwent a 1-in-100 serial passage into fresh BHI broth (with antibiotics and in normoxia/hypoxia as appropriate to maintain continuity of selection pressures) and optical density ($A_{600\ nm}$) was measured. 20% cryogenic glycerol stocks (section 3.2.2.3) of whole populations were prepared and stored at -80˚C every 5 transfers and a subsection plated on BHI agar. Population 6 of SH1000 in normoxia died out on day 14 and was excluded from subsequent analysis. Method summarised in Figure 3-2.

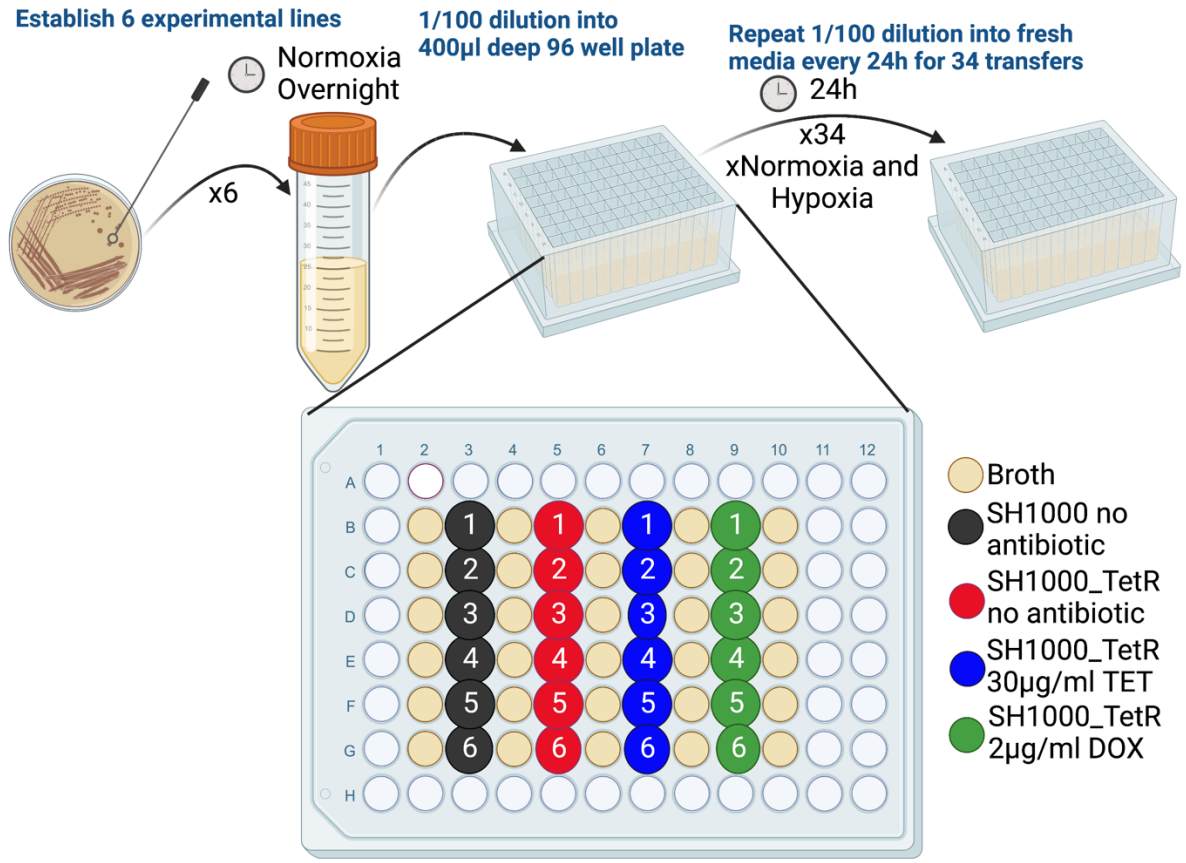

Figure 3-2: Method for SH1000_TetR evolution in hypoxia and tetracyclines

Schematic of selection assay method for SH1000_TetR evolution in normoxia and hypoxia. 6 experimental lines for both SH1000 and SH1000_TetR were established by inoculating individual colonies in 10 ml BHI broth and growing overnight. Overnight cultures were diluted 1-in-100 in pre-equilibrated media (with antibiotic were appropriate) in normoxia and hypoxia for SH1000 no antibiotic, SH1000_TetR no antibiotic, SH1000_TetR 30 µg/ml tetracycline, SH1000_TetR 2 µg/ml doxycycline and placed in deep well (1.2 ml) 96 well plates. Every 24 h bacteria were transferred into fresh media (and antibiotics as appropriate) with a 1-in-100 dilution. Bacteria were incubated in normoxia or hypoxia (280 rpm) with slitted 96 well plate seal on top of the deep well plate. Glycerol stocks were made and frozen every 5 transfers as contingency. Created with BioRender.com

The evolved populations were further analysed. For the work described in Chapter 5 the growth (section 3.2.7.2) and MIC (section 3.2.9) of whole populations arising from the above experiment were analysed. Overnight cultures at the start of each population assay were established by using a sterile inoculation loop and directly inoculating into 10 ml BHI broth in a 50 ml falcon tube before overnight incubation (37°C, 5% CO_2, 280 rpm). For the work described in Chapter 6 the growth (section 3.2.7.2), MIC (section 3.2.9) and genetics (section 3.2.14) of 1 clone from each population resulting from the evolution described above was analyses. 1 clone from each of the 47 populations (6 per evolution condition, but without population 6 of SH1000 in normoxia which died out) was selected by streaking out (section 3.2.2.1) a sub-section of each population, on to one BHI agar plate per population with a pre-marked cross, prior to overnight incubation (37°C). The colony closest to the pre-marked cross was selected to be the clone of the corresponding population. This colony was grown overnight in BHI broth and a glycerol stock (section 3.2.2.3) of each clone was made. Overnight cultures for experiments with clones were established as for populations above.

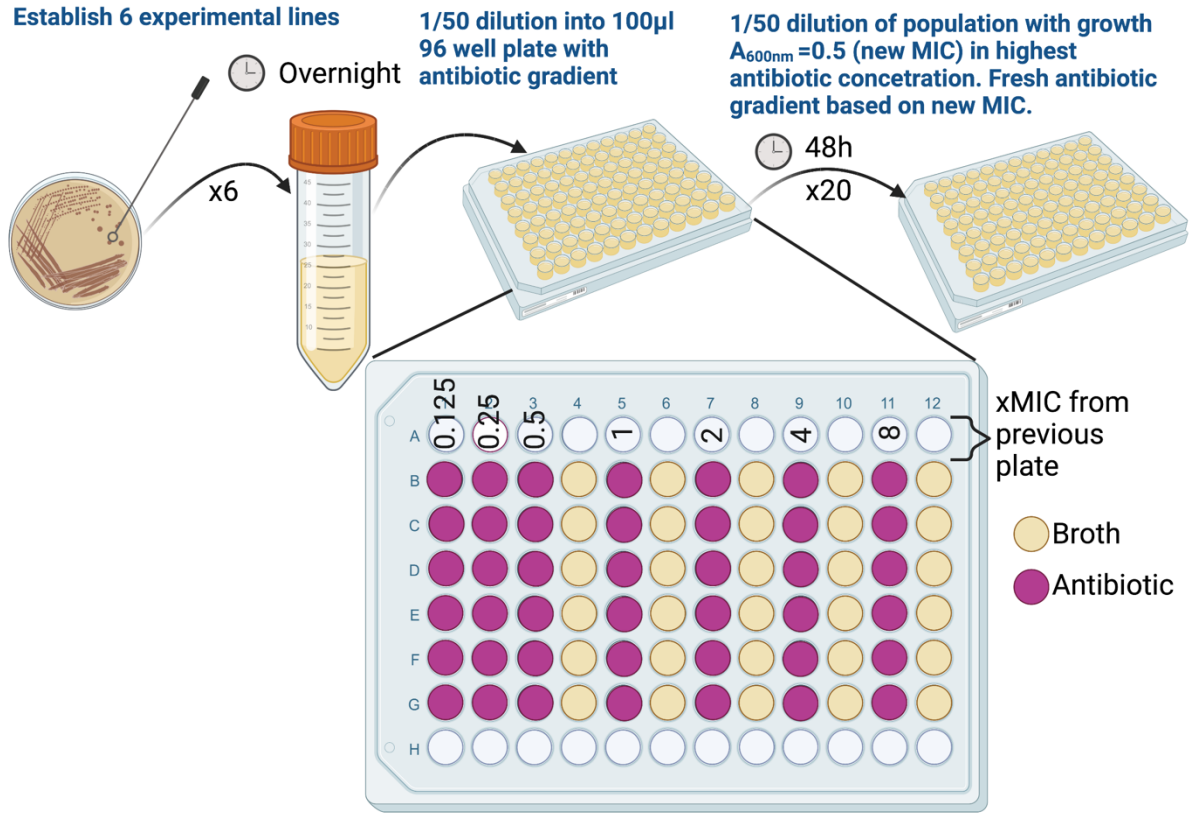

Figure 3-3: Selection method for SH1000 on an antibiotic gradient

Antibiotic resistance selection on an antibiotic gradient in normoxia. 6 experimental lines of SH1000 were established by picking individual colonies and growing overnight in 10 ml BHI broth. Overnight bacterial cultures were diluted 1-in-50 into an antibiotic gradient (clarithromycin, doxycycline, flucloxacillin, linezolid, tobramycin and no antibiotics) based on the bacterial MIC. Every 48 h bacteria were passaged with a 1-in-50 dilution into a new antibiotic gradient based on the current MIC of the evolving bacterial population. Between passages bacteria were incubated at 37℃, 5% CO_2. Glycerol stocks were made every 5 transfers and every time the populations MIC increased. Created with BioRender.com.

3.2.6.2. SH1000 selection on antibiotic gradient in normoxia (Chapters 4 and 7)

6 independent colonies of SH1000 were selected from streak plates to establish 6 experimental lines. These were added to 10 ml BHI broth and incubated overnight (37°C, 5% CO_2, 280 rpm). 6 standard 96 well plates (1 for each of the following experimental conditions- antibiotic free, clarithromycin, doxycycline, flucloxacillin, linezolid, tobramycin) were prepared with 98 µl of 0.125- 8 times the minimum inhibitory concentration (MIC, see below 3.2.9), with a doubling antibiotic gradient (7 doubling concentrations) in each antibiotic (Figure 3-3). The starting MIC for each antibiotic was: 0.5 µg/ml clarithromycin; 0.125 µg/ml doxycycline; 0.0625 µg/ml flucloxacillin; 4 µg/ml linezolid; 4 µg/ml flucloxacillin; no antibiotic control. 2 µl of the relevant bacterial culture was added to 98 µl of relevant antibiotic or antibiotic concentration and incubated for 48 h (37°C, 5% CO_2, static culture). 48 h was selected as some colonies on antibiotic plates took 48 h to appear in the fluctuation assay (section 3.2.4). At 48 h the optical density ($A_{600\ nm}$) was measured, and a new MIC was established as the highest concentration of antibiotic with a reading of at least $A_{600\ nm}$=0.5, now MIC=1. If there was clear growth but no population reached $A_{600\ nm}$=0.5, the well with the population with the highest level of growth was used. Based on these results, new antibiotic plates were made as above but with the new MIC as the bases. 2 µl bacteria from the previous plates was added to 98 µl of relevant antibiotic or antibiotic concentration each well in the new antibiotic gradient (new MIC, x 0.125-8). This was repeated every 48 h for 20 transfers, 40 days. 20% glycerol stocks (section 3.2.2.3) were made every 5 transfers and every time the populations MIC increased. Selection method summarised in Figure 3-3.

All subsequent assays were carried out on 1 clone per population (36 clones in total), which were prepared as for the selection assay above (section 3.2.6.1). Starting overnight cultures for each clone was established by selecting 1 colony from an agar streak plate (section 3.2.2.1) from each clones' glycerol stock.

3.2.7. Bacteria growth measurements

3.2.7.1. Ancestors' growth in normoxia and hypoxia (Chapter 5)

Bacterial growth curves were used to compare growth parameters in different oxygen tensions. Overnight cultures were prepared by inoculating strains directly from frozen stocks into 10 ml BHI broth before growing overnight in normoxia (37°C, 5% CO_2, 280 rpm). Optical density of overnight bacterial culture was measured at 600 nm and inoculated into equilibrated media to a density of $A_{600\ nm}$=0.05. Optical density measurements were then taken (hourly at 0-7 h plus a final reading at 24 h) at 600 nm, diluting in BHI broth to the range $A_{600\ nm}$= 0.1-1.0. Between readings cultures were incubated in a hypoxic (Ruskinn Sci-tive hypoxic chamber 0.8% O_2, 5% CO_2) or normoxic incubator as appropriate with shaking at 280 rpm. At 24 h final bacterial counts were calculated by serial dilution (section 3.2.2.4).

3.2.7.2. Growth of evolved populations (Chapter 5) or clones (Chapter 6) from hypoxia evolution experiment

Growth curves were carried out on evolved populations (Chapter 5) from the normoxia or hypoxia evolution experiment, section 3.2.6.1, or 1 clone from each of the 47 evolved populations (Chapter 6) using identical methodology to allow comparison. The need for the generating a hypoxic growth curve precluded the use of the plate reader method described below (3.2.7.3). Overnight cultures of all 47 populations or clones plus 3 repeats for the ancestors SH1000 and SH1000_TetR were grown directly from 20% glycerol stock (from normoxia/hypoxia evolution experiment, section 3.2.6.1) in normoxia (37°C, 5% CO_2, 280 rpm) in 400 µl BHI broth in deep well 96 well plates with slitted plate seals. 100 µl from each well of the overnight cultures was transferred into a shallow 96 well plate and optical density (600 nm) was measured. The mean optical density was calculated averaging the $A_{600\ nm}$ from all populations or clones irrespective of evolution conditions. All populations or clones were diluted to the same 1-in-10 mean $A_{600\ nm}$ in deep well 96 well plates in normoxia (stock plate). From the normoxia stock plate, each culture was diluted 1-in-10 (final 1-in-100 mean $A_{600\ nm}$) in pre-equilibrated media in 5 deep well 96 well plates place in normoxia and hypoxia in the respective incubators, to a final volume of 400 µl per well. The deep well plates were incubated at 280 rpm sealed with a slitted plate seal. At 0, 2, 4, 6 or 24 h optical density (600

nm) was measured of 1 deep 96 well plate per condition, with a separate plate used at each time point. Evolved population or clone growth was compared to ancestors grown simultaneously in identical conditions.

3.2.7.3. Plate reader growth curves of clones from antibiotic selection experiment (Chapter 4)

Clones from the antibiotic selection gradient were generated and selected as outlined in section 3.2.6.2. Overnight cultures were prepared by inoculating 1 colony per condition from streak plates into 10 ml BHI broth and growing overnight in normoxia (37°C, 5% CO_2, 280 rpm). Overnight bacterial culture optical density (600 nm) was measured, and samples were inoculated into 1 ml BHI broth to a final density of $A_{600\ nm}$=0.05. 100 µl of each adjusted bacterial culture was added to a 96 well plate. Broth blanks (to check shaking did not lead to contamination) and control populations (at least 3) were randomly dispersed throughout the 96 well plate. The outside rows and columns of the 96 well plate was filled with broth.

The prepared 96 well plate was placed in the Varioskan LUX Multimode Microplate Reader set at 37°C throughout the assay. Optical density readings were taken at 600 nm every 10 mins for 48 h with the plate shaking at 120 rpm between readings. At 48 h CFUs were determined through platting 10 µl of each well by serial dilutions (section 3.2.2.4).

3.2.7.4. Growth curve analysis

Bacterial growth curve analysis was carried out in R version 4.3, using the packages 'Rmisc' and 'flux'. For each growth curve, the area under the curve (integral), maximum optical density reading, maximum growth rate and lag phase was calculated (Figure 3-4A). When calculating the lag phase, a tangent is drawn from the maximum growth rate (blue line Figure 3-4B and C) and where it meets the x axis is the measured lag phase. However, in multiple curves the maximum growth rate did not occur at the beginning of the exponential phase (example Figure 3-4C), therefore without data manipulation (which could have introduced bias), the lag phase could not be accurately determined for these bacterial samples.

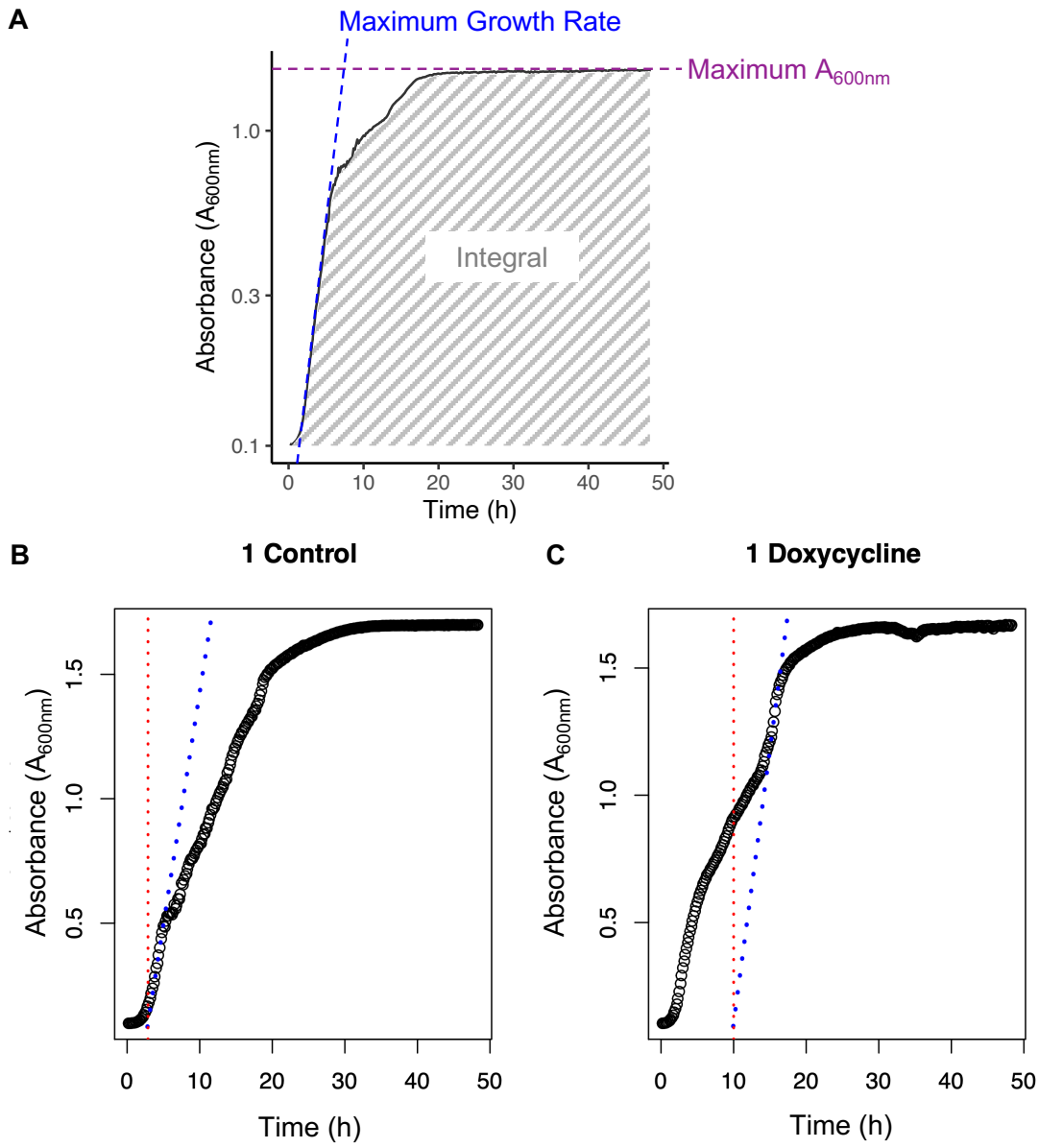

Figure 3-4: Growth curve analysis

Example growth curves measured in 96 well plates with readings every 10 mins taken automatically at $A_{600\ nm}$ by the Varioskan LUX Multimode Microplate Reader with the temperature set at 37℃. Between reading the plate was shaken at 120 rpm. A) Parameters measured from the growth curves were, the maximum growth rate (blue line), maximum $A_{600\ nm}$ (purple line) and integral (total growth, grey shading). B, C) The blue line shows the tangent created the show the maximum growth rate, the red line the tangent to determine the lag phase. In B) the lag phase is accurately determined. C) shows an inaccurate measurement of lag phase due to the maximum growth rate being at the end of the logarithmic phase.

3.2.8. Competition Assays (Chapter 5 and 6)

Strains were competed against each other to compare the fitness of two strains when grown in identical conditions in the same vessel. For each competing strain, the frozen bacterial stocks were inoculated directly into 10 ml BHI in a 50 ml falcon tube and grown for 24 h in normoxia (37°C, 5% CO_2, 280 rpm). After 24 h the optical density (600 nm) was measured for each bacterial culture to check similar initial growth (if not the volumes in the next step would have been adjusted, but this was not necessary in any experiment). 50 µl of each strain was then transferred into 10 ml equilibrated media (t=0 h) in a 50 ml falcon tube, and the combined cultures were incubated for 24 h at the appropriate oxygen tension (280 rpm shaking). When included, 0.125 µg/ml tetracycline as added to the media. At 0 h and 24 h optical density (600 nm) was measured and 50 µl bacteria were plated at between 10^{-3} and 10^{-5} as appropriate as a spread plate (section 3.2.2.5) onto both non-selective plates and selective plates with the corresponding antibiotic for the resistance marker (concentrations listed in Table 3-4). The fitness (for strains A and B) was then calculated as follows:

3.2.9. Antibiotic minimum inhibitory concentration (MIC)

Antibiotic MICs were measured to find the lowest antibiotic concentration required to prevent visible growth of bacteria. This allowed appropriate antibiotic concentrations to be used in fluctuation assays (section 3.2.4) as the antibiotic concentration which prevents bacterial growth, and selection assays (section 3.2.6) as ½ to ¼ the tetracycline or doxycycline MIC for SH1000_TetR. Following selection assays MICs of evolved clones and populations were compared to their ancestor to determine the influence of selection conditions on antibiotic susceptibility. Serial doubling dilutions of antibiotic were carried out with appropriate broth controls; the general plate layout for the assay is shown in Figure 3-5. Further details of the conditions specific to the measurements of MICs of normoxia versus hypoxia and following antibiotic selection are given below (sections 3.2.9.1 and 3.2.9.2 respectively). In MICs in atmospheric oxygen tensions 50 µl bacteria was added to 50 µl broth or diluted antibiotic. When MICs included a hypoxic condition, the media (or diluted antibiotic) volumes were adjusted to 90 µl broth with 10 µl bacteria added to increase the

volume of pre-equilibrated media used so the bacteria were immediately in hypoxic conditions. The methodology was adapted from the European Committee on Antimicrobial Susceptibility Testing (EUCAST) method[259] to match the media used in selection experiments.

In the analysis of MICs, breakpoints (the lowest antibiotic concentration with no visible growth) were primarily used to compare antibiotic sensitivity. Optical density (600 nm) readings were also measured at the end of each MIC experiment and the area under the curve (AUC) was measured to represent sensitivity to the antibiotics across a range of concentrations. AUC measurements also incorporate the impact of antibiotics on growth.

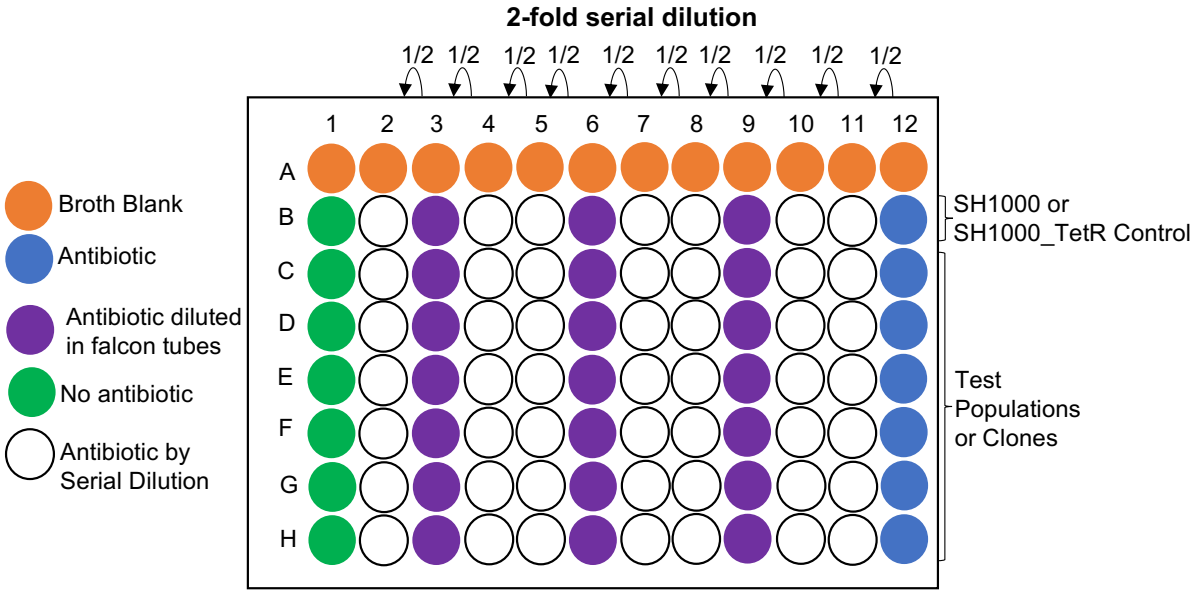

Figure 3-5: MIC 96 well plate layout.

1-in-2 serial dilutions of antibiotics were carried out from column 2-12 transferring media containing antibiotics from the adjacent well to the right (white wells). Antibiotics in columns 12, 9, 6, and 3 were prepared to the appropriate concentration in falcon tubes and used as the stocks for the dilutions (blue or purple wells). Green wells had no antibiotics in them. Orange wells were broth banks to control for contamination and to normalise absorbance readings. A control of SH1000 or SH1000_TetR as appropriate was added in row B. Row C-H had test populations or clones added with 1 row per subject.

3.2.9.1. Comparing normoxic and hypoxic MICs (Chapters 5 and 6)

Preliminary experiments determined the range of antibiotic concentrations (Table 3-5) to use. Assays were performed in 96 well plates with the general layout as shown in Figure 3-5. Antibiotics were diluted by serial half dilutions in equilibrated BHI broth in each column of wells from column 12 through to 2 of the plates to achieve a final volume of 90 μl per well; column 1 contained no antibiotic (diluent only). Antibiotic concentrations in columns 12, 9, 6 and 3 were prepared in falcon tubes before adding to the plates for the remaining dilutions. Broth controls (row 1 of the plate) were included to detect contamination.

Overnight populations or clones were grown from 20% glycerol stocks or microbank beads in 10 ml BHI broth in normoxia (37°C, 5% CO_2, 280 rpm). Overnight cultures were diluted in BHI broth so $A_{600\ nm}$=0.05. 10 μl of the diluted bacteria cultures was added to 90 μl antibiotics in the pre-prepared 96 well plate in both normoxia and hypoxia. Final 100 μl cultures were grown for 20 h (static) in normoxia or hypoxia. MIC cut-offs were determined as lowest concentration of antibiotic without visible growth. Optical density (600 nm) were also taken at 20 h to see the impact of lower antibiotic concentrations on growth, although these were not used for calculating the MIC cut-off.

3.2.9.2. Clones before and after antibiotic selection (Chapter 4)

MICs were carried out as described in 3.2.9.1 with the following changes. Overnight cultures of clones following antibiotic selection (section 3.2.6.2) were started from a single colony from a spread plate (section 3.2.2.1) placed into 10 ml BHI broth in a 50 ml falcon tube and incubated for 48 h in normoxia (37°C, 5% CO_2, 280 rpm). Antibiotic concentrations ranges were as shown in Table 3-5. Antibiotics were prepared so there were 50 μl in the 96 well plate and a 50 μl volume of bacteria at $A_{600\ nm}$=0.05 was added to each well. All stages were prepared at atmospheric oxygen tensions and pre-equilibrated media were not required. In the set-up of antibiotic selection assays, and MICs from clones from fluctuation assays, MIC plates were incubated for 20 h. Following antibiotic selection (section 3.2.6.2) MIC plates were incubated for 48 h to match the duration of the antibiotic selection assay. Preliminary experiments showed no consistent difference in MIC cut-offs measured at 20, 24 and 48 h in any of the antibiotics tested (Figure 3-6).

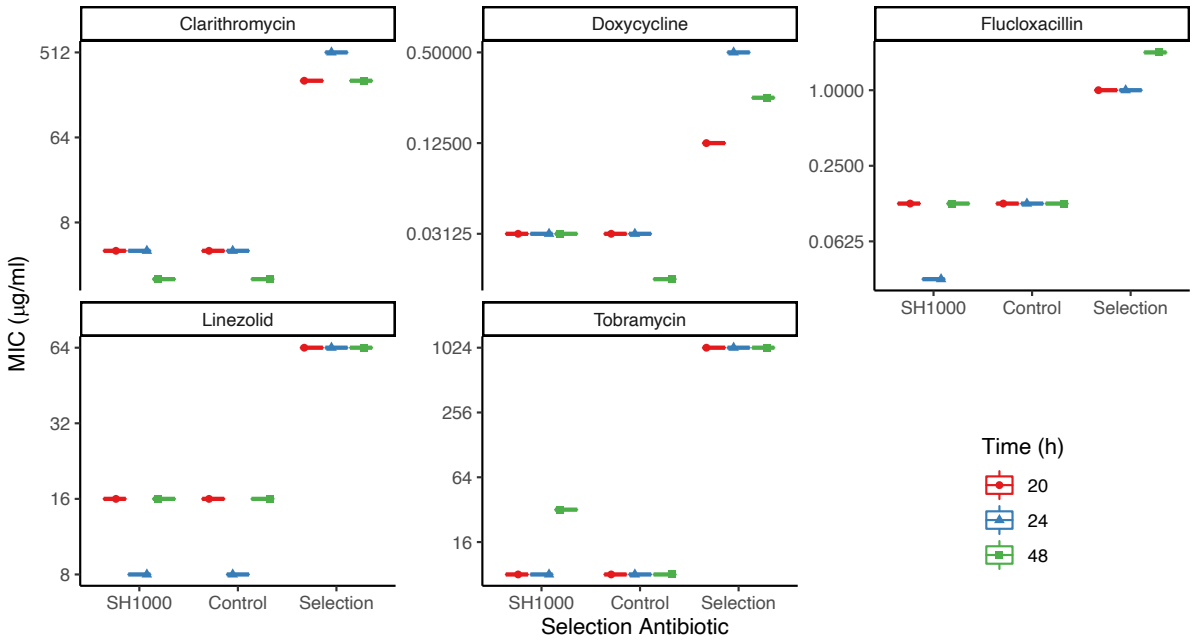

Figure 3-6: Lack of influence of time on measured MICs

MICs of ancestor (SH1000) or clones which had undergone 20-day selection under no antibiotic (control) or the corresponding antibiotic in each panel (selection). The antibiotic in each panel was prepared by serial dilutions in BHI broth in 96 well plates and incubated with bacteria for 20 h (red circles), 24 h (blue triangles) or 48 h (green squares). MIC cut-offs were defined as the lowest antibiotic concentration with no visible bacterial growth in the well, n=1 experiments. The same 96 well plate was used for repeat measurements at each time point.

Table 3-5: Antibiotic concentration ranges used for MIC measurements

Antibiotic	Figure	Highest Concentration (µg/ml) (Column 12)	Lowest Concentration (µg/ml) (Column 2)
Clarithromycin	4-1, 4-2, 4-10, 4-15	128	0.125
Daptomycin	4-1	64	0.0625
Doxycycline	4-1, 4-13, 4-15	128	0.125
	5-5 SH1000	128	0.125
	5-5 SH1000_TetR	256	0.25
	5-8	512	0.5
Flucloxacillin	4-1, 4-2, 4-14, 4-15	8	0.00781
Linezolid	4-1, 4-11, 4-15	256	0.25
Tetracycline	5-5 SH1000	128	0.125
	5-5 SH1000_TetR	256	0.25
	5-8	512	0.5
	6-5, 6-9, 6-11	256	0.25
Tobramycin	4-1, 4-2, 4-12, 4-15	64	0.0625

3.2.10.Detecting small colony variants (SCVs)

SCVs were observed following SH1000 selection on an antibiotic gradient (section 3.2.6.2) and SH1000 and SH1000_TetR selection in hypoxia and tetracyclines (section 3.2.6.1). To quantify SCVs for clones which had been selected on an antibiotic gradient (Chapter 4 and 7), each of the 36 clones were streaked out on BHI agar, incubated for 24 h (37°C) and colonies were compared to SH1000. Each clone was defined as a SCV or not. For populations evolved in hypoxia and tetracyclines (Chapter 5) there was a heterogeneous SCV phenotype within populations, therefore each of the 47 evolved populations were streaked out onto BHI agar, incubated for 24 h (37°C) and compared to their ancestor (SH1000 or SH1000_TetR). Evolved populations had a pre-defined area of SCVs and 'normal' colonies counted to give a percentage SCV for each population. Agar plates were blinded by covering labels while counting to remove unconscious bias. A SCV was defined as a colony lacking pigment which is smaller (approx. 10%) than the colonies ancestor (SH1000 or SH1000_TetR) incubated in identical conditions.

3.2.11.Neutrophil recombinant protein assays (Chapter 7)

Assays were carried out on recombinant proteins and peptides (BPI, cathepsin G, elastase, HNP-1 and LL-37) to establish whether they had antimicrobial activity against *S. aureus* (or *E. coli* for BPI and elastase), and subsequently to determine whether the evolution of *S. aureus* SH1000 in antibiotics (section 3.2.6.2) changed *S. aureus* sensitivity to LL-37. Recombinant proteins were prepared according to the manufacture's instructions with initial stock concentrations of: 200 µg/ml BPI (in 80 mM Citrate Phosphate, pH 5.6, 0.75 M NaCl); 400 µg/ml cathepsin G (in 150mM sodium acetate (pH 5.5), 150mM NaCl); 100 µg/ml elastase (in 50 mM sodium acetate (pH 5.5), 150 mM NaCl); 100 µg/ml HNP-1 (in H_2O); 100 µg/ml LL-37 (in H_2O). In all experiments, proteins were compared to protein and solute controls. Protein control was BSA prepared to the same stock concentration and in the same solute as the stock experimental proteins, BSA stocks were then treated identically to each of the proteins. The solute control was the same solute the neutrophil proteins were reconstituted in, at identical final experimental concentrations.

3.2.11.1. Concentration response (Chapter 7)

S. aureus SH1000 was grown overnight in 10 ml BHI broth in 50 ml falcon tubes (37°C, 5% CO_2, 280 rpm). Optical density of overnight cultures were adjusted to $A_{600\ nm}$=0.05. Recombinant neutrophil proteins, BSA control or control solute were diluted in BHI broth to achieve the desired final concentration ranges (BPI, 10 ng/ml-10 µg/ml; cathepsin G 100 ng/ml-100 µg/ml; elastase 1 ng/ml-50 µg/ml; HNP-1, 10 ng/ml-50 µg/ml; LL-37, 1 ng/ml-100 µg/ml). 50 µl recombinant proteins (or controls) were added to a 96 well plate, and 50 µl of the prepared bacteria was added, before a 4 h incubation (static, 37°C, 5% CO_2). 0 h and 4 h bacterial counts were measured by serial dilution and plating on to BHI agar before overnight incubation at 37°C (section 3.2.2.4).

E. coli concentration responses for BHI and elastase were measured as for *S. aureus* with appropriate media changes (LB broth and agar or RPMI 10 mM HEPES) and to quantify bacteria numbers spread plates were used due to the large colony size (section 3.2.2.5)

3.2.11.2. Evolved (no antibiotics) clone time course (Chapter 7)

Proteins and their corresponding controls were prepared to 10 µg/ml for LL-37 and HNP-1. Gentamycin was used as a positive control for bacterial killing at 50 µg/ml. Bacteria were prepared as for the concentration response assays (section 3.2.11.1), but using the 6 SH1000 clones evolved in no antibiotics for 20 transfers over 40 days (section 3.2.6.2). 1 well per time point was collected at 0, 2, 4, 8 h (and 24 h for LL-37) and plated by serial dilutions (section 3.2.2.4) to calculate bacterial numbers.

3.2.11.3. Antibiotic evolved clone sensitivity to LL-37 (Chapter 4 and 7)

Proteins and controls were prepared as above (section 3.2.11.1) but using the bacterial clones evolved from SH1000 in antibiotics (clarithromycin, doxycycline, flucloxacillin, linezolid, tobramycin) for 20 transfers over 40 days (section 3.2.6.2). Evolved clones were exposed to 10 µg/ml LL-37 or BSA control for 4 h before bacterial counts were measured by serial dilution (section 3.2.2.4).

3.2.11.4. pH of neutrophil protein (Chapter 7)

pH of neutrophil elastase was measured by pipetting 1 µl from 10 µg/ml elastase wells after 4 h incubation with *S. aureus* or *E. coli* from concentration response assays (section 3.2.11.1) onto each square on pH strips range pH 4.5-10 (Sigma-Aldrich P4536). pH was approximately identified by comparing colour change to the scale on for the pH strips.

3.2.12.Preparation and analysis of neutrophil products (Chapter 4 and 7)

3.2.12.1. Ethical approvals

Ethical approval was obtained for all work on human peripheral blood and patient samples. Approval for the work on neutrophils, plasma and serum had approval from the South Sheffield Research Ethics Committee. REC reference number 05/Q2305/4 and UOS 031773.

The **S**uperiority **T**rial **o**f **P**rotease inhibition in COVID-19 (STOP-COVID19) study[260] and sputum proteomic[261] analysis (Chapter 7) were approved by the South of Scotland Research Ethics Committee. STOP-COVID19 approval number 20/SS/0057, clinical trials registration number is ISRCTN30564012. All participants, patients or legal representatives gave written informed consent to participate. Inclusion criteria and patient demographics are in [260] (STOP-COVID19) and [261] (sputum proteomics).

3.2.12.2. Neutrophil isolation by Percoll™ density gradient centrifugation (Chapter 7)

The Percoll™ neutrophil isolation method is an adapted version of the isolation method described by Haslett et al.[262]. Neutrophil isolations were carried out by members of the Condliffe, Prince, Sabroe groups and by myself using blood drawn from healthy volunteers. The neutrophils were isolated by dextran sedimentation and plasma-Percoll™ density gradient centrifugation. All centrifugations were carried out in the MSE MISTRAL 3000i centrifuge.

40 ml venous blood from healthy volunteers via a 19G needle was added to sterile 3.8% tris-sodium citrate in a 50 ml falcon tube and gently mixed by inversion to prevent clotting. To remove the platelet rich plasma (PRP) blood was spun (330 x *g*, 20 mins, 20°C) and the upper

phase (PRP) was carefully removed. The PRP was centrifuged (912 x *g*, 20 mins, 20°C) and the platelets were discarded, leaving platelet poor plasma (PPP).

The lower cellular phase from the initial spin was added to 6 ml 6% dextran (pre-warmed to 37°C in water bath), and the volume was then made up to 50 ml with 0.9% sterile saline. The solution was gently mixed by inversion. The red blood cells (RBCs) were left to sediment for 20-30mins with the lid loose until a clear interface formed. The upper phase was then removed into a clean 50 ml falcon tube and centrifuged (230 x *g*, 6 mins, 20°C) to pellet the white blood cells (WBCs). WBCs were resuspended in 2 ml of PPP.

A discontinuous Percoll™ gradient was prepared in a 15 ml falcon tube overlaying the upper phase (840µl 90% Percoll™, 1.16 ml PPP) onto the lower phase (1.02 ml 90% Percoll™, 980µl PPP) with a Pasteur pipette. The WBCs were separated by laying them onto the top of the gradient, avoiding mixing the layers. The gradient was centrifuged (275 x *g*, 11min, 20°C, without braking) to yield 3 layers: top- peripheral blood mononuclear cells (PBMCs); middle- granulocytes; bottom- RBCs. The PBMCs were aspirated, followed by the granulocyte layer (neutrophils, eosinophils and basophils) into separate clean 50 ml falcon tubes and 10 ml PPP was added to each tube. The granulocyte volume was topped up to 50 ml with HBSS and 10µl was removed to count the cells under light microscopy using a haemocytometer. The calculated volume of granulocytes needed were centrifuged (511 x *g*, 6 mins, 20°C) and resuspended at the desired density. Preparations were routinely >95% neutrophils and were otherwise discarded.

3.2.12.3. Neutrophil supernatant generation (Chapter 7)

2.5 million neutrophils isolated using the Percoll isolation (no wash steps) (section 3.2.12.2) were resuspended in 1 ml RPMI 10% FBS or RPMI only (depending on the assay) at room temperature. Cells were then incubated (37°C, 5% CO_2) for 1 or 4 h in a 2 ml Eppendorf, which allowed cells to settle but not become adherent. 4h incubation time was used initially to allow maximum time for supernatant production before cells became apoptotic. After incubation, the neutrophils were centrifuged in a microfuge to pellet (300 x *g*, 2 mins). The supernatant was then removed. The supernatants were further centrifuged (2,000 x *g*, 3 mins), to ensure all cells were removed.

Heat-inactivated supernatants were produced by incubating 500 µl supernatant in a 1.5 ml Eppendorf for 10 mins at 95°C.

3.2.12.4. Neutrophil supernatants Time Course (Chapter 7)

Neutrophil supernatants produced by 1 h incubations in RPMI, heat inactivated supernatants or RPMI alone (section 3.2.12.3) were aliquoted into 96 well at 90 µl per well. *S. aureus* frozen stocks (section 3.2.2.6) were then defrosted at room temperature and centrifuged (2,000 x *g*, 6 mins). The bacterial pellet was resuspended in RPMI 10% FBS to give 1,125,000 CFU in 10 µl. 10 µl *S. aureus* were added to 90 µl neutrophil 'products' (derived from 225,000 neutrophils) giving a final neutrophil (product): bacteria of 1:5. Neutrophil products or controls were incubated with the *S. aureus* for 0.5, 1, 1.5, 2, 3, 4, 20, 24 h (37°C, 5% CO_2) with 3 wells per condition per time point. After incubation, bacteria numbers were measured by serial dilution (section 3.2.2.4). Bacteria counts were compared to bacteria grown in the corresponding media (RPMI 10% FBS) or heat inactivated supernatants.

3.2.12.5. Supernatant concentration response (Chapter 7)

Supernatants produced by 4 h incubation in RPMI 10% FBS (section 3.2.12.3) were diluted by 1-in-10 serial dilution in RPMI 10% FBS, with the lowest concentration 1-in-1000. 90 µl diluted supernatants were plated with 10 µl bacteria prepared as with previous experiments (section 3.2.12.4) with a 1:5 neutrophil (product): bacteria ratio based on 100% supernatant. Supernatants were incubated for 24 h with bacteria, before bacterial counts were assessed by serial dilution (section 3.2.2.4).

3.2.12.6. Antimicrobial activity of washes following neutrophil isolation (Chapter 7)

To understand the unexpectedly high level of killing by unstimulated neutrophils, assays were undertaken to assess the antimicrobial activity of residual plasma following the plasma-Percoll™ neutrophil isolation (section 3.2.12.2). The neutrophils were washed twice and the elute from these washes were tested for its antimicrobial activity.

Following the Percoll™ isolation (section 3.2.12.2), instead of resuspending neutrophils to the desired cell density, neutrophils were initially resuspended in 10 ml HBSS then centrifuged

(511 x *g*, 6 mins, 20°C), the supernatant was collected as the first wash. The neutrophils were then resuspended in 10 ml RPMI then centrifuged (511 x *g*, 6 mins, 20°C), this supernatant was collected as the second wash.

To assess the antimicrobial activity of the neutrophil washes, bacteria growth was compared in neutrophil washes or the HBSS/RPMI media. *S. aureus* frozen stocks (section 3.2.2.6) were defrosted at room temperature and centrifuged (2,000 x *g*, 6 mins). The bacteria pellet was resuspended in RPMI 10% FBS to give 1,125,000 CFU in 10 µl. 10µl *S. aureus* were added to 90 µl neutrophil wash material (derived from 225,000 neutrophils) giving a final neutrophil (product): bacteria of 1:5 before 4 h incubation (37°C, 5% CO_2). 0 h and 4 h bacterial counts were measured by serial dilution and plating on BHI agar (section 3.2.2.4).

3.2.12.7. Coomassie staining (Chapter 7)

Coomassie staining was used to visualise the protein content in neutrophil supernatants. A 15% or 10% SDS polyacrylamide gel was made by thoroughly mixing the reagents of the resolving gel (Table 3-6) and pipetting between a 1.5 mm spacer plate with a short plate up to ¾ of the plate by height. A layer of isopropanol (IPA) was added to level the gel before allowing the gel to set. Once set, the IPA was removed and the stacking gel reagents were combined before adding to the gel, filling the plate, before adding a Min-PROTEAN® 10-well comb and allowing the gel to set.

Table 3-6: 15% SDS polyacrylamide gel reagents

Reagents were thoroughly mixed in the following order. It was made and used on same day.

Reagent	15% resolving gel	10% resolving gel	Stacking gel
H_2O	3.48 ml	5.99 ml	2.79 ml
30% Acrylamide	7.52 ml	5.01 ml	826 µl
1.5M Tris buffer pH 8.8	3.8 ml	3.8 ml	-
0.5M Tris buffer pH6.8	-	-	1260 µl

20% SDS	75 µl	75 µl	25 µl
20% Ammonium persulfate	150 µl	150 µl	50 µl
N,N,N',N'-Tetramethylethylenediamine (TEMED)	6 µl	6 µl	5 µl

Samples were prepared by mixing 6.25 µl 4x Laemmli sample buffer (Table 3-1) to 18.75 µl sample before heating at 95°C for 5 mins. Samples were then quenched on ice for 5 mins. 10 µl BLUeye pre-stained protein ladder (Geneflow S6-0024) was added to the first lane of the gel. 20 µl sample (supernatant) was added to subsequent lanes. A media negative control and 1% FBS positive control was also prepared and run on the gel. Samples were run in 1 x running buffer (Table 3-1) at 100V.

The gel was fixed by mixing on Stuart mini orbital shaker SSM1, 72 rpm, with fixing solution (Table 3-1) for 10 mins. After removing the fixing solution, the gel was stained with Coomassie blue solution for 1 h. The gel was de-stained overnight in de-staining solution (Table 3-1). All solution compositions are in (Table 3-1). The gel was imaged on BIO-RAD Gel Doc™ EZ imager.

3.2.12.8. Neutrophil isolation by negative selection (Chapter 4 and 7)

Neutrophil isolation by antibody-coupled magnetic bead negative selection is a quicker isolation method, with fewer centrifugation steps (less potential for operator exposure), is less likely to activate the neutrophils[263] and gives neutrophil higher purity compared to the Percoll neutrophil isolation (section 3.2.12.2). Although not routinely used due to the expense of the required reagents, it was used when studying neutrophil function in the STOP-COVID19 clinical trial for intracellular survival assays (section 3.2.12.9).

20 ml venous blood was collected in 10 ml EDTA vacutainers (STOP-COVID19) or in a syringe (intracellular survival assay) and added to a 50 ml falcon tube (Falcon® 50 ml high clarity polypropylene centrifuge tube) with EDTA (ethylene-diaminetetraacetic acid) with final EDTA concentration 1.8 mg/ml to prevent clotting. Neutrophils were isolated using the EasySep™

isolation kit following the manufactures instructions, in a Category III laboratory when working with COVID-19 patient samples. All steps are carried out at room temperature (15-25°C). The EasySep™ isolation kit contains an antibody cocktail with magnetic particles. Unwanted cells (non-neutrophils) are targeted for removal with antibodies recognizing specific cell surface markers and separated by passing the cell-antibody cocktail over an Easy 50 EasySep™ magnet. Antibody-bound cells (all cells other than neutrophil) are retained by the magnet whilst neutrophils flow through. In detail, 20 ml of blood was added to a 50 ml falcon tube, the RapidSpheres™ were vortexed for 30 s before adding 1 ml to the blood, 1 ml of isolation cocktail was then added to the blood and it was mixed by inversion. The blood sample was left to stand for 5 mins. The blood was then topped up to approximately 50 ml with PBS (Ca^{2+} and Mg^{2+} free) with 1 mM EDTA and mixed by inversion, prior to placing on the magnet for 10 mins. Subsequently, the eluate (containing neutrophils) was carefully collected with a 25 ml stripette and transferred to a new 50 ml falcon tube, the old tube was discarded. The eluate was incubated on the magnet twice more, without any additional antibody cocktail, to ensure all non-neutrophil cells had been removed. 1 ml RapidSpheres™ was then added to the supernatant, mixed by inversion, left to stand from 5 mins, put in the magnet for 5 mins. The neutrophil supernatant was then removed with a 25 ml stripette into a new 50 ml falcon tube. The neutrophil supernatant was then place back in the magnet for a final 10 min incubation before the supernatant was removed with a 25 ml stripette and put in a new 50 ml falcon tube. The isolated neutrophils were then washed twice by pelleting the cells (300 x *g*, 6 mins), removing the supernatant and gently resuspending the cells in PBS (Ca^{2+} and Mg^{2+} free) twice. The cells could then be pelleted (300 x *g*, 6 mins) and resuspended in the desired media at the correct concentration.

3.2.12.9. Intracellular survival assay (Chapter 4)

The neutrophil intracellular survival assay is used to measure if bacteria can survive intracellularly, following phagocytosis, when all bacteria have been removed from the extracellular environment, within a set period (30mins). Timings of the assay is summarised in Figure 3-7.

S. aureus was grown in normoxia or hypoxia overnight by inoculating 1 colony in 10 ml equilibrated BHI broth in a 50 ml falcon tube (280 rpm). 1 ½ h before the end of the neutrophil

isolation, the optical density of the overnight cultures was measured, and 10 ml equilibrated BHI broth was inoculated with bacteria so $A_{600\,nm}$=0.05. Bacteria were grown for 2-2 ½ h until in mid-log phase where $A_{600\,nm}$ = 0.6-0.8. Optical density (600 nm) of mid-log cultures was measured before being centrifuged (2000 x *g*, 6 mins). The supernatant was removed, and cells were resuspended to achieve a starting MOI=5 using the following equation based of a previous calibration curve:

All steps are carried out within the normoxic and hypoxic chamber, timed so bacteria are ready at the same time as the neutrophils (Figure 3-7, 0 h). To test bacteria in different incubation oxygen tensions, all bacteria are first taken into hypoxia and added to the neutrophils, and then immediately after added to the normoxic neutrophils.

Neutrophils isolated by negative selection (section 3.2.12.8) were resuspended in RPMI 10% FBS ($5x10^6$ cells/ml, 2.5 million cells per oxygen tension) in normoxia and hypoxia. 90 µl of neutrophils were added to a 96 well plate and incubated for 1 h in normoxia or hypoxia to ensure at the correct oxygen tension. At 0 h 10 µl bacteria (prepared above) were added to the neutrophils and incubated for 30 mins giving an multiplicity of infection (MOI)=5. At 30 mins, 20 µg/ml lysostaphin was added to the intracellular survival cells. At the same time, cells and bacteria from 2 wells per condition were removed, by scrapping the well for 5 s, before pipetting up and down, and pooling the content of both wells is put into an Eppendorf. These cells and bacteria were washed twice in 200 µl ice cold PBS (400 x *g*, 4 mins), before resuspending in 200 µl ice-cold pH 11 alkaline water, vortex vigorously (2x10 s), sit for 5 mins, vortex vigorously (2x10 s). The vortex in the hypoxic chamber (Cole-Parmer™ Stuart™ Variable Speed Mini Vortex Mixer) and normoxic chamber (Vortex-Genie 2) were both set to their maximum speed. Lysates were then removed from the hypoxic chamber. Hypoxic and normoxic lysates were stored on ice before plating. After the intracellular survival cells have a further 30 mins incubation, cells and bacteria were removed and washed using the same method above. Bacteria counts were measured by serial dilution (section 3.2.2.4) plated on BHI agar and incubated overnight (37°C).

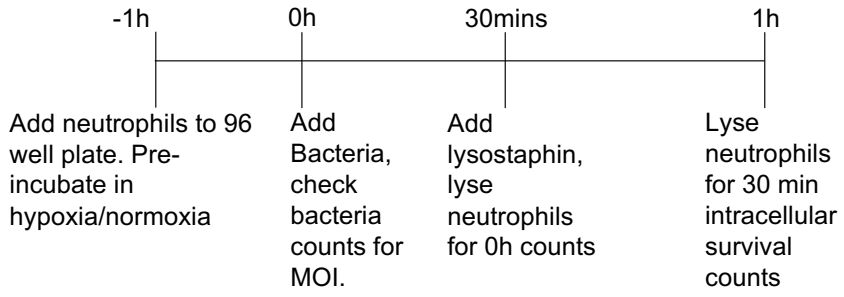

Figure 3-7: Timeline for intracellular survival assay

Neutrophils are pre-incubated in hypoxia or normoxia for 1 h, before mid-log bacteria are added (MOI=5) at 0 h. Following a 30 min co-incubation, lysostaphin (20 µg/ml) is added to kill extracellular bacteria. Bacteria is collected at 0 h and plated to check the starting MOI. At 30 mins and 1h neutrophils and bacteria are removed from wells by scrapping and pipetting up and down, before neutrophils are washed twice in PBS before lysis in pH 11 alkaline water and plating lysates on BHI agar to measure surviving bacteria.

3.2.12.10. STOP-COVID19 CD63 surface marker (Chapter 7)

Eppendorf tubes were prepared for labelling neutrophil surface markers. 2 Eppendorf tubes were prepared for the unlabelled control and CD63 condition. In each Eppendorf tube 100 µl of 2% BSA solution in PBS was added, 10 µl PE-CD63 antibody was then added to the CD63 tube. These Eppendorf's were then covered in foil, to protect from light, and stored in the fridge before use (no more than 6 h). Of note, other surface markers were also studied for the trial but only the CD63 data are relevant to the work in this thesis and presented herein.

20 ml EDTA blood was obtained by clinical research nurses from patients enrolled in the STOP-COVID trial (all patients hospitalised with COVID-19 requiring oxygen and treated with study drug brensocatib or placebo in a double-blind study design). Neutrophil were isolated from by magnetic negative selection (section 3.2.12.8) and resuspended in PBS to achieve final concentration $5x10^6$ cells/ml. 100 µl suspension ($0.5x10^6$ neutrophils) were added to each of the pre-prepared unlabelled and CD63 Eppendorf tubes. Samples were covered in foil and incubated in the fridge (4°C) for 30 mins. Following incubation, 300 µl 2% BSA in PBS was added to each tube, cells were then centrifuged (300 *x g*, 5mins). The supernatant was removed and cells were resuspended in 500µl PBS to wash the cells before centrifuging again (300 x *g*, 5 mins). Pelleted cells were then re-suspended in 250µl 4% PFA at 4°C for 90 mins to fix. The fixed cells were centrifuged (300 x *g*, 5 mins), PFA was removed by aspiration, cells resuspended were in 500 µl PBS to wash prior to a final centrifugation (300 x *g*, 5 mins). Cells were then resuspended in 500 µl 2% BSA in PBS, before transferring the cells to 5 ml round bottom tubes to be analysed by flow cytometry.

3.2.12.11. Flow cytometry analysis (Chapter 7)

Flow cytometry samples (section 3.2.12.10) were analysed by BD LSRFortessa™ Cell Analyzer (Dundee) or BD® LSR II Flow Cytometer (Sheffield). As samples were run on different machines it was necessary for data to be normalised to an unlabelled control (prepared as above but without antibody labelling). 10,000 events were measured on the flow cytometers, with the laser set at 575 nm. Analysis was carried out on FlowJo (version 10). Cells expressing CD63 were selected by: gating neutrophils by forward and side scatter (Figure 3-8A); gating single cells by forward scattered area and signal height (Figure 3-8B). The number of cells expressing

CD63 by selecting cells with PE levels above that of unlabelled cells was measured (Figure 3-8C). An example of cell numbers after each step are shown in Figure 3-8D. The geometric mean of single cells fluorescence at 575 nm was measured, with the mean of CD63 labelled cells normalised to unlabelled cells.

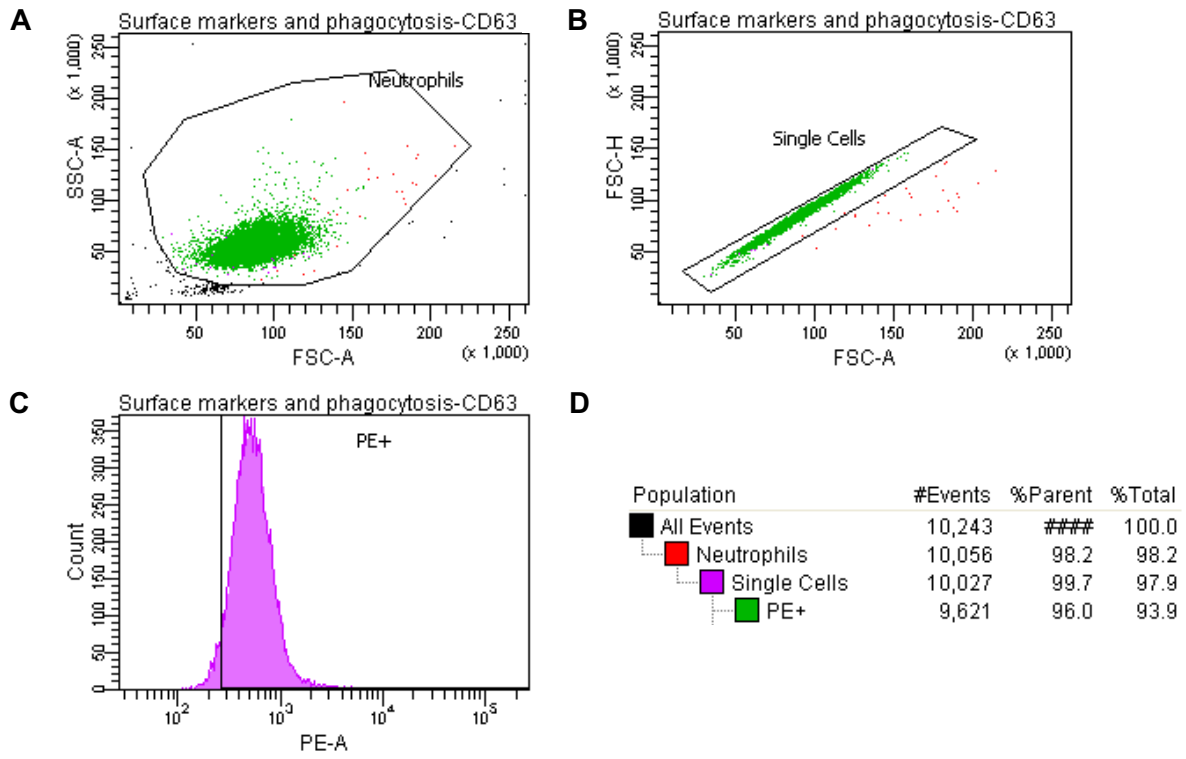

Figure 3-8: Example CD63 surface marker flow cytometry analysis

Example of gating from cells for analysis of surface marker CD63 after CD63-PE antibody has bound to neutrophils. A) The neutrophils population are selected from other cells by forward scatter and side scatter, B) single cells are selected by linear relationship between forward scattered area and signal height, C) cells with florescent CD63-PE antibody bound can be identified by gating and cells with florescence above the unlabelled cells (black vertical line). D) Shows the number of cells in each group.

3.2.13.Proteomic analysis (Chapter 7)

Proteomic analysis was carried out as described in full in [261]. The sputum protein profiling was performed by other members of the group by means of a label-free shotgun proteomic workflow with a nanoflow liquid chromatography system (Agilent 1200; Agilent) linking to an Orbitrap mass spectrometer (LTQ-Orbitrap; Thermo Scientific). Protein identification and label- free quantification were performed by using MaxQuant version 1.4.1.2 (Max Planck Institute of Biochemistry) against the UniProt/ human database (version 2019-09-29; UniProt Consortium). False discovery rate for protein identification was set to 1% at peptide-spectrum match level.

Proteomic statistical analysis was carried out in R version 4.0.3. Principal component analysis (PCA) is a method whereby a single line of best fit is added to a dataset, minimising the averaged squared distances for all the data set, while maintaining the variance within data[264]. The strongest contributing factors (highest variance) in each dimension can be seen as a predictor of where the difference between the samples lies. This is a good technique to detect correlations which can then be tested further. The PCA dimensional reduction of 693 protein abundances per patient (n=55 patients) was conducted by using 'prcomp' (in default R 'stats' package). Visualization of PCAs was performed through R package 'ggbiplot' with ellipses around groupings representing 68% CIs. The top 15 loading variables were shown as the proteins with the highest level of variation within the model.

From the PCA it is possible to see where differences may lie within a dataset. Volcano plots were then used to visualise proteins significantly changed between 2 groups. In the generated Volcano plot, significant differences in relative abundance of proteins between the groups were calculated using the Student t test with Benjamini and Hochberg correction for multiple comparisons (R package 'rstatix', 'stats') and the mean $\log_2$(fold change) was calculated using basic function in the R base package to show the direction (up or down regulated) and extent of any change in expression. These parameters were visualised within the volcano plot constructed in R (package 'ggplot2').

3.2.14.Whole genome sequencing and analysis

Whole genome sequences using 2x250 paired-end Illumina sequencing was outsourced and undertaken by MicrobeNG (microbesng.com). The genomes were compared to the reference genome NCTC 8325, and the bacteria's ancestor (SH1000 or SH1000_TetR) where appropriate, to identify genetic changes. The forwards and backwards reads were then provided as trimmed.fastq.gz data files for analysis.

3.2.14.1. Bacterial preparation

S. aureus samples were prepared as specified by MicrobesNG. Briefly *S. aureus* clones for sequencing were streaked onto BHI agar (section 3.2.2.1) (containing antibiotic if the strain carried a resistance marker). For clones sequenced in (Chapter 5 and 6) a single colony was picked using a sterile inoculation loop and mixed in 100µl PBS. This was spread onto a BHI agar plate to cover 1/3 of the area and then streaked out in the other 2/3 to ensure the purity of the sample. All colonies were collected with a sterile inoculation loop and mixed in the appropriate tubes purchased from MicrobesNG.

Over this PhD the MicrobesNG changed their required method for bacterial preparation before they isolated the DNA and carried out sequencing. Therefore, clones sent for sequencing in Chapter 4 were streaked out to obtain a single colony. 1 colony was picked using a sterile inoculation loop and mixed in 200 µl PBS. 100 µl was then transferred into 15 ml BHI broth in a 50 ml falcon tube and the bacteria were grown to mid log phase ($A_{600\,nm}$=0.6-1) (37°C, 5% CO_2, 280 rpm). Bacteria was pelleted at 2000 g, 6 mins, resuspended in 1 ml PBS and transferred into a 1.5 ml Eppendorf before pelleting (2000 x *g*, 2 mins). Bacteria were resuspending in 500 µl RNA/DNA SHIELD buffer before being sent to MicrobesNG. The remaining 100 µl of bacteria, PBS suspending was streaked out onto BHI agar to check for purity.

To reduce bias, the colony selected for sequencing was pre-selected by marking the streak plate with a cross prior to incubation. The colony closest to the cross was picked for sequencing. A glycerol stock (section 3.2.2.3) from the same clone was generated for further analysis.

3.2.14.2. Sequence analysis

All sequence analysis was carried out using the data supplied by MicrobesNG. MicrobesNG carried out quality control of the data before the analysis was carried out including: mean genome coverage; number of reads per genome; total genome length and GC content. Basic taxomic description was also provided which confirmed *S. aureus* as the most frequent species for all genomes. MicrobesNG provided me with forward and backward trimmed.fastq files which were then processed and analysed for any genetic variants compared to reference sequences. The reference genome NCTC 8325 (genome accession number: CP000253) was used as the closest available annotated genome for mapping the sequencing reads. Bioinformatics analysis was used to detect mutations: Burrows-Wheeler Aligner aligned short-reads to an annotated NCTC 8325 reference genome, Single nucleotide polymorphisms (SNPs) and small indel variants were identified by GATK Haplotype Caller, gene information was annotated using SNPeff. Quality of the called variants were confirmed by frequency of alternative allele (>80% of reads match alternative), and coverage (>30 reads per bp). Analysis of coverage depth in R was used to identify large genetic variation, including duplication events and deletions over 100 bp. Larger genetic variations, including deletions over 100bp and duplication events, were identified by analysing changes in coverage depth in R version 4.0.3. The Breseq pipeline[265] was used to check for additional variants. Integrative Genomics Viewer (IGV) was used to visually verify all variants[266]. Genomic rearrangements were not investigated as this would have required long read sequencing[267].

For clones in Chapter 6 the *TetL* insertion was interrogated through extraction of unmapped reads before de novo assembly using SPAdes[268]. Mutations were checked for using the sequence analysis above with SH1000_TetR SPAdes assembly of the resistance gene as the reference. Change in *TetL* coverage was determined by comparison of mean coverage within the *TetL* gene to the mean coverage of the corresponding genome. Additional insertion sites were checked for through extraction and sorting of unmapped reads (from initial pipeline) where at least 1 read aligns to SH1000_TetR SPAdes assembly using Burrows-Wheeler Aligner[269] followed by SPAdes assembly to compile contigs to identify insertion sites by ncbi BLAST[270] .

3.2.15.Mutation structural analysis (Chapter 6)

Structural predictions were carried out using Phyre2[271] which compares the amino-acid sequence of the mutant protein being studied to similar structures in the protein data bank[272]. The resulting structures were analysed using PyMOL[273] where the prediction was structurally aligned to the closed protein structure (DNA gyrase B: CryoEM structure from *E. coli* 6rkw.pdb[274]; rluD-like protein: Xray-diffraction model from *E. coli* 2ist.pdb (to be published)).

3.2.16.Statistical analysis

All statistical analysis was carried out in R version 4.0.3 (R Foundation for Statistical Computing). Prior to statistical analysis, normality of data was tested with Shapiro-wilk test. Statistical analysis of parametric data was carried out by paired T-test for 2 groups of unpaired data; analysis of variance models (ANOVA) was used to compare data with 2 or more groups followed by Tukey's multiple comparisons of evolution phenotype data. When there were 3 variables in the ANOVA model, the nested approach prevents the need to use repeated statistical testing increasing the likelihood of type I statistical error. Non-parametric data were analysed by Kruskal-Wallis rank sum test with Wilcoxon rank sum post-hoc testing and Benjamini-Hochberg correction for multiple comparisons.

In data with repeated measured (evolution data in Chapter 5, STOP-COVID19 CD63 surface marker expression in Chapter 7) a linear mixed effects model (r package 'lme4') was used to test for interaction between 3 factors (fixed effects), and specifying the random effects (population or patient number). The data in the evolution experiment (chapter 5), was box cox transformed prior to putting in a linear mixed effects model to meet underlying test assumptions of the model (linearity of the data; homogeneity of variance; normal distribution of the residuals of the model). p values were derived from the linear mixed effects model with a type III ANOVA with Satterthwaite's method to predict the degrees of freedom within the model.[275]

Phylogenetic distances were calculated using a Jaccards index based on presence or absence of mutations within a gene or *TetL* duplication followed by a permutational ANOVA (package 'vegan') (used for calculating differences between distance matrices). An unrooted neighbour

joining phylogenetic tree was constructed using the Jaccards index distances using the R package ‘ggtree’.

Data presented as box and whisker plots (Figure 3-9) present median, 25/75% quantile (upper and lower hinge), smallest/ largest observation within the 1.5 inter quantile range are shown as the upper/lower hinge. The range of the data beyond the 1.5 inter quantile range is shown as filled circles, this is not a data point on the graph.

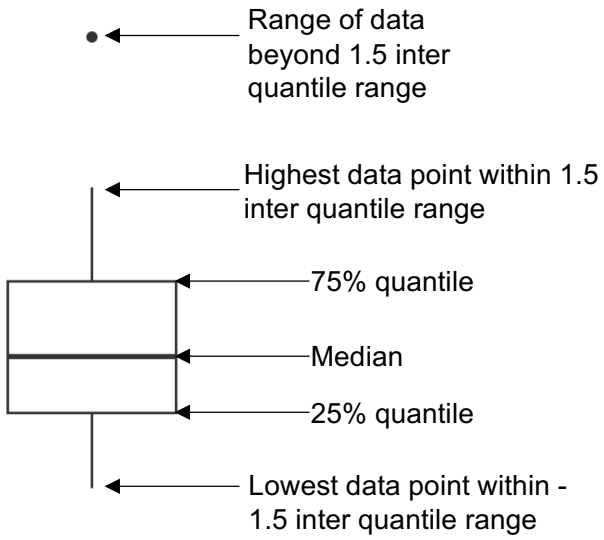

Figure 3-9: Box and whisker plot

Example of box and whisker plot to show the distribution of data. Median is the central line, upper and lower hinge show the 25/75% quantile, whiskers show the smallest/largest data point within the +/- 1.5 inter quantile range, filled circle show range of data beyond the whiskers.

4 The Evolution of Resistance and Cross-Resistance to Antibiotics

4.1 Introduction

The evolution of antibiotic resistance is a major challenge for human and animal health. Antibiotic resistance can be acquired through chromosomal mutations, horizontal gene transfer, or a combination of both[276-278]. *S. aureus* is a highly adaptable pathogen and has developed resistance against every antibiotic used to treat it[3].

4.1.1 Antibiotics used to treat *Staphylococcus aureus*

A range of antibiotics are used to treat *S. aureus* infections, chosen based on efficacy, side effects, cost, allergy status plus current and future risk of resistance[279,280] with choices often specified by locally applicable guidelines. Commonly used anti-staphylococcal antibiotics (Table 4-1) include flucloxacillin, doxycycline and clarithromycin. Vancomycin is frequently used to treat severe MRSA infections but requires intravenous administration and has the potential for severe toxicity. Daptomycin is sometimes used to treat MRSA or severe MSSA infections in patients with penicillin allergy[281]. Oral linezolid is also used to treat severe *S. aureus* infections including MRSA but again confers a substantial risk of side effects[282]. Use of daptomycin and linezolid is generally restricted in the UK. Nebulised tobramycin is available for patients with cystic fibrosis with *Pseudomonas* infections[283] and is also occasionally used to treat chronic respiratory *S. aureus* airway colonisation/infection in bronchiectasis (personal communication, Professor Alison Condliffe). Many patients with cystic fibrosis are co-infected with *P. aeruginosa* and *S. aureus*[284] so in this setting *S. aureus* will also be exposed to long term tobramycin. These agents alone represent 6 classes of antibiotics targeting a range of cellular functions, with flucloxacillin (a penicillin) targeting the cross linking within the cell wall, daptomycin (a cyclic lipopeptide) forming pores in the cell wall, and the rest with targets within the ribosome: clarithromycin (a macrolide) and linezolid (an oxazolidinone) the 50s ribosomal subunit, and doxycycline (a tetracycline) and tobramycin (an aminoglycoside) the 30S ribosomal subunit[168]. Despite targeting different components within the ribosome, the shared target of the ribosome increases the risk of cross antibiotic resistance occurring[285-287]. Other antibiotics used in certain situations include the lincosamide antibiotic clindamycin

(good tissue penetration but has a high risk of causing *Clostridium difficile* overgrowth)[288], and the phenicol antibiotic chloramphenicol (risk of bone marrow suppression)[289].

4.1.2 Resistance mechanisms for antistaphylococcal antibiotics

Resistance mechanisms have evolved against all of these clinical antibiotics and the main mechanisms are summarised in Table 4-1.

***Table 4-1: Antibiotics to treat* S. aureus infections**

Antibiotics to treat S. aureus *and non-exhaustive list of genes involved in antibiotic resistance, with mutations in chromosomal genes causing resistance in bold. Examples of use in clinical infections from NICE guidelines.*

Antibiotic	**Class**	**Clinical Infections**	**Gene**	**Resistance Mechanism[290]**	**Refs.**
Clarithromycin	Macrolide	Boils and carbuncles; dental abscess; COPD; skin ulcers. Useful in penicillin allergy.	*ermA/B/C*	23S rRNA methyltransferase	291-296
			msrA/B	Ribosomal protection	
			ereA/B	Esterase	
			mefE/A	Efflux pump	
			rplD	**50S ribosomal protein L4**	
			rplV	**50S ribosomal protein L22**	
			mphA/B	Phosphorylates macrolides	

Daptomycin	Cyclic lipopeptides	Complicated skin and soft-tissue infections caused by Gram-positive bacteria	***mprF***	**Modifies charge of phosphatidylglycerol**	188,297,298
			yycG	**Controls peptidoglycan metabolism**	
			rpoB/C	**β and β' subunits of RNA polymerase**	
Doxycycline	Tetracycline	COPD exacerbations; skin ulcers; skin infections	*tetK/L*	Efflux pump	2,292,293,299,300
			tetO/M	Ribosome protection	
			tetX	Hydroxylates antibiotic	
			norB	Efflux Pump	
			rpsJ	**30S ribosomal subunit protein S10**	
Flucloxacillin	β-lactam	Boils and carbuncles; skin ulcer; diabetic foot infection	*mecA*	Penicillin-binding protein 2a	291,293,301,302
			PBP1/2	**Point mutations in penicillin binding proteins**	
Linezolid	Oxazolidinones	Skin ulcers, hospital	***rplD***	**50S ribosomal protein L4**	293,301,303-305

		acquired pneumonia, moderate or severe diabetic foot infection*	***rplC***	**50S ribosomal protein L3**	
			Cfr	23S rRNA methyltransferase	
Tobramycin	Aminoglycoside	Lung infections in patients with cystic fibrosis, endocarditis.	***rpsL***	**Ribosomal protein S12**	178,306-308
			fusA1	**Elongation factor G**	
			gyrA	**DNA gyrase A**	
			armA	16S rRNA methyltransferase	
			rmtC/D/E/F/G/H	16S rRNA methyltransferase	
			aadA	aminoglycoside nucleotidyltransferase	

** "Antibiotics to be added if methicillin-resistant Staphylococcus aureus infection is suspected or confirmed- if vancomycin cannot be used; specialist advice only"*

The resistance mechanisms outlined in Table 4-1 can be either horizontally acquired (usually by plasmid transfer) or arise by chromosomal mutations. Mutations often modify the antibiotic target. The frequency of chromosomal mutations and horizontal elements differ for each antibiotic. In vitro studies frequently identify chromosomal mutations associated with resistance.

Mechanisms of resistance to the macrolide erythromycin has been more thoroughly studied than the more recent derivative, clarithromycin. The most frequently described mechanism of macrolide resistance, in *S. aureus* and other organisms, is through horizontally acquired *erm* genes encoding 23S rRNA methylases, which modify the 50S ribosomal subunit to prevent clarithromycin (or other macrolides) from target binding[295]. Chromosomal mutations in ribosomal genes are also able to cause resistance against macrolides including through mutations within the 23S rRNA binding site. Spontaneous mutations in 23S rRNA arise at low frequency in antibiotic-free settings, for example conferring clarithromycin resistance in *Helicobacter pylori*[309]. Mutations in the 50S ribosomal proteins L4 and L22 reduce binding of macrolides[310,311] with mutations in L22 changing the surface charge of the polypeptide exit tunnel[312]. Resistance to macrolides is easily acquired, with in vitro evolution experiments under macrolide selection reporting resistance associated with point mutations in L4, L22 and 23S rRNA in *Streptococcus pneumoniae*[311]. Similar ribosomal point mutations have been observed in clinical isolates of multiple species including *S. aureus*[313,314], *H. pylori*[315], *E. coli*[316].

Chromosomal mutations in the 50S ribosomal subunit L3, L4 and L22 have been shown to confer resistance to linezolid[304] in many species including *S. aureus, S. epidermidis, Enterococcus faecalis*[305,317]. In vitro testing of linezolid, before completion of clinical trials, found one strain of *E. faecalis* developed low level resistance to linezolid when passaged on a spiral gradient plate of linezolid for 5 days, although the mechanism for resistance was not described. During pre-clinical testing, no spontaneous mutants to linezolid or resistant strains were detected against *S. aureus*[318]. A recent in vitro selection assay, with 3 linezolid-resistance selection steps, found mutations in L3 conferred low level resistance to *S. aureus* by altering the linezolid binding site. Horizontally acquired genes *cfr* (23 rRNA methylation), *optrA* (ribosomal protection) and *poxtA* (ribosomal protection) also cause resistance to linezolid although are rare in *S. aureus* isolates from human infections[319,320]. Linezolid

resistance is uncommon[321], in part due to the restricted use, but has been found in hospitalised patients with no prior exposure to linezolid, with the source of resistance unknown[322].

Resistance to tetracyclines such as doxycycline is predominantly mediated by horizontally acquired genes. There are 63 known horizontally acquired resistance genes against tetracycline, which drive resistance through efflux (36 genes), ribosomal protection (13 genes), enzymatic inactivation (13 genes) and 1 by an unknown mechanism (*tetU*)[323] (section 1.3.1.1). In contrast, chromosomal point mutations causing resistance to doxycycline are challenging to acquire. An experimental evolution experiment by Narendrakumar et al.[324] of *Vibrio cholerae* in increasing concentrations of doxycycline with 12 h transfers, took ~210 days to establish resistance at the MIC breakpoint. Resistant *V. cholerae* clones from this experiment had mutations in 30S ribosomal protein S10 (*rspJ)*, the Gram-negative 2-component system CpxA/CpxR (*cpxA*) and hypothetical proteins[324]. *rpsJ* causes resistance to tetracyclines by altering interactions of tetracyclines with the 16S rRNA region[300]. *rspJ* variants have been found to decrease susceptibility of *S. aureus*, *A. baumannii,* and *E. coli* to tetracyclines in experimental evolution experiments[325].

Aminoglycoside (tobramycin) resistance is mainly driven by horizontally acquired aminoglycoside-modifying enzymes. There are over 100 aminoglycoside-modifying enzymes which inactivate aminoglycosides by: acetylation of aminoglycosides; phosphorylation of hydroxyl groups on aminoglycosides or transferring AMP from an ATP donor to hydroxyl groups on aminoglycosides[178]. *fusA1* encodes elongation factor G, which catalyses translocation within the ribosome and ribosome recycling. Chromosomal mutations in *fusA1* can confer resistance to tobramycin[308], inhibiting bacterial growth by preventing ribosomal recycling[326]. *fus1A* mutations have been found in *P. aeruginosa* clinical isolates and following in vitro evolution of *P. aeruginosa* and *A. baumannii*[308,326].

Resistance against daptomycin in *S. aureus* is predominantly due to mutations associated with the cell wall, both in clinical isolates and in clones from evolution experiments[327]. These mutations target genes including: *mprF* which alters the phospholipid composition of the cell membrane[328,329]; *yycG* which changes expression of the 2-component system which regulating cell wall synthesis and homeostasis by influencing the expression of 163

genes[188,330]; and *rpoB* and *rpoC* which encode β and β' subunits of RNA polymerase[328,331,332]. Resistance via horizontal elements is rare, although it is present in Vancomycin-resistant enterococci[333].

Resistance to β-lactams is typically conferred by horizontally acquired elements. The horizontally acquired *mecA* encodes PBP2a, causing resistance by bypassing the β-lactam target PBP2, which cross links the cell wall[302]. β-lactamases cause resistance to β-lactams by cleaving the β-lactam ring. Flucloxacillin is resistant to β-lactamases, as it was designed with the β-lactam ring protected by steric hinderance[169,334]. Small increases in resistance to β-lactams can occur through point mutations in PBP-1, PBP-2 and through increases in expression of PBP-4[335].

There is thus varied understanding of anti-staphylococcal resistance mechanisms against the commonly used antibiotics flucloxacillin, clarithromycin, doxycycline, daptomycin, linezolid, tobramycin. Many resistance mechanisms have been studied in other organisms and/or in derivatives or antibiotics from the same class, meaning chromosomal mutations in *S. aureus* conferring resistance against some antibiotics are likely to have been missed. Overall, chromosomal mutations in ribosomal proteins are important for resistance against macrolides and linezolid, with chromosomal mutations conferring resistance to daptomycin associated with cell wall synthesis and RNA polymerase. Horizontally acquired elements appear to be the predominant drivers of resistance against tetracyclines, aminoglycosides and β-lactams, although horizontally acquired elements have been attributed to resistance against all these anti-staphylococcal antibiotics. It is unknown if the frequency of chromosomal mutations, against commonly used antistaphylococcal antibiotics, influences the acquisition or persistence of horizontal resistance determinants.

Horizontal gene transfer can lead to multi-drug resistance if a gene is acquired which confers resistance to multiple antibiotics[336]. For *S. aureus,* one multi-drug resistance element is the SCC*mecII* horizontally acquired resistance cassette. SCC*mecII* contains *ermA* (macrolide and lincosamide resistance, 23S rRNA methyltransferase) and *mecA* (methicillin resistance gene, PBP2a)[3,336]. Multi-drug resistance can also be conferred by a single gene. The chromosomally encoded efflux pump MepA confers resistance to multiple compounds including the

antibiotics tigecycline (glycylcycline), ciprofloxacin and norfloxacin (fluoroquinolones) by removing the antibiotics from the cell[337].

Importantly, chromosomal resistance mutations can arise through spontaneous mutations in an antibiotic-free environment[278]. Additionally, sub-MIC antibiotic concentrations, typical of those found in hospital sewage outlets, water and soil, as well as present in the setting of inadequate dosing/poor compliance/poor tissue penetration, can select for chromosomal mutations which can cause high level resistance[277].

4.1.3 Antibiotic cross resistance

When bacteria acquire mutations which confer resistance against one antibiotic, cross-resistance or collateral-sensitivity against another antibiotic can develop[286,336]. Cross-resistance occurs when one mutation results in resistance against multiple antibiotics through a shared mechanism. Collateral sensitivity is where increased resistance to one antibiotic causes decreased resistance to another antibiotic. A systematic study of *E. coli* antibiotic cross resistance networks by Lázár, et al.[286], which selected for resistance against 12 antibiotics individually and then tested these evolved clones for change in susceptibility to the other 11 antibiotics, found changes in sensitivity of clones to other antibiotics in 52% of antibiotic pairs, including across different functional classes of antibiotics (with cross-resistance between targets of protein synthesis and the cell wall). The only functional class in this *E. coli* cross-resistance network without interactions with other classes was the aminoglycosides[286]. Interestingly, in another study in *E. coli*, aminoglycoside resistance drove 44% of the collateral sensitivity interactions between clones evolved against 24 antibiotics, associated with decreased activity of an efflux pump; collateral sensitivity was not found between the same antibiotic class[338]. Similarly, other studies of *E. coli* evolved against 23 or 15 antibiotics found collateral sensitivity or cross-resistance, including interactions between different classes of antibiotics[287,339]. The relevance of these in vitro studies is supported by an analysis of 448,563 antimicrobial susceptibility tests of clinical bacterial isolates (172,139 *E. coli*, 76,620 *S. aureus*), which found 240 antibiotic resistance pairs for *E. coli* and 56 antibiotic resistance pairs for *S. aureus*. In the *S. aureus* isolates the strongest interacting antibiotic resistance pairs were between oxacillin/ clindamycin and tetracycline/ levofloxacin[340]. The genetic

determinants of cross-resistance can be hard to determine. In *S. aureus,* Evgrafov et al.[191] tested for cross resistance between clones evolved in vitro against six individual antibiotics in parallel, plus 5 drug pairs, and found cross-resistance between ciprofloxacin (targets DNA synthesis) and ampicillin (targets cell wall), ciprofloxacin and doxycycline (target 30S ribosome), doxycycline and erythromycin (target 50S ribosome), erythromycin and fusidic acid (target protein synthesis), fusidic acid and amikacin (target 30S ribosome) plus collateral sensitivity between fusidic acid and erythromycin. This study carried out whole genome sequencing on clones with high-level resistance and identified commonly known resistance targets, but was unable to show which mutations were driving cross-resistance[191]. Another study evolved *S. aureus* and five other bacterial species in cefepime (target cell wall synthesis), gentamicin (target 30S ribosome), meropenem (target cell wall synthesis), and tetracycline. This study showed *S. aureus* collateral sensitivity to ciprofloxacin for all 4 antibiotics. Again, only the most resistant clones were sequenced with individal target mutations identified, but no genes were associated with collateral sensitivity or cross-resistance[341]. Some studies have also shown patterns of cross-resistance for *S. aureus* and identified responsible genes, including: trimethoprim collateral sensitivity to ciprofloxacin mediated by mutations in *rsbW* (inhibits the stress-response regulator sigma factor B)[243], and vancomycin cross-resistance to daptomycin via *mprF* mutations[241,342,343]. Considering evidence of antibiotic cross-resistance and collateral sensitivity in *S. aureus*, a systematic study of antibiotic cross-resistance between clinically utilised antibiotics, exploring genetic mechanisms including those in low resistance clones, is justified.

4.1.4 Bacterial lifestyle changes altering antibiotic sensitivity

Bacterial lifestyle changes (i.e. biofilm and small colony variants formation) can also alter *S. aureus* antibiotic sensitivity. Lifestyle changes are often reversible and may be governed by genetic mutations (sometimes selected for by antibiotics) or by alterations in gene expression which can be triggered by environmental factors[344]. Switching to a slow growing phenotype often increases persistence, for example small colony variants (SCVs) exhibit slower growth rates as well as reduced pigmentation and haemolysis. Mutations in biosynthetic pathways have been linked to this SCV phenotype, although there are multiple SCVs where no genetic determinants have yet been identified. Some SCVs can easily revert to their parental

phenotype, while others retain the SCV phenotype with serial passage. SCVs have been associated with clinical infections, for example prosthesis-associated infections[345]. Changing to a SCV lifestyle is commonly associated with antibiotic resistance including resistance against aminoglycosides and vancomycin[346-348]. I wished to further explore the contribution of SCVs in the development of antibiotic resistance in different classes of antibiotics.

To compare the resistance evolvability of *S. aureus* SH1000 against a range of clinical antibiotics I first quantified the MIC of ancestral SH1000 against each antibiotic. I then quantified the spontaneous mutation rate for resistance in an antibiotic free setting and the resistance level of the spontaneous mutants for each antibiotic. Next, I performed a selection experiment with gradually increasing antibiotic doses to test if SH1000 could evolve higher levels of resistance against these antibiotics. I measured the growth and MIC of clones evolved in antibiotics to see how they were affected by antibiotic selection. Whole genome sequencing of clones tested the genetic divergence of clones and number of mutations based on antibiotic selection. Comparison of sequencing and MIC data for each clone identified genes associated with increased antibiotic resistance. Finally, the MIC was measured for each clone in the other antibiotics, allowing patterns of cross-resistance to be identified and mutations associated with cross resistance to be interrogated.

4.2 Hypothesis and aims

In this chapter I have tested the hypothesis:

Antibiotic resistance will evolve against clinically used anti-staphylococcal antibiotics, with overlapping antibiotic targets facilitating cross-resistance.

The aims of the work in this section are:

- To quantify *S. aureus* SH1000 sensitivity to antibiotics commonly used in clinical practise
- To test the ability of SH1000 to evolve resistance by spontaneous mutations against a range of antibiotics
- To explore changes in growth, antibiotic sensitivity and mutations selected for by prolonged antibiotic exposure

- To test the propensity for antibiotic cross-resistance to occur and test whether this is more likely for antibiotics that share similar cellular targets

4.3 Results

4.3.1 Sensitivity of *S. aureus* to antibiotics

Depending on the site and characteristics of a *S. aureus* infection, a range of antibiotics can be used alone, in combination or sequentially[169]. I sought to further understand the development of resistance in the presence and absence of antibiotics representing several different classes. To do this I initially investigated 6 antibiotics from different classes used to treat *S. aureus* infections. These were clarithromycin (macrolide), daptomycin (lipopeptide), doxycycline (tetracycline), flucloxacillin (β-lactam), linezolid (oxazolidinone) and tobramycin (aminoglycoside).

Before selecting for resistance, a baseline sensitivity of the ancestor (*S. aureus* SH1000) to each antibiotic was determined. The antibiotic breakpoint was established by exposing SH1000 to a gradient of each of the 6 antibiotics for 20 h (clarithromycin, 0.125-128 μg/ml; daptomycin, 0.0625-64 μg/ml; doxycycline, 0.125-128 μg/ml; flucloxacillin, 0.00781-8 μg/ml; linezolid, 0.25-256 μg/ml; tobramycin, 0.0625-64 μg/ml). At 20 h bacterial optical density (Figure 4-1A) and breakpoints (Figure 4-1B) were measured. Unexpectedly, it was not possible to measure a breakpoint for daptomycin as DMSO, the antibiotic solute, had equivalent killing to daptomycin at all concentrations used (data not shown). As I was unable to establish an MIC daptomycin was not taken forward.

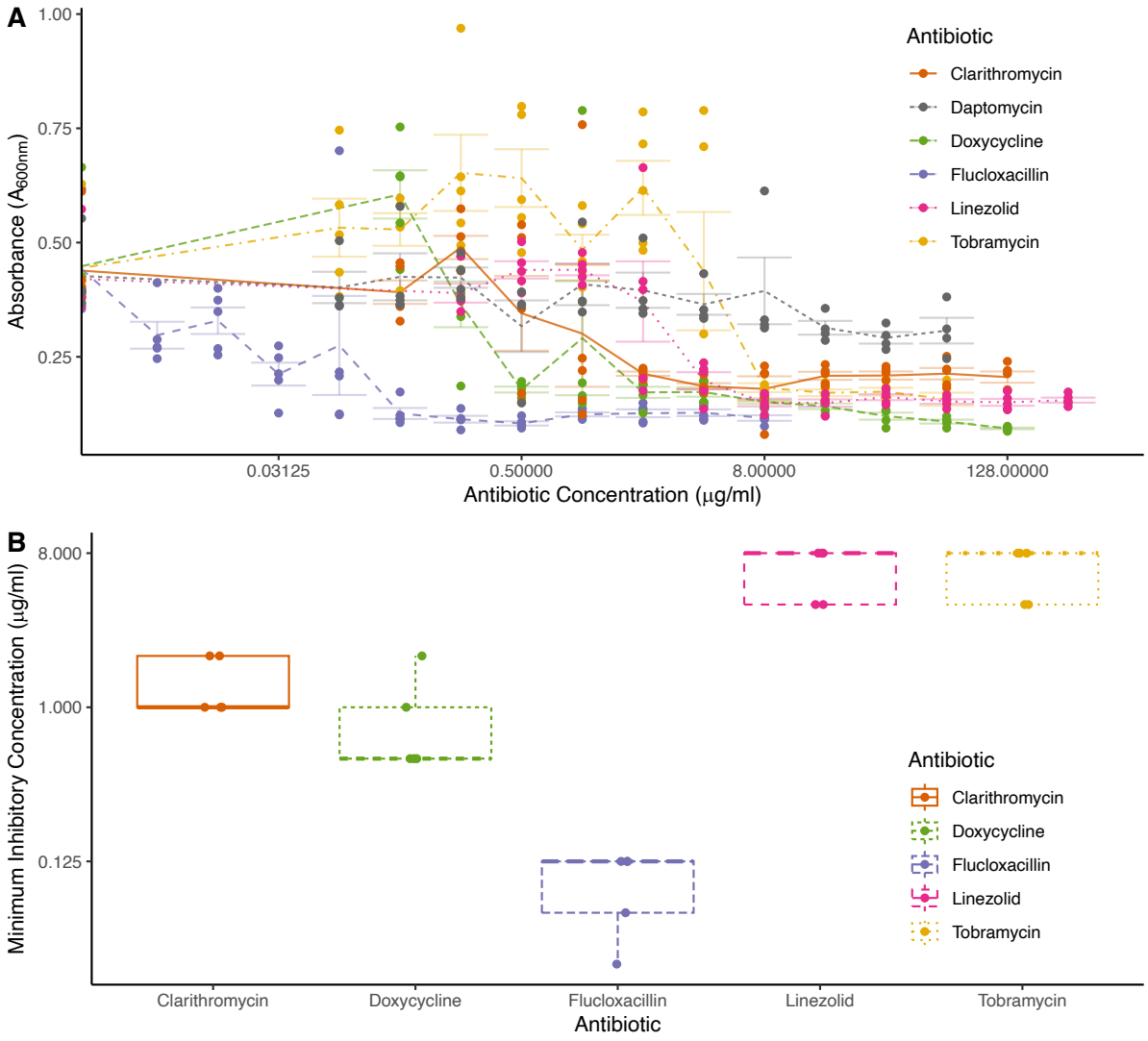

Figure 4-1: Sensitivity of* S. aureus *to anti-staphylococcal antibiotics.

MICs of SH1000 for clarithromycin (orange, 0.125-128 µg/ml), daptomycin (grey, 0.0625-64 µg/ml), doxycycline (green, 0.125-128 µg/ml), flucloxacillin (purple, 0.00781-8 µg/ml), linezolid (pink, 0.25-256 µg/ml), tobramycin (yellow, 0.0625-64 µg/ml). Antibiotics prepared by serial dilutions in 96 well plates before 20 h incubation with bacteria (37℃, 5% CO_2). Overnight cultures were diluted to $A_{600\ nm}$=0.05 before 50 µl was added to 50 µl antibiotic preparation. A) Optical density ($A_{600\ nm}$) at antibiotic concentrations shown. B) MIC cut-offs (breakpoints) defined as the lowest antibiotic concentration with no visible bacterial growth in the well. Daptomycin not included as the solute DMSO induced equal bactericidal effect. n=4/5 with A) mean +/- se, B) Box and whisker plots present median, 25/75% quantile (upper and lower hinge), smallest/ largest observation ≤ upper/lower hinge +/- 1.5 inter quantile range (whiskers).

4.3.2 The spontaneous mutation rate for resistance varies among the clinical antibiotics

Fluctuation assays in antibiotic-free conditions can be used to quantify the spontaneous mutation rate of *S. aureus* conferring resistance against clinical antibiotics[257,349]. Mutation rates were measured by establishing 10 independent lines of SH1000, growing individual colonies overnight in 10 ml BHI broth. Overnight cultures were then plated onto separate BHI agar plates containing the individual antibiotics at the breakpoints established in 4.3.1 above. After 24 h and 48 h, I compared the colony counts on BHI agar with antibiotics (clarithromycin, doxycycline, flucloxacillin, linezolid or tobramycin) to BHI agar plates with no antibiotics. Colonies appeared after 24 h on flucloxacillin plates but took 48 h to appear on clarithromycin and tobramycin plates. Knowing the number of colonies on antibiotic plates compared to no antibiotics allowed a mutation rate against each antibiotic to be calculated (Table 4-2) using the R package flan[258], which uses a probability generating function to estimate the mutation rate (section 3.2.5.1). The calculated mutation rate (m/Nt, where m represents the number of clones which grew in each antibiotic combined with the probability of mutations occurring and Nt the final number of cells cultured with no antibiotics) for conferring flucloxacillin resistance was much higher than that for clarithromycin or tobramycin (mutation rates per genome: clarithromycin, 0.075; flucloxacillin, 550.89; tobramycin, 0.040), suggesting spontaneous mutations in a higher number of genetic loci are associated with resistance to flucloxacillin. No clones were isolated on doxycycline or linezolid plates, showing the development of resistance to some antibiotics by spontaneous mutations is restricted.

Next, I quantified the level of resistance conferred by spontaneous mutations. I selected one clone from each antibiotic plate with growth from the fluctuation assays and determined antibiotic resistance by measuring their MICs against the same antibiotic in liquid culture. There was a significant decrease in antibiotic sensitivity (increased antibiotic resistance) of clones following selection on clarithromycin and flucloxacillin (Figure 4-2A; clarithromycin, $p=0.017$; flucloxacillin, $p=0.015$). There was a trend towards increased tobramycin resistance in the clones from the tobramycin fluctuation assays, although antibiotic resistant clones only grew on 3 tobramycin plates and $n=3$ is not high enough to reach significant in a non-parametric dataset (Figure 4-2A, $p=0.072$). However, this equated to low level increases in

antibiotic resistance for clarithromycin and flucloxacillin, with higher increases seen in the small number of tobramycin resistant clones (Figure 4-2A, median fold increase compared to ancestor: clarithromycin, 2.6 fold; flucloxacillin, 2 fold; tobramycin, 16 fold). To explain these somewhat counter-intuitive results I studied the antibiotic concentration curves (Figure 4-2B) from these MIC measurements. These suggest growth was affected in clones selected by growth on tobramycin plates. These clones had lower growth in liquid culture than their ancestor in sub-MIC antibiotic concentrations. The influence on clone growth at lower antibiotic concentrations likely accounts for there being no significant difference in the area under the curve of the concentration gradients measured in Figure 4-2B (Kruskal Wallis rank sum test with pairwise-Wilcoxon rank sum: clarithromycin, $p=0.6$; flucloxacillin, $p=0.57$; tobramycin, $p=0.2$).

Table 4-2: Spontaneous mutation result in antibiotic resistance determined by growth on agar plates

Mutation rate of 10 independent clones of SH1000 when grown overnight in antibiotic free conditions (10 ml BHI broth, 37℃, 280 rpm) followed by selection against 5 antibiotics. SH1000 (10 µl tobramycin, 50 µl all other antibiotics) was plated BHI agar containing the MIC of each antibiotic: clarithromycin, 0.5 µg/ml; doxycycline, 0.125 µg/ml; flucloxacillin, 0.0625 µg/ml; linezolid, 4 µg/ml or tobramycin, 4 µg/ml, prior to 48 h incubation (37℃). n=10, mutations calculated using a probability generating function (GF-test).

Antibiotic	Plates with colonies (/10)	Mutation Number (Nt)	p-value for mutation number	Mutation rate (m/Nt)	Lower bound	Upper bound	Mutation rate per genome
Clarithromycin	9	4.74	0.114	$2.66x10^{-8}$	$5.84x10^{-10}$	$5.27x10^{-8}$	0.075
Doxycycline	0	-	-	-	-	-	-
Flucloxacillin	10	34982.44	0.108	$1.97x10^{-4}$	0	$4.36x10^{-4}$	550.89
Linezolid	0	-	-	-	-	-	-
Tobramycin	3	2.53	0.473	$1.42x10^{-8}$	0	$3.77x10^{-8}$	0.040

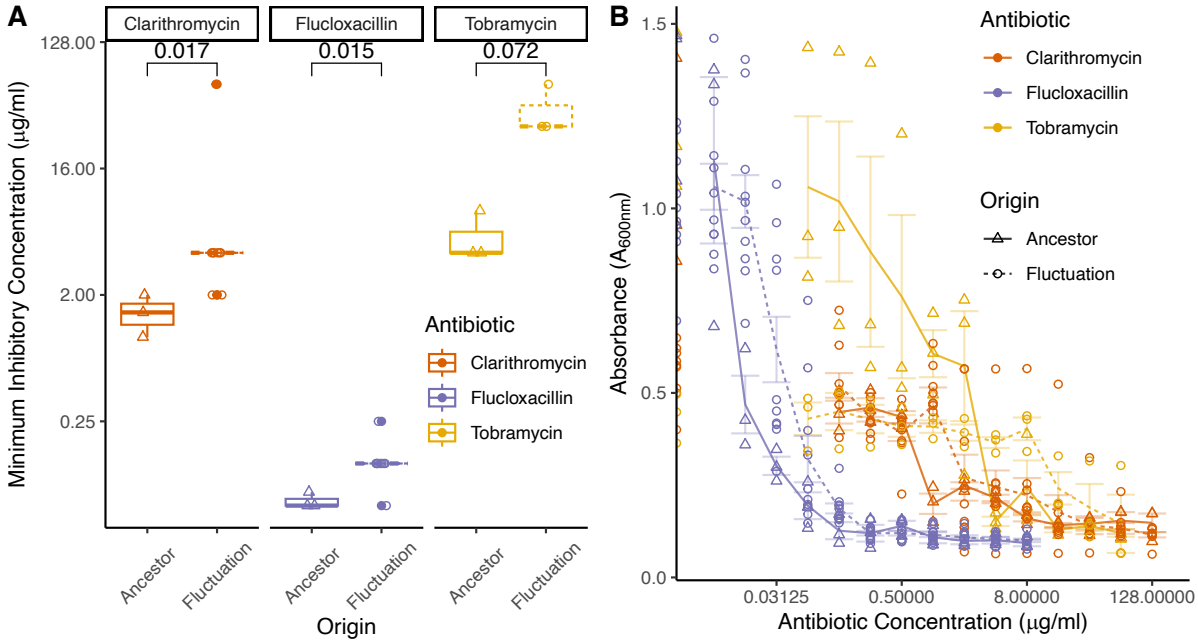

Figure 4-2: Antibiotic resistant clones from spontaneous mutations have modest gains in resistance.

MICs of single randomly selected clones from each agar plate with resistant colonies (described in Table 4-2) in clarithromycin (orange, 0.125-128 µg/ml), flucloxacillin (purple, 0.00781-8 µg/ml) or tobramycin (yellow), 0.0625-64 µg/ml) prepared by ½ serial dilution in BHI broth before 48 h incubation with bacteria in 96 well plate (37℃, 5% CO_2). Clones from fluctuation assays (dashed line, triangle) compared to their ancestor (solid line, circle). A) MIC cut-offs defined as the lowest antibiotic concentration with no visible bacterial growth in the well. n=3-10 of experiment carried out in triplicate. B) Optical density ($A_{600\ nm}$) at antibiotic concentrations shown. A) Statistical analysis by Kruskal-Wallis rank sum test with Wilcoxon rank sum post-hoc testing, B) mean+/- se. Box and whisker plots present median, 25/75% quantile (upper and lower hinge), smallest/ largest observation ≤ upper/lower hinge +/- 1.5 inter quantile range (whiskers), filled circle show range beyond whiskers in A. Additional statistical analysis comparing area under the curve (B) of ancestor to clones from fluctuation assays, Kruskal Wallis rank sum test with pairwise-Wilcoxon rank sum: clarithromycin, p=0.6; flucloxacillin, p=0.57; tobramycin, p=0.2.

4.3.3 Selection under increasing antibiotic concentration produces clones with high antibiotic resistance phenotypes and limited fitness costs

From the fluctuation assays I inferred that there are likely more individual loci which confer resistance to flucloxacillin than clarithromycin and tobramycin, with doxycycline and linezolid resistance evolution being more constrained, perhaps requiring multiple mutations. To further study this, I established 6 lines and selected for resistance against the 5 antibiotics above in a liquid antibiotic gradient, from 0.125-8 x MIC determined in Figure 4-1 (starting concentration range: clarithromycin, 0.0625-4 μg/ml; doxycycline, 0.0156-1 μg/ml; flucloxacillin, 0.0078-0.5 μg/ml; linezolid, 0.5-32 μg/ml; tobramycin, 0.5-32 μg/ml). Every 48 h the new MIC of the population was established, and populations were passaged into a doubling antibiotic gradient based on the new MIC. Following selection, each line showed usually modest increases in antibiotic concentration tolerance (Figure 4-3, fold increase: A) clarithromycin, 16-4096; B) doxycycline, 2-4; C) flucloxacillin, 4-16; D) linezolid, 2-16; E) tobramycin, 8-256). Interestingly, clarithromycin induced much greater increases in antibiotic resistance, and the clarithromycin gradient reached its maximum concentration range (16-2048 μg/ml) without precipitating out of solution at transfer 16 for clarithromycin population 3 (C3). The experiment was ended at transfer 20 (day 40), as each population no longer appeared to be increasing antibiotic resistance at each transfer.

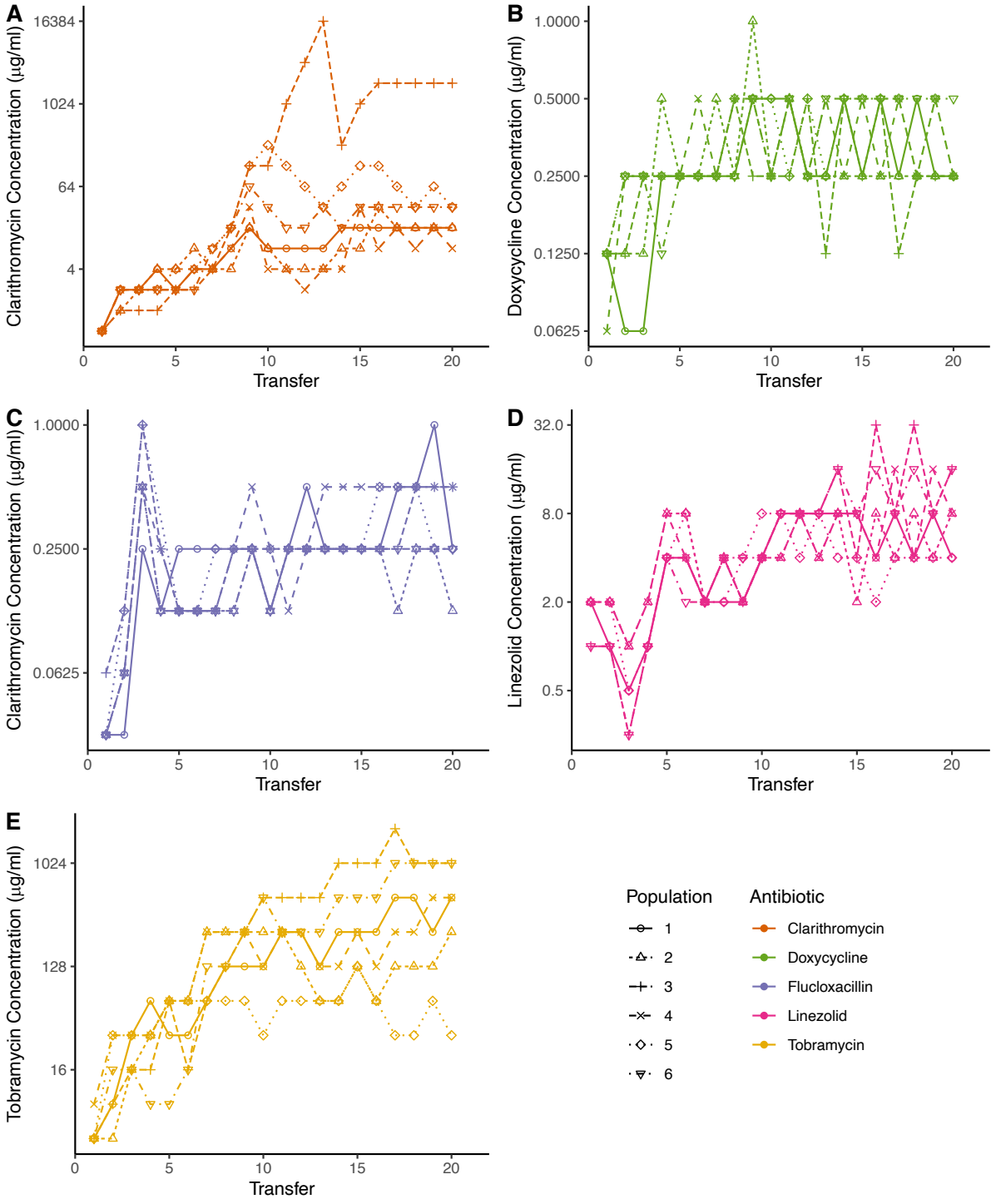

Figure 4-3: Antibiotic resistance increases following selection in antibiotic gradient

Antibiotic concentration with bacterial growth at transfer 1-20 for clones evolving in an antibiotic gradient. Bacterial growth cut-off was set at A $_{600\ nm}$=0.5 or the closest non-0 value, this then set the new MIC for making the next transfers antibiotic gradient. The antibiotic gradient was 0.125 to 8 x previous transfers MIC cut-off in BHI media. Transfer 0 concentrations: A) clarithromycin, 0.0625-4

µg/ml; B) doxycycline, 0.0156-1 µg/ml; C) flucloxacillin, 0.0078-0.5 µg/ml; D) linezolid, 0.5-32 µg/ml; E) tobramycin, 0.5-32 µg/ml. 1/50 transfers carried out every 48 h with 1x96 well plate per antibiotic at 37℃, 5% CO_2. 6 independent lines originating from distinct clones with lines connecting antibiotic concentrations at each transfer.

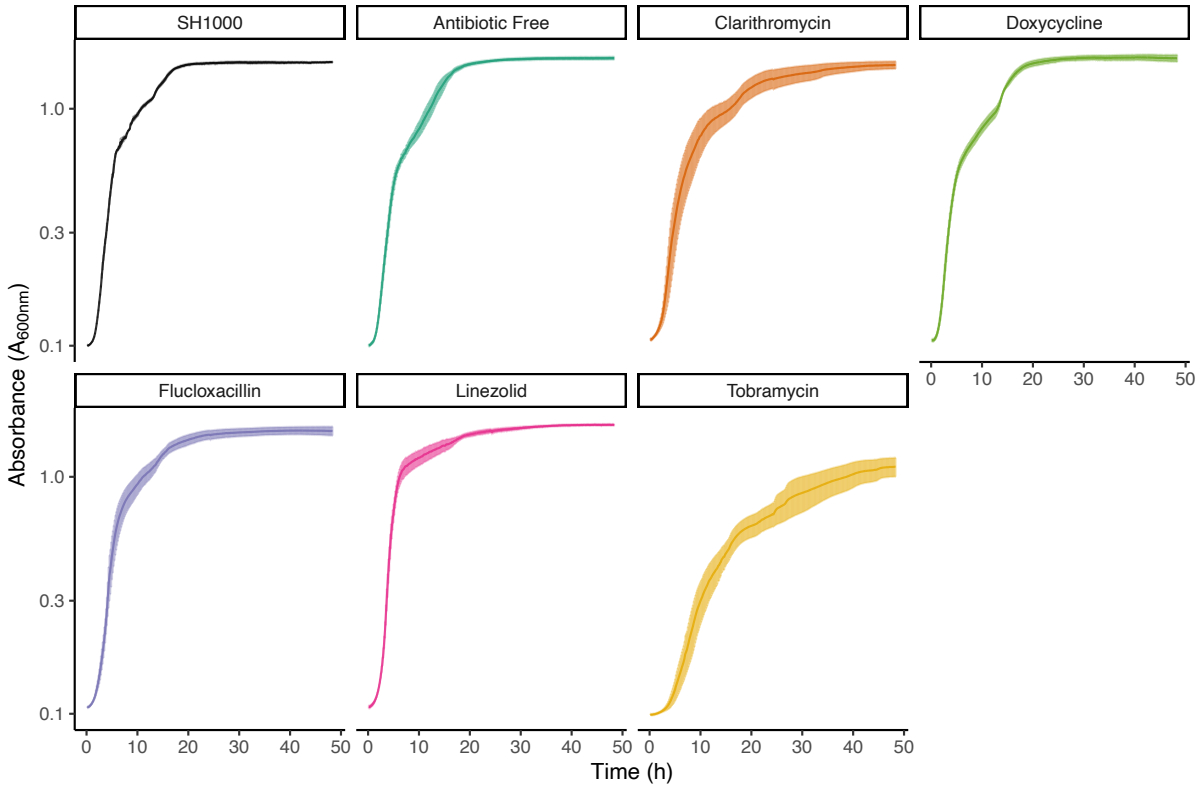

Figure 4-4: Growth curves of clones following antibiotic selection

Growth curves of evolved clones following selection in antibiotic free BHI broth, clarithromycin, doxycycline, flucloxacillin, linezolid or tobramycin compared to their ancestor, SH1000. An overnight culture for each clone was diluted in BHI broth to $A_{600\ nm}$=0.05 before 100µl was added to a 96 well plate. Optical density readings were taken at 600 nm every 10 mins for 48 h by the Varioskan LUX Multimode Microplate Reader. Between readings the plate was shaken at 120 rpm, 37°C. n=3/6 carried out in triplicate. Data shows mean +/- SE.

To determine whether the observed changed in antibiotic sensitivity influenced bacterial phenotypes, growth curves and MICs of one clone per population was carried out (36 in total, 6 antibiotic conditions x 6 populations). Growth was measured in a 96 well plate reader for 48 h (Figure 4-4). Determination of growth parameters (integral, maximum growth rate, maximum growth) allows comparison between selection settings. There was a significant decrease in the total growth of clones in antibiotic-free conditions following selection in tobramycin compared to selection in no antibiotics (Figure 4-5A: tobramycin, p=<0.001). This effect was not seen for clones following selection in other antibiotics (clarithromycin, p=0.259; doxycycline, p=>0.999; flucloxacillin, p=0.996; linezolid, p=0.970). Similar patterns were also observed for maximum growth achieved (Figure 4-5C), but not maximum growth rate (Figure 4-5B), showing tobramycin selection limited maximum population size rather than growth rate per se as measured by optical density. In contrast, the 48 h CFU values from these growth curves (Figure 4-6) did not show a significant reduction in the number of colonies growing on solid agar following tobramycin selection, perhaps reflecting inaccuracies in optical density readings due to cell morphology[350]. When plating the bacteria on agar to measure CFUs I observed a SCV phenotype, with very small colonies lacking pigment often appearing after 48 h incubation, always in clones which had been evolved in antibiotics. It was hypothesised the discrepancy between 48 h CFU values and optical density readings could vary between antibiotic treatments or reflect the development of SCVs, but there was a poor correlation between optical density readings and bacterial counts for each antibiotic treatment (Figure 4-6B) and likewise a poor correlation with the number of small colony variants (Figure 4-6C). Therefore, the $A_{600\,nm}$ growth readings and deduced parameters need to be interpreted with caution. The CFU values were measured at 48 h compared to the optical density values over the entire growth cycle. Clones evolved in all antibiotics other than tobramycin reached stationary phase within the first 12-24 h so will be in the death phase by 48 h, therefore the 48 h CFU values could be compromised as many cells will no longer be viable. As discussed in the methods (section 3.2.7.4) the lag phase could not be accurately determined for these growth curves, and a prolonged lag phase could also be affecting total growth in liquid culture. Limited total growth suggests a possible fitness cost associated with tobramycin selection, which is not seen in other antibiotics either due to low-cost mutations or to compensatory mutations, as seen in other studies[245,351,352].

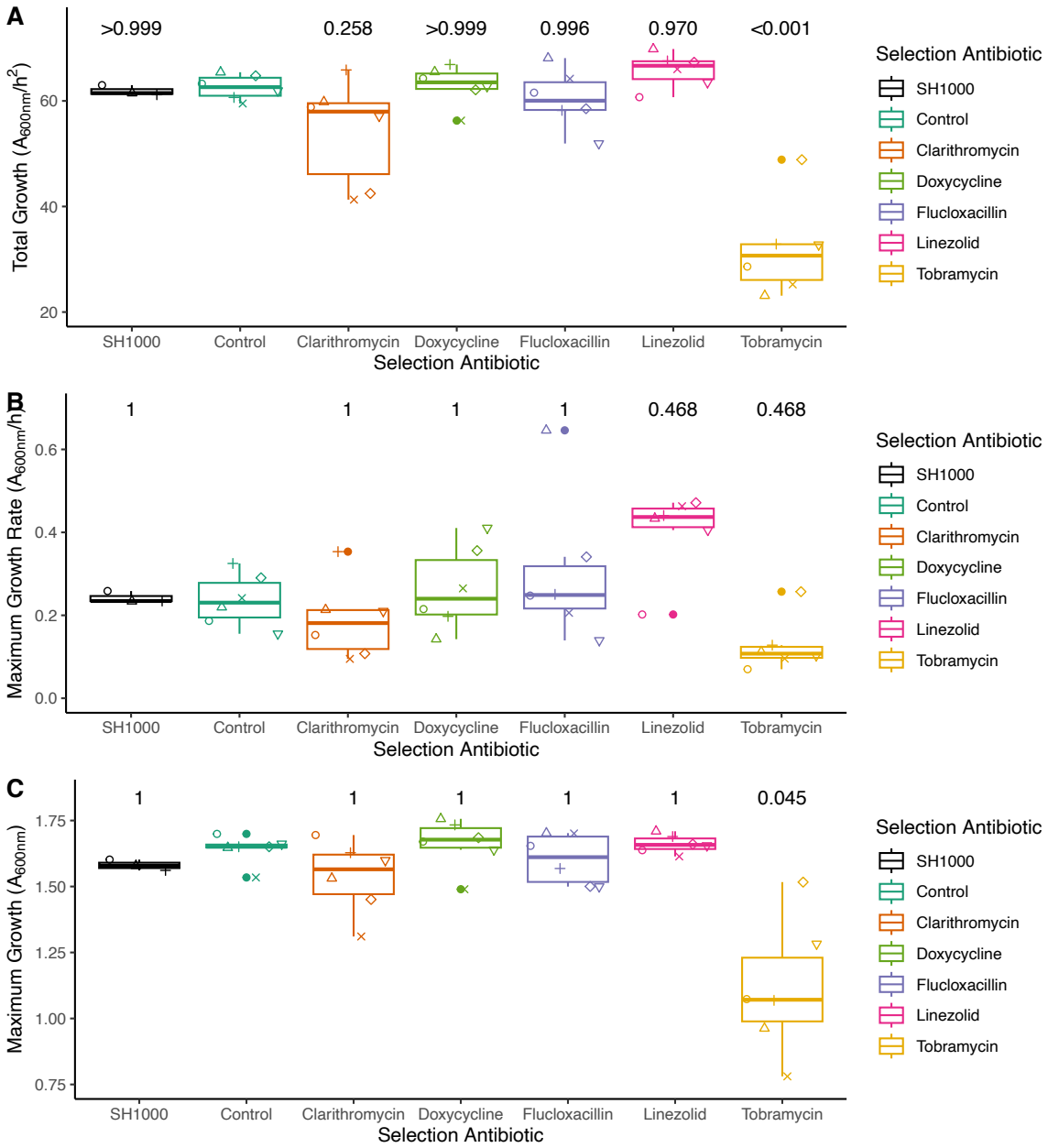

Figure 4-5: Antibiotic free growth in liquid culture is reduced following selection in tobramycin

Growth parameters of clones following 20 transfers in an antibiotic gradient, compared to ancestor (SH1000) and to populations with transfers in antibiotic-free media (control). Parameters from 48 h growth curves of overnight cultures diluted to a starting density of $A_{600\,nm}$=0.05 at 37°C, 120 rpm. Readings taken every 10 mins for 48 h by Varioskan LUX Multimode Microplate Reader at 600 nm. Parameters are A) area under the curve, B) maximum growth rate, C) maximum $A_{600\,nm}$ reading. n=3-6 carried out in triplicate, statistical analysis compared to control group by A) 2-way ANOVA with Tukey's multiple comparisons, B, C) Kruskal Wallis rank sum test with pairwise-Wilcoxon rank sum post-hoc testing. p values of each condition versus evolution in no antibiotic shown above each condition.

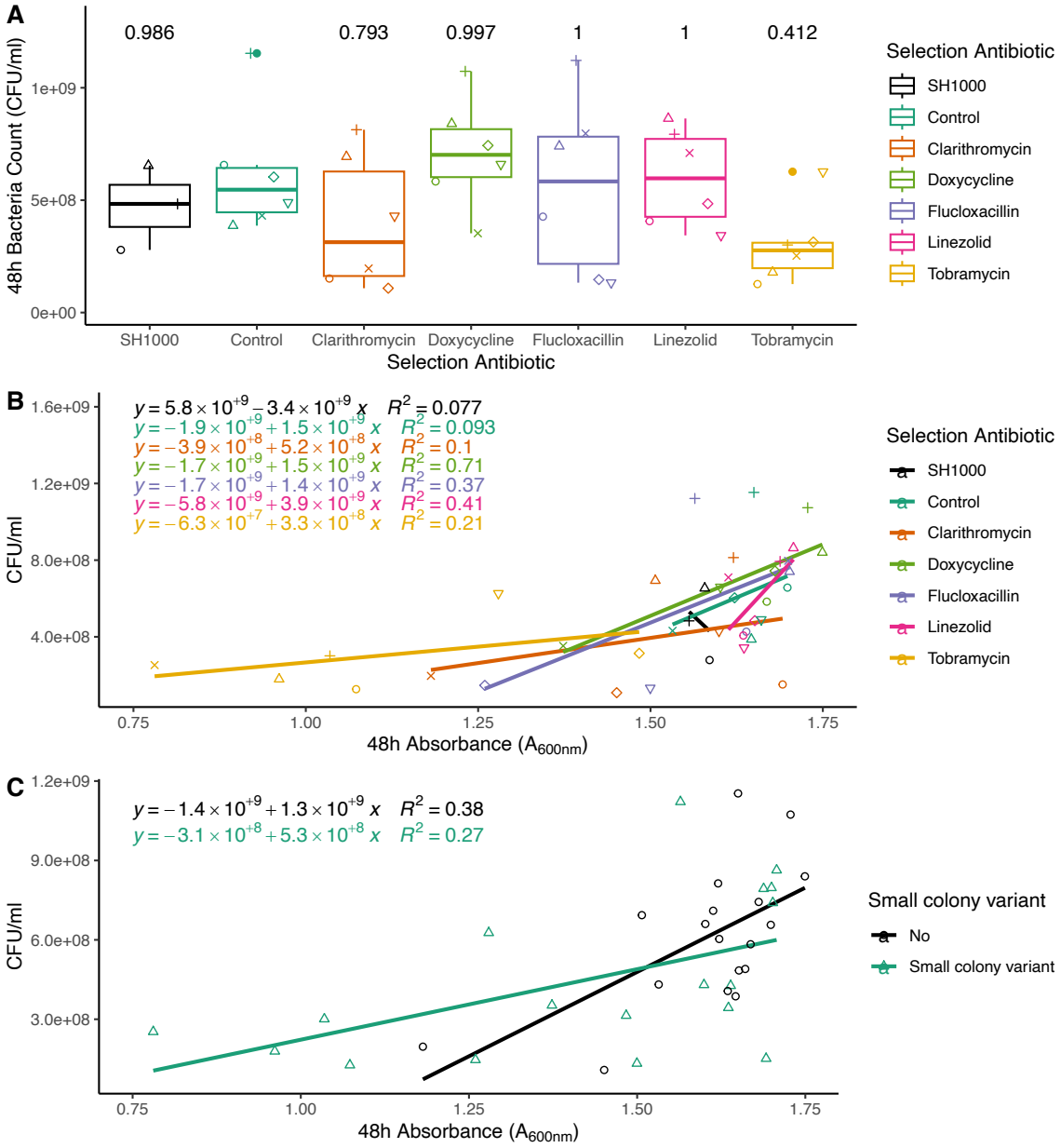

Figure 4-6: No difference in CFUs of clones after antibiotic selection

Bacterial counts at 48 h of clones from experiment shown in Figures 4-4 and 4-5 grown in BHI at 37°C, 120 rpm, following 20 transfers in an antibiotic gradient, 20 transfers in no antibiotic (control) or ancestor (SH1000). Bacterial counts were determined by serial dilution in PBS before plating. A) Bacterial counts for each selection antibiotic, B) A $_{600\,nm}$ readings compared to CFU/ml values for clones after antibiotic selection, C) A $_{600\,nm}$ readings compared to CFU/ml grouped by clones having a small colony variant phenotype (triangle) on BHI agar plates, or not (circle). n=3-6 carried out in triplicate. Statistical analysis by A) 2-way ANOVA with Tukey's multiple comparisons compared to control group, p values of each condition versus evolution in no antibiotic shown above each condition, B, C) linear regression.

4.3.4 Distinct genetic signatures follow evolution in different antibiotics

Whole genome sequencing was used to characterise genetic responses to antibiotic selection. The 36 clones for which I quantified growth were compared to their ancestor, SH1000. I carried out whole genome sequence analysis by 2 pipelines (3.2.14.2) both of which mapped the Illumina sequence reads to the reference genome NCTC 8325, identified differences with the reference, which I then check against the reference and their ancestor (SH1000) in IGV[266] (Integrative Genomics Viewer, which visualises the genome sequence). 156 variants were detected compared to their ancestor (main variants labelled in Figure 4-7), comprising 7 deletions, 8 insertions, 22 frameshift mutations, 24 intergenic mutations, 85 missense mutations, 4 nonsense mutations and 3 synonymous mutations. There were 3 large deletions affecting more than 1 gene. There was a significant difference in the number of mutations based on treatment condition (2-way ANOVA, Pr(>F)=0.00179: Tukey's multiple comparisons: flucloxacillin-control, p=0.00645; flucloxacillin-clarithromycin, p=0.0231; flucloxacillin-doxycycline, p=0.00645; flucloxacillin-linezolid, p=0.00415; flucloxacillin-tobramycin, p=0.354) with a significant increase in variants following selection in flucloxacillin compared to all antibiotic conditions other than tobramycin (consistent with the high mutation or fixation rates seen in the fluctuation assays for flucloxacillin). The genomic location of variants also varied depending on antibiotic treatment (Permutational ANOVA, F= 2.3887, Pr(>F)= 0 0.012). This resulted in genetic divergence between treatments (Figure 4-8: Permutational ANOVA, F= 4.3278, Pr(>F)=0.001) with clones from the same antibiotic selection environment clustering together. These results demonstrate that there are distinct genetic changes relating to selection in each antibiotic condition.

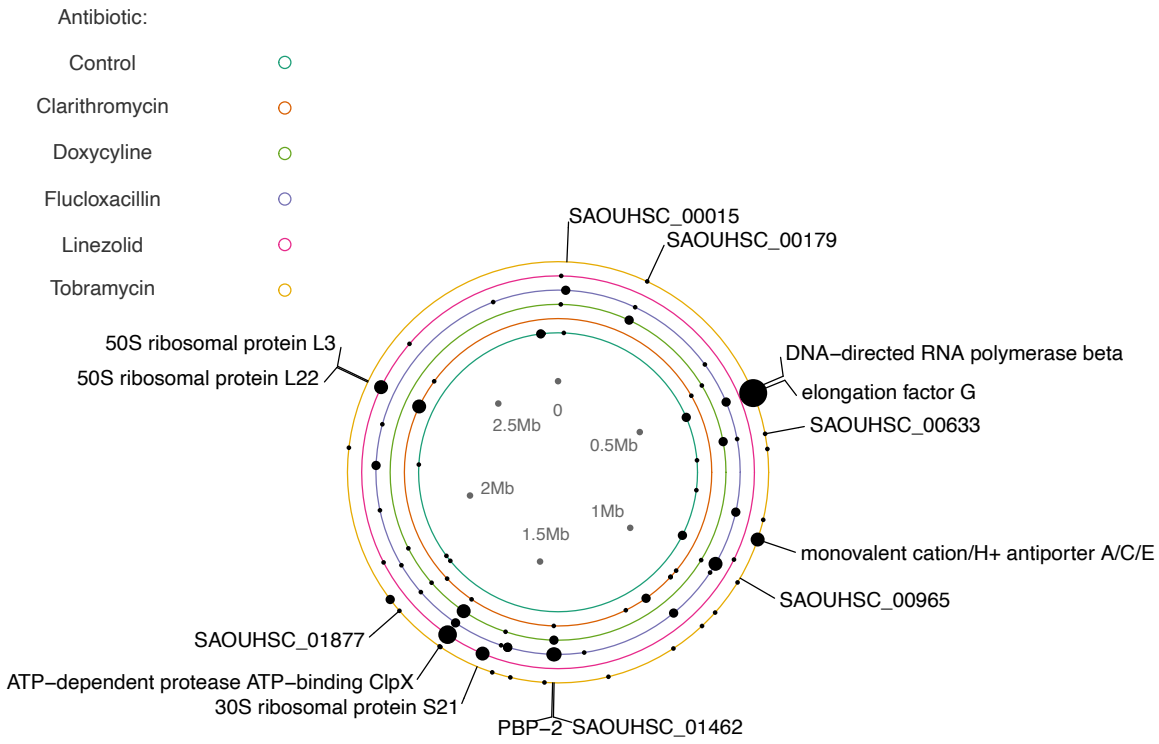

Figure 4-7: Overview of mutations across antibiotic selection conditions

Non-synonymous mutations in clones following 20 transfers at 48 h in antibiotic gradients. Teal=no antibiotic (control), orange=clarithromycin, green= doxycycline, purple=flucloxacillin, pink= linezolid and yellow=tobramycin. Size of filled circle is proportional to the numbers of variants in different clones. Labels for >2 variants in all clones. n=6 clones assessed in each condition. PBP-2= penicillin-binding protein 2. Hypothetical proteins are indicated by their chromosomal identification number (prefix: SAOUHSC).

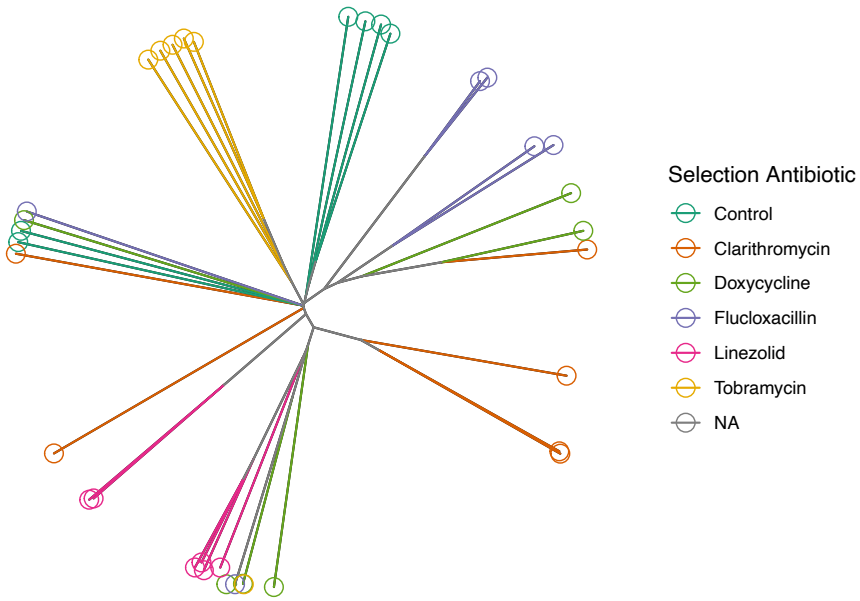

Figure 4-8: New phylogenetic distances display clusters based on antibiotic treatments.

Unrooted neighbour joining phylogeny of clones following 20 transfers on antibiotic gradients. Distances based on matrix of non-synonymous variants in a binary change or no-change in a gene. Evolution antibiotics are represented by teal=no antibiotic, orange=clarithromycin, green= doxycycline, purple=flucloxacillin, pink=linezolid, yellow=tobramycin, grey= branch shared by 2 or more antibiotics. n=6 in each antibiotic condition. Permutational ANOVA model of genetic distances between branches in phylogenetic tree grouped by selection antibiotic, p=0.001.

4.3.5 Genetic responses to antibiotic selection

The genetic divergence of clones based on evolution antibiotics indicated specific mutational targets were associated with different antibiotics. The MICs for each clone were measured to allow comparison of the effects of putative antibiotic resistance mechanisms upon resistance level.

For clones evolved in no antibiotic, 2-4 variants were identified per clone (Figure 4-9). These variants indicate those likely arise during adaptation to the laboratory environment or random genetic drift. Laboratory adaptation has also been seen in the long-term evolution experiment of *E. coli* with improved nutrient utilisation and transient polymorphisms in the populations[353]. I identified 5 genes designated as hypothetical proteins as they have not been characterised (prefix: SAOUHSC). If variants occur in a gene in more than 1 clone (parallel mutations) this increases the likelihood of the variant being important for bacterial adaptation rather than due to random genetic drift. 2 clones had variants in DNA-directed RNA polymerase β, which may optimise transcription in the antibiotic-free BHI environment. The *sasA* gene also had variants in 2 clone; this encodes a cell surface protein which modulates bacterial adhesion[354], hence these mutations could aid growth in the plastic 96 well plate in which these bacteria were evolved.

Clarithromycin binds within the 50S ribosomal subunit. Accordingly, I detected mutations in the binding site of the 50S ribosomal subunits (Figure 4-10A) L4 and L22[355,356]. There were also variants in the 50S ribosomal subunit L32 (*rpmF*)[357] in 5/6 clones subject to clarithromycin selection, of which 4 clones had deletions within or entire deletion of the *rpmF* gene. There is a redundancy in genes encoding L32, so this does not eliminate the expression of L32[358]. When the MIC of clarithromycin-evolved clones was measured on a clarithromycin antibiotic gradient (0.125-128 μg/ml), there was a 64-512 fold increase in MIC compared to clones selected without antibiotic (Figure 4-10B, p=0.036), supporting the potential role of these mutations in clarithromycin resistance. To test specific mutations' roles in resistance, clarithromycin resistance of all 36 evolved clones were compared according to whether or not they were carrying specific mutations. Mutations within the 50S ribosomal subunit L22 were associated with a significant increase in the clarithromycin MIC (Figure 4-10C, p=0.012).

Unexpectedly clone C3, evolved in clarithromycin, only carried a single mutation in PBP-2 (Figure 4-10D) and displayed high level clarithromycin resistance (MIC= 512, Figure 4-10B), putatively and unexpectedly linking this mutation with clarithromycin resistance, discussed further below.

A

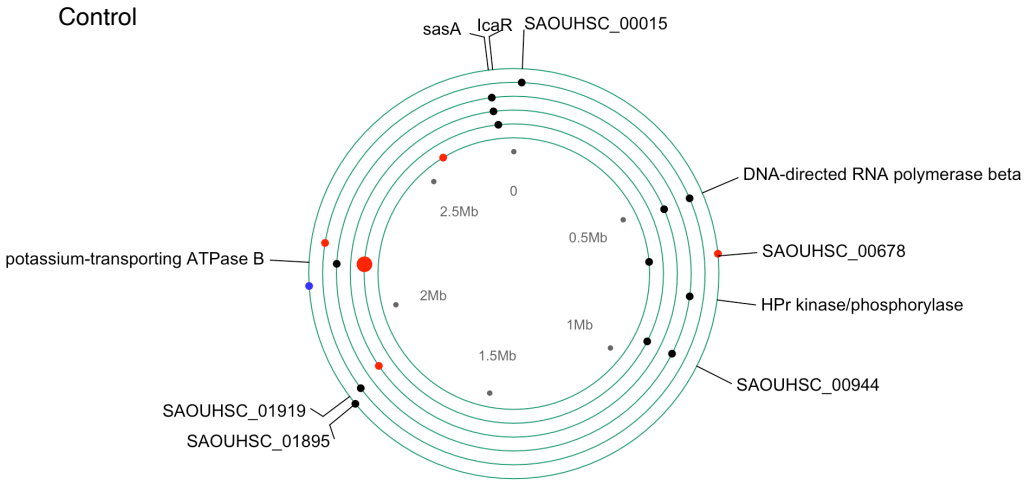

B

Clone	Variants
Con1	Hypothetical protein, intergenic mutation, deletion covering: abortive infection protein; membrane anchored protein; hypothetical protein; Aliphatic amidase amiE; accessory gene regulator protein B AGRB
Con2	Hypothetical protein, 2x intergenic mutations, ica operon transcriptional regulator IcaR
Con3	DNA-directed RNA polymerase subunit beta, intergenic mutation, sasA
Con4	Hypothetical protein, HPr kinase/phosphorylase, potassium-transporting ATPase subunit B, sasA
Con5	2x hypothetical proteins, DNA-directed RNA polymerase subunit beta, intergenic mutation
Con6	Intergenic mutation, hypothetical protein

Figure 4-9: Clones evolved in no antibiotics have mutations likely associated with laboratory adaptation

A) Circle plot of non-synonymous mutations in clones following 20 transfers (40 days) under antibiotic free selection. 1 clone sequenced from each evolved population (n=6). Each ring represents 1 clone with the inner ring representing clone 1, through to clone 6 in the outer ring. Size of filled circle is proportional to the numbers of variants in each gene, black=non-synonymous variants, red=intergenic variants, blue=deletion greater than 1 gene. Labels for all coding variants. SAOUHSC prefix and chromosomal number are for hypothetic proteins. B) Location of the variants in each clone in A. Each clone was evolved in no antibiotics, Con1=clone 1, Con2=clone 2, Con3=clone 3, Con4=clone 4, Con5=clone 5, Con6=clone 6.

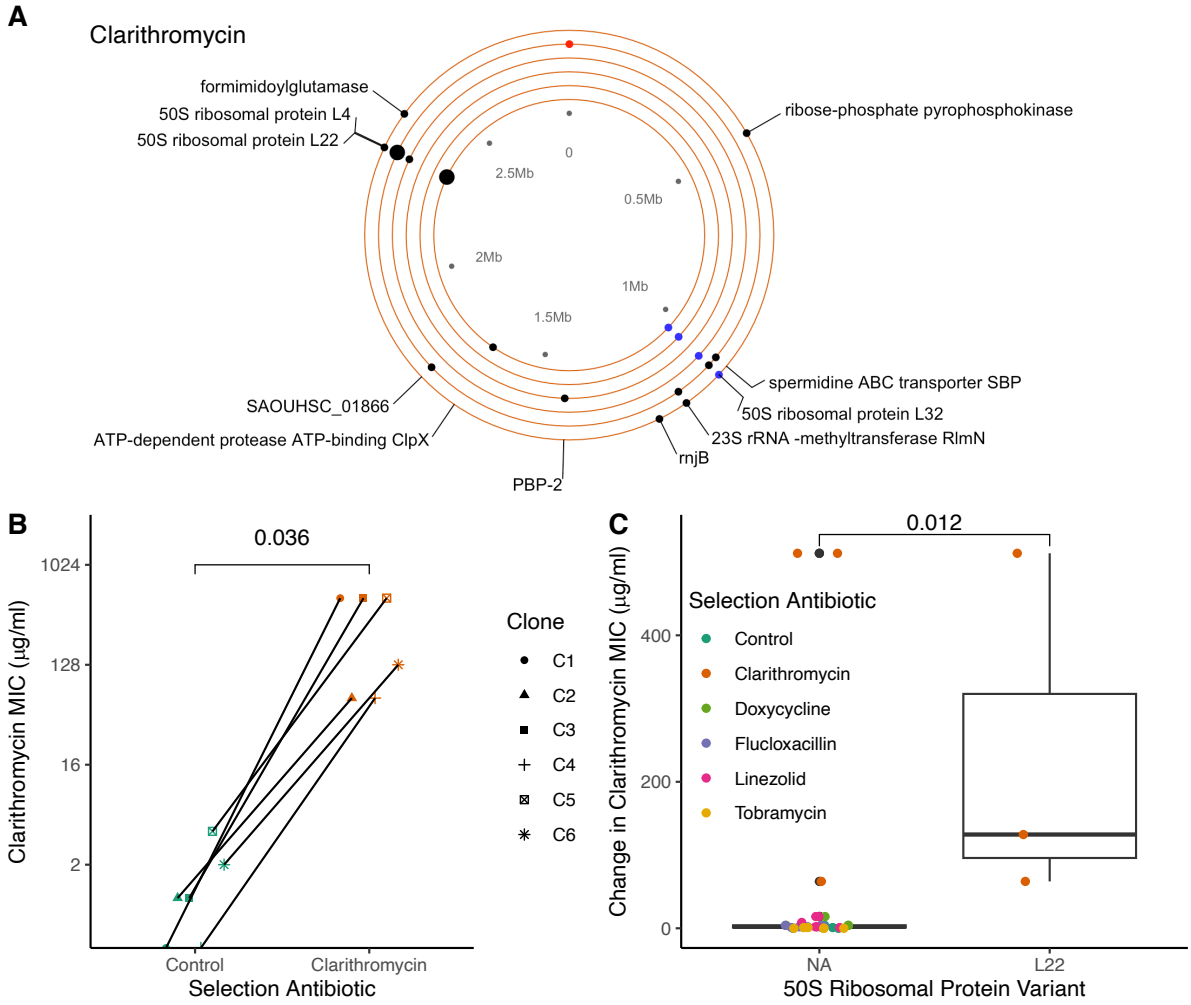

D

Clone	Variants
C1	Intergenic deletion, ATP-dependent protease ATP-binding subunit ClpX, 2x 50S ribosomal protein L22
C2	Deletion covering 2 hypothetical proteins and 50S ribosomal protein L32
C3	Penicillin-binding protein 2
C4	50S ribosomal protein L32, 50S ribosomal protein L22
C5	1x hypothetical protein, 1 intergenic mutation, spermidine/putrescine ABC transporter substrate-binding protein, rpmF, 23S rRNA (adenine(2503)-C(2))-methyltransferase RlmN, 2x 50S ribosomal protein L4
C6	Ribose-phosphate pyrophosphokinase, intergenic deletion, 50S ribosomal protein L32, 23S rRNA (adenine(2503)-C(2))-methyltransferase RlmN, rnjB, 2x50S ribosomal protein L22, formimidoylglutamase

Figure 4-10: Evolution in clarithromycin selects for mutations in ribosomal proteins

A) Circle plot of non-synonymous mutations in clones following 20 transfers (40 days) in a clarithromycin gradient. 1 clone from each evolved population (n=6) was sequenced. Each ring represents 1 clone with the inner ring representing clone 1, through to clone 6 in the outer ring. Size of

filled circle is proportional to the numbers of variants in each gene, black=non-synonymous variants, red=intergenic variants, blue=deletion greater than 1 gene. Labels for all coding variants. SAOUHSC prefix and chromosomal number are for hypothetic proteins. B, C) Clarithromycin minimum inhibitory concentration (MIC) for B) clones evolved in antibiotic free media (control, n=6) or clarithromycin gradient (n=6) or C) all 36 evolved clones. Clarithromycin prepared by serial dilutions in 96 well plates (0.125-128 µg/ml) before 48 h incubation with bacteria at 37℃, 5% CO_2. B) MICs of clarithromycin evolved clones compared to their ancestor evolved in no antibiotics. MIC cut-off defined as the lowest antibiotic concentration with no visible bacterial growth. C) Change in sequenced clone MIC compared to their ancestor (SH1000) with (n=3) or without (n=33) mutations in 50S ribosomal subunit L22. D) Location of the variants in each clarithromycin evolved clone in A. Each clone was evolved in clarithromycin (C), with the number as the clone number. B, C) Statistical analysis by Kruskal Wallis rank sum test with pairwise-Wilcoxon rank sum post-hoc testing vs. control. C) Box and whisker plots present median, 25/75% quantile (upper and lower hinge), smallest/ largest observation ≤ upper/lower hinge +/- 1.5 inter quantile range (whiskers).

Linezolid also targets 50S ribosomal subunit and prevents the formation of the initiation complex[359]. Mutations in 50S ribosomal protein L3 (L3), and 23S ribosomal RNA are known to be associated with linezolid resistance due to the interaction with the binding site[360,361]. Not unexpectedly, 4/6 clones evolved in linezolid had mutations at these sites (Figure 4-11A). The MIC of these clones, measured on a linezolid gradient (0.25-256 µg/ml), showed a modest but significant increase in linezolid MIC (Figure 4-11B; 2-8 fold increase compared to their ancestor, p=0.036). All clones carried a variant in L3 or in the 30S ribosomal protein S21 (S21) (Figure 4-11C). The S21 variant types include disruptive mutations of 2 clones with large deletions, 1 with a stop mutation and 1 clone with a frameshift mutation. There was a significant increase of the MIC in linezolid of clones carrying a L3 variant when compared to the linezolid MIC of all clones (irrespective of evolution condition) without such variants (Figure 4-11D, p=0.0039). 4 clones had variants in S21, which has not previously been associated with linezolid resistance as far as I can ascertain. In keeping with this, variants in S21 did not confer a significant increase in linezolid resistance (Figure 4-11E).

In clones evolved in tobramycin, there were no genomic variants in tobramycin's target, the 30S ribosomal subunit[216]. However, a variant was found in 50S ribosomal subunit L10 (*rplJ*) (1/6 clones, Figure 4-12A) which may relate to the fact that tobramycin blocks the formation of the initiation complex between these 2 subunits. Mutations in *rplJ* have also been found in *P. aeruginosa* when it was experimentally evolved against tobramycin[362]. In line with recent studies identifying elongation factor G as an under-reported mechanism of tobramycin resistance[308,326], herein 5/6 *S. aureus* clones evolved in tobramycin had variants in the gene encoding this protein (Figure 4-12A). There was a large and significant increase in tobramycin resistance for clones following tobramycin selection (Figure 4-12B, 16-64 fold increase compared to their ancestors, p=0.036), and this strongly associated with mutations in elongation factor G. The 5 clones with elongation factor G variants exhibited a significant increase in tobramycin MIC compared to clones without variants (Figure 4-12C, Kruskal-Wallis rank sum test, p=0.00048), although as all clones contain additional mutations these could also be contributing to tobramycin resistance.

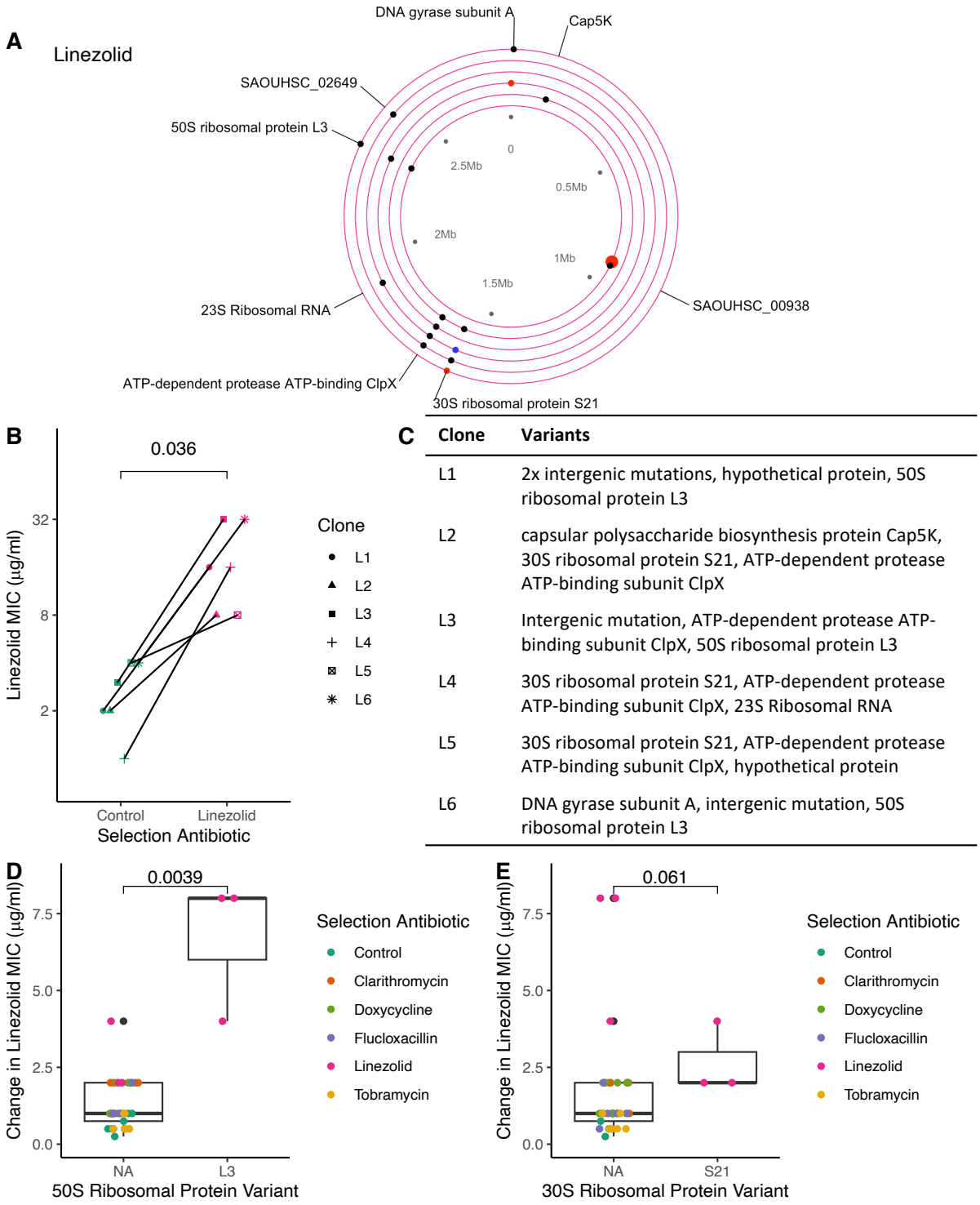

Figure 4-11: Evolution in linezolid selects for mutations in ribosomal proteins

A) Circle plot of non-synonymous mutations in clones following 20 transfers (40 days) in a linezolid gradient. 1 clone from each evolved population (n=6). Each ring represents 1 clone with the inner ring representing clone 1, through to clone 6 in the outer ring. Size of filled circle is proportional to the numbers of variants in each gene, black=non-synonymous variants, red=intergenic variants,

blue=deletion greater than 1 gene. Labels for all coding variants. SAOUHSC prefix and chromosomal number are for hypothetic proteins. B, D, E) Linezolid minimum inhibitory concentration (MIC) for B) clones evolved in antibiotic free media (control, n=6) or linezolid gradient (n=6) or D) all 36 clones evolved clones. Linezolid prepared by serial dilutions in 96 well plates (0.25-256 µg/ml) before 48 h incubation with bacteria at 37℃, 5% CO_2. MIC cut-off defined as the lowest antibiotic concentration with no visible bacterial growth. B) MICs of linezolid evolved clones compared to their ancestor evolved in no antibiotics. D, E) Change in sequenced clone linezolid MIC compared to their ancestor (SH1000) D) with (n=3) or without mutations (n=33) in the 50S ribosomal subunit L3 or E) with (n=3) or without mutations (n=33) in the 30S ribosomal protein S21, independent of other mutations within their genomes. C) Location of the variants in each linezolid evolved clone in A. Each clone was evolved in linezolid (L), with the number as the clone number. B, D, E) Statistical analysis by Kruskal Wallis rank sum test with pairwise-Wilcoxon rank sum post-hoc testing vs. control. D, E) Box and whisker plots present median, 25/75% quantile (upper and lower hinge), smallest/ largest observation ≤ upper/lower hinge +/- 1.5 inter quantile range (whiskers). Cap5K = capsular polysaccharide biosynthesis protein Cap5K.

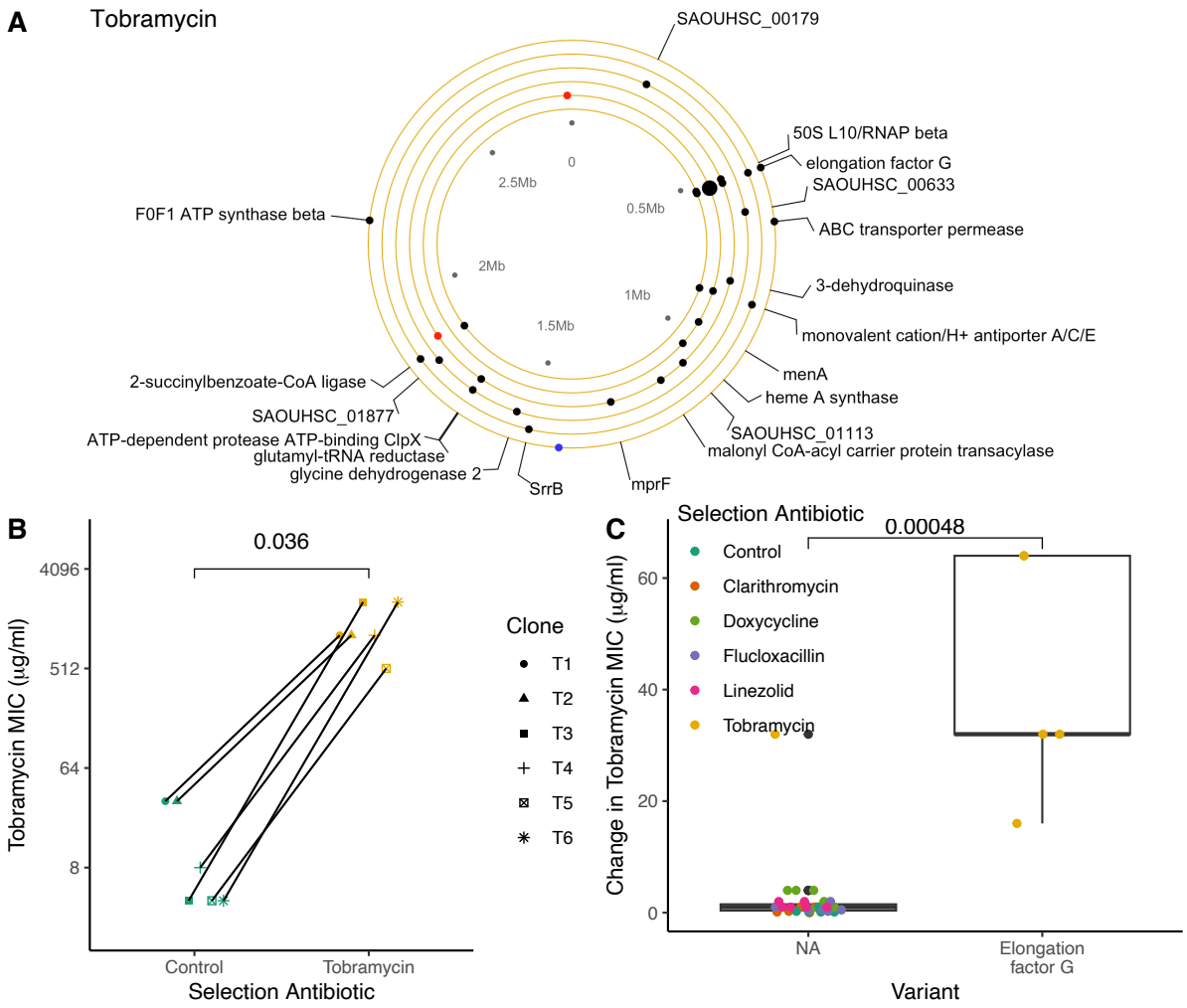

D

Clone	Variants
T1	DNA-directed RNA polymerase subunit beta, elongation factor G, monovalent cation/H+ antiporter subunit A, 2-succinylbenzoate-CoA ligase
T2	2x elongation factor G, monovalent cation/H+ antiporter subunit E, 1,4-dihydroxy-2-naphthoate octaprenyltransferase, heme A synthase, intergenic variant
T3	50S ribosomal protein L10, elongation factor G, 3-dehydroquinase, hypothetical protein, malonyl CoA-acyl carrier protein transacylase, mprF, glutamyl-tRNA reductase, intergenic mutation
T4	3x hypothetical proteins, glycine dehydrogenase subunit 2, ATP-dependent protease ATP-binding subunit ClpX
T5	elongation factor G, monovalent cation/H+ antiporter subunit C, respiratory response protein SrrB, 2-succinylbenzoate-CoA ligase
T6	elongation factor G, ABC transporter permease, 642bp deletion including aroB (3-dehydroquinate synthase), F0F1 ATP synthase subunit beta

Figure 4-12: Evolution in tobramycin selects for variants in elongation factor G

A) Circle plot of non-synonymous mutations in clones following 20 transfers (40 days) in a tobramycin gradient. 1 clone from each evolved population (n=6). Each ring represents 1 clone with the inner ring representing clone 1, through to clone 6 in the outer ring. Size of filled circle is proportional to the

numbers of variants in each gene, black=non-synonymous variants, red=intergenic variants, blue=deletion greater than 1 gene. Labels for all coding variants. SAOUHSC prefix and chromosomal number are for hypothetic proteins. B, C) minimum inhibitory concentration (MIC) for B) clones evolved in antibiotic free media (control, n=6) or tobramycin gradient (n=6) or D) all 36 evolved clones. Tobramycin prepared by serial dilutions in 96 well plates (0.0625-64 µg/ml) before 48 h incubation with bacteria at 37℃, 5% CO_2. MIC cut-off defined as the lowest antibiotic concentration with no visible bacterial growth. B) MICs of tobramycin evolved clones compared to their ancestor evolved in no antibiotics. C) Change in sequenced clone tobramycin MIC compared to their ancestor (SH1000) with (n=4) or without mutations (n=32) in the elongation factor G, independent of other mutations within their genomes. D) Location of the variants in each tobramycin evolved clone in A. Each clone was evolved in tobramycin (T), with the number as the clone number. B, C) Statistical analysis by Kruskal Wallis rank sum test with pairwise-Wilcoxon rank sum post-hoc testing vs. control. C) Box and whisker plots present median, 25/75% quantile (upper and lower hinge), smallest/ largest observation ≤ upper/lower hinge. SrrB = staphylococcal respiratory response protein B, 50S L10/RNAP beta= 50S ribosomal protein L10/ DNA-directed RNA polymerase subunit beta.

No variants in doxycycline's target, the 30S ribosomal subunit, nor in the transcriptional machinery were identified (Figure 4-13A) in clones that underwent selection in doxycycline. There were 2-5 variants detected per doxycycline evolved clone. Many of these were in hypothetical proteins (6 genes) or genes associated with a more general antibiotic stress response, discussed below (ATP-dependent protease ATP-binding ClpX, PBP-2). These could be associated with adaptation to the laboratory environment plus permitting survival in doxycycline prior to development of resistance. This is consistent with the modest, non-significant, increases in doxycycline MICs seen (Figure 4-13B, 1-4 fold increase, p=0.104).

Flucloxacillin (Figure 4-14A) is a β-lactam antibiotic, targeting cell wall crosslinking through inhibition of penicillin binding proteins (PBPs)[168] rather than binding the ribosomal apparatus. Correspondingly, 3/6 clones had gained mutations in PBP-2. All 3 of these clones (Figure 4-14B, clones F1, F2 and F5) had higher MICs compared to the same experimental line evolved in no antibiotics, although they all had additional variants within their chromosome (Figure 4-14C). The flucloxacillin clones with PBP-2 variants had significantly higher flucloxacillin resistance than clones without PBP-2 variants (Figure 4-14D, p=0.0049); the influence of PBP-2 on cross-antibiotic resistance is explored further below (Figure 4-17A,B). Additionally, mutations in the cell division protein FtsZ were found in 2/6 clones. This can be linked to the target of flucloxacillin as FtsZ has been shown to recruit PBP-2 and inhibitors of FtsZ synergise with β-lactam antibiotics[363,364]. Clones with FtsZ variants show a trend towards increased flucloxacillin resistance, although it was not possible do statistics for n=2 (Figure 4-14E). One of these clones (clone F5 evolved in flucloxacillin, Figure 4-14C), had variants in both PBP-2 and FtsZ, which are likely working collaboratively to achieve resistance. In addition to these commonly reported resistance mechanisms to β-lactams, 2 clones had no mutations directly associated resistance to β-lactams following flucloxacillin selection (clones F3 and F6 evolved in flucloxacillin, Figure 4-14C). Clones F3 and F6 have 4 or 6 variants in hypothetical proteins, respectively, which have yet to be characterised but which may be driving resistance. In clone F6 evolved in flucloxacillin, ncbi BLAST[270] for these variants identified 2 variants in the hypothetical protein SAOUHSC_00826, in a clinical MRSA strain (KUH140331)[365]. Mutations in ATP-dependent protease ATP-binding subunit ClpX[366,367] (ClpX) in clone F3 and diadenylate cyclase CdaA[368,369] in clone F6, are associated with broader antibiotic resistance.

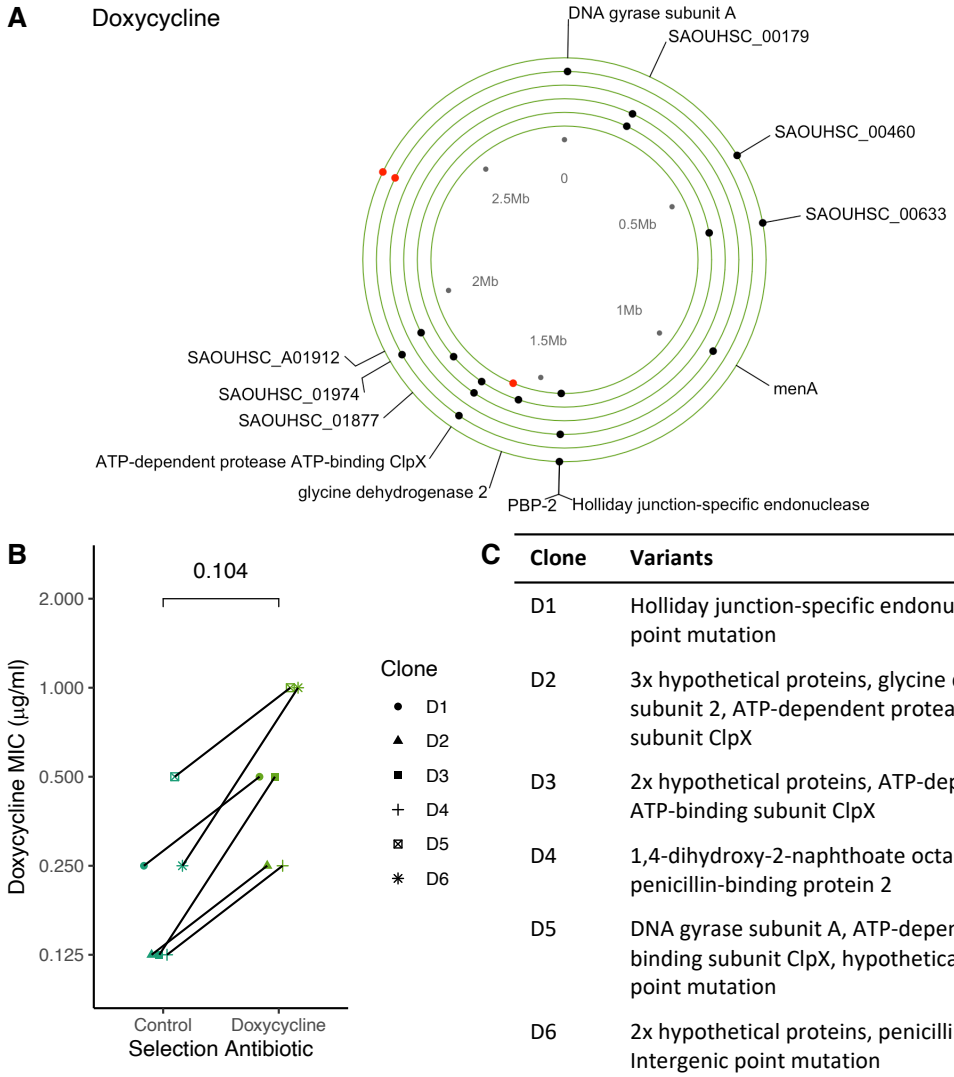

C

Clone	Variants
D1	Holliday junction-specific endonuclease, Intergenic point mutation
D2	3x hypothetical proteins, glycine dehydrogenase subunit 2, ATP-dependent protease ATP-binding subunit ClpX
D3	2x hypothetical proteins, ATP-dependent protease ATP-binding subunit ClpX
D4	1,4-dihydroxy-2-naphthoate octaprenyltransferase, penicillin-binding protein 2
D5	DNA gyrase subunit A, ATP-dependent protease ATP-binding subunit ClpX, hypothetical protein, Intergenic point mutation
D6	2x hypothetical proteins, penicillin-binding protein 2, Intergenic point mutation

Figure 4-13 Evolution in doxycycline selects for mutations in non-ribosomal targets

A) Circle plot of non-synonymous mutations in clones following 20 transfers (40 days) in a doxycycline gradient. 1 clone from each evolved population (n=6). Each ring represents 1 clone with the inner ring representing clone 1, through to clone 6 in the outer ring. Size of filled circle is proportional to the numbers of variants in each gene, black=non-synonymous variants, red=intergenic variants. Labels for all coding variants. SAOUHSC prefix and chromosomal number are for hypothetic proteins. B) minimum inhibitory concentration (MIC) for n=6 clones evolved in doxycycline gradient versus ancestor evolved in antibiotic free media (control, n=6). Doxycycline prepared by serial dilutions in 96 well plates (0.125-128 µg/ml) before 48 h incubation with bacteria at 37℃, 5% CO_2. MIC cut-off defined as the lowest antibiotic concentration with no visible bacterial growth. C) Location of the variants in each doxycycline evolved clone in A. Each clone was evolved in doxycycline (D), with the number as the clone number. B) Statistical analysis by Kruskal Wallis rank sum test with pairwise-Wilcoxon rank sum post-hoc testing vs. control.

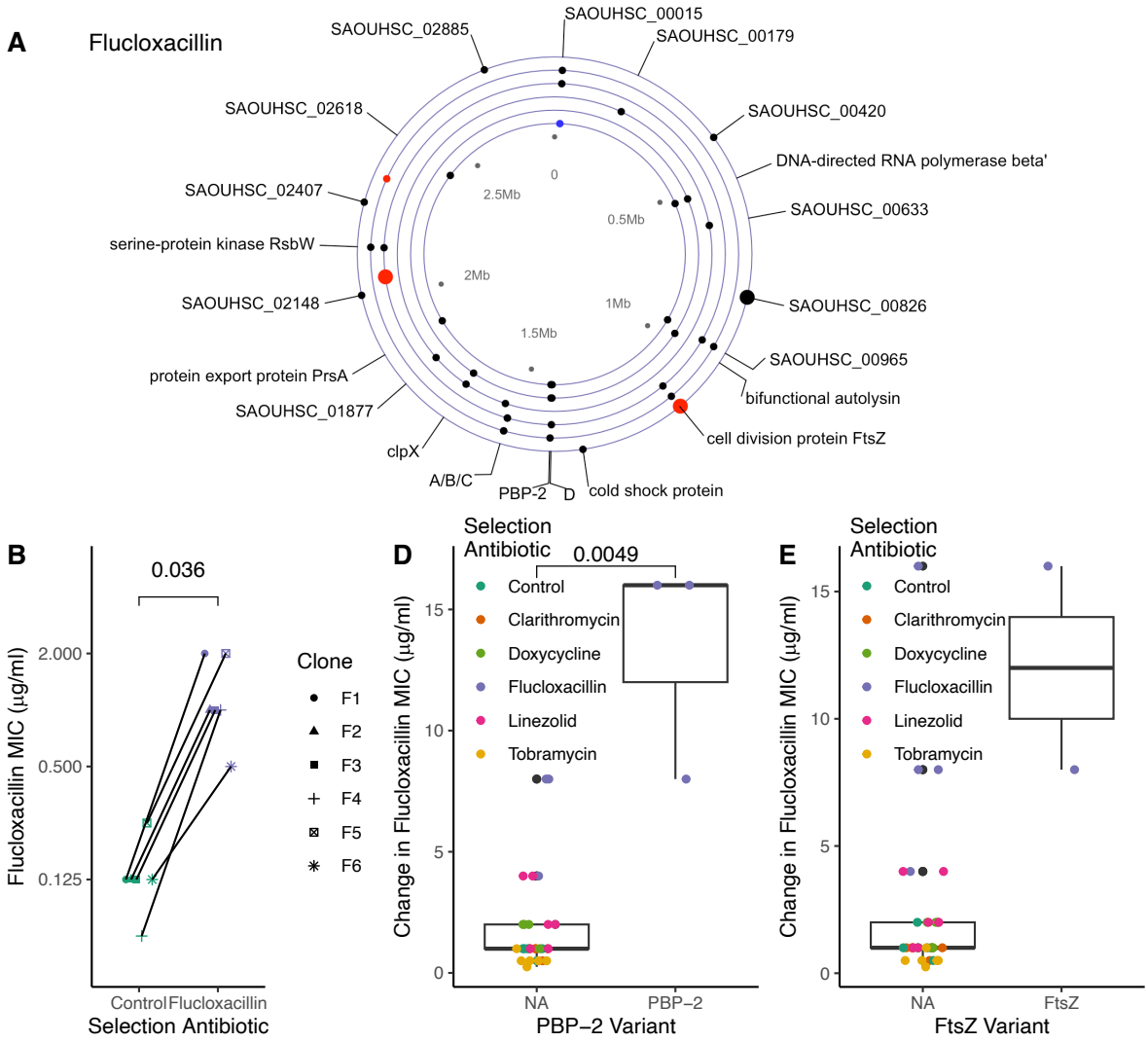

C

Clone	Variants
F1	3x hypothetical proteins, 325bp deletions covering a hypothetical protein and cyclic-di-AMP phosphodiesterase GdpP, DNA-directed RNA polymerase subunit beta', penicillin-binding protein 2, protein export protein PrsA
F2	Hypothetical protein, DNA-directed RNA polymerase subunit beta', bifunctional autolysin, penicillin-binding protein 2, ATP-dependent protease ATP-binding subunit ClpX
F3	3x hypothetical proteins, glycine dehydrogenase subunit 2, ATP-dependent protease ATP-binding subunit ClpX
F4	4x hypothetical proteins, cell division protein FtsZ, 2-oxoisovalerate dehydrogenase, E1 component subunit beta, 2x intergenic mutations
F5	3x hypothetical proteins, cell division protein FtsZ, penicillin-binding protein 2, 2-oxoisovalerate dehydrogenase, E1 component subunit beta, serine-protein kinase RsbW, intergenic mutation
F6	6x hypothetical proteins, 2x intergenic mutations, cold shock protein

Figure 4-14: Evolution in flucloxacillin selects for variants in PBP-2 and FtsZ

A) Circle plot of non-synonymous mutations in clones following 20 transfers (40 days) in a flucloxacillin gradient. 1 clone from each evolved population (n=6). Each ring represents 1 clone with the inner ring

representing clone 1 through to clone 6 in the outer ring. Size of filled circle is proportional to the numbers of variants in each gene, black=non-synonymous variants, red=intergenic variants, blue=deletion greater than 1 gene. Labels for all coding variants. SAOUHSC prefix and chromosomal number are for hypothetic proteins. B, D, E) minimum inhibitory concentration (MIC) for B) clones evolved in antibiotic free media (control, n=6) or flucloxacillin gradient (n=6), D) all 36 clones evolved on antibiotic free media, or antibiotics or E) all clones evolved on antibiotic free media, or antibiotics excluding 3 clones with PBP-2 mutations evolved in antibiotics other than flucloxacillin. Flucloxacillin prepared by serial dilutions in 96 well plates (0.0078-8 µg/ml) before 48 h incubation with bacteria at 37℃, 5% CO_2. MIC cut-off defined as the lowest antibiotic concentration with no visible bacterial growth. B) MICs of flucloxacillin evolved clones compared to their ancestor evolved in no antibiotics. D) Change in sequenced clone flucloxacillin MIC compared to their ancestor (SH1000) with mutations in PBP-2 following evolution in flucloxacillin (n=3) or without mutations (n=30) in PBP-2, independent of other mutations within their genomes. E) Change in sequenced clone flucloxacillin MIC compared to their ancestor (SH1000) with (n=2) or without mutations (n=34) in FtsZ, independent of other mutations within their genomes. C) Location of the variants in each flucloxacillin evolved clone in A. Each clone was evolved in flucloxacillin (F), with the number as the clone number. B, E) Statistical analysis by Kruskal Wallis rank sum test with pairwise-Wilcoxon rank sum post-hoc testing vs. control. A=SAOUHSC_01612, B= glycine dehydrogenase 2, C=2-oxoisovalerate dehydrogenase subunit beta, D= SAOUHSC_01462, Cap5K= capsular polysaccharide biosynthesis protein Cap5K.

4.3.6 Some genes contribute to resistance against multiple antibiotics

Previous studies have described cross-resistance and collateral sensitivity following bacterial evolution in antibiotics, particularly when antibiotics have shared targets, with lower levels of cross-resistance between aminoglycosides and other classes of antibiotics[286,287,338,339,341]. All 5 antibiotics used here are from different classes, however, clarithromycin, doxycycline, linezolid and tobramycin all target the ribosome, whilst flucloxacillin targets the cell wall. To see if having a shared target influenced cross resistance, either by mutations in genes specifically associated with the mechanisms of action or indirectly via other genes, I compared cross-resistance for evolved resistant clones against all antibiotics. The MICs of all study antibiotics (clarithromycin, doxycycline, flucloxacillin, linezolid and tobramycin) were measured for each of the 36 evolved clones (6 per evolution antibiotic plus 6 in no antibiotics) and for each antibiotic the MICs of the clones grouped by evolution antibiotic was compared to clone evolved in no antibiotics (control) (Figure 4-15).There was no significant increase in overall clarithromycin MICs (Figure 4-15A), doxycycline MICs (Figure 4-15B), flucloxacillin MICs (Figure 4-15C) or tobramycin MICs (Figure 4-15D) for clones grouped by antibiotic against any other antibiotic. There was a small but significant increase in linezolid resistance overall for all clones selected in clarithromycin (1-2 fold increase, p=0.036, Figure 4-15E) suggesting consistent but low-level cross-resistance in this setting. There was variation in the MICs of individual clones evolved in each antibiotic, with some specific clones displaying higher levels of resistance and a degree of cross-resistance (Figure 4-16). Specifically, multiple clones had 4-fold or greater increases in clarithromycin resistance following selection in doxycycline, linezolid or flucloxacillin. There was also a 4-fold increase in tobramycin MIC for 3 clones under doxycycline selection. I saw no evidence for collateral sensitivity between clones. The sequence analysis of these clones showed mutations in many ribosomal targets which I look at in more detail below to see if these are driving cross-resistance. The interaction between clarithromycin and flucloxacillin resistance, with different antibiotic targets, suggests non-ribosomal mutations are driving cross resistance in this setting.

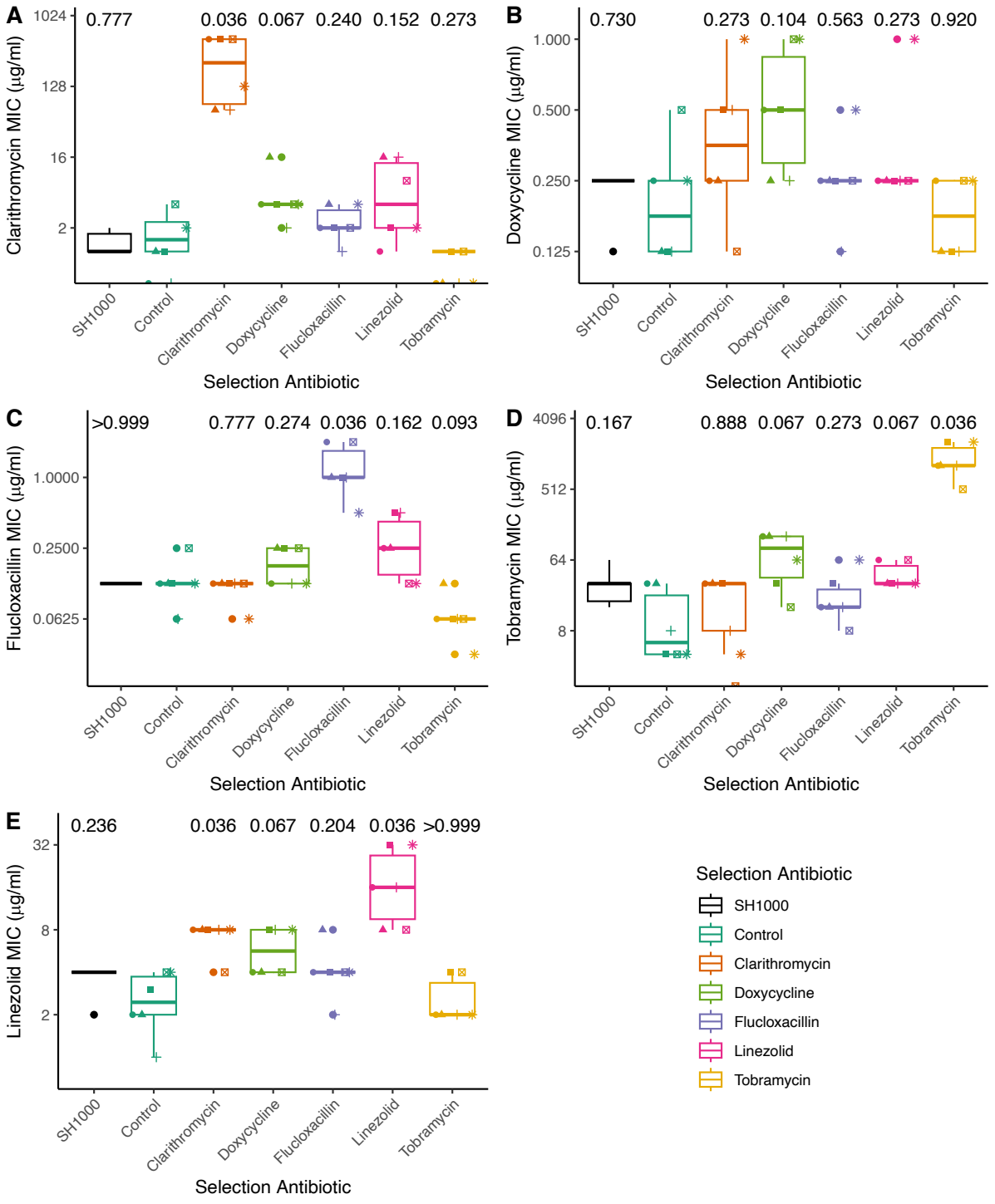

Figure 4-15: Antibiotic selection drives resistance to the same antibiotic with limited impact of resistance to other antibiotics at population level

Minimum inhibitory concentrations (MICs) for clones following selection in 5 different antibiotic gradients or antibiotic free media (control) or ancestor (SH1000). Antibiotics prepared by serial dilutions in 96 well plates of clarithromycin (0.125-128 µg/ml), doxycycline (0.125-128 µg/ml),

flucloxacillin (0.00781-8 µg/ml), tobramycin (0.0625-64 µg/ml) or linezolid (0.25-256 µg/ml) before 48 h incubation with bacteria at 37℃, 5% CO_2. MIC cut-offs defined as the lowest antibiotic concentration with no visible bacterial growth in the well. n=6. Statistical analysis by Kruskal Wallis rank sum test with pairwise-Wilcoxon rank sum post-hoc testing vs. control. Box and whisker plots present median, 25/75% quantile (upper and lower hinge), smallest/ largest observation ≤ upper/lower hinge +/- 1.5 inter quantile range (whiskers). p values of each condition versus evolution in no antibiotic shown above each condition. These data are a different representation of the MIC data for all clones in Figures 4-10-14.

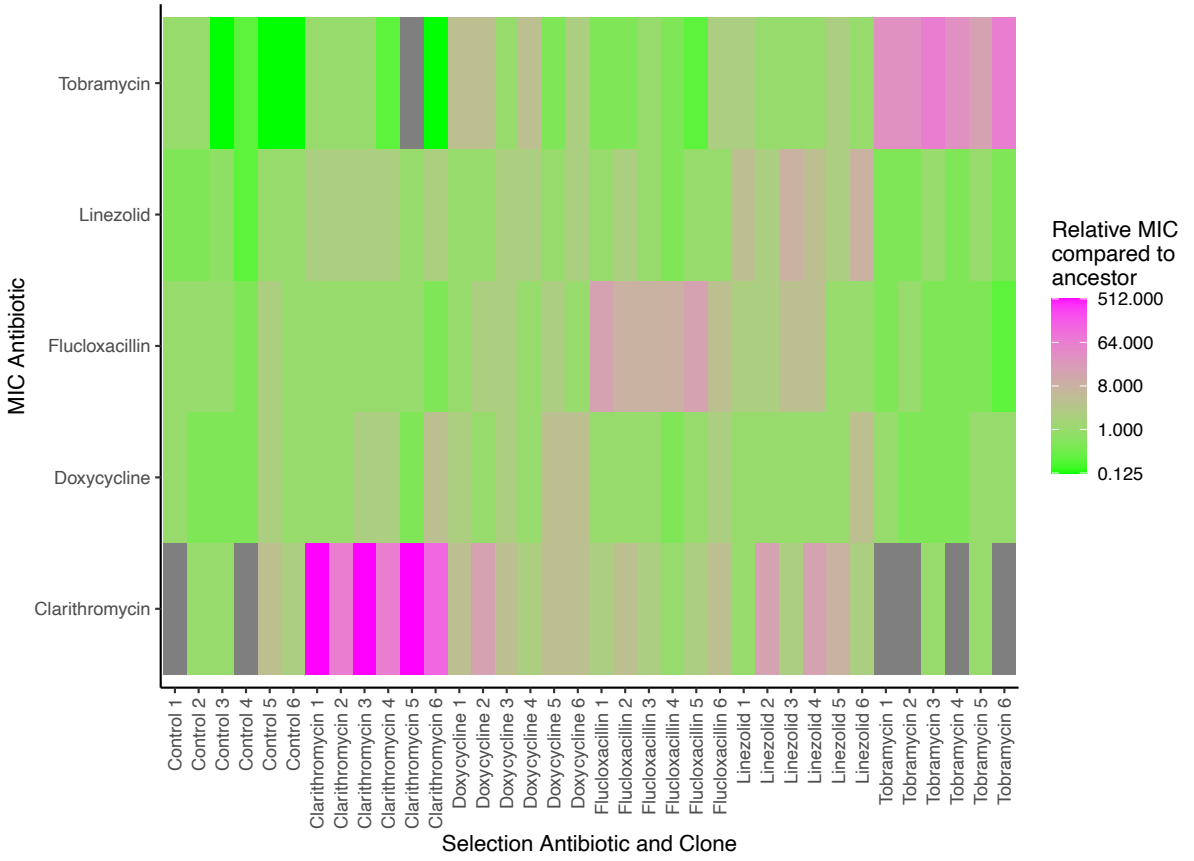

Figure 4-16: Some individual clones display cross antibiotic resistance

Relative MICs of each clone measured in Figure 4-15 on an antibiotic gradient of clarithromycin (0.125-128 µg/ml), daptomycin (0.0625-64 µg/ml), doxycycline (0.125-128 µg/ml), flucloxacillin (0.00781-8 µg/ml), linezolid (0.25-256 µg/ml) or tobramycin (0.0625-64 µg/ml) before 48 h incubation with bacteria at 37℃, 5% CO_2. Normalisation by dividing by ancestor MIC in the respective antibiotic. Antibiotic selection for 20 transfers in selection antibiotic gradient or antibiotic free conditions (control) for 6 independent lines (1-6). Grey= no change in MIC compared to ancestor, green= lower MIC and pink=higher MIC compared to ancestor. These data are a different representation of the MIC data for all clones in Figures 4-10-15.

Mutations in the ribosomal antibiotic targets may contribute to cross resistance between antibiotics with such targets. Clones evolved in clarithromycin with mutations in the 50S ribosomal subunit L22 showed a trend to higher linezolid MICs compared to all clones other than those evolved in linezolid, although this did not reach significance (Figure 4-17A, p=0.14). This, perhaps in combination with other mutations, may contribute to the significant, albeit small (2-fold) increase in linezolid MICs of clones evolved in clarithromycin noted above (Figure 4-15E). This synergy is potentially due to clarithromycin and linezolid both targeting the 50S ribosomal subunit, resulting in minor changes in the sensitivity of these clarithromycin evolved clones to linezolid.

As well as the expected mutations in PBP-2 in response to flucloxacillin, variants in PBP-2 were unexpectedly also found in 2 clones under doxycycline selection and 1 clone under clarithromycin selection. These mutations were at different loci (Met1-start codon lost, Ala132Thr, Gln528Pro) compared to flucloxacillin (Arg128Cys, Gly142Ser, Ala553Val). There was no significant overall increase in flucloxacillin MIC of these clones with PBP-2 variants (Figure 4-17B, p=0.097). However, the clones displaying PBP-2 variants that evolved under flucloxacillin selection have higher MICs than clones without PBP-2 variants (Figure 4-14D, p=0.0049). Strikingly, the only variant in clone C3 was p.Gln528Pro in PBP-2, implying a direct link to clarithromycin resistance. The population this clone was derived from diverged from the rest of the populations in clarithromycin at transfer 11 (Figure 4-3A), and rapidly reached the maximum attainable concentration of clarithromycin. PBP-2 variants do not ubiquitously result in clarithromycin resistance (Figure 4-17C, p=0.45) highlighting the importance of specific variants.

ATP-dependent protease ATP-binding subunit ClpX (*cplX*) was also strongly associated with selection in multiple different antibiotics. This is a subunit of the Clp protease which can degrade unfolded proteins in an energy dependent manner and is involved in regulating widespread functions across the cell[370,371]. *clpX* variants were found in 11/30 clones under antibiotic selection, with at least 1 clone in each antibiotic treatment but none in antibiotic free selection (Figure 4-17D). These variants had higher flucloxacillin MICs (Figure 4-17D, p=0.036), but no increase in MIC to other antibiotics (clarithromycin, p=0.085; doxycycline, p=0.87; linezolid, p=0.066; tobramycin, p=0.66).

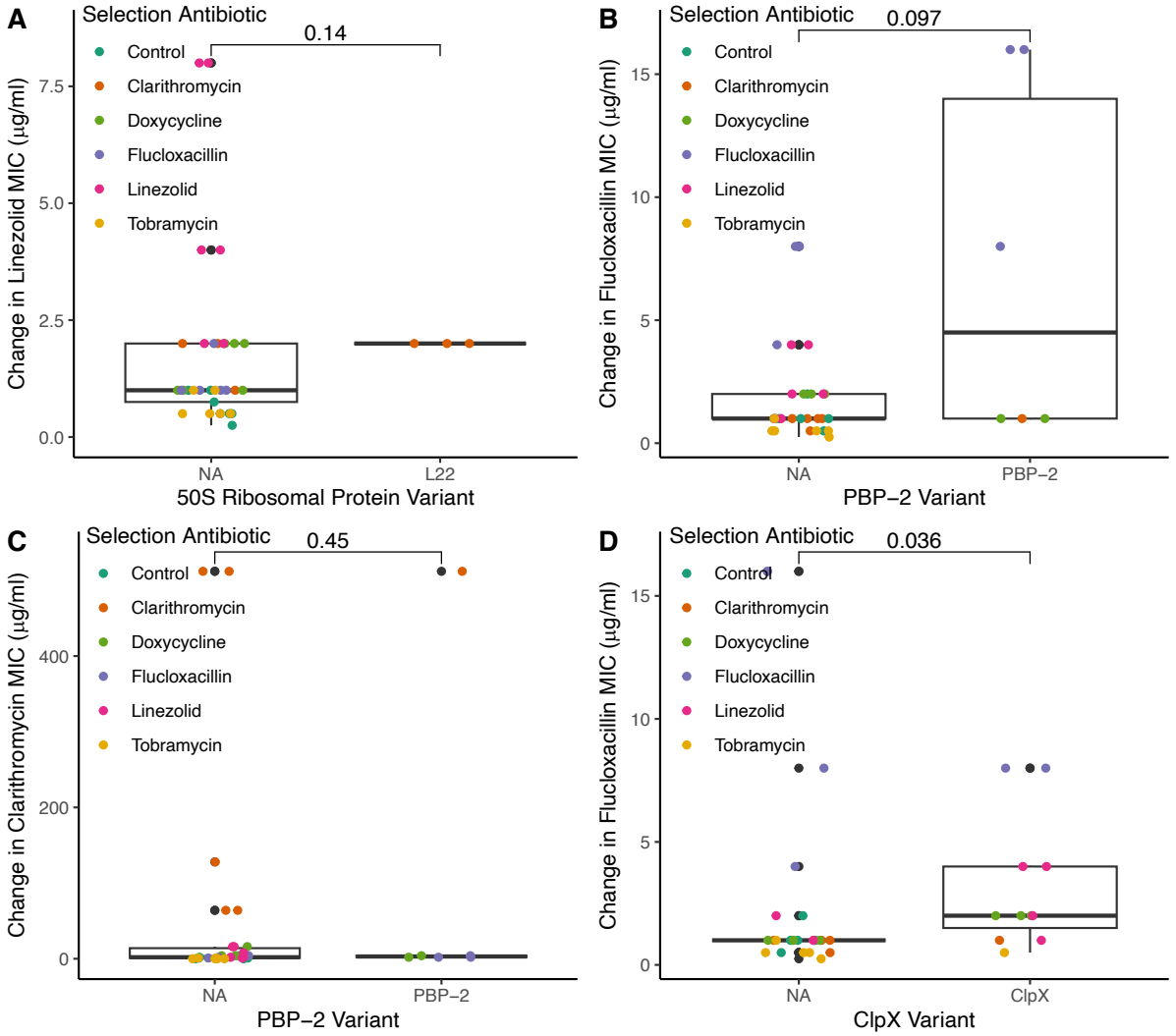

Figure 4-17: Influence of mutations selected across multiple antibiotic conditions on cross antibiotic resistance

MICs from data displayed in Figure 4-15 to A) linezolid, B, D) flucloxacillin, C) clarithromycin or prepared by serial dilutions in 96 well plates (flucloxacillin (0.0078-8 µg/ml), clarithromycin (0.125-128 µg/ml), linezolid (0.25-256 µg/ml)) before 48 h incubation with bacteria at 37℃, 5% CO_2. MIC cut-offs were defined as the lowest antibiotic concentration with no visible bacterial growth. Change in sequenced clone MIC compared to ancestor. Sequenced clone MICs A) with (n=3) or without mutations (n=33) in the 50S ribosomal subunit L22, B, C) with (n=6) or without mutations (n=30) in penicillin-binding protein 2, D) with (n=11) or without mutations (n=25) in ATP-dependent protease ATP-binding subunit ClpX, independent of other mutations within their genomes. Statistical analysis by Kruskal Wallis rank sum test with pairwise-Wilcoxon rank sum post-hoc testing vs. control. Box and whisker plots present median, 25/75% quantile (upper and lower hinge), smallest/ largest observation ≤upper/lower hinge +/- 1.5 inter quantile range (whiskers).

Discussion

Using in vitro evolution, I show that variants in multiple genes of *S. aureus* SH1000 were associated with the evolution of antibiotic resistance, including mutations that have also been reported in clinical isolates. Fluctuation assays showed higher resistance mutation rates against flucloxacillin than clarithromycin and tobramycin, but resistance by spontaneous mutations was not observed against doxycycline or linezolid. Using serial passage of clones with individually optimised antibiotic concentrations to maintain evolutionary pressure, I identified several mutations in the bacterial ribosomal apparatus driven by antibiotics that target the ribosome (particularly clarithromycin and linezolid) in addition to mutations in PBP-2 in response to flucloxacillin exposure. Finally, I showed low level cross-resistance among antibiotics associated with their sharing of antibiotic target (e.g. 50S ribosomal protein L22) or the general resistance gene *clpX* which provided broad cross-resistance across all antibiotic classes.

Clones from fluctuation assays had MICs above the clinical breakpoint for: clarithromycin clones, 2-62 μg/ml above breakpoint; tobramycin clones, 30-62 μg/ml above breakpoint. Clones following selection on an antibiotic gradient had MICs above the clinical breakpoint for: clarithromycin, 62-510 μg/ml above breakpoint; linezolid, 4-28 μg/ml above breakpoint; tobramycin, 510-2046 μg/ml above breakpoint. Clones following selection in doxycycline did not have MICs above the clinical breakpoint and for flucloxacillin no breakpoint is provided. Clones in flucloxacillin had high relative gains in resistance, which equated to low absolute increase in resistance (fluctuation assays, 0.0625-0.1875 μg/ml increase; antibiotic gradient, 0.375-1.875 μg/ml increase). 5/6 clones following selection in clarithromycin had clinical levels of linezolid resistance (4 μg/ml increase), although as this is only a 2-fold increase this is within the error of the assay, especially as conditions did not match the EUCAST method. Overall, these could suggest the development of low-level resistance to flucloxacillin and linezolid plus high-level resistance to clarithromycin and tobramycin.

Low-level antibiotic resistance against clarithromycin and tobramycin developed from de novo mutations in an antibiotic-free setting in fluctuation assays and high-level resistance developed in the presence of antibiotics when selected for on an antibiotic gradient.

Horizontal transfer could not contribute to the high-level resistance in fluctuation assays or resistance selection on an antibiotic gradient as these experiments were closed systems without input of external genetic material. The development of high-level resistance against clarithromycin and tobramycin has also been found in clinical settings. Clarithromycin resistance was identified in clinical trials[372] in *H. parainfluenzae* prior to patients receiving clarithromycin, supporting the existence of resistance in the environment which have not been selected for by antibiotics. Tobramycin resistance is common in MRSA strains with resistance in 99% of isolates in one study in Iran[373] and 85% in a study in Japan[374] suggesting regional variation which could be influenced by antibiotic availability and prescribing regimes.

Spontaneous mutations in antibiotic-free or sub-MIC antibiotic concentrations can drive the acquisition of high-level resistance in the presence of antibiotics[375,376] as seen in clarithromycin and tobramycin selection on an antibiotic gradient. The increase in MICs between antibiotic resistance clones selected for in fluctuation assays compared to those on an antibiotic gradient suggest bacteria further adapt to the antibiotic environment following spontaneously acquired antibiotic resistance. Clones following selection on a clarithromycin gradient had no change in growth compared to antibiotic free conditions, suggesting any fitness cost associated with acquisition of resistance has been overcome by compensatory mutations[377]. To confirm this, clarithromycin evolved clones from earlier points in the selection experiment (i.e. transfers 5 and 10) could be sequenced and their growth measured to see if in the acquisition of resistance caused a decrease in growth which was subsequently compensated for. In contrast, clones in tobramycin had a significant decrease in growth that was still apparent at the end of the 40-day experiment. This is a cost of resistance and would be expected to be outcompeted in an antibiotic-free environment in vivo, limiting the spread of resistance, unless other factors such as reduced nutrient requirements, compensated for the reduced growth rate. Competition assays or a more complex assay environment would be needed to test this.

Most variants with high level resistance to clarithromycin and tobramycin had mutations within genes directly associated with the antibiotics target, or to closely related targets as also found in clinical isolates. Clarithromycin resistant clones predominantly had mutations within the 50S ribosomal subunit (L4, L22 or L32)[355-357]. Multiple different mutations were

found in the same genes, but at different loci. Reliance on the same targets in this rapid phase of resistance development has previously been described as “gambling for existence”; these mutations may not be beneficial for long term existence in the environment[378,379]. All but one of these clones also carried variants in multiple sites. Further study would be required to see if these are facilitating the gain of high-level resistance mutations, compensating for the cost of resistance, or inconsequential mutations[199]. This might require complex and time-consuming techniques such as site-directed mutagenesis to re-create single mutations in isolation which was felt to be beyond the scope of this thesis.

Evolution in tobramycin was strongly associated with mutations in elongation factor G[308,326], with limited efficacy in driving ribosomal mutations. 5/6 clones evolved in tobramycin developed mutations in Elongation Factor G encoded by *fusA*; such mutations have been widely reported in clinical *S. aureus* isolates, for example associated with resistance to fusidic acid[380]. Importantly, fusidic acid (used as both an oral and topical anti-staphylococcal agent) inhibits protein synthesis by binding Elongation Factor G, inhibiting both peptide translocation and ribosome disassembly[381]. Unfortunately, I did not include fusidic acid in my antibiotic panel, but it would have been of interest to see if tobramycin induced cross-resistance with this agent as this could be a clinically relevant interaction.

Low-level antibiotic resistance can be defined as “MIC higher than is common for the susceptible population, devoid of any acquired resistance mechanism”[382]. This can be, but is not inevitably, a gateway to higher level resistance. Gomez et al.[383], found low level resistance in *Mycobacterium smegmatis* from ribosomal mutations facilitated high level resistance in a multi-drug setting[383]. In my assays, low-level resistance was seen in clones following selection on an antibiotic gradient in flucloxacillin and in most resistant linezolid clones. Low level resistance will increase the duration of antibiotic treatment needed to effect a cure, and therefore may also increase the likelihood of cooperative resistance mechanisms to arise or a horizontal gene transfer event with a relevant resistance gene to occur in vivo[377,384,385]. Antibiotic concentrations vary spatially in the human body in due to variations in metabolism, cell binding, access, rate of elimination, time since dosing, and interactions with normal or pathogenic flora[386]. Additionally, there are environmental sources of antibiotics, including

sewage, animal feed and water sources[387]. Hence, bacteria are exposed to a range of antibiotic concentrations to be able to develop these low-level resistance phenotypes.

Doxycycline was the only antibiotic where clones did not display a significant increase in MIC compared to their ancestor in the corresponding antibiotic following exposure to the antibiotic gradient (Figure 4-13B). This is consistent with the whole genome sequencing analysis which did not find any genes directly related to doxycycline's target, 30S ribosomal subunit, nor any translational proteins (Figure 4-13A). Depending on the selection experiment, levels of doxycycline resistance and mutated targets have been found. *E. coli* has been shown to develop doxycycline resistance following selection on an antibiotic gradient, with mutations in ribosomal proteins and reduction in carbon metabolism[325]. In contrast, Toprak et al.[388] developed ~10 fold increased in doxycycline resistance in *E. coli* and also found no mutations in ribosomal genes. This could be due to ribosomal mutations having a high growth cost[383] in the competitive environment of the populations within liquid culture selection experiments. Two previous studies also found evolving resistance to doxycycline was slow, with the clinical breakpoint not reached in *S. aureus* after 5 transfers[191] or, in *V. cholerae*, ~210 days (220 transfers) were required to reach MIC breakpoint[324]. However, both these studies identified on target mutations in 30S ribosomal subunit S10[191,324]. My work likely did not evolve *S. aureus* in doxycycline for long enough to acquire resistance. I did identify some general antibiotic resistance genes, including PBP-2 and *clpX*, which account for the non-significant trends in doxycycline resistance seen. Since doxycycline resistance is common in clinical settings (e.g. 31% of MSSA and 49% of MRSA isolates from a hospital in Iran were doxycycline resistant in a recent study[389]), additional drivers may contribute to such resistance to arising. I explore one such additional mechanism (namely hypoxia) in subsequent work (see Chapters 5 and 6).

Mutations that confer more general resistance mechanisms were seen across antibiotic treatments but not in the antibiotic-free controls. These included mutations within ClpX and PBP-2. ClpX is involved in a broad range of regulation mechanisms within the cell, acting as a chaperone or, in combination with ClpP and protease to degrade proteins and peptides. It influences cellular processes including cell division, in the synthesis of the septum, degradation of *ftsZ,* and it is important for resistance to immune peptides including LL-37.

This observation was influential in my choice of LL-37 as a factor that might interact with antibiotics to modify bacterial killing (see Chapter 7). *clpX* mutations have previously been identified as driving resistance in the evolution of *E. coli* in neomycin and ciprofloxacin[243]. When *clpX* was inactivated in MRSA (clone USA300), bacteria were highly resistant to β-lactams and had increased susceptibility to daptomycin[202]. Deletion of *clpX* causes high-level β-lactam resistance with cells being smaller, associated with higher levels of peptidoglycan crosslinking and thicker cell walls[199,367,390,391]. PBP-2 has 2 functional domains, the transpeptidase domain essential for growth and survival, and the transglycosylase domain for cell wall biosynthesis and growth. The transpeptidase domain catalyses peptidoglycan chain crosslinking and elongation. It is directly targeted by β-lactam antibiotics, with its activity compensated for by *mecA* inducing PBP-2a in MRSA. The transglycosylation domain catalyses the elongation of un-crosslinked peptidoglycan chains[392,393]. Across all antibiotic conditions, 6 clones acquired PBP-2 mutations. Interestingly, 1 clone evolved in doxycycline had lost the start codon; it is unknown how this clone was able to survive as PBP-2 is an essential gene[394]. This clone needs to be re-sequenced and analysed to verify this result. For 3 flucloxacillin-evolved clones, PBP-2 variants could be leading to resistance through decreased affinity to the binding site, driving the low level of resistance seen[395]. The other 3 clones which evolved in doxycycline or clarithromycin did not confer a change in sensitivity to flucloxacillin. PBP mutations influencing low level resistance to clarithromycin and doxycycline have been identified in clinical isolates of *Streptococcus pneumoniae*[396]. This change in antibiotic sensitivity could be due to altered cell surface properties[397] altering antibiotic cell penetration and access to the ribosome. However, Clone 3 evolved in clarithromycin had only a single PBP-2 mutation and this was associated with high level resistance to clarithromycin. This might be confirmed in future studies by site-directed mutagenesis and the mechanism further explored, for example by in silico modelling.

Physiological changes which alter bacterial growth rate can influence ribosome number and sensitivity to antibiotics. Antibiotics which bind reversibly, such as clarithromycin and doxycycline, have been shown to be less efficient in the setting of reduced growth rates[398]. However, I found no significant change in bacterial growth of clones evolved in clarithromycin or doxycycline compared to clones evolved in no antibiotic. In the fluctuation assays, clarithromycin resistant clones only appeared after 48 h incubation. Growth curves of clones

from fluctuation assays were not measured, although a growth defect would be expected. These results suggest any initial defect in growth as clarithromycin resistance is acquired is compensated for by subsequent mutations. Further study could show if the changes in PBP-2 in these non-flucloxacillin clones influences growth rate and antibiotic susceptibility, either by selecting clones early in the selection process before compensatory mutations have been acquired or by carrying out site directed mutagenesis to study specific mutations.

The increased number of variants in clones following selection in flucloxacillin, compared to clones in other antibiotic and controls, suggests flucloxacillin is driving enhanced rate of de novo mutations. This has also been seen for other antibiotics in a range of bacterial species with norfloxacin and streptomycin increasing mutation rates in *E. coli*[399,400], and quinolones increasing the mutation rate in *Salmonella*[401]. This can be due to a bacterial stress response, selection of mutations which increase mutability or some antibiotics themselves increasing mutability[402-404]. Higher mutation rates in flucloxacillin could reflect its bactericidal mechanism, compared to the other antibiotics which are bacteriostatic through targeting the ribosome[404]. Additionally, the fluctuation assays with highest mutation rate was for flucloxacillin, where antibiotic exposure was after mutation selection, suggests this could be from a high number of cooperative targets or access pathways leading to resistance[405]. This is supported by 2 clones, following flucloxacillin evolution , with multiple variants in targets not known to be directly related flucloxacillin resistance.

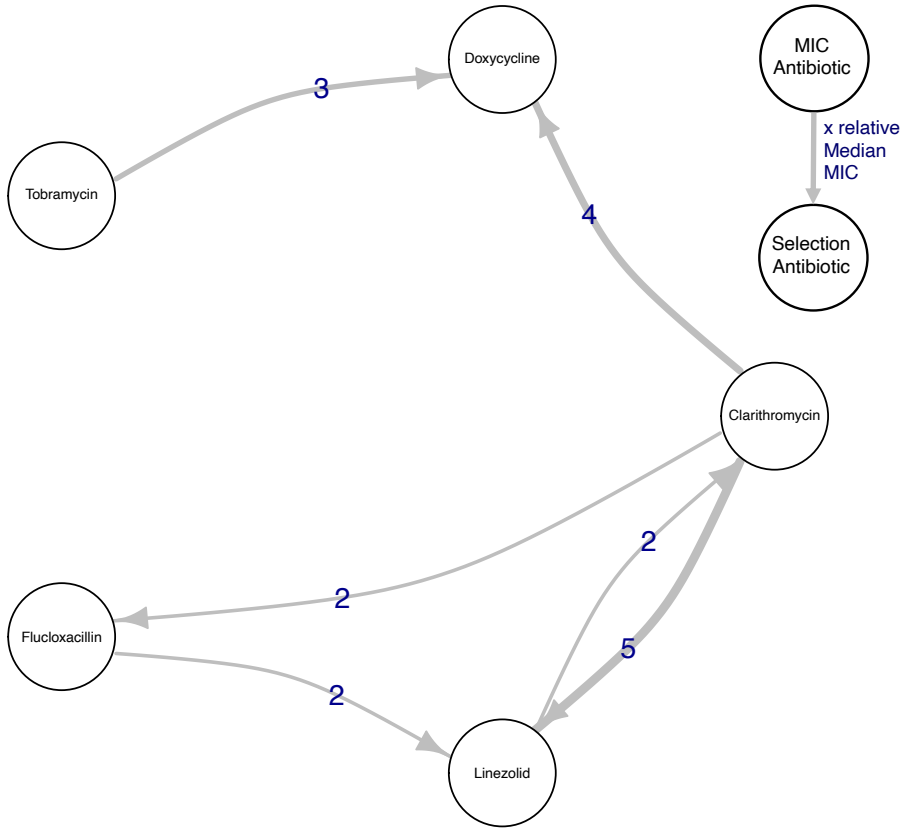

Figure 4-18: Schematic summarising cross resistance networks.

Antibiotic cross resistance network from MICs in Figure 4-15. Based on median of relative MIC for each group calculated by dividing MICs by the ancestor. Relative median MIC increases of ≥2 shown and labelled, with magnitude proportional to arrow width. Arrows from the antibiotic the MIC was measured in to the antibiotic resistance had been selected against by 20 transfers on an antibiotic gradient.

In this study I identified clones with antibiotic cross-resistance following evolution in other antibiotics. To summarise changes in cross-resistance, I normalised the median MIC of clones evolved in the same antibiotics and normalised these data to the ancestors MIC in the same antibiotics to create a cross resistance network (Figure 4-18) which is shown here due to the extent these data have been normalised and averaged to create this network. This cross-resistance network indicates where low levels of cross resistance may be occurring, even if no significant interactions were identified when comparing the MICs of groups of clones based on evolution antibiotics in Figure 4-15. Only clarithromycin selection led to a significant, albeit very small, decrease in linezolid sensitivity (Figure 4-15E), with all other changes being clone specific. These changes in sensitivity are small and do not equate to resistance. However, small changes in low-level resistance can facilitate high level resistance particularly when acting cooperatively when a horizontal element is acquired[199].

The cross-resistance network in Figure 4-18 shows cross-resistance is not necessarily bi-directional, as previously described for *E. coli*[406]. Strikingly, clones evolved in doxycycline had an increase in median MIC in tobramycin and clarithromycin, which was not recipricated. This is despite clones evolved in doxycycline not developing significant levels of doxycycline resistance (Figure 4-13) or having any mutations in doxycycline's target the 30S ribosomal subunit. Clones evolved in doxycyline did have mutations in *clpX* and PBP-2 which could be contributing to resistance in tobramycin and clarithromycin. Previously, aminoglycoside (tobramycin) resistant *E. coli* has been shown to have few cross resistance interactions[286], including against doxycycline. This difference could be due to different mutations accumulated between species when clones acquire low versus high level doxycycline resistance.

Four of the antibiotics studied in this chapter target the ribosome, and despite having different specific targets, which may increase the likelihood of cross-resistance. A previous study in *S. aureus* found no relationship between the antibiotic target and cross-resistance when high level resistance developed[191]. I did not include enough antibiotic targets to fully assess this. The high number of ribosomal mutations I found, and trend towards 50S ribosomal protein L22, contributing to clarithromycin, linezolid cross resistance, supports mutations in antibiotic targets driving low levels of cross resistance. The contribution of

mutations in the antibiotic targets support previous calls for new antibiotic classes and targets[407], despite these proving challenging to achieve.

Some elements of the experimental design limit how relevant these findings are to clinical infections. The MIC values measured in this work are not directly comparable with EUCAST values[259], since media and incubation times differed from the standard method to match evolution conditions, so can only be indicative of the extent of resistance. Additionally, these clones evolved from the laboratory adapted strain SH1000, which has a divergent phenotype from clinical isolates[408], so these antibiotic evolved clones would not be likely to be pathogenic or even to survive in an in vivo setting.

The different mechanisms for the development and retention of antibiotic resistance have important possible implications for the spread of antibiotic resistance. The lack of detectable spontaneous mutations causing linezolid and doxycycline resistance means lower levels of resistance would be expected to exist against these antibiotics prior to treatment starting, increasing the likelihood of successful treatment. There was no significant decrease in *S. aureus* growth in antibiotic-free settings of clones with point mutations causing clarithromycin, flucloxacillin and linezolid resistance compared to their ancestor, SH1000. Limited fitness costs once *S. aureus* has evolved in the antibiotics means resistance would be expected to persist after antibiotics are removed from the environment which could be contributing to the limited success of antibiotic cycling reducing antibiotic resistance in previous clinical studies[409].

5 Adaptation of Antibiotic Resistant Populations to Hypoxia and Antibiotics

5.1 Introduction

Staphylococcus aureus is a Gram-positive commensal bacterium capable of causing a wide range of infections[1]. Although naturally highly susceptible to antibiotics, *S. aureus* has proven adept at acquiring resistance mechanisms, and its consequently increased level of antibiotic resistance poses a serious challenge for the effective treatment of infections[2,3]. Of particular concern is the ability of *S. aureus* to acquire novel resistance mechanisms by horizontal gene transfer[2]. Antibiotic resistance necessitates changes to the standard antibiotic treatments for example in the setting of methicillin, vancomycin or tetracycline resistance[410,411]. Methicillin resistance is mostly caused by the acquisition of *mecA*, encoding the alternative penicillin binding protein 2a[199]. Vancomycin resistance is caused by the *vanA* operon, with multiple genes coordinated to induce resistance, although this is still uncommon[412]. Resistance to tetracyclines in encoded by genes including the tetracycline-specific efflux pumps, Tet(K) and Tet(L), conferring resistance to multiple tetracyclines[300,413]. Tetracyclines are inexpensive broad-spectrum antibiotics widely used to treat both human and animal *S. aureus* infections globally. Doxycycline is commonly used to treat community acquired *S. aureus* infections, as it is often effective against MRSA[414]. It is recommended for the treatment of outpatients with community-acquired pneumonia[415], and for many other respiratory and skin infections[292,416], particularly in the context of penicillin allergy. Outpatient prescribing of doxycycline has recently increased with the onset of the COVID-19 pandemic, accounting for 10.5% of prescriptions in one study in 2020 compared to 4.9% in 2019[417]. Therefore, limiting the spread of tetracycline resistance is an urgent priority.

Horizontally acquired resistance mechanisms are unlikely to be well adapted to their new genomic context. Indeed, newly acquired resistance mechanisms are often associated with fitness costs[352,418], which may in turn limit the survival and further spread of these resistant genotypes upon removal of antibiotic selection[419]. Such fitness costs can be due to a variety of causes, including the metabolic costs of transcribing and translating the resistance genes[420], or the incoming genes being mismatched with the new genomic environment (e.g.

in terms of GC-content or codon usage) or in conflict with other genes resident in the genome[418]. Experimental evidence from a range of systems suggests that some of these initial fitness costs of acquiring resistance genes can be rapidly negated through compensatory evolution[245,421,422]. Compensatory mutation(s) may directly affect the newly acquired genes themselves, or occur at other genomic loci[423], and have been shown to enable the maintenance of resistant genotypes both in laboratory and natural populations of bacteria[422,424].

Variation in infection-relevant physiological parameters could also affect the fitness cost of newly acquired resistance mechanisms in pathogens. Conditions at infection sites can vary substantially, both between different types of infection and across spatiotemporal microenvironments within an infection[425,426]. Tissue oxygen levels even in health are low, with oxygen tension falling to 20–30 mmHg (3.6-3.9 kPa) in capillaries and further as oxygen diffuses into the surrounding tissues. This 'physiological' hypoxia is further enhanced during infections due to the high respiratory demands of pathogens and immune cells, which result in marked oxygen consumption[16,64]. 'Pathological' hypoxia is a common feature of *S. aureus* infections: for example, the archetypal *S. aureus* abscess can prevent material exchange and antibiotic penetration through its fibrous capsule, exacerbated by poor blood supply to the necrotic centre[62,63]. *S. aureus* is thus exposed to profound hypoxia (or even anoxia) in many chronic infections including the cystic fibrosis airway[65], chronic osteomyelitis[66] and diabetic foot ulcers[67], resulting in phenotypic changes to bacteria[427-429]. *S. aureus* responds to the hypoxic environment through the two-component system *ssrAB* (staphylococcal respiratory response AB) regulating the production of virulence factors to resist oxidative stress and allowing metabolic adaptation[16,430,431]. Additionally, short term exposure to hypoxia *in vitro* has been shown to influence key pathogenic characteristics, including biofilm formation and adhesion[45]. However, the effect of hypoxia on the fitness costs of horizontally acquired resistance mechanisms, such as tetracycline efflux pumps, is currently unknown, although niche adaptation has been shown to enhance the stability of newly acquired resistance plasmids[432].

To study the impact of hypoxia on horizontally acquired resistance genes, I first tested the fitness cost associated with 3 antibiotic resistance genes in hypoxia. I then evolved

tetracycline resistant *S. aureus* in hypoxia with and without tetracyclines to see how *S. aureus* adapts to a recently acquired gene when it is, or is not, essential for survival. Finally, to see the impact of evolution in hypoxia and tetracyclines on tetracycline resistance *S. aureus*, I measured evolved population growth and antibiotic resistance.

5.2 Hypothesis and aims

In this chapter I have tested the following research hypothesis:

Environmental hypoxia will interact with antibiotics to impact the fitness cost of horizontally acquired resistance genes, but evolutionary adaptation over longer timescales will enable bacteria to ameliorate these fitness costs.

The specific aims addressed in this chapter are:

- Determine if hypoxia influences the fitness cost and resistance associated with acquiring resistance genes
- Characterise population behaviour of *S. aureus* during prolonged exposure to hypoxia with or without tetracyclines
- Examine the growth and antibiotic resistance of evolved populations following selection in tetracyclines and hypoxia

5.3 Results

5.3.1 Tetracycline resistance is costly in hypoxia but not in normoxia

To mimic the horizontal acquisition of a new antibiotic resistance gene I used *S. aureus* strains SH1000 and NewHG, with resistance genes, *tetL, kan and erm* (tetracycline, kanamycin and erythromycin resistance, respectively) inserted into the chromosome at the *lysA* locus[232,433,434] (hereafter SH1000_TetR, SH1000_KanR, SH1000_EryR, NewHG_TetR, NewHG_KanR and NewHG_EryR). SH1000_TetR was made by McVickers et al.[435] using the *tetL* gene from pAISH1[436] inserted into the pMUTIN4 suicide vector[433] which inserted *tetL* after the *lysA* site in SH1000. *lysA* remained intact evident by SH1000_TetR's ability to grow on minimal media. To test the immediate impact of acquiring these resistance genes on fitness and how this varied with oxygen availability, each resistance clone was competed against the relevant parental strain over 24 h in normoxia (21% O_2, 5% CO_2, 37°C) or hypoxia (0.8% O_2, 5% CO_2, 37°C), herein referred to in the text simply as 'normoxia' and 'hypoxia'. Fitness was assessed by plating onto BHI agar with/without the corresponding antibiotic (section 3.2.8).

SH1000_TetR, NewHG_TetR, and NewHG_EryR showed significantly lower fitness relative to their parent in hypoxia compared with normoxia (Figure 5-1: A) SH1000_EryR, p=0.823; SH1000_KanR, p=0.837; SH1000_TetR, p=0.003; B) NewHG_EryR, p=<0.001; NewHG_KanR, p=>0.999; NewHG_TetR, p=0.018). These data suggest that hypoxia can significantly increase the fitness cost of horizontally acquired genes. Both strains carrying *tetL* consistently present a decrease in fitness in hypoxia compared to their parent. In contrast, strains carrying *kan* did not show a significant decrease in fitness in hypoxia. The *erm* gene was only associated with a fitness cost in hypoxia only in the NewHG background. Together these suggest the fitness cost of SH1000_TetR and NewHG_TetR in hypoxia is not associated with disruption to the LysA insertion locus. This is also unlikely due to mismatching with the genetic background as there was the fitness cost when *tetL* was inserted into both SH1000 and NewHG. In addition to the relative fitness cost between normoxia and hypoxia, SH1000_TetR also displayed a large fitness cost compared to their ancestor in hypoxia but not normoxia (one sample t-tests against 1, normoxia p=0.74, hypoxia p=0.0064).

To determine whether the fitness cost in hypoxia influenced bacterial growth, growth curves were carried out for SH1000 and SH1000_TetR (Figure 5-2A) with optical density assessed at 0, 1, 2, 3, 4, 5, 6, 7, 24 h. Statistical analysis of the area under the curve (Figure 5-2B) shows no significant difference between the growth of SH1000 and SH1000_TetR in the same oxygen tension (normoxia $p=0.490$; hypoxia $p=0.749$). As previously established[437], there was a significant decrease in growth in hypoxia compared to normoxia for both strains (SH1000 $p<0.001$; SH1000_TetR $p<0.001$). These growth patterns were also seen when comparing normoxic and hypoxic growth NewHG to NewHG_TetR (Figure 5-3). The detection of fitness costs due to antibiotic resistance genes in hypoxia using fitness assays and not growth curves likely represents the higher sensitivity of fitness assays, which incorporate all aspects of the growth cycle and allow direct competition between clones[438].

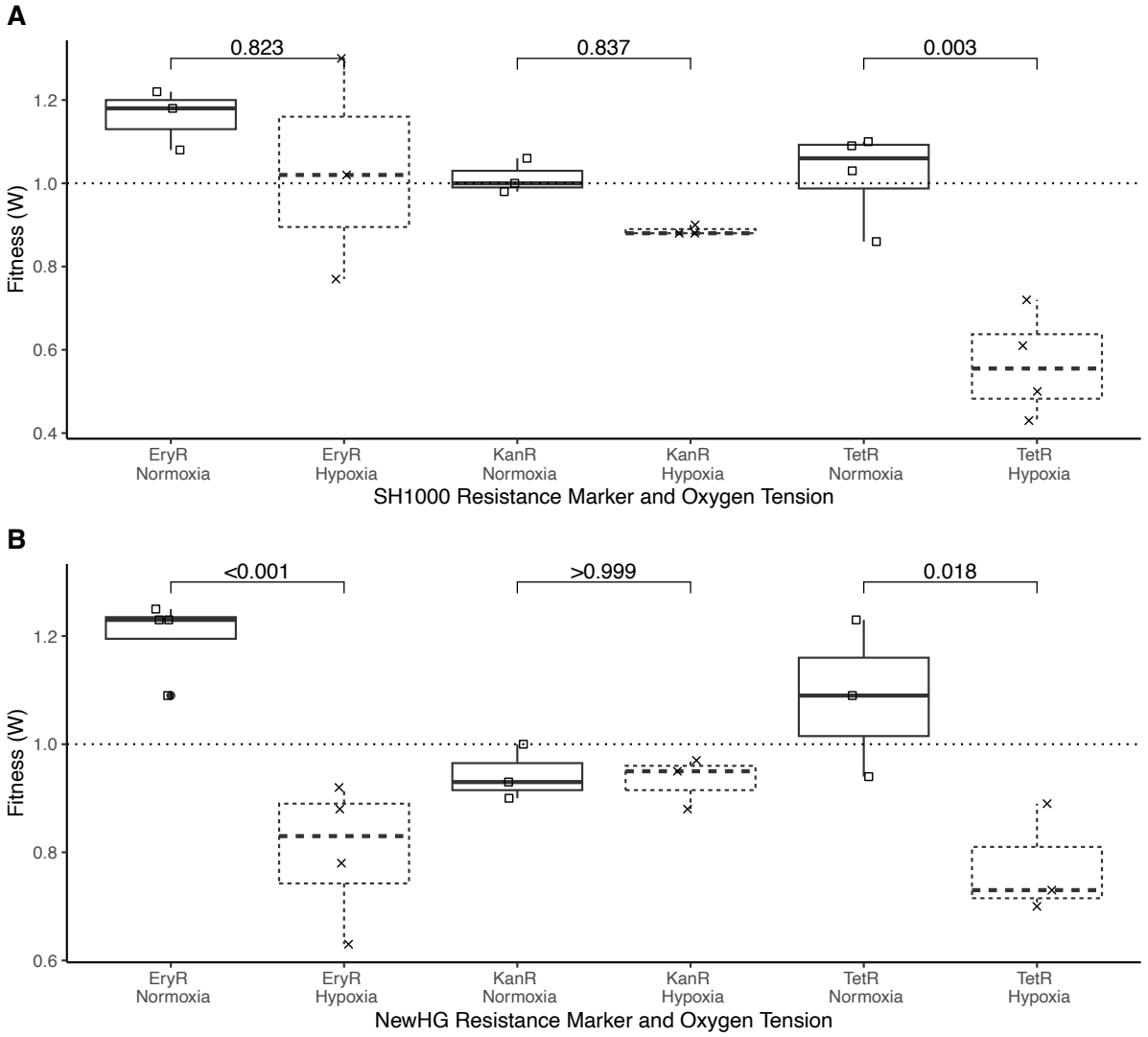

Figure 5-1: Fitness cost of antibiotic resistance genes in hypoxia

Competition assay showing the fitness of A) SH1000 or B) NewHG competed against the isogenic strain with antibiotic resistance insertion tetL*,* kan *or* erm *at* lysA *site, in normoxia or hypoxia after 24 h competition. A 1:1 ratio of competing strains was established from normoxic overnight cultures at 0h before 24 h incubation in normoxia (21% O_2, 5% CO_2, 37°C; squares) or hypoxia (0.8% O_2, 5% CO_2, 37°C; crosses) with initial and final ratios confirmed by plating on selective/non-selective agar, enabling calculation of fitness index (section 3.2.8). Dashed line at 1 indicates no fitness cost, <1 show a fitness cost of the resistance gene. Results are n=3/4 independent experiments performed in triplicate with lines connecting linked results. Statistical analysis by paired t-test. Additional statistical analysis in A) SH1000_TetR one-sample t-test against 1: normoxia p=0.74, hypoxia p=0.0064.*

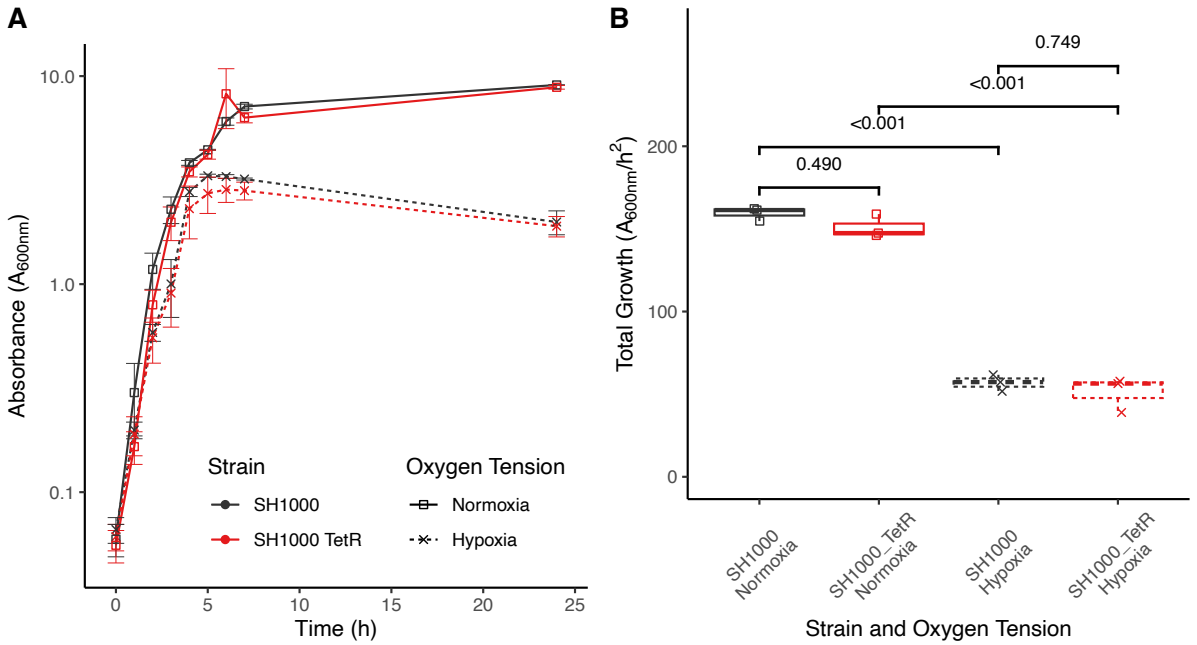

Figure 5-2: TetR does not influence total growth of SH1000 in normoxia or hypoxia

Growth curves of SH1000 (black) and SH1000_TetR (red) in normoxia (squares, solid lines), (21% O_2, 5% CO_2, 37°C) and hypoxia (crosses, dashed lines), (0.8% O_2, 5% CO_2, 37°C). A) A starting density of $A_{600\ nm}$=0.05 was established from normoxic overnight cultures in hypoxia and normoxia. $A_{600\ nm}$ measurements were taken at timepoints shown. Data represent mean +/- SE. B) Integrals of growth curves in A. Statistical analysis by 2-way ANOVA with Tukey's multiple comparisons, n=3. Box and whisker plots present median, 25/75% quantile (upper and lower hinge), smallest/ largest observation ≤upper/lower hinge +/- 1.5 inter quantile range (whiskers).

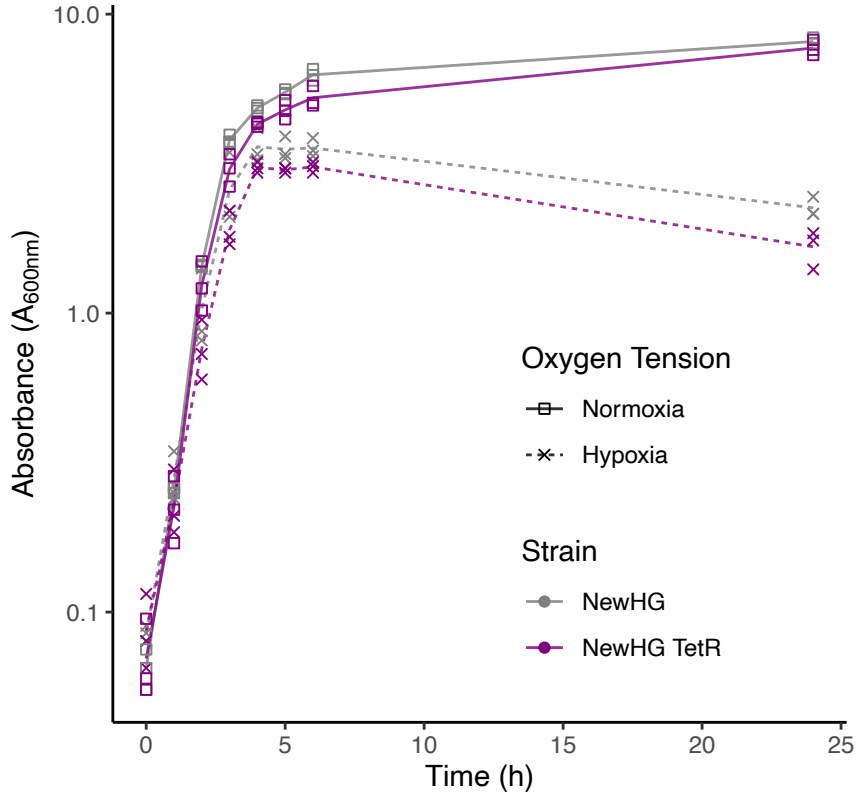

Figure 5-3:Tetracycline resistance had little impact on NewHG growth

Growth curves of NewHG (grey) and NewHG_TetR (purple) in normoxia (squares, solid lines), (21% O_2, 5% CO_2, 37°C) and hypoxia (crosses, dashed lines), (0.8% O_2, 5% CO_2, 37°C). A starting density of $A_{600\ nm}$=0.05 was established from normoxic overnight cultures in hypoxia and normoxia. $A_{600\ nm}$ measurements were taken at timepoints shown. Data represent n=1. Mean and technical replicates shown.

Since no clear explanation was apparent for the increased fitness cost of SH1000_TetR in hypoxia, whole genome sequencing was carried out to confirm the resistant gene location, identity and any SNPs or indels. Illumina sequencing by MicrobesNG (www.microbesng.com), followed by alignment to the reference NCTC 8325 (genome accession number: CP000253) allowed analysis to identify any genetic differences between SH1000 and SH1000_TetR. Both strains were isogenic other than the *tetL* insertion, which was confirmed at the *lysA* insertion site within the pMUTIN2 integrational vector, as expected. Unexpectedly, a SNP at 1,720,851bp on the NCTC 8325 genome was identified in SH1000_TetR within the protein Universal Stress Protein A (UspA). This could influence the fitness of SH1000_TetR in hypoxia, as UspA has been associated with the stringent response[439]. Within the UspA variants' amino acid sequence, this SNP is predicted to cause a missense mutation, resulting in the amino acid change from leucine to glutamine. This changes the residue polarity from non-polar to polar which could influence hydrogen bonding and the residues possible conformations within UspA. To see if UspA influences hypoxic growth, growth curves were carried out with the UspA transposon mutant from the Nebraska library (UspA_KO) compared to its parent, USA300 LAC JE2[254]. The location of the transposon mutant has not been verified. There were no significant differences between the growth of USA300 LAC JE2 and UspA_KO in normoxia or hypoxia (Figure 5-4: normoxia p=0.092; hypoxia p=0.998) suggesting UspA is unlikely to be causing a large change in hypoxic growth. UspA variants will be closely interrogated in subsequent sequencing of clones as it could still influence the fitness cost seen in hypoxia, given this is a more sensitive assay than growth curves (Figure 5-1 versus Figure 5-2). Importantly, no SNPs were found in NewHG_TetR UspA, although variants were found at 1,163,029 (*uvrC*, Leu205Ile), 1,443,839 (*lysA*, Asn24Ser), 1,449,010 (Unknown protein, Gly14 frame shift) and 1,838,239 (unknown protein, Gly396Asp). It was decided to take SH1000_TetR forward for further investigation as it contained fewer SNPs compared to its parent and *uspA* had no clear impact on hypoxic growth.

Antibiotic breakpoints in normoxia and hypoxia were checked for the functionality of *tetL* plus any impact of hypoxia on antibiotic sensitivity. Minimum inhibitory concentrations (MICs) were determined following 20 h incubations of bacteria within an antibiotic gradient with serial 2-fold dilutions (SH1000: 0.125-128 µg/ml; SH1000_TetR: 0.25-256 µg/ml) in tetracycline (TET) and doxycycline (DOX). SH1000_TetR showed substantially increased

resistance to TET (mode TET MIC: SH1000, 0.5 μg/ml; SH1000_TetR, 64 μg/ml) and DOX (mode DOX MIC: SH1000, 0.5 μg/ml; SH1000_TetR, 8 μg/ml) relative to SH1000 both in hypoxia and normoxia (Figure 5-5, TET: normoxia p=0.005; hypoxia p=0.0025; DOX: normoxia p=0.072; hypoxia p=0.0053), although the DOX MICs were insufficiently powered to show significant differences. This confirms activity of *tetL* in the target and likely a second-generation tetracycline that is widely used clinically. No significant differences were seen in MICs measured in normoxia or hypoxia (Figure 5-5, TET: SH1000 p=0.209; SH1000_TetR p=1; DOX: SH1000 p=0.161; SH1000_TetR p=0.606) indicating hypoxia has no significant impact on antibiotic sensitivity.

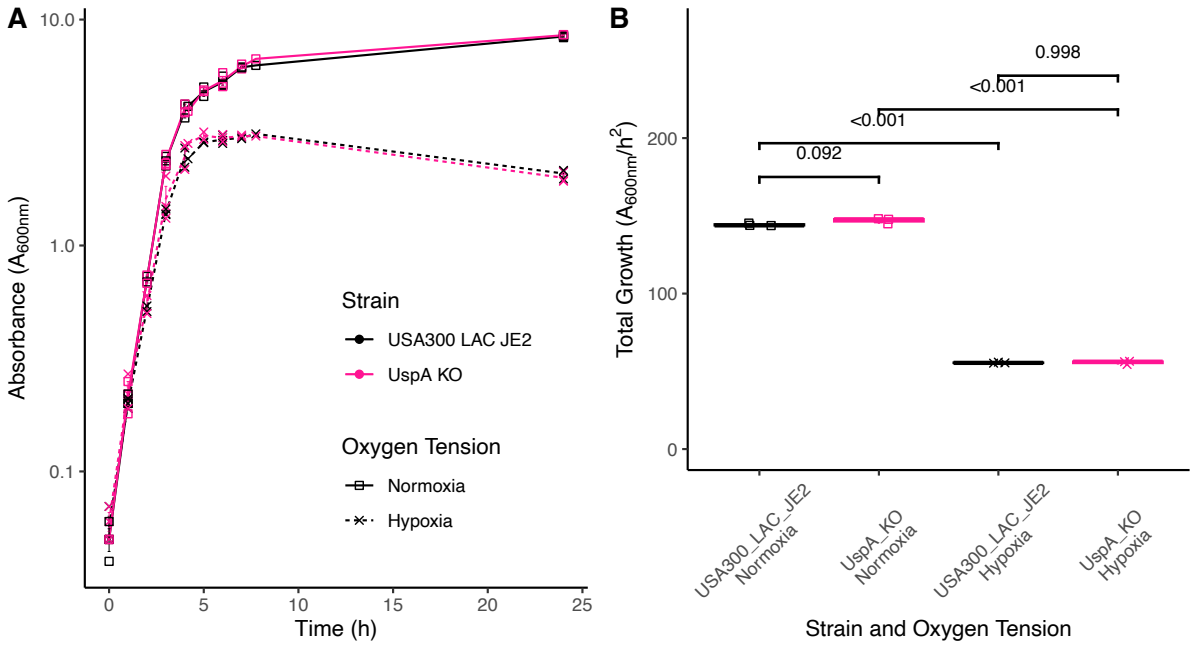

Figure 5-4: UspA transposon mutant has similar growth to ancestor.

Growth curves of USA300 LAC JE2 (black) compared to UspA transposon mutant from the Nebraska library[254] (pink) in normoxia (squares, solid lines), (21% O_2, 5% CO_2, 37°C) and hypoxia (crosses, dashed lines), (0.8% O_2, 5% CO_2, 37°C). A) A starting density of A_{600nm}=0.05 was established from normoxic overnight cultures and cultures transferred to normoxic and hypoxic conditions. A $_{600\,nm}$ measurements were taken at timepoints shown. Data represent mean +/- SE. B) Integrals of growth curves from A. Statistical analysis by 2-way ANOVA with Tukey's multiple comparisons, n=3 carried out in triplicate. Box and whisker plots present median, 25/75% quantile (upper and lower hinge), smallest/ largest observation ≤upper/lower hinge +/- 1.5 inter quantile range (whiskers).

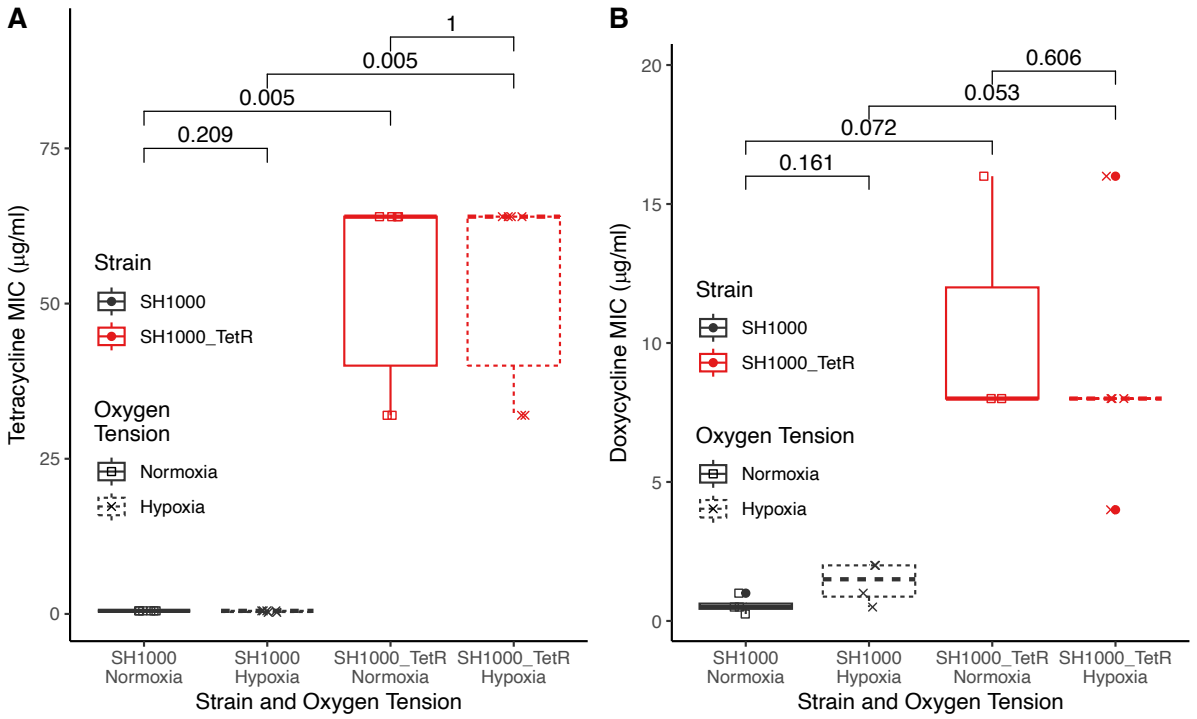

Figure 5-5: Increase in tetracycline resistance from* tetL *insertion

MICs for SH1000 (black) and SH1000_TetR (red) in A) TET or B) DOX in normoxia (squares, solid lines), (21% O_2, 5% CO_2, 37°C) or hypoxia (crosses, dashed lines), (0.8% O_2, 5% CO_2, 37°C). Antibiotics were prepared by ½ serial dilutions (SH1000: 0.125-128 µg/ml; SH1000_TetR: 0.25-256 µg/ml) in equilibrated BHI broth in 96 well plates. Normoxic overnight cultures were diluted to $A_{600\ nm}$=0.05 before 10 µl was added to 90 µl antibiotics then 20 h co-incubation. MIC cut-offs were defined as the lowest antibiotic concentration with no visible bacterial growth in the well, A) n=6, B) n=3-5 independent experiments. Statistical analysis by Kruskal-Wallis rank sum test with Wilcoxon rank sum post-hoc testing and Benjamini-Hochberg correction for multiple comparisons. Box and whisker plots present median, 25/75% quantile (upper and lower hinge), smallest/ largest observation ≤ upper/lower hinge +/- 1.5 inter quantile range (whiskers).

5.3.2 Antibiotic treatment selected for increased resistance but no improvement in growth

To determine the longer-term evolutionary response to resistance gene acquisition and how this varied according to antibiotic selection and oxygen levels, I experimentally evolved 6 replicate populations of SH1000 and SH1000_TetR with or without TET or DOX under either hypoxia or normoxia (SH1000 no antibiotic, SH1000_TetR no antibiotic; SH1000_TetR 30 µg/ml TET; SH1000_TetR 2 µg/ml DOX). Antibiotic concentrations were ¼ (DOX) or ½ (TET) of SH1000_TetR's MIC in each antibiotic as measured (Figure 5-5), aiming to provide a high selective pressure without killing the evolving populations as described in other studies[307]. Every 24 h each population was passaged with a 1-in-100 dilution, routinely used in other studies[243,308,325,353]. Every 24 h optical density was measured and every 5 days a sample from each population was plated to check for contamination, and 20% glycerol stocks were made to store an archive. The evolution, with daily transfers, was continued for 34 days (~200 generations) out of a planned 60 days, cut short due to the COVID-19 lockdown. Therefore, subsequent analysis of populations and clones was carried out from day 30 glycerol stocks. Population 6 of SH1000 in normoxia died out on day 14 and was excluded from subsequent analysis.

Population densities and the factors that influenced them were assessed by a linear mixed effects model, which can incorporate both fixed and random effects, and is useful when there are repeated measures. First, I looked at control SH1000 and SH1000_TetR populations in no antibiotics to see if there is a significant impact of *tetL* in the evolution of SH1000. In the absence of antibiotics, population densities were not influenced by the presence of *tetL* (Strain interaction: Pr(>F) = 0.654; Figure 5-6A, Table 5-1). These populations showed adaptation to the laboratory environment and oxygen tensions over time (Time by Oxygen Tension by Strain interaction: Pr(>F) = 0.000759; Figure 5-6A, Table 5-1). Next, I analysed the SH1000_TetR populations to look at the interaction between antibiotics and hypoxia on the evolution of SH1000_TetR. On exposure to antibiotics, SH1000_TetR population density increased over time, reaching the level of those in antibiotic free conditions. SH1000_TetR populations increased population densities at a greater rate when selected under normoxia than hypoxia, whereas the density of populations evolved without antibiotics did not increase

over time (Time by Antibiotic by Oxygen Tension interaction: Pr(>F) = 0.0055; Figure 5-6B, Table 5-2). Overall, oxygen tension and presence of antibiotics influenced the population densities over the course of the selection experiment.

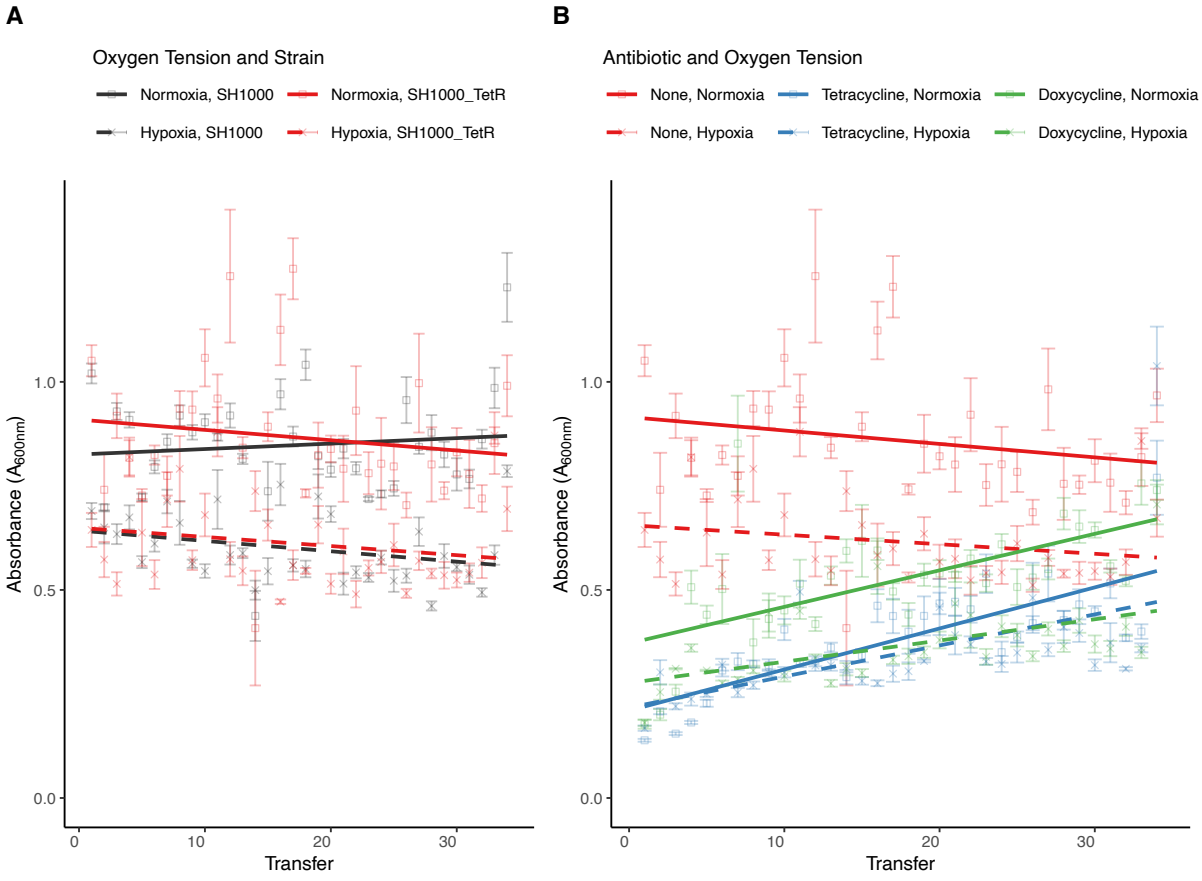

Figure 5-6: Prolonged exposure to tetracyclines and hypoxia influences 24 h growth of SH1000_TetR

24 h $A_{600\,nm}$ measurements from bacteria under selection from hypoxia or tetracyclines. 24 h readings are prior to 1/100 dilution in pre-equilibrated BHI broth in normoxia (solid line, square) (21% O_2, 5% CO_2, 37°C) or hypoxia (dashed line, cross) (0.8% O_2, 5% CO_2, 37°C). A) Antibiotic free conditions, with SH1000 (black) and SH1000_TetR (red). B) SH1000_TetR in antibiotic free media (red, same data as A), in TET (30 µg/ml) (blue), and in DOX (2 µg/ml) (green); antibiotics which were added to the media before each transfer. Results show mean of n=6 populations in each evolution condition, started from 6 independent clones. Error bars show +/- SE. Trend lines show linear model fitted to these data. Statistical analysis by linear mixed effects model, A) time: oxygen tension: strain, Pr(>F)= 0.00076, B) time: oxygen tension: antibiotic, Pr(>F) = 0.0055. Full data and interactions shown in Table 5-1 and Table 5-2.

Table 5-1: Linear mixed effects model interactions from antibiotic free selection of SH1000 and SH1000_TetR.

*Type III Analysis of Variance Table with Satterthwaite's method of linear mixed effects model of box-cox transformed data in Figure 5-6A. Signif. codes: 0 '***' 0.001 '**'.*

Interaction	Sum Sq	Mean Sq	NumDF	DenDF	F value	Pr(F)	
Transfer	10.617	10.617	1	1727	39.685	3.777×10^{-10}	***
Oxygen Tension	9.749	9.749	1	1727	6.443	1.920×10^{-9}	***
Strain	0.0537	0.0537	1	1727	0.201	0.654	
Transfer: Oxygen Tension	1.706	1.706	1	1727	6.376	0.0117	*
Transfer: Strain	2.542	2.542	1	1727	9.502	0.00208	**
Oxygen Tension: Strain	0.136	0.136	1	1727	0.508	0.476	
Transfer: Oxygen Tension: Strain	3.0443	3.0443	1	1727	11.380	0.000759	***

Table 5-2: Linear mixed effects model interactions from SH1000_TetR selection in hypoxia and tetracyclines.

*Type III Analysis of Variance Table with Satterthwaite's method of linear mixed effects model of box-cox transformed data from Figure 5-6B. Signif. codes: 0 '***' 0.001 '**'.*

Interaction	Sum Sq	Mean Sq	NumDF	DenDF	F value	Pr(F)	
Transfer	32.43	32.43	1	1801.7	307.52	$< 2.2x10^{-16}$	***
Oxygen Tension	0.92	0.92	1	1801.1	8.72	0.0032	**
Antibiotic	134.19	67.09	2	1801.3	636.15	$< 2.2x10^{-16}$	***
Transfer: Oxygen Tension	3.98	3.98	1	1801.1	37.71	$1.003x10^{-9}$	***
Transfer: Antibiotic	26.72	13.36	2	1801.7	126.68	$< 2.2x10^{-16}$	***
Oxygen Tension: Antibiotic	4.28	2.14	2	1801.1	20.28	$1.950x10^{-9}$	***
Transfer: Oxygen Tension: Antibiotic	1.10	0.55	2	1801.1	5.22	0.0055	**

The antibiotic sensitivity of all SH1000 and SH1000_TetR evolved populations was measured to test for any change in antibiotic resistance associated with the selection conditions. MICs were carried out by 20 h incubations of bacteria within an antibiotic gradient with serial 2-fold dilutions. The MIC of the evolved populations' were normalised to the ancestors' (SH1000 or SH1000_TetR) MIC. There was no change in tetracycline resistance of SH1000 population following selection in no antibiotics in hypoxia or normoxia (Figure 5-8). Looking only at the SH1000_TetR evolved populations, antibiotic treated populations evolved higher antibiotic resistance , such that populations treated with TET or DOX had higher resistance against both antibiotics by the end of the experiment (SH1000_TetR MIC increase compared to ancestor: TET, TET evolved 112-240 μg/ml, DOX evolved 16-240 μg/ml, DOX MICs, TET evolved 6-30 μg/ml, DOX evolved 6-62 μg/ml), whereas populations evolved without antibiotics showed no change in resistance to either antibiotic (Kruskal-Wallis rank sum test comparing MIC of SH1000_TetR populations based on evolution antibiotic, $p< 4.34x10^{-12}$) (Figure 5-9).

Growth curves were performed to determine if growth of SH1000 and SH1000_TetR populations evolved in hypoxia or normoxia and no antibiotic, TET or DOX was influenced by selection conditions. To match the evolution environment, populations were grown in deep well plates for 2, 4, 6, 24 h in normoxia and hypoxia, with one plate per timepoint as all the sample was used to take readings. To allow comparison between normoxic and hypoxic growth, all growth metrics were normalised to ancestral growth in the same oxygen tension. Growth of SH1000 populations was not influenced by evolution oxygen tensions (Figure 5-10A: integral growth: normoxia p=0.988; hypoxia p=0.831) seen in all growth parameters measured (Figure 5-10). Additional statistical analysis of these growth data was carried out, to see if there was a significant increase in total growth of these populations compared to their ancestor (Figure 5-10A), independent of evolution oxygen tension. Other parameters were not compared as the integral measures cumulative growth which correlates with the other growth measurements and is normally distributed here. For populations that evolved without antibiotics, significant, albeit modest increases in both normoxic and hypoxic growth were observed by the end of the experiment (Figure 5-10A) (1-sample T-test of integrals against 1 (ancestor), normoxic growth: $p=9.298x10^{-7}$, hypoxic growth: $p= 1.524x10^{-5}$). Hypoxic but not normoxic growth of SH1000_TetR populations evolved without antibiotics was significantly higher than those evolved with TET or DOX treatment (SH1000_TetR ANOVA

model: normalised integral ~ (Oxygen*Antibiotic*Condition), Antibiotic: Pr(>F)= $1.64x10^{-5}$, full interactions Table 5-3) (Figure 5-11). SCVs were observed while plating populations during the evolution experiment. SCVs were measured for each evolved population, to see if the occurrence is associated with an evolution condition and potentially influencing changes in growth, however, no significant changes in the occurrence of SCV formation was observed based on evolution oxygen tension nor evolution antibiotic (Figure 5-7). These data suggest antibiotic treatment prevents SH1000_TetR populations evolving increased hypoxic growth which is not influenced by SCVs.

Together these data suggest that the horizontal acquisition of a tetracycline resistance gene came at a fitness cost apparent only under hypoxia, and that this cost could be overcome through evolution only in the absence of antibiotics; antibiotics instead selected for higher levels of resistance.

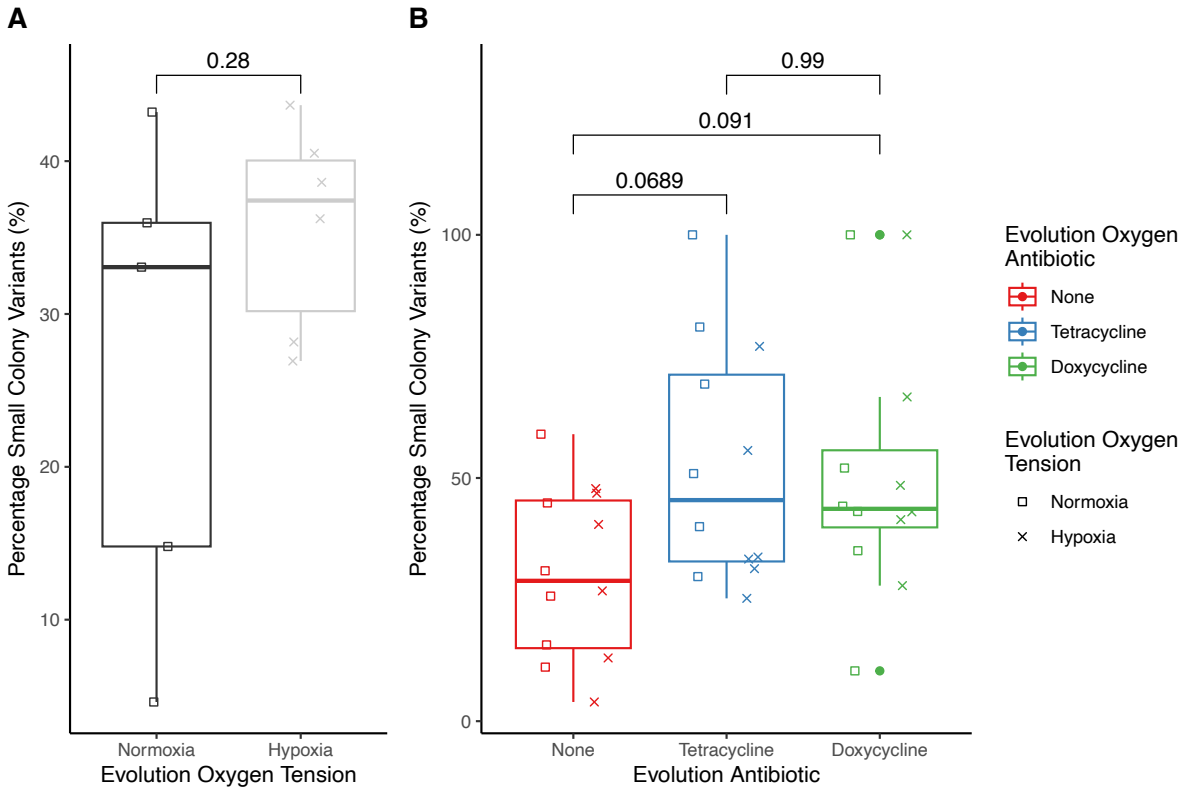

Figure 5-7: There is no change in small colony variants for SH1000 or SH1000_TetR evolved in hypoxia or antibiotics

*Percentage of small colony variants from populations of A) SH1000 or B) SH1000_TetR evolved in hypoxia or normoxia with or without antibiotics. Percentage of small colony variants determined by streaking out populations onto BHI agar, incubating for 24 h (37℃), and counting number of 'small' colonies compared to colonies size of their ancestor (SH1000 or SH1000_TetR) incubated for the same period of time. Statistical analysis by A) T-test, B) ANOVA model (SCV~ Evolution Antibiotic*Evolution Oxygen Tension) with Tukey's multiple comparisons. ANOVA model: evolution antibiotic, p=0.0515; evolution oxygen tension, p=0.5713. Box and whisker plots present median, 25/75% quantile (upper and lower hinge), smallest/ largest observation ≤ upper/lower hinge +/- 1.5 inter quantile range (whiskers).*

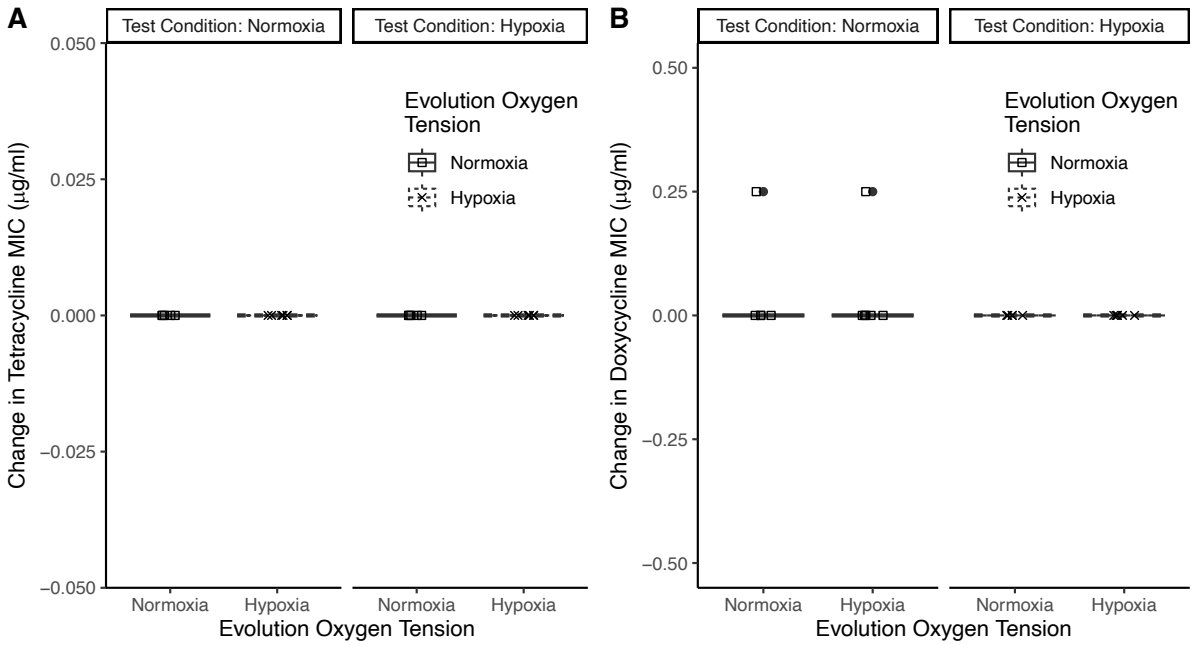

Figure 5-8: SH1000 evolved population antibiotic sensitivity is unchanged

Change in MIC of SH1000 populations evolved in hypoxia (n=6) or normoxia (n=5) in no antibiotics compared to their ancestor measured in A) TET or B) DOX, prepared by serial dilutions of antibiotics in equilibrated BHI broth in normoxia, (21% O_2, 5% CO_2, 37°C) or hypoxia, (0.8% O_2, 5% CO_2, 37°C) in 96 well plates before 20 h incubation with bacteria. Normoxic overnight cultures were diluted to $A_{600\ nm}$=0.05 before 10 µl was added to 90 µl antibiotics preparation. SH1000 populations following 30 days selection in normoxia (squares, solid lines) or hypoxia (crosses, dashed lines). MIC Cut-offs were defined as the lowest antibiotic concentration with no visible bacterial growth in the well. Kruskal-Wallis rank sum test of all data independent of test oxygen tension by evolution oxygen tension, A) NA, all 0 values, B) p= 0.895. Box and whisker plots present median with filled circle showing range beyond whiskers.

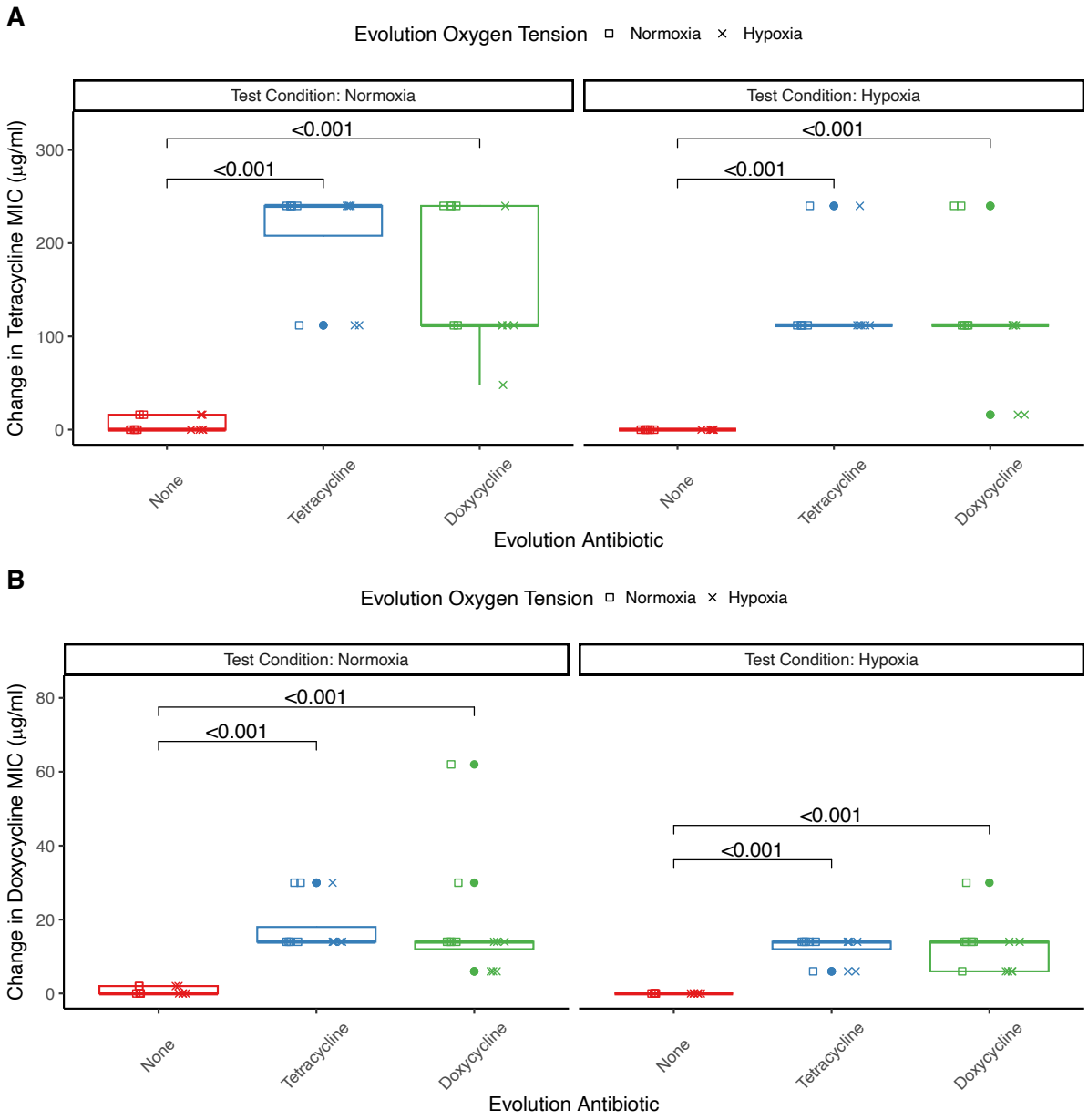

Figure 5-9: Susceptibility to tetracyclines decreases following selection in tetracyclines

Change in MIC of SH1000_TetR populations compared to their ancestor measured in A) TET (0.5-512 µg/ml) or B) DOX (0.5-512 µg/ml), prepared by serial dilutions of antibiotics in equilibrated BHI broth in normoxia, (21% O_2, 5% CO_2, 37°C) or hypoxia, (0.8% O_2, 5% CO_2, 37°C) in 96 well plates before 20 h incubation with bacteria. Normoxic overnight cultures were diluted to A_{600nm}=0.05 before 10 µl was added to 90 µl antibiotics preparation. SH1000_TetR following 30 days selection in red= no antibiotic, blue= TET, Green= DOX in normoxic (square) or hypoxic (cross) oxygen tensions. MIC cut-offs were defined as the lowest antibiotic concentration with no visible bacterial growth in the well. Statistical analysis by Kruskal-Wallis rank sum test with Wilcoxon rank sum post-hoc testing and Benjamini-

Hochberg correction for multiple by evolution antibiotic with no separation by evolution oxygen tension. Kruskal-Wallis rank sum test of all data independent of test oxygen tension by evolution antibiotic, A) $p< 2.2x10^{-16}$ B) $p< 2.2x10^{-16}$. Box and whisker plots present median, 25/75% quantile (upper and lower hinge), smallest/ largest observation ≤upper/lower hinge +/- 1.5 inter quantile range (whiskers), fill circle show range beyond whiskers.

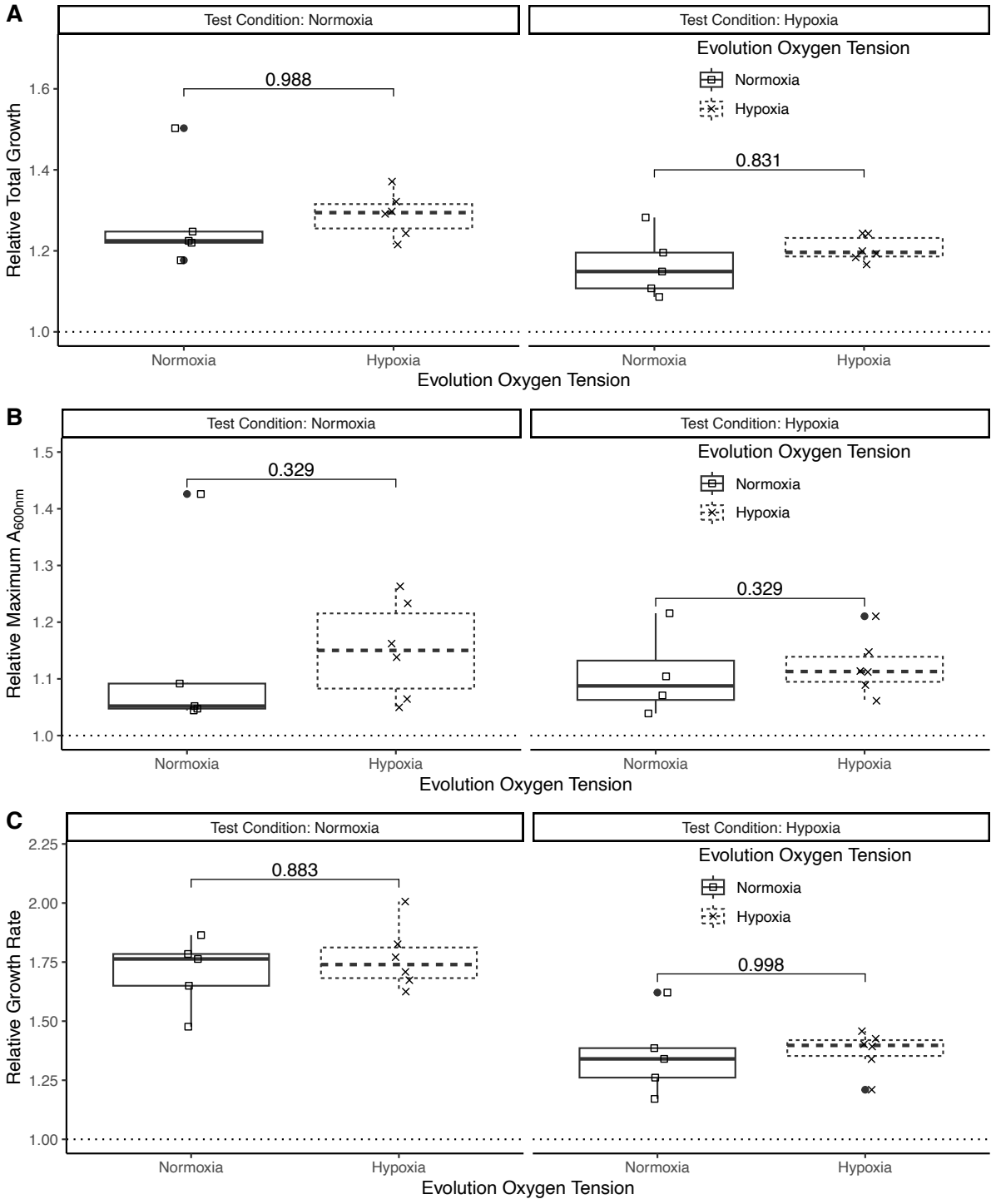

Figure 5-10: Increased in growth of SH1000 populations is unaffected by selection in hypoxia

Growth parameters of populations of SH1000 following selection in normoxia (square, solid line), (21% O_2, 5% CO_2, 37°C) or hypoxia (cross, dashed line), (0.8% O_2, 5% CO_2, 37°C). Parameters calculated from growth curves of evolved populations grown in deep 96 well plates to match evolution condition. $A_{600\ nm}$ readings were taken at 0, 2, 4 ,6, 24 h. Relative growth was calculated through division of population growth by the ancestor (SH1000) growth in matching test oxygen tensions (dashed line at 1). Growth

parameters shown are A) integral of growth curves, B) maximum recorded A $_{600\ nm,}$ C) growth rate between 2-6 h. Results represent n=3 experimental repeats. Statistical analysis by A, C) 2-way ANOVA with Tukey's multiple comparisons, B) Kruskal-Wallis rank sum test with Wilcoxon rank sum post-hoc testing and Benjamini-Hochberg correction for multiple comparisons. Additional statistical analysis only of A) 1-sample T-test of integrals against 1, normoxia: $p=9.298x10^{-7}$, hypoxia: $p= 1.524x10^{-5}$. Box and whisker plots present median, 25/75% quantile (upper and lower hinge), smallest/ largest observation ≤ upper/lower hinge +/- 1.5 inter quantile range (whiskers), fill circle show range beyond whiskers.

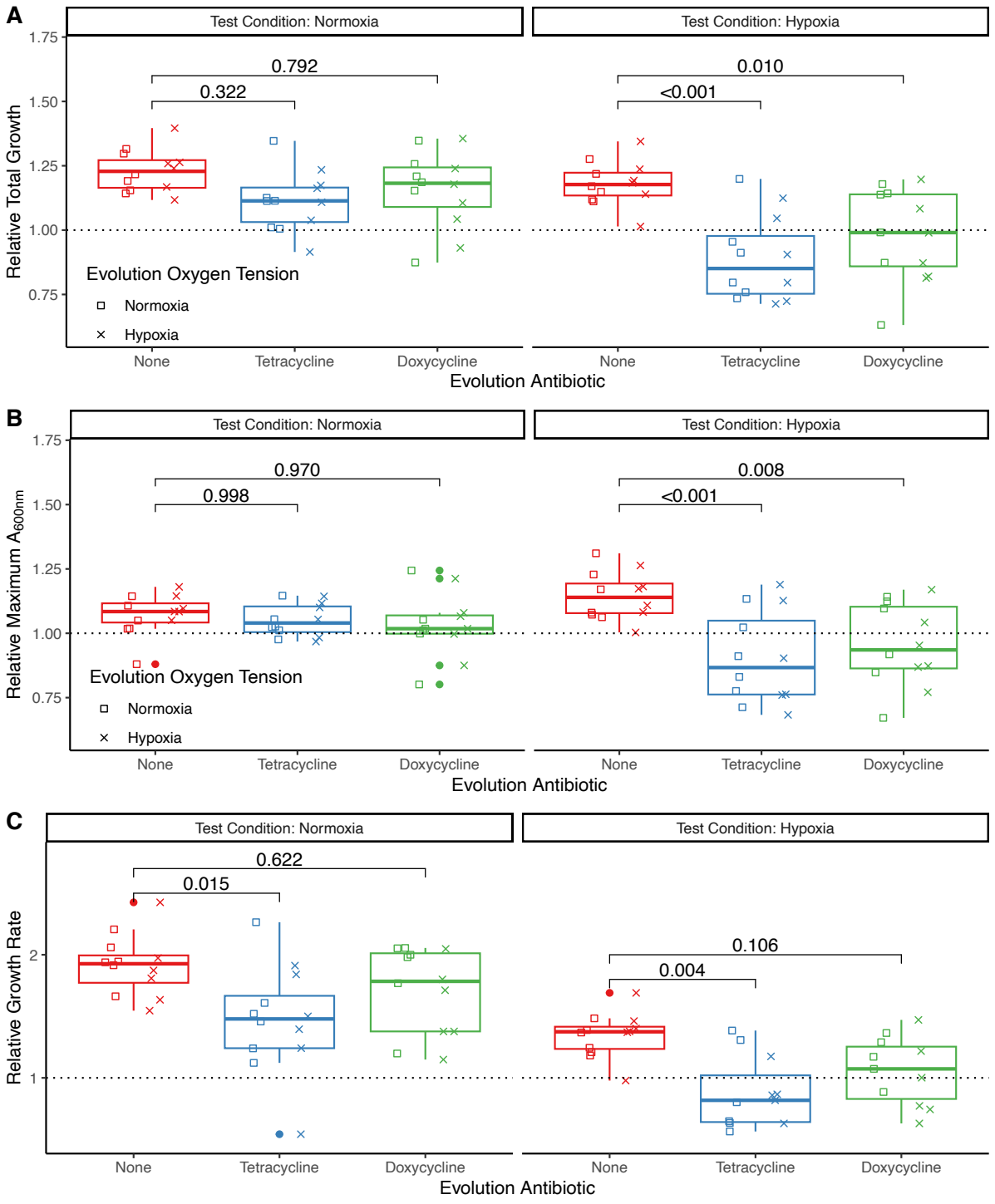

Figure 5-11: SH1000_TetR Growth is reduced following selection in antibiotics and hypoxia

Growth parameters of populations of SH1000_TetR following selection in normoxia (square), (21% O_2, 5% CO_2, 37°C) or hypoxia (cross), (0.8% O_2, 5% CO_2, 37°C) in no antibiotics (red), TET (blue) or DOX (green). Parameters calculated from growth curves of evolved populations grown in antibiotic free BHI broth deep 96 well plates to match evolution condition. A_{600nm} readings were taken at 0, 2, 4, 6, 24 h.

*Relative growth was calculated through division of population growth by the ancestor (SH1000_TetR) growth in matching test oxygen tensions (dashed line at 1). Growth parameters shown are A) integral of growth curves, B) maximum recorded $A_{600\ nm}$, C) growth rate between 2-6 h. Results represent n=3 experimental repeats. Statistical analysis by ANOVA model (growth metric ~ (Evolution Oxygen*Evolution Antibiotic*Test Oxygen Tension) with Tukey's multiple comparisons by "Antibiotic: Test Oxygen Tension" presented. ANOVA model, evolution antibiotic, A) $Pr(>F)= 2.11x10^{-5}$, B) $Pr(>F)= 0.0011$, C) $Pr(>F)= 1.96x10^{-5}$. Full interactions for A) in Table 5-3. Box and whisker plots present median, 25/75% quantile (upper and lower hinge), smallest/ largest observation ≤ upper/lower hinge +/- 1.5 inter quantile range (whiskers), fill circle show range beyond whiskers.*

Table 5-3: Interaction from ANOVA model of integral growth of evolved SH1000_TetR populations in Figure 5-11A.

*Model: normalised integral ~ (Evolution Oxygen*Evolution Antibiotic*Test Oxygen Tension)*

Interaction	DF	Sum Sq	Mean Sq	F value	Pr(F)	
Evolution Oxygen Tension	1	0.012	0.0012	0.060	0.0868	
Evolution Antibiotic	2	0.521	0.261	13.313	1.64×10^{-5}	***
Test Oxygen Tension	1	0.410	0.410	20.958	2.42×10^{-5}	***
Evolution Oxygen Tension: Evolution Antibiotic	2	0.0063	0.0031	0.160	0.852	
Evolution Oxygen Tension: Test Oxygen Tension	1	0.0000	0.0000	0.001	0.982	
Evolution Antibiotic: Test Oxygen Tension	2	0.0971	0.0485	2.479	0.0924	
Evolution Oxygen Tension: Evolution Antibiotic: Test Oxygen Tension	2	0.0002	0.0001	0.005	0.995	
Residuals	60	1.175	0.0196			

5.4 Discussion

In this chapter, I have shown that hypoxia, a common physiological stressor at infection sites[16,429], influences the fitness costs associated with horizontally acquired resistance genes, in particular the tetracycline resistance gene *tetL*. During prolonged exposure to hypoxia and antibiotics, populations of SH1000_TetR evolved increased antibiotic resistance or hypoxic growth based on evolution conditions. Populations exposed to antibiotics increased total growth over time, and developed decreased antibiotic sensitivity – these phenotypes were not seen in populations evolved in antibiotic-free conditions. However, populations which had evolved high levels of antibiotic resistance had lower levels of hypoxic growth in an antibiotic free setting compared to populations which had evolved in an antibiotic-free setting. These dynamics suggest an evolutionary trade-off between adaptation to antibiotics and hypoxia which will be explored further at a genetic level in chapter 6.

The horizontal acquisition of new resistance genes is often expected to be associated with fitness costs[352,418], which could limit the persistence of antibiotic-resistant genotypes in the absence of antibiotics. My data demonstrate that such fitness costs depend critically upon environmental oxygen availability, with a high cost of acquiring a tetracycline efflux pump observed under hypoxia but not normoxia. This suggests that measurements made under standard normoxic laboratory conditions may underestimate the fitness costs of tetracycline resistance. Importantly, the efficacy *tetL* is not compromised in hypoxia and still confers resistance to the widely-used second-generation tetracycline, doxycycline, so *tetL* remains an important clinical challenge if *tetL* persists in populations. Hypoxia is common in a range of infection environments, with oxygen tensions of 20–30 mmHg in normal capillaries[16] and 2.5 mmHg in the mucus of patients with cystic fibrosis[429]. The high cost of tetracycline resistance under hypoxia may therefore help to explain why tetracyclines continue to be effective treatments against *S. aureus* infections within such hypoxic infection environments.

Despite investigations, the SNP in *uspA* cannot be totally exonerated from influencing SH1000_TetR fitness in hypoxia. UspA has previously been reported to have increased expression in *S. aureus* during the stringent response within a kidney abscess[439] which would be expected to be hypoxic. The fact that the Nebraska transposon mutant[254] did not have

altered growth characteristic from its parent strongly suggests that this protein does not influence hypoxic growth. However, to confirm this, the identity of the mutant needs to be confirmed by PCR and transduced into the SH1000 genetic background, where the SNP in *uspA* was found. This would not eliminate a gain of function mutation influencing fitness in hypoxia. However, as noted, NewHG_TetR also carried fitness cost in hypoxia compared to normoxia with a wildtype *uspA*. Furthermore, no variants in *uspA* were observed in any evolved clone following selection in hypoxia or normoxia. Thus, it is highly unlikely that the *uspA* SNP is the cause of the impaired fitness of SH1000_TetR I observed in hypoxia.

For TET and DOX the EUCAST breakpoint are: sensitive 1 μg/ml≤, resistant 2 μg/ml> for both TET and DOX[259]. These breakpoints compare to the median MIC recorded for SH1000 of 0.5 μg/ml TET (normoxia and hypoxia), 0.5 μg/ml DOX normoxia, 2 μg/ml DOX hypoxia and SH1000_TetR 64μg/ml TET (normoxia and hypoxia), 8 μg/ml DOX (normoxia and hypoxia) of *S. aureus* ancestors before the evolution experiment. Caution needs to be applied to interpreting DOX MICs due to low experimental repeats and variation between experiments. The method used to measure these MICs differed from the EUCAST method in media, antibiotic volumes, and strain to allow relevant readings relevant to evolution conditions to be determined. Therefore, these measurements are not directly comparable. However, the results are as expected indicative of *tetL* inducing resistance that exceeds the clinical breakpoints, reducing the clinical utility of these tetracyclines. The SH1000_TetR MICs recorded are comparable to those seen in clinical isolates which carry the *tetK* efflux pump or *tetM* mediating ribosomal protection, when tested on Mueller–Hinton agar as in the EUCAST guidelines. SH1000_TetR's MICs are still lower than in *S. aureus* clones carrying *tetK* and *tetM* supporting higher levels of TET resistance is still possible in these populations[440].

In common with other studies[441] I observed that prolonged antibiotic selection induced increased antibiotic resistance in clones despite clones already possessing a resistance mechanism that was sufficient to protect the cells at the antibiotic concentrations used. This supports previous studies showing the acquisition of a resistance gene is not an evolutionary endpoint[423,442]. Genetic analysis of individuals within these populations, in the next chapter, will determine if this increased resistance is from mutations directly impacting resistance mechanisms, compensatory mutations against acquisition of the resistance genes, or direct

mutations within *tetL*. The increase in tetracycline resistance for SH1000_TetR could prevent the treatment of this infection by an alternative antibiotic within the same class, as *tetL* is conferring cross resistance to second-generation antibiotics.

In contrast to the chapter hypothesis, populations selected in antibiotic-free environments maintained tetracycline resistance even in hypoxia where these genes were costly. This was unexpected given the high fitness cost of *tetL* in hypoxia, and Dunai et al. has previously shown the loss of tetracycline resistance in *E. coli*[286,419] when it is not essential for survival in an antibiotic free setting. However, other studies have shown compensatory mutations can offset for costly elements such as plasmids[245]. The next chapter will use whole genome sequencing to see if chromosomal mutations or gene deletions can explain the retention of costly tetracycline resistance.

Additional selective pressures, as well as hypoxia and antibiotics, will have been experienced by evolving populations. One limitation of the experimental design is the serial dilution setup causes inherent fluctuating population sizes and nutrient availability[443-446]. Every cycle equates to approximately 6.7 generations growth prior to dilution. Population size and nutrient fluctuations were not controlled as in vivo infection conditions are not constant[447]. Populations in no antibiotics in normoxia were exposed to less stringent conditions and a larger bottleneck than populations in hypoxia and antibiotics, with a significant decrease in SH1000 and SH1000_TetR growth in hypoxia compared to normoxia (Figure 4-2). This change in bottleneck size will also be the case during hypoxic infections with antibiotics compared to those without. Comparison of genetics of populations evolved in antibiotics and hypoxia, to those evolved in normoxia without antibiotics, will show if the size of the bottleneck influences the number of mutations within populations (chapter 6).

Hypoxia is common in many *S. aureus* infections and these results highlight the potential for such host-relevant physiological stresses to interact with antibiotic selection in complex and unpredictable ways. By modulating fitness costs, hypoxia may select against antibiotic resistance, whereas antibiotic selection may constrain adaptation to hypoxic conditions, thus potentially limiting the persistence of these highly-resistant but poorly-adapted genotypes once antibiotic treatment ceases. Together these combined effects may help to explain why

tetracyclines remain a useful treatment against *S. aureus* infections where hypoxia is a prominent feature within host environment.

6 Genetic Changes Evolved in Response to Oxygen Tension and Exposure to Tetracyclines

6.1 Introduction

Tetracyclines are bacteriostatic antibiotics, which bind to 16S rRNA within the 30S ribosomal subunit, preventing transcription by weakening the affinity of tRNAs to the A site where the ribosome accepts incoming tRNA's[177]. Correspondingly, single point mutations within the 16SrRNA subunit can confer high level resistance to tetracyclines[190,448,449]. Alternatively, additional mechanisms of tetracycline resistance can be encoded on horizontally acquired elements including ribosomal protection proteins (TetO, TetM), tetracycline specific efflux pumps (TetA, TetB, TetK, TetL) and antibiotic inactivating enzymes (TetX)[300]. As shown in chapter 5, populations of bacterial cells carrying *tetL* can evolve an increased level of tetracycline resistance following prolonged exposure to tetracyclines. This is consistent with other studies showing that antibiotic exposure can alter the evolutionary response of bacteria to the horizontal acquisition of resistance genes. Exposing resistant cells to antibiotics commonly selects for additional resistance-associated mutations affecting the horizontally acquired resistance mechanism itself and/or other genomic loci linked to resistance, potentially leading to the emergence of evolved genotypes with high-level resistance[441,450]. For example, under tetracycline selection, populations of *E. coli* carrying a plasmid encoding the TetA tetracycline-specific efflux pump evolved more than 32-fold increased tetracycline resistance despite gaining mutations that impaired the activity of the TetA efflux system. Increased tetracycline resistance arose through compensatory missense mutations in chromosomal genes that reduced cellular permeability to tetracycline and increased its efflux[441]. A *S. aureus* strain with a chromosomal copy of the methicillin resistance gene *mecA* evolved more than 2000-fold increased oxacillin resistance through gain of missense mutations in *rpoB* or *rpoC*, encoding subunits of RNA polymerase, when selected on a gradient of oxacillin. The *rpo* mutations caused increased expression of *mecA* and other chromosomal genes, causing high-level resistance whilst also restoring the redox balance of the cell, which had been disrupted by the introduction of *mecA*[204].

Less is known about the potential evolutionary responses to hypoxia, a common physiological stressor at the site of infection. To investigate this, Wilde and colleagues undertook TnSeq analysis using a recently described *S. aureus* transposon insertion library in a hypoxic osteomyelitis murine model (bone infection is a profoundly hypoxic environment with the authors detecting a value falling from 45mmHg in uninfected bone to 14.3 mmHg at 10 days post infection). These investigators found 65 genes to be essential for *S. aureus* infections in bone rather than in atmospheric oxygen conditions in vitro, with a further 148 mutants displaying compromised fitness in vivo[428]. The 65 essential genes for bone infection include those associated with nitrosative stress, *cydB* and *qoxC*, and metabolic pathways. Unsurprisingly, *srrA* and *srrB* of the SrrAB 2-component system were essential genes due to this systems role in regulation of the oxidative and nitrosative stress response[44]. The SrrAB 2-component system also regulates the expression of virulence genes, signifying an interplay between the hypoxic response and virulence[451]. Thirty-seven genes were associated with uncharacterised hypothetical proteins, with more work needed to understand their potential role in survival under hypoxia. In other studies, genetic variants within metabolic pathways key to oxygen utilisation (TCA cycle, glycolytic pathway) have been enriched in clones isolated from skin-adapted *S. aureus* strains[452]. Skin is a hypoxic environment[453], however, it was not tested whether these genetic variants represented hypoxia specific adaptations.

In addition to its impact on bacterial responses, hypoxia is known to regulate the essential antimicrobial activity of neutrophils against *S. aureus*. Activation of the PHD/HIF pathway leads to increased neutrophil persistence, migration, glycolytic capacity and survival[140]. Hypoxia has also been shown to increase intra-neutrophil *S. aureus* persistence through the reduction in killing by ROS[91]. *S. aureus* can evade killing by neutrophils through the expression of multiple virulence factors including expression of aureolysin, phenol-soluble modulins and SodA/M[16]. Additionally, metabolic adaptation of *S. aureus* through point mutations in *cls2* have been shown to modify the bacterial membrane, which facilitated evasion of neutrophil chemotaxis and resistance to daptomycin[454]. Mutations in *cls2* occurred in clinical isolates and it is unclear if this is adaptation to the immune environment, stress conditions or antibiotic treatment.

Here I used whole genome sequencing of evolved clones from the end of the selection experiments reported in chapter 5 to understand the genetic basis of adaptation to hypoxia and antibiotic exposure. I identified mutations and gene duplications associated with SH1000 and SH1000_TetR adaptation to low oxygen tensions and tetracyclines and measured their impact on tetracycline sensitivity and fitness of clones in hypoxia. I then carried out structural predictions to see the potential impact of mutations on protein function. Finally, I carried out neutrophil intracellular survival assay of DNA gyrase B mutants to see if mutations driving adaptation to hypoxia impact bacterial survival in an immune setting.

6.2 Hypothesis and aims

In this chapter I have tested the following research hypothesis:

Specific mutations will be associated with SH1000_TetR's adaptation to hypoxia and increased tetracycline resistance.

The specific aims addressed in this chapter are:

- Characterise genetic changes in clones that are associated with hypoxia and tetracyclines selection.
- Determine the how mutated genes influence bacterial fitness according to oxygen levels and tetracycline exposure.
- Investigate the neutrophil-mediated killing of selected mutants associated with hypoxia.

6.3 Results

6.3.1 Clone phenotypes are broadly consistent with population phenotypes

In the previous chapter, I found a significant fitness cost associated with *tetL* in hypoxia, with SH1000_TetR populations evolved in hypoxia and/or tetracyclines gaining increased antibiotic resistance at the cost of increased growth in hypoxia in an antibiotic free setting. To investigate the genetic response to selection, I selected one randomly chosen clone per replicate population from the evolution experiment in chapter 5 (overview in Figure 6-1). This totalled 47 clones, including SH1000_TetR evolved in normoxia or hypoxia with or without TEX or DOX, and SH1000 controls evolved in normoxia or hypoxia without antibiotics. The growth and resistance phenotypes of the evolved clones were broadly consistent with those of the populations from which they were sampled, as assayed in chapter 5 (Figure 6-3, Figure 6-4, Figure 6-5, Table 6-1). As before, growth curves were carried out in parallel in hypoxia and normoxia from the same starting $A_{600\,nm}$ for all clones, with readings at 2, 4, 6, 24 h (Figure 6-2). To allow comparison, growth rate, maximum $A_{600\,nm}$ and the integral of these growth curves was calculated. Growth of SH1000 clones was not significantly influenced by evolution oxygen tension as assessed by integral growth (for normoxic versus hypoxic evolution, tested in normoxia p=0.11, tested hypoxia p=0.576, Figure 6-3A), maximal A_{600nm} (for normoxic versus hypoxic evolution, tested in normoxia p=0.931, tested in hypoxia p=0.583, Figure 6-3B) or maximal growth rate (for normoxic versus hypoxic evolution, tested in normoxia p=0.317, tested hypoxia p=0.619, Figure 6-3C).

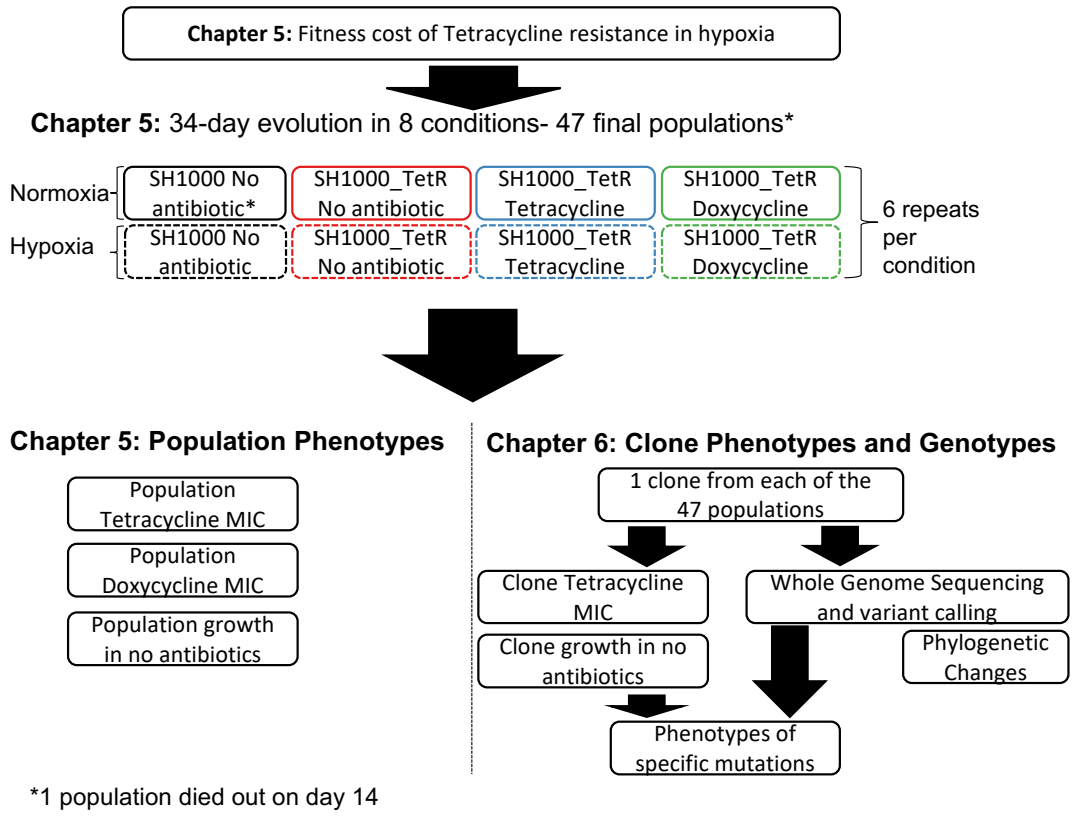

Figure 6-1: Chapter overview

Overview of analysis following 34-day evolution experiment in Chapter 5 where 5 experimental lines were evolved: SH1000, no antibiotic, normoxia; SH1000, no antibiotic, hypoxia; SH1000_TetR, no antibiotic, normoxia; SH1000_TetR, no antibiotic, hypoxia; SH1000_TetR, TET, normoxia; SH1000_TetR, TET, hypoxia; SH1000_TetR, DOX, normoxia; SH1000_TetR, DOX, hypoxia. In the previous chapter 5 population phenotypes were established. In this chapter, one clone from each experimental line in the evolution experiment will be characterised for their specific genotype and phenotype. Following this, an in-depth analysis will be carried out showing specific genetic variants associated with phenotypic changes.

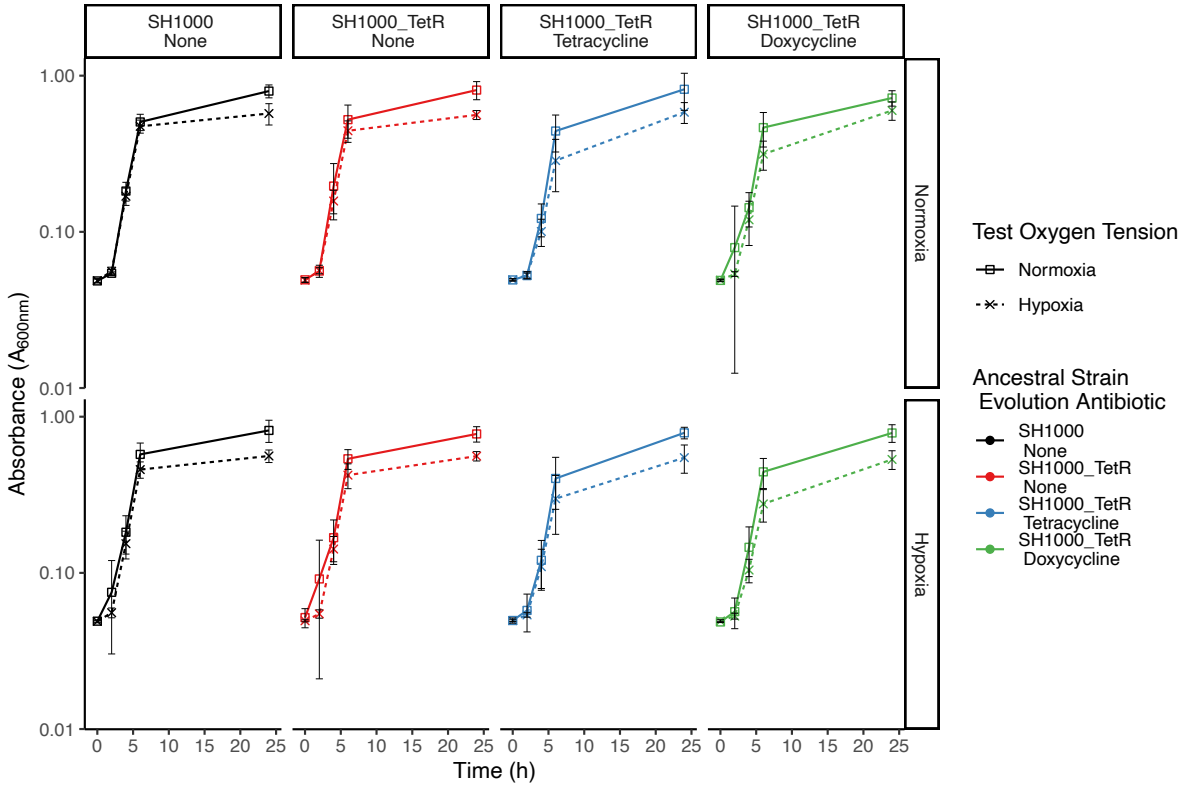

Figure 6-2: Growth curves of evolved clones

Growth curves of evolved clones following selection in normoxia (21% O_2, 5% CO_2, 37°C) (top row), or hypoxia (0.8% O_2, 5% CO_2, 37°C) (bottom row) in no antibiotic (black or red), TET (blue) or DOX (green). Ancestral strains were SH1000 (black) or SH1000_TetR (red, blue or green). Growth curves of evolved populations grown in deep 96 well plates to match evolution condition. A $_{600\,nm}$ readings were taken at 0, 2, 4, 6, 24 h and measured in normoxia (square, solid line), (21% O_2, 5% CO_2, 37°C) or hypoxia (cross, dashed line), (0.8% O_2, 5% CO_2, 37°C). n=6 carried out in triplicate. Data show mean +/- SE.

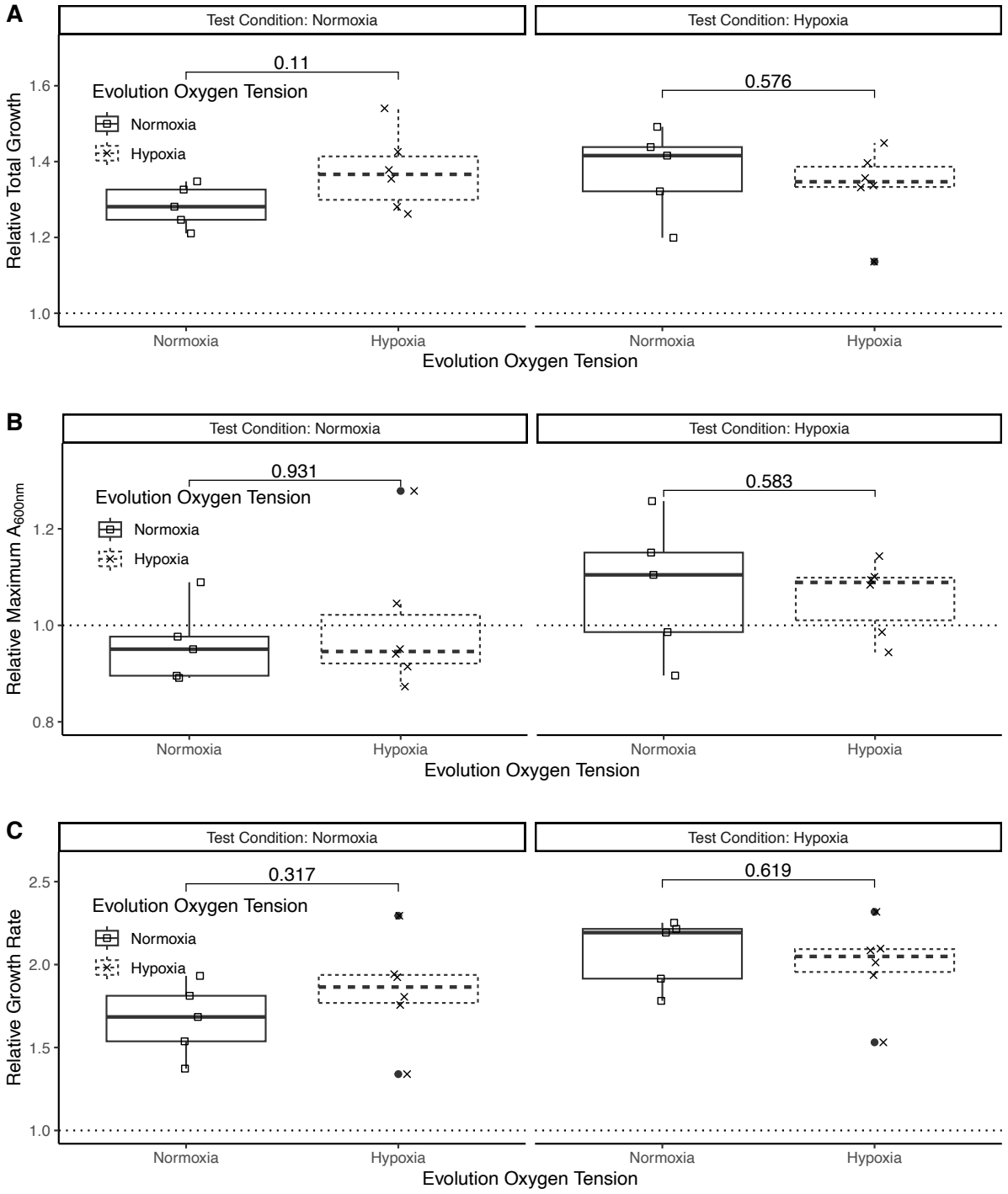

Figure 6-3: Growth of SH1000 clones are unaffected by selection in hypoxia

Growth parameters of clones of SH1000 following selection in normoxia (square, solid line), (21% O_2, 5% CO_2, 37°C) or hypoxia (cross, dashed line), (0.8% O_2, 5% CO_2, 37°C). Parameters calculated from growth curves of evolved populations grown in deep 96 well plates to match evolution condition. $A_{600\ nm}$ readings were taken at 0, 2, 4, 6, 24 h. Relative growth was calculated through division of population

growth by the ancestor (SH1000) growth in matching test oxygen tensions (dashed line at 1). Growth parameters shown are A) integral of growth curves, B) maximum recorded $A_{600\ nm}$, C) growth rate between 2-6 h. Results represent n=3 experimental repeats. Statistical analysis by A, C) 2-way ANOVA with Tukey's multiple comparisons, B) Kruskal-Wallis rank sum test with Wilcoxon rank sum post-hoc testing and Benjamini-Hochberg correction for multiple comparisons. Box and whisker plots present median, 25/75% quantile (upper and lower hinge), smallest/ largest observation ≤ upper/lower hinge +/- 1.5 inter quantile range (whiskers), filled circle show range beyond whiskers.

Unlike growth in SH1000_TetR populations (Chapter 5), SH1000_TetR clones showed a trend toward increased total growth following antibiotic free selection compared to populations in TET or DOX. Overall, evolution of SH1000_TetR in antibiotics is restricting increases in bacterial growth in no antibiotics (Figure 6-4: ANOVA model: normalised integral ~ (Evolution Oxygen*Evolution Antibiotic*Test Oxygen Tension), Evolution Antibiotic: Pr(>F)= 0.0084, full interactions Table 6-1).The increases in the total growth of clones in an antibiotic free setting (Figure 6-4) appears to be due to clones evolved in antibiotic free conditions having increases in total hypoxic growth, with clones evolved in TET or DOX having restricted hypoxic growth limiting their adaptation to hypoxia, although there are no significant pairwise interactions between evolution antibiotics in either oxygen tension (normoxic growth: no antibiotic-TET, p=0.475; no antibiotic-DOX, p=0.418; hypoxic growth: no antibiotic-TET, p=0.212; no antibiotic-DOX, p=0.244). The maximum hypoxic and normoxic growth of clones was unaffected by the clones evolution antibiotics (normoxic maximum growth: no antibiotic-TET, p=0.887; no antibiotic-DOX, p=0.887; hypoxic maximal growth: no antibiotic-TET, p=0.887; no antibiotic-DOX, p=0.887) (Figure 6-4B). In contrast, there were significant pairwise interactions in the hypoxic growth rate by selection antibiotic with clones evolved in no antibiotics having an increased hypoxic growth rate than clones evolved in no antibiotics (normoxic maximum growth rate: no antibiotic-TET, p=0.301; no antibiotic-DOX, p=0.569; hypoxic maximal growth rate: no antibiotic-TET, p=0.021; no antibiotic-DOX, p=0.026) (Figure 6-4C). Increased growth rates in clones evolved in no antibiotics indicates the advantage in total hypoxic growth following evolution in no antibiotics compared to TET and DOX is from clones evolved in no antibiotics reaching maximum growth quicker than clones evolved in TET or DOX with no change in the maximum growth depending on evolution antibiotic. All increases in hypoxic growth were associated with evolution antibiotic and were unaffected by evolution oxygen tensions with no significant difference in growth related to evolution oxygen tension (ANOVA model: normalised integral ~ (Evolution Oxygen*Evolution Antibiotic*Test Oxygen Tension), Evolution Oxygen Tension: Pr(>F)= 0.392, Table 6-1) showing adaptation to hypoxia is limited in these clones. There was also no interaction between test evolution oxygen tension interaction with evolution oxygen tension or evolution antibiotic (full interactions Table 6-1) hence, grouping data from clones evolved in normoxia or hypoxia in Figure 6-4. In the previous chapter, significant pairwise interactions were seen

between populations evolved in no antibiotics compared to TET or DOX for hypoxic total growth, maximum growth and maximum growth rate (Figure 5-11). The slight differences between population and clone growth parameters, are likely from the averaging effect of population readings in optical measurements. Additionally, clones do not represent the genetic diversity, or necessarily the dominant phenotype within a population due to random selection.

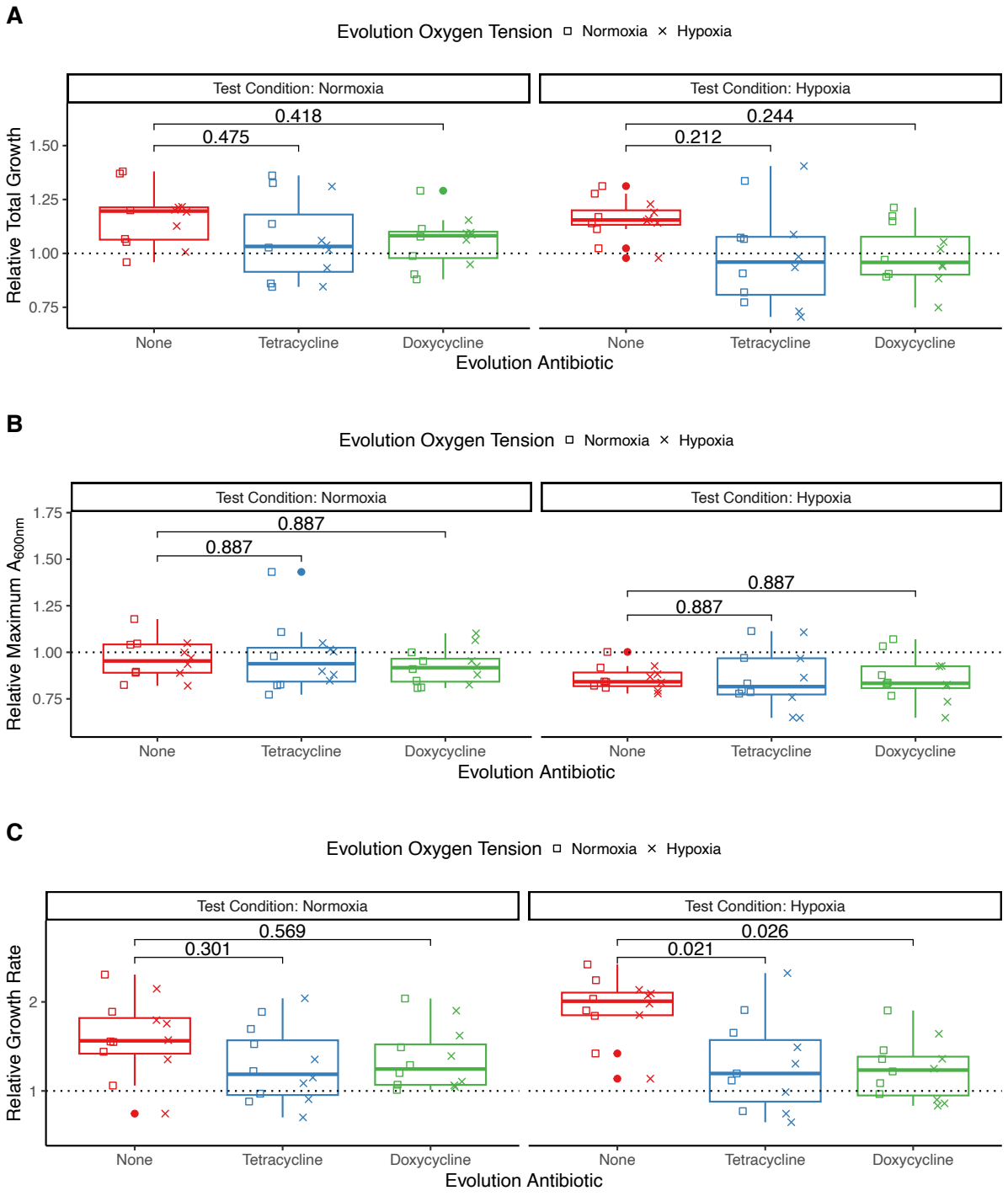

Figure 6-4: SH1000_TetR growth is reduced following selection in antibiotics and hypoxia

Growth parameters of clones of SH1000_TetR following selection in normoxia (square), (21% O_2, 5% CO_2, 37°C) or hypoxia (cross), (0.8% O_2, 5% CO_2, 37°C) in no antibiotics (red), TET (blue) or DOX (green). Parameters calculated from growth curves of evolved clones grown in antibiotic free BHI broth deep 96 well plates to match evolution condition. A_{600nm} readings were taken at 0, 2, 4, 6, 24 h. Relative

*growth was calculated through division of population growth by the ancestor (SH1000_TetR) growth in matching test oxygen tensions (dashed line at 1). Growth parameters shown are A) integral of growth curves, B) maximum recorded $A_{600\ nm}$, C) growth rate between 2-6 h. Results represent n=3 experimental repeats. Statistical analysis by A, C) ANOVA model (growth metric ~ (Evolution Oxygen*Evolution Antibiotic*Test Oxygen Tension) with Tukey's multiple comparisons by "Antibiotic: Test Oxygen Tension" presented. ANOVA model, evolution antibiotic, A) Pr(>F)= 0.00584, C) Pr(>F)= 0.00046. Full interactions for A) in Table 6-1. B) Kruskal-Wallis rank sum test with Wilcoxon rank sum post-hoc testing and Benjamini-Hochberg correction for multiple comparisons. Kruskal-Wallis rank sum test by antibiotic p = 0.872. Box and whisker plots present median, 25/75% quantile (upper and lower hinge), smallest/ largest observation ≤upper/lower hinge +/- 1.5 inter quantile range (whiskers), filled circle show range beyond whiskers (not a data point).*

Table 6-1: Interaction from ANOVA model of integral growth of evolved SH1000_TetR clones in Figure 6-4.

*Model: normalised integral ~ (Evolution Oxygen*Evolution Antibiotic*Test Oxygen Tension)*

Interaction	DF	Sum Sq	Mean Sq	F value	Pr(F)	
Evolution Oxygen Tension	1	1.79	1.79	0.743	0.392	
Evolution Antibiotic	2	27.11	13.56	5.611	0.0084	**
Test Oxygen Tension	1	200.55	200.55	83.007	6.43×10^{-13}	***
Evolution Oxygen Tension: Evolution Antibiotic	2	0.15	0.07	0.031	0.970	
Evolution Oxygen Tension: Test Oxygen Tension	1	0.50	0.50	0.208	0.650	
Evolution Antibiotic: Test Oxygen Tension	2	0.31	0.16	0.64	0.938	
Evolution Oxygen Tension: Evolution Antibiotic: Test Oxygen Tension	2	2.61	1.31	0.541	0.585	
Residuals	60	144.96	2.42			

In accordance with population data there was no change in SH1000 clone MICs following selection in no antibiotics (Figure 6-5A) and there was a significant increase in SH1000_TetR clones MICs following selection in TET or DOX (TET MIC increase compared to ancestor: 0-192 μg/ml for both TET and DOX evolved clones) (Kruskal-Wallis rank sum test comparing MIC of SH1000_TetR clones based on evolution antibiotic, $p=6.44x10^{-9}$) (Figure 6-5B). Unlike for population data, the tetracycline MICs of SH1000_TetR evolved normoxia were significantly higher than for clones evolved in hypoxia (Kruskal-Wallis rank sum test comparing MIC of SH1000_TetR clones based on evolution oxygen tension, p=0.0217), with the difference in MICs by evolved oxygen tension only apparent in normoxic test conditions (normoxia, p=0.032, hypoxia, p=0.321) (Figure 6-5B). The difference between population (Chapter 5) and clones MICs could be from populations MICs only showing the maximum MICs of any individual within a population however rare the phenotype. Growth characteristics and MICs from clones support previous conclusions from population data that evolution in the absence of antibiotics can overcome the resistance cost associated with *tetL* but antibiotic instead select for higher levels of resistance.

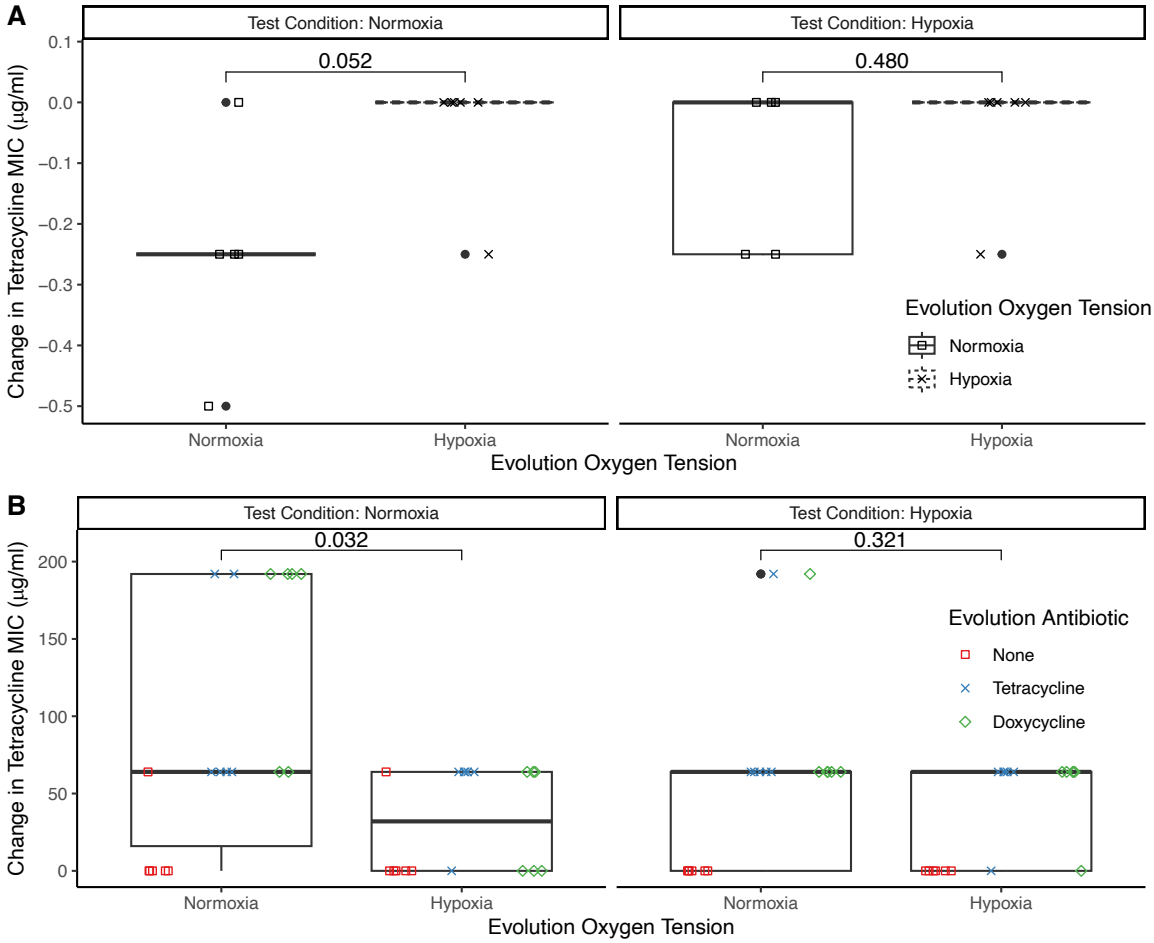

Figure 6-5: MICs of clones are not consistently influenced by evolution oxygen tension

Change in MIC compared to their ancestor measured in TET (0.25-256 µg/ml), prepared by serial dilutions of antibiotics in equilibrated BHI broth in normoxia, (21% O_2, 5% CO_2, 37°C) or hypoxia, (0.8% O_2, 5% CO_2, 37°C) in 96 well plates before 20 h incubation with bacteria. Normoxic overnight cultures were diluted to $A_{600\ nm}$=0.05 before 10 µl was added to 90 µl antibiotics preparation. A) SH1000 following 30 days selection in normoxia (square, solid line) or hypoxia (cross, dashed line). B) SH1000_TetR following 30 days selection in red square= no antibiotic, blue cross= TET, green diamond= DOX in normoxic or hypoxic oxygen tensions. MIC Cut-offs were defined as the lowest antibiotic concentration with no visible bacterial growth in the well. Statistical analysis by Kruskal-Wallis rank sum test with Wilcoxon rank sum post-hoc testing and Benjamini-Hochberg correction for multiple by evolution oxygen tension. Kruskal-Wallis rank sum test of B) independent of test oxygen tension and evolution oxygen tension by evolution antibiotic, $p=6.44x10^{-9}$, by evolution oxygen tension, p= 0.0217. Box and whisker plots present median, 25/75% quantile (upper and lower hinge), smallest/ largest observation ≤upper/lower hinge +/- 1.5 inter quantile range (whiskers), filled circle show range beyond whiskers.

6.3.2 Distinct genetic loci are selected by antibiotic- versus hypoxia-mediated selection

To investigate the genetic mutational landscape in response to selection in antibiotics and/or hypoxia, I performed whole genome sequencing on 47 clones, 1 from each of the 6 evolved population of SH1000 or SH1000_TetR in no antibiotic, TET or DOX and normoxia or hypoxia. These were randomly selected and were characterised above. As noted (Figure 6-3, Figure 6-5), these clones seemed representative of the evolved populations in terms of growth characteristics. I carried out whole genome sequence analysis by 2 pipelines (section 3.2.14.2) both of which mapped the illumina sequence reads to the reference genome NCTC 8325, identified differences with the reference, which I then check against the reference and their ancestor (SH1000 or SH1000_TetR) in IGV which visualises the genome sequence. I also checked the unmapped reads and coverage read depth for any differences compared to their ancestor. Over all evolution conditions, 115 mutations (Figure 6-6) were identified compared to the ancestor, comprising 8 deletions, 7 frame shift mutations, 31 intergenic mutations, 7 synonymous mutations, 48 missense mutations, 11 nonsense mutations plus 3 large deletions affecting more than 1 gene. There was no significant difference in the number of variants per clone between the evolution conditions (2-way ANOVA, Pr(>F)= 0.326).

Clones evolved in different treatment conditions varied in the loci that had acquired mutations (Permutational ANOVA, F=7.427, Pr(>F)= 0.001). A phylogenetic tree was constructed to model this divergence between clones. Jaccard's distances were used, categorically defining presence or absence of a mutation, before mapping these distances on an unrooted neighbour joining phylogeny using the R package ggtree (section 3.2.16). The phylogenetic tree showed clustering mainly based on antibiotic treatment and then evolution oxygen tension within antibiotic treatments (Figure 6-7) indicating clones evolved in the same antibiotics and oxygen tension had mutations in the same genes. Distinct sets of mutated loci were associated with the response to antibiotic- or oxygen-mediated selection and hence substantial genetic divergence between treatments (Figure 6-7; antibiotics, $p< 2x10^{-16}$, oxygen tension, $p= 1.84x10^{-11}$). This suggests that the evolutionary environments impact differential selective pressures leading to discrete subsets of adaptive mutational changes.

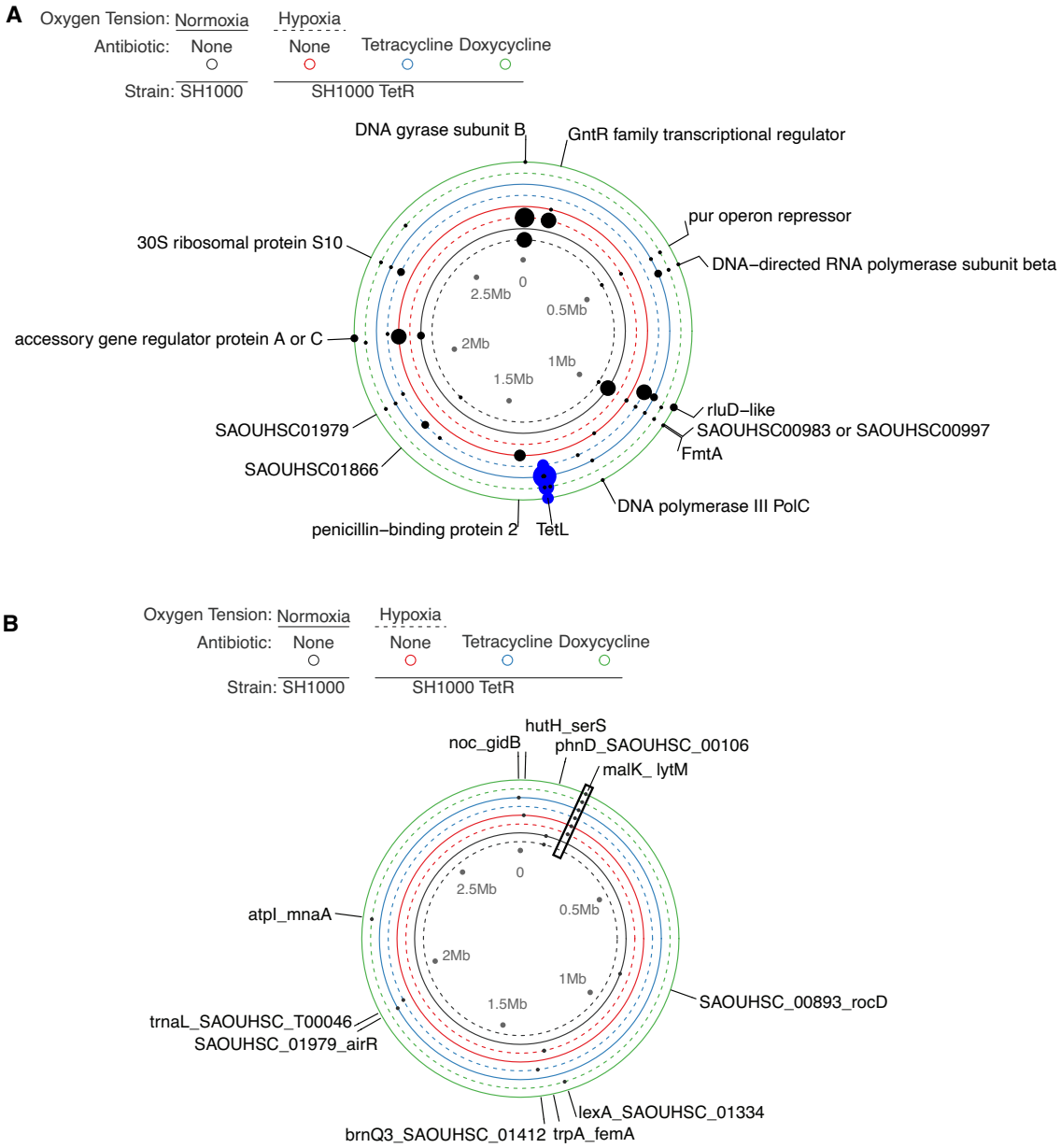

Figure 6-6: Parallel mutations associated with evolution conditions

Mutations from day 30 evolved isolates. Size of filled circle is proportional to the numbers of variants in different clones. Black= SH1000 no antibiotic, red= SH1000_TetR no antibiotic, Blue= SH1000_TetR TET, Green= SH1000_TetR DOX. Evolution conditions are represented by: normoxia=solid line, hypoxia=dashed line. A) Non-synonymous (black filled circles) mutations plus TetL duplication (blue filled circles) from day 30 evolved isolates, synonymous mutations have been excluded for clarity. Labels for >1 variants in different clones. B) Intergenic (black) mutations from day 30 evolved isolates. Genes flanking intergenic mutations are labelled. Black box around variant at 191203 in all SH1000_TetR repeat 2 derived clones. Filled circles represent 1 clone with an intergenic mutation at that position.

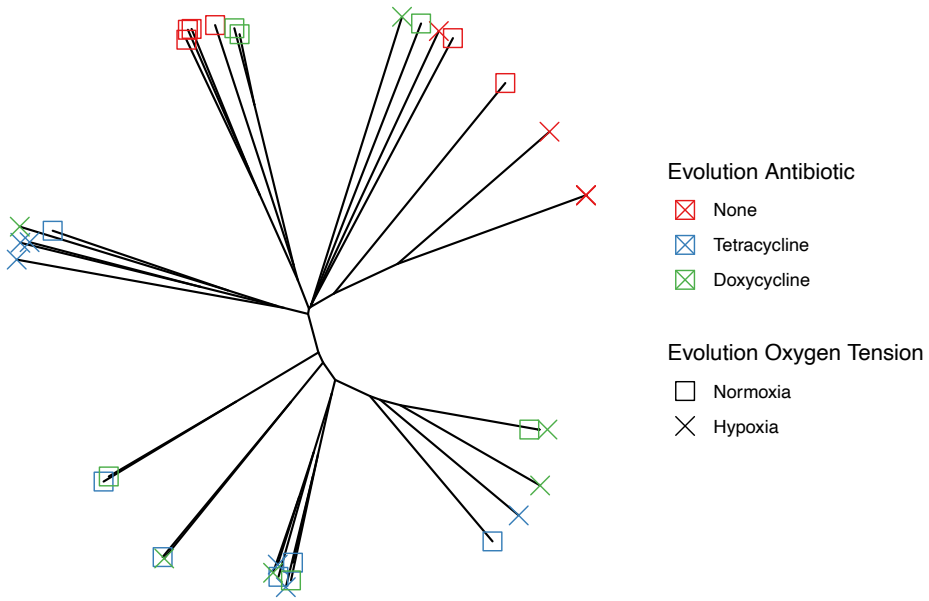

Figure 6-7: Phylogenetic clusters are based on presence of tetracyclines in evolution

Unrooted neighbour joining phylogeny of SH1000_TetR clones. Distances based on matrix of non-synonymous mutations in a binary change or no-change in a gene, TetL duplication recorded as duplicated or not. Evolution antibiotics are represented by red= no antibiotic, blue= TET, Green= DOX with evolution oxygen tensions denoted as normoxia=cross or hypoxia=square. ANOVA model of Jaccard's index of genetic distances based on selection conditions: evolution antibiotics, $p< 2x10^{-16}$, evolution oxygen tension, $p= 1.84x10^{-11}$. Tukey's multiple comparison, Antibiotics: None: TET $p<1x10^{-7}$, None: DOX $p<1x10^{-7}$, TET: DOX p= 0.133

To identify candidate putatively adaptive mutations associated with the response to antibiotic and hypoxia selection, I focused on those non-synonymous mutations which had variants in multiple independently evolving populations within treatments at the same loci (Figure 6-6A), because such parallel evolution is strong evidence for the operation of positive selection at these loci[455]. Generally, I did not focus on the intergenic mutations (Figure 6-6B) as I do not have transcriptional data which would be needed to establish if these had any impact on the expression of upstream/downstream genes. All evolved clones retained the *tetL* gene irrespective of treatment, however in those evolved with antibiotic selection I observed a range of mutations at the site of the *tetL* insertion. Interrogation of the pMUTIN2 integration vector by carrying out de novo assembly of the unmapped reads in SH1000_TetR ancestor to get a reference sequence, and then mapping the clones unmapped reads to this sequence, revealed that 2 of the 6 clones evolved in DOX in normoxia had large deletions (of 995 bp in 2 sections in 1 clone, and 7659 bp in the other) in the pMUTIN2 vector after the *lysA* insertion site, but retained the entire *tetL* gene. Elevated (>2-fold) coverage (i.e. increased illumina read depth) of the *tetL* was observed in 15 clones of the 24 that had evolved under TET or DOX selection, suggesting gene duplication had occurred (Figure 6-8). The maximum coverage of *tetL* was 29 times in a clone that had evolved under TET selection in normoxia. The location of the gene duplication was inspected, and no additional insertion sites were identified suggesting the gene duplications are within the *lysA* insertion site.

Several genes with roles in the transcription and translation processes acquired mutations in evolved clones that had undergone prolonged selection with antibiotics. Unsurprisingly, these included the 30S ribosomal protein S10 (4/47 clones all evolved in antibiotics (24 clones)), which is the target of tetracycline[456]. Unexpectedly, the most frequent target of antibiotic selection was a gene encoding an RluD-like protein (10/47 clones all of which had been evolved in antibiotics (24 clones)).

I also observed a hypoxia-associated mutational profile in evolved clones. Parallel mutations in genes encoding DNA gyrase B (10/47 clones, 9 evolved in hypoxia) and the GntR family transcriptional regulator (5/47 clones, 4 evolved in hypoxia) were observed more often in clones evolved under hypoxia in the absence of antibiotics, suggesting these are involved in adaptation to hypoxia. Finally, parallel mutations were also identified in genes with no clear

association with antibiotics or hypoxia, including penicillin-binding protein 2 (2/47 clones) and FmtA (10/47 clones) both of which are associated with cell wall synthesis[393,457]; these mutations may therefore be associated with adaptation to the laboratory conditions present during the prolonged evolution experiment.

Given the above findings, I decided to explore in more detail the RluD-like protein mutations and TetL duplications (as the most frequent targets of prolonged tetracycline exposure) and the DNA gyrase B mutations (strongly associated with evolution in low oxygen tensions).

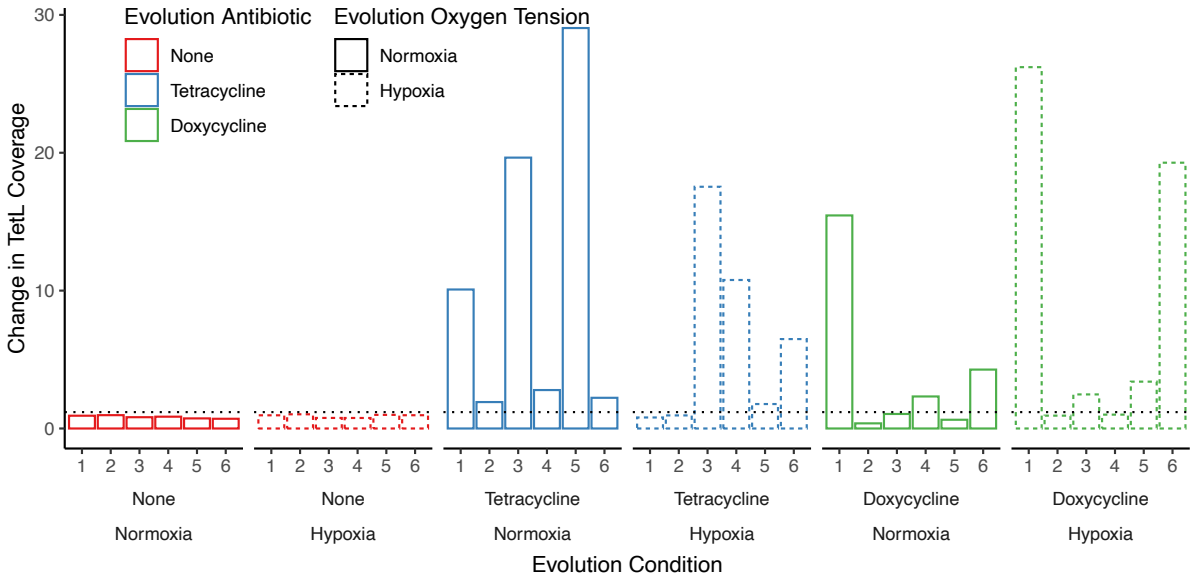

Figure 6-8: TetL duplications in SH1000_TetR following evolution in tetracyclines

Change in the TetL mean sequencing coverage compared to the mean coverage across the entire genome. This was calculated by mean coverage depth of a 1000 bp region within the resistance gene normalised by mean coverage depth across the entire genome. 1-6 represent the 6 different SH1000_TetR clones in each evolution condition. Dashed black line at 1.18 shows mean coverage of TetL in SH1000_TetR ancestor. Evolution conditions are: red=no antibiotic, blue=TET, green=DOX, solid line=normoxia, dashed line=hypoxia.

6.3.3 Mutations affecting the RluD-like protein alter antibiotic resistance

To associate the observed genetic variants with specific phenotypes of interest, the tetracycline MICs and growth of clones with and without mutations at loci of interest were compared. The poorly-characterised rluD-like protein is a pseudouridine synthase which carries out post-transcriptional modification of 23S rRNA[458]. 10 clones carried a mutation within the *rluD*-like gene, all of which had evolved in the presence of antibiotics. These variants were in 5 different positions in the gene. Residue 29 was mutated in 4 clones, with 3 clones having the Ala29Thr variant and 1 Ala29Ser. All clones carrying a *rluD*-like variant also had 1 or more mutations elsewhere in their genomes compared to their ancestor. Importantly, mutations in the gene encoding this RluD-like protein were associated with a large increase in tetracycline MIC of already resistant clones (mean+/- SE: normoxia: WT, 73.8 +/-10.8 µg/ml; *rluD,* 179.2 +/-20.9 µg/ml; hypoxia: WT, 65.9 +/-8.4 µg/ml, *rluD,* 154.0 +/-17.1 µg/ml) which was significant when tested in both normoxia and hypoxia (Figure 6-9A, normoxia, p=0.00019, hypoxia, p=0.00017).

To further study the role of RluD-like protein in tetracycline resistance the transposon mutant obtained from the Nebraska mutagenesis library (NE822) (rluD_KO) was studied compared to its parent the MRSA strain USA300_LAC_JE2 which has had all plasmids removed. Unexpectedly given the above results from the antibiotic-evolved clones, I found rluD_KO had increased sensitivity to TET compared to its ancestor (Figure 6-9B, normoxia, p=0.00061; hypoxia, p=0.0027), independent of oxygen tension. To see if rluD-like protein influenced *S. aureus* fitness, competitions assays of USA300_LAC_JE2 and rluD_KO compared to erythromycin resistant USA300_LAC_JE2 (USA300_LAC_JE2_eryR), as the only antibiotic resistant USA300_LAC_JE2 derivative available, were carried out. 0.125µg/ml TET was included as a subinhibitory concentration to check if TET influences fitness. There was no significant difference in the fitness of USA300_LAC_JE2 or rluD_KO independent of the presence of TET or oxygen tension (Figure 6-9C). This is important as it suggests *rluD* is not having a large influence on bacterial fitness so the mutations found are more likely to be neutral or beneficial in an antibiotic free setting, increasing likelihood of mutations being maintained within a population.

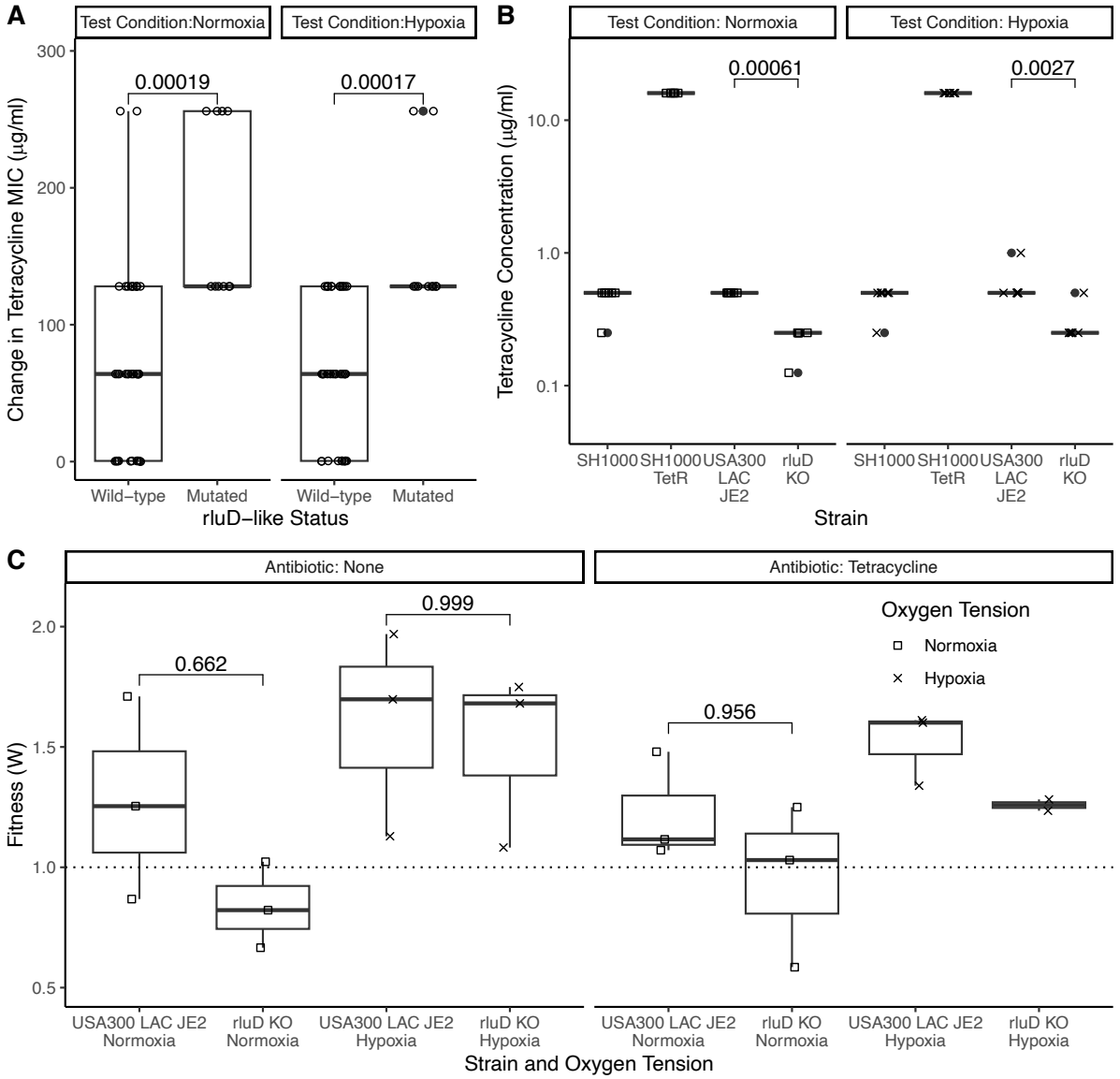

Figure 6-9: rluD mutations may influence tetracycline resistance

A, B) MICs measured in TET prepared by serial dilutions of TET (0.25-256 µg/ml) in equilibrated BHI broth in normoxia and hypoxia prior to 20 h incubation with MIC cut-offs were defined as the lowest antibiotic concentration with no visible bacterial growth. A) Change in sequenced clone MIC compared to ancestor. Sequenced clone MICs with (n=10) or without mutations (n=37) in the rluD-like gene independent of mutations elsewhere in their genome. B) MICs of SH1000, SH1000_TetR, USA_300_JE2, and rluD transposon mutant from Nebraska mutant library. C) Competition assays of S. aureus USA300_LAC_JE2 competed against USA300_LAC_JE2_EryR for 24 h in normoxia or hypoxia. Starting and final ratios were determined by selective plating with or without erythromycin. Dashed line at 1 indicates no fitness cost. <1 show a fitness advantage compared to USA300_LAC_JE2_EryR. When included TET is included in the competitions for the 24 h incubation at 0.125 µg/ml. Results are n=2/3

clones carried out in triplicate. Statistical analysis by A, B) Kruskal-Wallis rank sum test with Wilcoxon rank sum post-hoc testing and Benjamini-Hochberg correction for multiple comparisons. C) 2-way ANOVA with Tukey's multiple comparisons. No comparison on group where n=2. Box and whisker plots present median, 25/75% quantile (upper and lower hinge), smallest/ largest observation ≤ upper/lower hinge +/- 1.5 inter quantile range (whiskers), filled circle show range beyond whiskers.

The MIC data from rluD_KO in TET were the opposite of what I expected given the rluD mutations in the evolved clones led to increased tetracycline MICs. It is possible that the observed mutations led to improved function of the RluD protein (i.e. 'gain-of-function') that would not be captured using a deletion mutant. Structural analysis was carried out, using Phyre2[271] to predict the structure and PyMOL[273] to align the prediction to a CryoEM structure (section 3.2.15). It was not possible to predict the consequence of the 3 rluD-like protein variants (Figure 6-10) with any confidence. Ala29Thr (3 clones) and Gly34Ser (2 clones) both occur on the same alpha-helix and could influence interactions with the other domain or a quaternary structure unseen in this structural predication. 1 clone had a 5 bp deletion at residue 163. This would be predicted to cause major disruption to a large proportion of the protein (Figure 6-10, affected region in black) and hence might be expected to be detrimental to protein function. This clone had a TET MIC of 256 μg/ml compared to its ancestor of 64 μg/ml. This clone did have another mutation in DNA gyrase B as well as the rluD-like protein mutation so unfortunately it is impossible to form firm conclusions based on these data alone; however, if there was a decrease in MIC from loss of function in rluD-like protein this might have been expected to be reflected in this clone.

Due to these inconsistencies, Dr Joshua Sutton kindly transduced the rluD_KO transposon into the SH1000_TetR genetic background so we could see if this was influencing these data. In doing this he found the transposon had the incorrect insertion locus, hence the rluD-protein was not in fact deleted as expected in this clone. When the Nebraska library was constructed, the insertions were not confirmed by sequencing, therefore this was likely an error in library construction. Other errors in the library have been found (Professor Simon Foster, personal communication). Therefore, the data obtained with the supposed rluD_KO cannot be used to further our analysis of the mutations we observed. Due to the time constraints of a PhD I did not pursue these findings further.

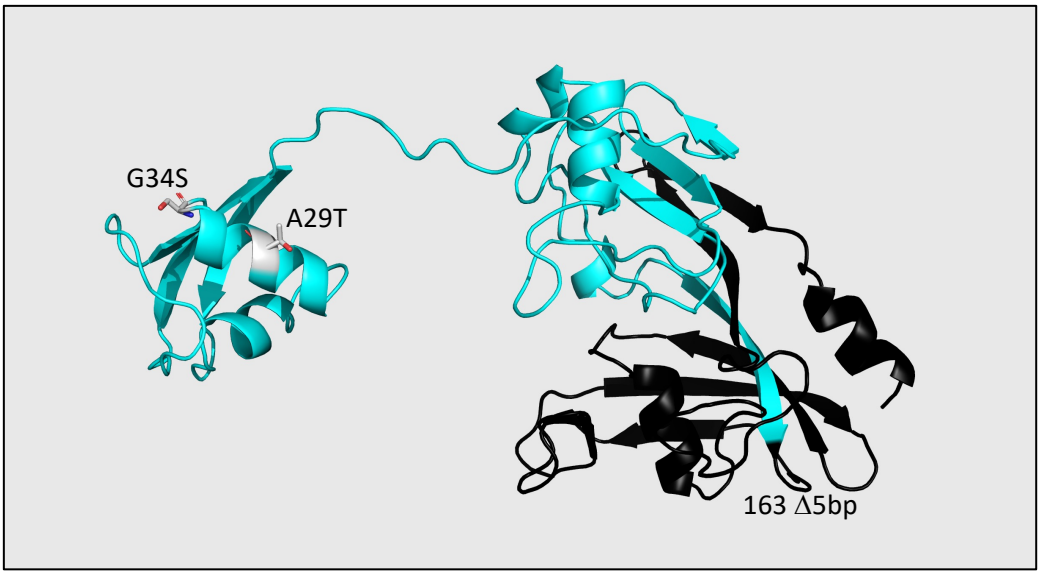

Figure 6-10: Location of mutations on rluD structure.

Computational structural analysis of Ala29Thr, Gly34Ser mutations (white) and the location of the 5 bp deletion at residue 163 and downstream region predicted to be influenced (black). Phyre2 model [271] aligned to Xray-diffraction model reported for E. coli *RluD (2ist.pdb) in the protein data bank[274].*

Another genetic variant favoured by antibiotic selection was the *tetL* duplication (15/24 clone evolved in TET or DOX) (Figure 6-8). Two such clones had no mutations elsewhere in their genomes, both evolved in DOX either in normoxia (15.6 times coverage) or hypoxia (26.2 times coverage).

To estimate the fitness effect of *tetL* duplications, clones with duplications were competed against SH1000_KanR. SH1000_KanR was used as a consistent resistance clone which could be used for tetracycline resistant and sensitive clones, and importantly, in chapter 5 it did not cause a differential fitness cost in hypoxia or normoxia (Figure 5-1A). Competing evolved clones with *tetL* duplications but no other mutations show no change in fitness compared to the SH1000_TetR ancestor with or without tetracycline, irrespective of oxygenation (antibiotic free: normoxia, p=0.932, hypoxia, p=0.989, TET: normoxia, p=0.99, hypoxia, p=0.763) (Figure 6-11A) suggesting that the *tetL* duplications did not lead to a higher fitness cost in any of the conditions explored, including tetracycline exposure. Furthermore, there was no clear association between the increase in *tetL* coverage of clones and their tetracycline MICs (Figure 6-11B); 3/8 clones had the maximum TET MIC of 256 μg/ml without *tetL* duplication. Increased resistance in these evolved clones with *tetL* duplications was instead associated with a combination of additional mutations. These were seen in genes encoding *rluD*-like (2 clones), accessory gene regulator protein A (1 clone), RpoB (1 clone), 30S ribosomal protein S10 (1 clone), and a hypothetical (1 clone) protein and a 7,659bp deletion in the tetL insertion cassette (1 clone, resistance gene complete). A non-coding region was also mutated in 2 clones, including 1 with this as the only additional mutation. The non-coding SNP which was found to be the only variant in this clone was highly parallel, found in all SH1000_TetR derived lines of clone 2 (highlighted with a box in Figure 6-6B) and thus likely occurred when these lines were established. Further study could establish if expression of the 2 flanking genes, *lytM* and *malK*, has been affected by this SNP as these genes have been previously associated with vancomycin resistance[459] and multiple antibiotic stresses[460], respectively. These variants achieve the same high-level tetracycline resistance, thus obscuring any benefit of *tetL* duplication. Overall, these results suggest that chromosomal point mutations elsewhere in the genome might contribute to high-level resistance in the antibiotic-evolved clones with *tetL* duplications.

6.3.4 DNA gyrase B mutation increases *S. aureus* fitness in hypoxia

Mutations in DNA gyrase B were associated with evolution in hypoxia (Figure 6-4). Evolved clones with mutations in *gyrB* showed increased growth in both normoxia (p=0.021) and hypoxia (p=0.0014) (Figure 6-12A). DNA gyrase B is a topoisomerase which catalyses the negative supercoiling of double-stranded DNA[461] opening up the structure for transcription. Overall, 10 clones (SH1000 or SH1000_TetR lineage) carried a DNA gyrase B variant, of which 9 were evolved in hypoxia with no antibiotics and one in normoxia with DOX. 4 clones carried the A439S variant, of which 3 had no additional mutations. Competition assays of these clones against their ancestor showed significantly increased fitness relative to the ancestor in hypoxia compared to normoxia (p=0.019) (Figure 6-12B). The strong association of *gyrB* mutations with the antibiotic free environment was interrogated through competition assays performed with or without tetracycline (0.125 μg/ml). Clones with the DNA gyrase B A439S variant showed increased fitness in antibiotic free hypoxic conditions compared to their ancestor (Figure 6-12C; hypoxia, p=0.005) but not in normoxia (p=0.138) or in the presence of TET (normoxia, p=0.051, hypoxia, p=0.876). These data support increased fitness in antibiotic free conditions in hypoxia driving the selection of DNA gyrase B mutations, with the addition of antibiotics in hypoxia eliminating this fitness advantage.

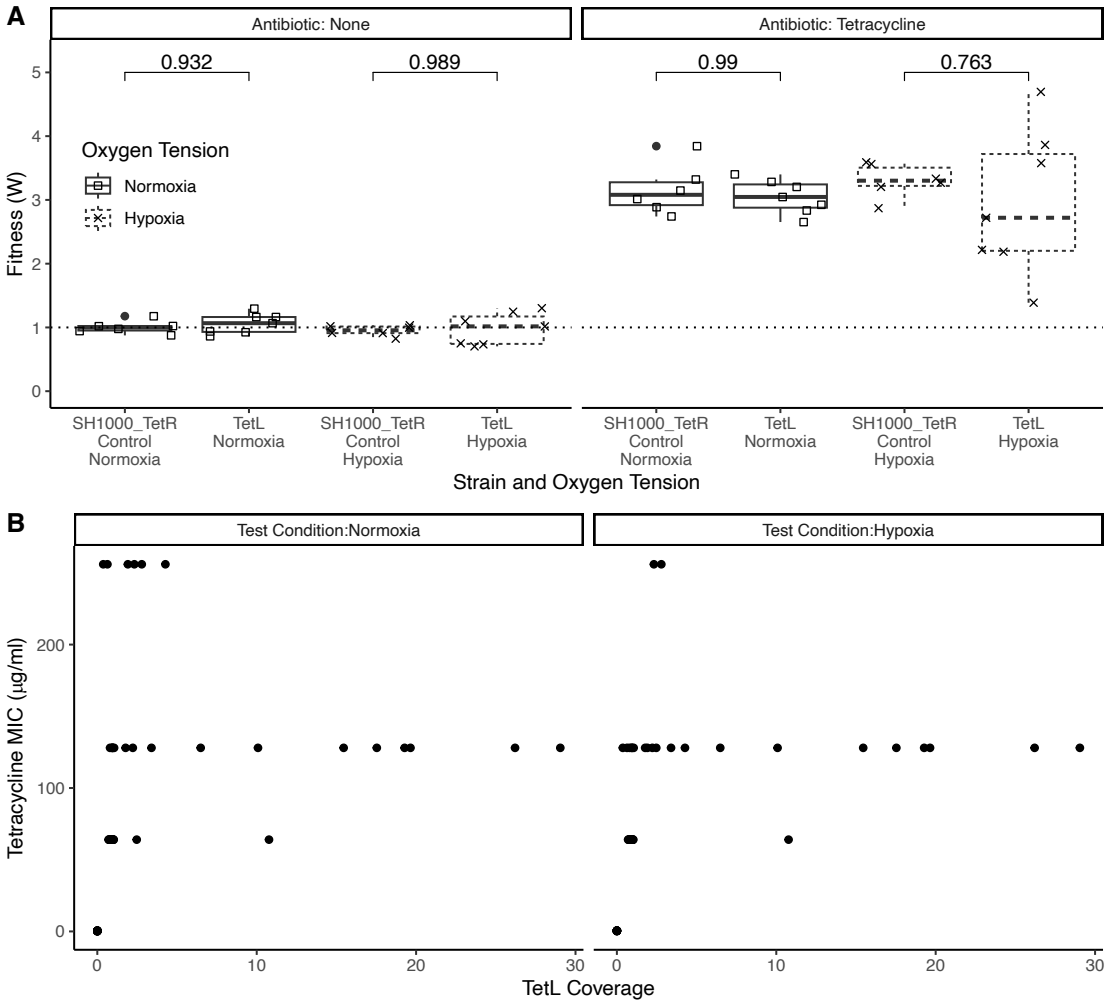

Figure 6-11: TetL duplications do not influence* S. aureus *fitness nor have a linear correlation with tetracycline resistance

A) Competition assay of kanamycin resistant SH1000 (SH1000_KanR) competed against SH1000_TetR clones with 26 times (n=4) or 15 times (n=3) TetL coverage compared to its ancestor (SH1000_TetR) in normoxia or hypoxia +/- TET (0.125 µg/ml) for 24 h starting from a 1:1 ratio performed in triplicate. Dashed line at 1 indicates no fitness cost, <1 show a fitness advantage over SH1000_KanR. Statistical analysis by 2-way ANOVA with Tukey's multiple comparisons. B) MICs measured in TET prepared by serial dilutions of antibiotics in equilibrated BHI broth in normoxia or hypoxia in 96 well plates. Bacteria were grown overnight before dilution to A $_{600\ nm}$=0.05 before adding to TET dilutions. Following 20 h incubation MIC cut-offs were defined as the lowest antibiotic concentration with no visible bacterial growth. n=6 clones evolved in each evolution condition. Change in the TetL mean sequencing coverage compared to the mean coverage across the entire genome. Box and whisker plots present median, 25/75% quantile (upper and lower hinge), smallest/ largest observation ≤ upper/lower hinge +/- 1.5 inter quantile range (whiskers), filled circle show range beyond whiskers in A Antibiotic: tetracycline.

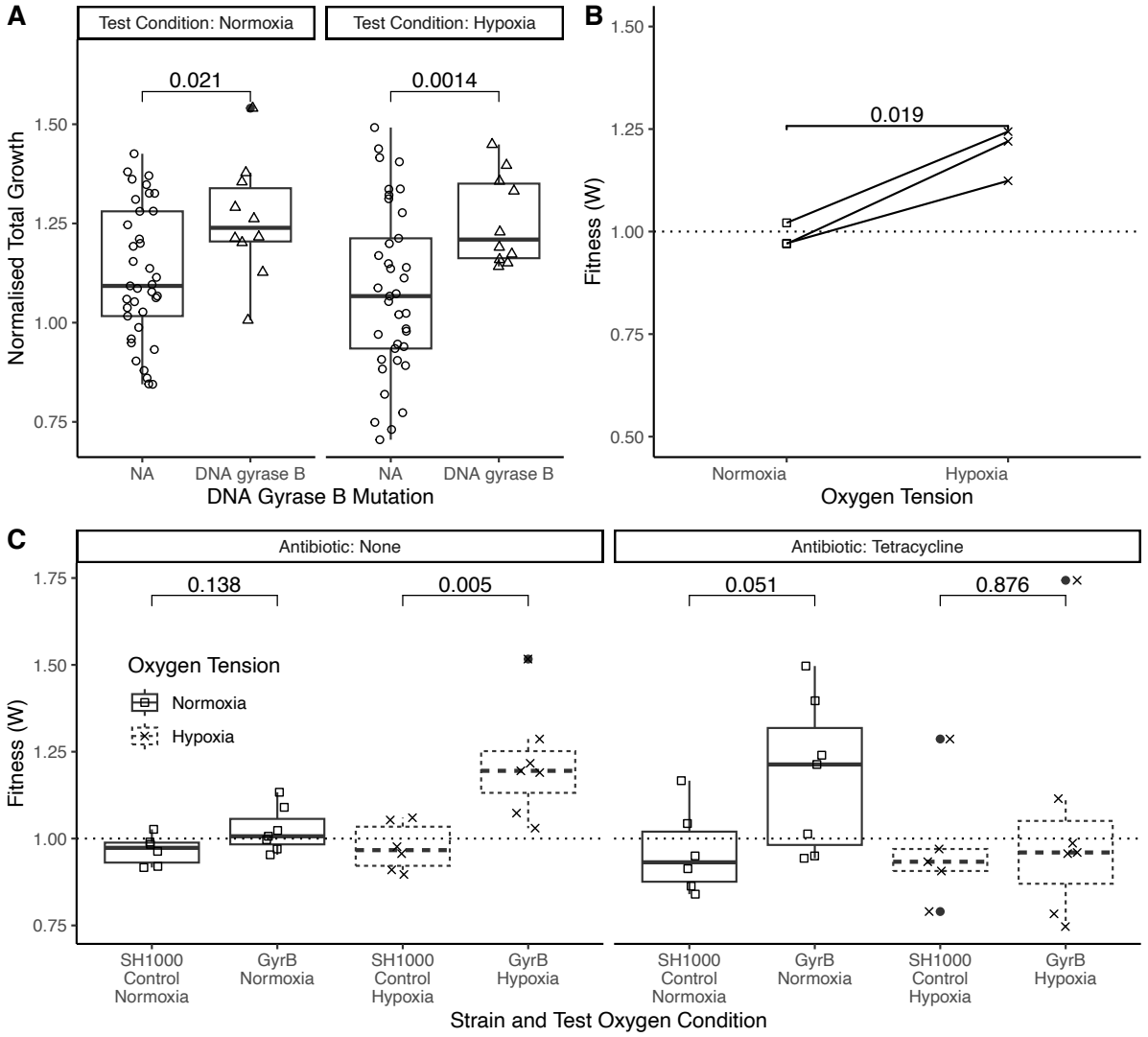

Figure 6-12: DNA gyrase B mutations detected predominantly in hypoxia increase fitness in hypoxia

A) Integral calculated from growth curves of clones from SH1000. Growth curves were carried out in deep 96 well plates in to match evolution condition. A $_{600\,nm}$ readings were taken at 0, 2, 4, 6, 24 h. The relative integral was calculated by division by the mean integral of the ancestor growth in matching test oxygen tensions. Clones without DNA gyrase B mutations (n=37) compared to variants with DNA gyrase B mutations (n=10) independent of whether clone carried other mutations within their genomes. B, C) Competition assays of SH1000 with DNA gyrase B variants Ala439Ser and no other mutations, following evolution in hypoxia, competed against SH1000_KanR for 24 h in normoxia or hypoxia. Starting and final ratios were determined by selective plating with or without kanamycin. Dashed line at 1 indicates no fitness cost. <1 show a fitness advantage compared to SH1000_KanR B) 3 clones carrying A439S variant in DNA gyrase B and no other. Results are n=3 clones carried out in triplicate with line connecting the same clone. C) Ancestor SH1000 compared to 2 clones (n=3/4) carrying Ala439Ser variant and no other mutations. TET is included in the competitions for the 24 h

incubation at 0.125 μg/ml. Results are n=7 carried out in triplicate. Statistical analysis by A) t-test, B) paired t-test, C) Kruskal-Wallis rank sum test with Wilcoxon rank sum post-hoc testing and Benjamini-Hochberg correction for multiple comparisons. Box and whisker plots present median, 25/75% quantile (upper and lower hinge), smallest/ largest observation ≤upper/lower hinge +/- 1.5 inter quantile range (whiskers), filled circle show range beyond whiskers.

To better understand the role of *gyrB* mutations, I performed computational structural analysis of the DNA gyrase B variant proteins with input from Professor Jon Sayers. The variant Ala439Ser arose independently in 4 clones. Residue 439 lies within a relatively hydrophobic pocket in the active site, thus alanine to serine mutation could be making it more hydrophilic. When including the DNA chain within the structure, the change to Ser439 (subunit B) is in close proximity with Tyr122 (subunit A) which forms a phosphotyrosine interaction with the DNA. The space between Ser439 and Tyr122 creates a space and appropriate bonding for an H_2O molecule or ion (Figure 6-13 A, B), which could create a network of H bonds to stabilise the active site affecting DNA binding. As such, this mutation would potentially alter the function of DNA gyrase B consistent with the functional data in Figure 6-12.

An additional DNA gyrase B variant, Ile284Leu, could also potentially influence its function. This was found in 2 clones, although each clone also had mutations elsewhere in their genomes. The isoleucine to leucine mutation is predicted to introduce steric clashes with arginine 347 (Figure 6-13C). This could drive a conformational change of arginine 347 which would bring it within hydrogen bonding distance of ATP (Figure 6-13D). If this would enhance or reduce the catalytic rate of DNA gyrase B is unknown. Although not supported by functional data, together with the Ala439Ser this supports a functional change in DNA gyrase B following evolution in hypoxia.

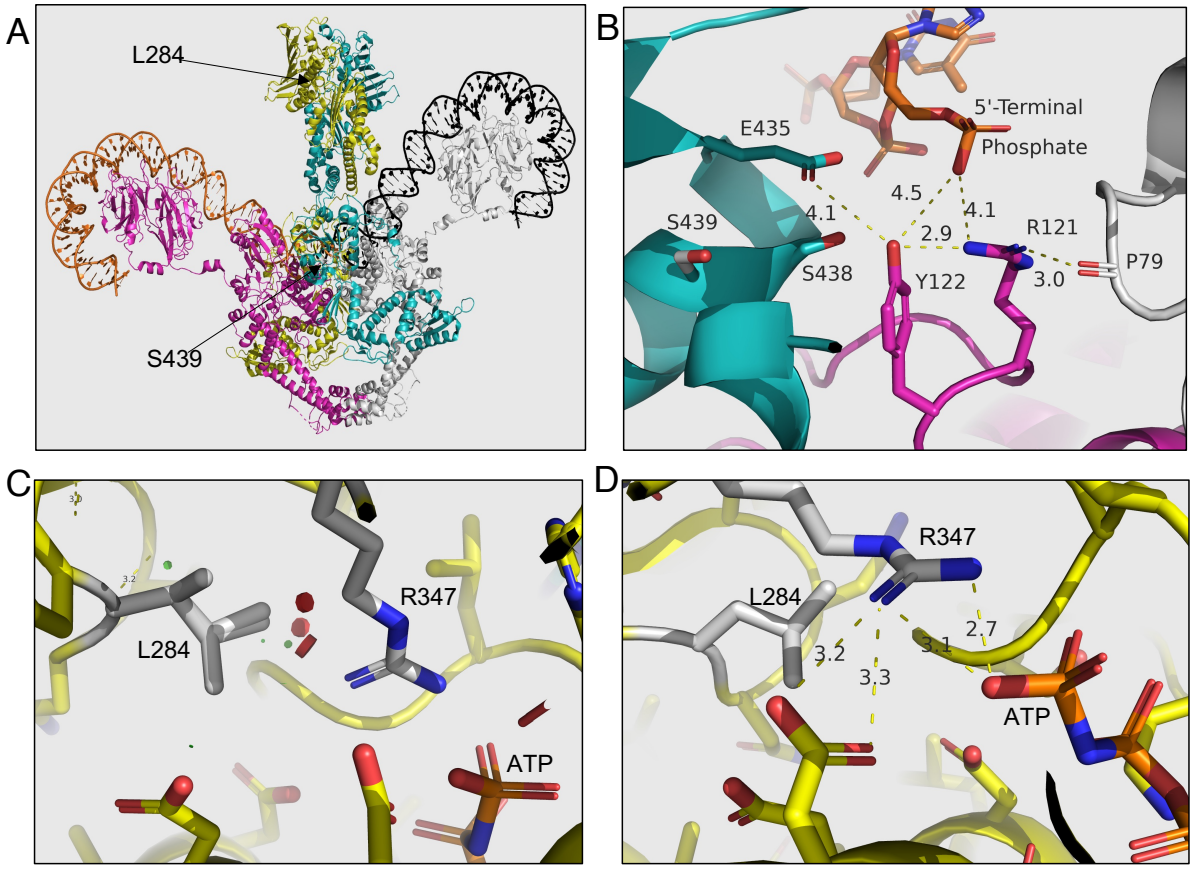

Figure 6-13: DNA gyrase B mutation structural prediction

Computational structural analysis of Ala439Ser and Ile284Leu DNA gyrase B mutation using Phyre2 model[271] aligned to Cryo-EM structure reported for E. coli *DNA Gyrase structure of (6rkw.pdb) in the protein data bank[274]. Grey=chain A, cyan= chain B, pink= chain C, yellow= chain D, orange/black=DNA before/after cleavage. A) Overview of whole structure with arrow indicating location of Leu284 and Ser429. B) Ser 439 mutations increasing H bond networks and creates a pocket possibly suitable for H_2O or ion which could enhance H bond network and phospho-tyrosine DNA interaction. C) Mutated Ile to Leu 284 resulting in steric clashes (red circles) with Arg347. D) Leu284 with Arg347 in possible new conformation plus resulting H bond distances with ATP. All distances are measured in Å.*

6.3.5 DNA gyrase B mutation does not influence neutrophil intracellular survival

Within the hypoxic host environment, neutrophils are key host effectors of the immune response required to clear *S. aureus* infections[16]. Neutrophil killing of *S. aureus* is predominantly an intracellular process, and intracellular survival within neutrophils is therefore important for *S. aureus* pathogenicity[16,49]. Since the DNA gyrase B mutation arises predominantly in hypoxia, I quantified the intracellular survival of the 439 Ser DNA gyrase B variant within neutrophils to test if this mutation enhanced survival of the host response to infection. DNA gyrase B variants were strongly associated with hypoxia, therefore live mid-log cultures in hypoxia were used, compared to matched normoxic cultures. Following isolation by negative selection, neutrophils were resuspended in equilibrated RPMI 10% media and pre-incubated in normoxia or hypoxia to ensure the correct starting oxygen tension, as previously established by the group[91]. Intracellular survival was measured as described in section 3.2.12.9 for 439 Ser DNA gyrase B variant and SH1000 with mid-log cultures in normoxia and hypoxia. The use of live mid-log bacteria cultures, increased the variability of the MOI (mean +/- SD: SH1000 normoxia, 7.2 +/- 2.7; SH1000 hypoxia, 4.9 +/- 2.0; GyrB normoxia 6.5 +/- 1.7; GyrB hypoxia 5.6 +/- 2.0). To account for differences in initial MOI all data was shown as a percentage killing, which also corrects for any differences in phagocytosis between experiments or conditions. Of note, only a very small percentage of any staphylococcal strain remained viable. I found no significant difference of intracellular survival of 439 Ser *gyrB* mutants compared to its ancestor SH1000 (Figure 6-14, Table 6-2: 2-way ANOVA by strain: p=0.417) independent of bacteria or test oxygen tension. Unlike previous studies[91], there was no significant influence of neutrophil oxygen tension on intracellular survival (Table 6-2: 2-way ANOVA by neutrophil oxygen tension: p=0.718). I did unexpectedly see a significant decrease in killing of hypoxic mid-log *S. aureus* (Table 6-2: 2-way ANOVA by bacteria oxygen tension: p=0.0025). As the bacterial preparation contributes to neutrophils killing ability this could have contributed to discrepancies with previous studies. Overall however, these data suggest there was no difference in the neutrophil host response to 439 Ser *gyrB* mutants.

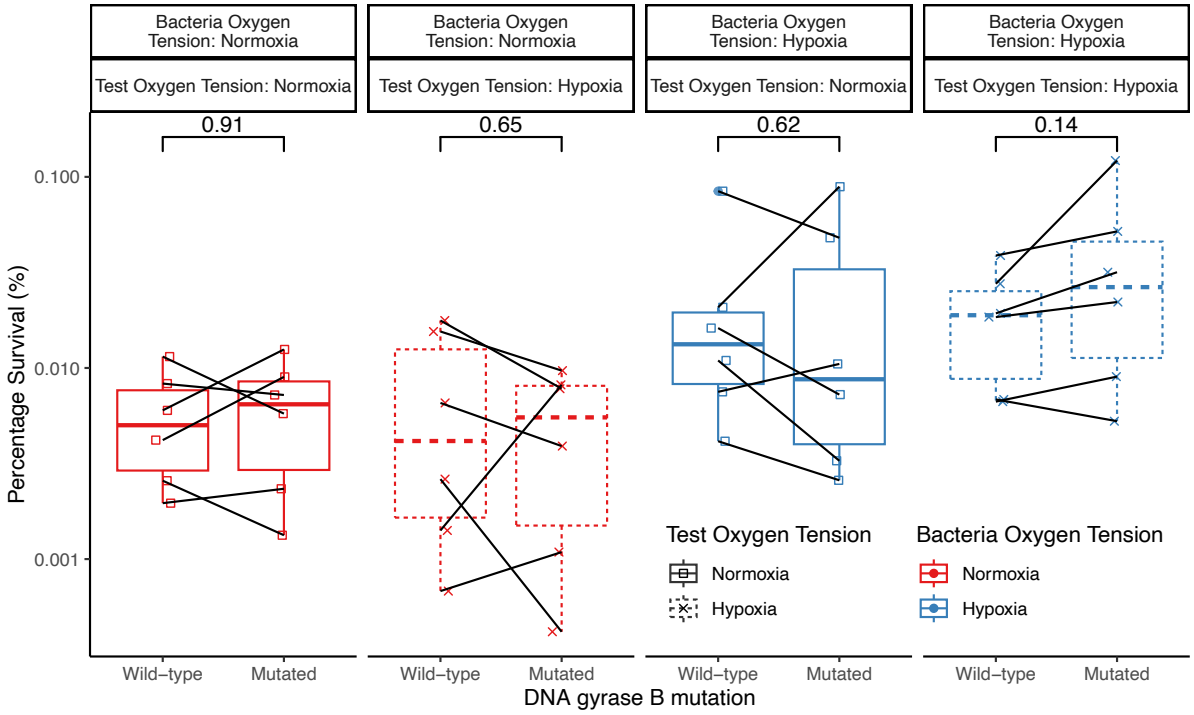

Figure 6-14: DNA GyrB Ala439Ser mutation does not influence intracellular survival in neutrophils.

Neutrophil killing of S. aureus *carrying the gyrB Ala439Ser mutation (mutated) compared to ancestor (SH1000). Mid-log bacteria cultures were grown in BHI broth in normoxia (red) (21% O_2, 5% CO_2, 37°C) or hypoxia (blue) (0.8% O_2, 5% CO_2, 37°C), before resuspending in equilibrated RPMI 10%FBS at MOI~5. Neutrophils were resuspended in pre-equilibrated RPMI 10% FBS (5x10^6 cells/ml 90 μl) in normoxia (square) and hypoxia (cross) and pre-incubated in 96 well plates for 1h. At 0 h bacteria were added, after 30 min incubation lysostaphin (20 μg/ml) killed extracellular bacterial and a 0 h bacteria intracellular counts were taken. 30 mins later neutrophils were collected, and intracellular counts were taken. Intracellular bacteria numbers were measured by washing neutrophils in dPBSx2 prior to cell lysis in pH 11 water and plating supernatants on BHI agar. Percentage killing calculated as (60 mins counts/ 30 mins counts) x 100. n=6 experiments from healthy volunteer neutrophil donors carried out in duplicate. Statistical analysis by paired T-test by donor. Box and whisker plots present median, 25/75% quantile (upper and lower hinge), smallest/ largest observation ≤ upper/lower hinge +/- 1.5 inter quantile range (whiskers).*

Table 6-2: Interactions from 2-way ANOVA for gyrB percentage killing data in Figure 6-14.

	Df	**Sum Sq**	**Mean Sq**	**F value**	**Pr (>F)**
Strain	1	0.000357	0.000357	0.672	0.4171
Bacteria Oxygen Tension	1	0.00553	0.00553	10.409	0.0025
Test Oxygen Tension	1	0.000070	0.000070	0.132	0.7183
Strain: Bacteria Oxygen Tension	1	0.000472	0.000472	0.889	0.3514
Strain: Test Oxygen Tension	1	0.000169	0.000169	0.319	0.5755
Bacteria Oxygen Tension: Test Oxygen Tension	1	0.000057	0.000057	0.107	0.7457
Strain: Bacteria Oxygen Tension: Test Oxygen Tension	1	0.000322	0.000322	0.607	0.4406
Residuals	40	0.0212	0.000531		

6.4 Discussion

In this chapter I have shown mutations in SH1000_TetR evolved clones diverge based on evolution in different oxygen tensions and antibiotics. The evolution of increased resistance to TET and DOX following prolonged antibiotic treatment, via mutations including in a *rluD*-like gene and *tetL* duplications, constrained adaptation to hypoxia, which otherwise arose via mutations affecting *gyrB*. 2 *gyrB* mutations, found following hypoxic evolution, were associated with changes in the active site for DNA gyrase. Crucially, the fitness benefit of *gyrB* mutations in hypoxic conditions were entirely negated when there were low levels of tetracycline present in competition assays. *gyrB* mutations did not change intracellular killing of *S. aureus.* Together, this supports the evolution data suggesting the advantage of *gyrB* variants in hypoxia is only in an antibiotic free setting.

The conditions I used in the 30-day evolution experimental scenario were chosen to re-capitulate important environmental conditions that might occur in chronic staphylococcal infections. Whilst some infections are readily and rapidly resolved, others (such as bone and joint infections[66], some skin conditions[462] and infective endocarditis[12]) require weeks or months of treatment with antibiotics. As previously noted, these infection sites are profoundly hypoxic with oxygen tensions as low (or lower) than those I have employed[58,61,66]. Of course, there are also important differences. Most chronic infections are treated with combinations of antibiotics rather than a single agent, and would commonly involve drugs such as flucloxacillin or gentamicin[463]. The access of antibiotics (as well as oxygen) to infection sites will be hindered by the ability to diffuse from the blood, which may be hindered by impaired capillary penetration or physical barrier[464]; hence the antibiotic concentrations at such infection sites are often unknown. In the evolution experiment I used 2 µg/ml DOX or 30 µg/ml TET to select for the *tetL* efflux pump and study the interaction with the fitness cost in hypoxia, however this is far in excess of the concentration either of these antibiotic would be found in humans[465]. I chose to study tetracyclines as I had already found in Chapter 5 that tetracycline resistance conferred by *tetL* was associated with a fitness cost in hypoxia, suggesting a possible interaction with this environmental stressor. Of course, the culture conditions will also differ from the micro-environment at an infections site including nutrient

availability[466], pH[464], biofilm formation[467] and bacteria surface interactions with cells rather than plastic[468].

As shown in the previous chapter, and other studies[441], prolonged antibiotic selection drove already resistant clones to further increase their resistance. Increased resistance to tetracycline and doxycycline arose via two distinct mechanisms. First, I observed duplication of *tetL,* the gene encoding the tetracycline efflux pump, although there was not a linear relationship between *tetL* copy number and TET resistance. *tetL* duplications were rarely in isolation and often occurred alongside mutations in the rluD-like protein. Increases in resistance were likely limited as *tetL* already conferred high levels TET resistance. Gene duplication events are commonly observed under antibiotic selection in vitro[469], including the duplication of plasmid-encoded *tetL* in *Enterococcus faecalis*[470], which was reversed on removal of tetracycline. Gene duplications mediating antibiotic resistance have also been detected in *S. aureus* isolated from clinical infections[471,472]. Resistance gene duplication events increasing resistance are likely to be more common than observed because these genomic changes are typically rapidly reversed when cultured without antibiotic[469-471], although I did not test this on our evolved clones. The *tetL* duplication events did not incur a fitness cost in line with previous studies, although I cannot guarantee they did not lose duplications during the assay in due to genomic mismatching[469].

A second and unexpected mutational mechanism I identified that led in the setting of persistent exposure to tetracycline antibiotics was the occurrence of mutations affecting an RluD-like protein. These mutations which were strongly associated with increased tetracycline resistance which has not previously been associated with antibiotic resistance. The RluD-like protein is a pseudouridine synthase which carries out posttranscriptional modification of 23S rRNA[458], and therefore is associated with the target of tetracyclines, the 30S ribosomal protein. The potential clinical relevance of these mutations is supported by identification of a rluD-like protein mutations (Ala29Thr) in a clinical isolate[473]. Mutations within the rluD-like protein have been observed in a previous laboratory evolution experiment where the same *S. aureus* background SH1000 was selected in the presence of the antimicrobial peptide melittin[474]. All 3 melittin-resistant strains identified in that study had mutations in residue 35 of the rluD-like protein, as was 1/10 rluD-like variants identified

in our study. However, the mechanism of resistance is likely to be different as melittin is an antimicrobial peptide which targets the bacterial membrane resulting in cell lysis[475]. It would be of interest to study the interactions of these rluD-like mutations in the context of tetracycline resistance, which could be done by site directed mutagenesis of *S. aureus* to test if these mutations confer antibiotic resistance in the absence of other mutations and the *tetL*. If variants in rluD-like protein do increase tetracycline resistance, the variant and wildtype proteins could be compared in vitro for binding to 23S substrate to identify if this is the cause of the change in resistance.

In the absence of antibiotics, *S. aureus* adapted to hypoxia often via mutations affecting *gyrB*. DNA gyrase B is the second subunit of the gyrase type II topoisomerase responsible for simultaneously catalysing the breakage and formation of double stranded DNA and for removing negatively supercoiled DNA in an ATP dependent manner. As such, DNA gyrase has broad influences on bacterial processes including: DNA replication initiation and elongation facilitating movement along the replication fork; transcription which can be activated and inhibited by supercoiling; promoting recombination and repair events[461,476]. Importantly, DNA gyrase has been shown to be essential for anaerobic but not aerobic growth[477] whilst increases in supercoiling have been associated with short term transitions to anaerobic conditions. Thus, the mutations are highly plausible with regard to adaptation to persistent hypoxia. A *gyrB226* mutation in *E. coli* has previously been shown to decrease supercoiling associated with a shift to anaerobic conditions[478]. I hypothesise, therefore, that the mutations I observed in DNA gyrase B may have increased bacterial fitness in hypoxia through modulating negative supercoiling and associated regulation of gene expression. By increasing fitness in low oxygen environments, *gyrB* mutations may enhance the competitiveness and survival of *S. aureus* in hypoxic infection sites. These findings thus suggest a previously unknown mechanism for adapting to hypoxia. Somewhat unexpectedly, I did not observe mutations in genes previously associated with responding to hypoxia, such as the *srrAB* encoding a 2-component system[430], although I cannot rule out that changes in gene expression levels could be occurring in parallel which could be further explored with RNA-seq experiments.

The DNA gyrase B mutation did not display altered neutrophil intracellular survival compared to its ancestor. Other *S. aureus* mutants have been shown to influence neutrophil killing, including *mprF* and *dlt,* through mediating antimicrobial peptide resistance[479,480]. Within a hypoxic neutrophil *S. aureus* is required to survive enhanced neutrophil degranulation compared to a normoxic neutrophil[89,142]. The high cost of antimicrobial attack within a neutrophil appear to negate any increases in hypoxic survival. Unexpectedly I saw no difference in neutrophil killing of internalised bacteria in hypoxia compared to normoxia. Previously there has been shown to be decreased intracellular killing of *S. aureus* in hypoxic neutrophils attributed to loss of ROS production[91] which has recently been repeated by other members of the group. This could be attributed to a combination of methodological differences including: different neutrophil isolation method; studying intracellular survival instead of whole cell killing; bacterial preparation method including opsonisation and washing, plus habituation to hypoxia; *S. aureus* strain or neutrophil lysis method; and also method of analysis (% killing versus CFU numbers). I found a significant decrease in *S. aureus* killing of hypoxic bacteria independent of neutrophil oxygen tension; I hypothesize this difference is caused by hypoxic bacteria being in a preconditioned 'stress response'. This is plausible, as the global virulence regulator *sar*, which is upregulated in low oxygen tensions[481], has already been shown to influence neutrophil intracellular survival with *sar* mutants less able to survive in neutrophils[49].

Although I used hypoxia as an infection-relevant selection pressure, a limitation of our study is that our experimental conditions do not fully capture the complexity of the infection environment. Conditions within infections are likely to vary with time and include additional stressors such as acidosis and nutrient deprivation, immune factors and interactions with other microbes in mixed infection[62,63,225]. Whilst some studies have explored the influence of fluctuating conditions[441,482], more studies incorporating a range of host specific stresses are needed to understand both the mechanisms of pathogen adaptation to these conditions and how such conditions affect the fitness costs of acquiring resistance genes. Neutrophils are a key regulator of *S. aureus* infections in hypoxia[16], with hypoxia increasing neutrophil degranulation[89], therefore next I investigate the interplay between antimicrobial products released at hypoxic sites and antibiotic resistance.

7 The Interaction Between Neutrophil-derived Proteins and Antibiotic Resistance

7.1 Introduction

During an infection, bacteria are exposed to multiple biotic and abiotic stresses. So far, I have studied the impact of hypoxia and of antibiotic exposure on the development of *S. aureus* bacterial growth and antibiotic resistance, and have identified mutations associated with these changes. In addition to hypoxia and antibiotics, during an infection *S. aureus* must escape or circumvent the immune system to successfully establish and maintain an infection. The predominant immune cell responsible for *S. aureus* clearance is the neutrophil, as evidenced by the severe staphylococcal infections suffered by patients with neutrophil defects[16]. In hypoxic conditions, neutrophil degranulation and the release of antimicrobial proteins is increased[89]. These neutrophil antimicrobial proteins are also of increased importance to bacterial killing mechanisms in hypoxia due to decreased activity of oxygen dependent mechanisms, including reactive oxygen species (ROS)[91]. Neutrophil granule proteins are pre-packaged during neutrophil development. The neutrophil granule types are azurophilic granules (primary granules, containing proteins or peptides including elastase, cathepsin G, bactericidal permeability increasing protein (BPI), human neutrophil peptide -1 (HNP-1) and myeloperoxidase (MPO))[124,483-485] specific granules (secondary granules, containing the antimicrobial peptide LL-37 or cathelicidin)[127] and gelatinase granules (tertiary granules, proteins include matrix metalloproteinases such as gelatinase) and secretory vesicles[483]. The release of granule proteins is hierarchical, dependent on the level of neutrophil activation, with secretory vesicles released readily followed by tertiary, specific then finally azurophilic granules with increased strength of stimulation[486].

In a hypoxic environment in vitro, neutrophil degranulation is markedly increased with enhanced liberation of (amongst others) elastase, neutrophil gelatinase-associated lipocalin (NGAL) and MPO; the same neutrophil-derived proteins were found to be upregulated in the plasma from patients with chronic obstructive pulmonary disease (COPD) during exacerbations (which are associated with inflammation/infection and hypoxia) compared to healthy controls[142], again illustrating the links between infection, neutrophils and their

products and hypoxia. In addition to the systemic neutrophil response, the signature of a neutrophilic inflammatory response is evident locally in many disease settings, including in the lungs in bronchiectasis (BE). Patients with BE have permanent airway dilation, which leads to increased sputum production and recurrent infections with organisms that include *S. aureus*[487]. The causes of bronchiectasis are complex and poorly understood. They include previous severe respiratory tract infections, COPD, asthma and immunodeficiency[488]. Cystic fibrosis (CF) also causes severe bronchiectasis due to mutations in the cystic fibrosis transmembrane conductance regulator (CFTR) gene[489], leading to dehydrated and thickened sputum, and infection with organisms such as *S. aureus* and *P. aeruginosa* as well as non-tuberculous mycobacteria (NTM). Sputum proteomics in 40 patients with bronchiectasis (20 severe vs 20 mild) identified 96 proteins that were associated with disease severity, including neutrophil azurophil granule proteins NGAL and MPO. Of note, sputum is a hypoxic environment[429], again linking hypoxia and neutrophilic inflammation in the setting of infection. Additionally, a study of participants with acute BE exacerbations (n=20) found 39 proteins that were significantly associated with antibiotic response. Of these, several proteins associated with neutrophil degranulation had differential regulation following 14 days antibiotic treatment (predominantly for *Pseudomonas* infections) including a significant decrease in MPO[487]. During my PhD, I undertook a placement in Dundee and had access to sputum proteomic data from patients with a range of chronic lung infections.

Infection with SarsCoV2 (COVID-19) is also strongly associated with neutrophilic inflammation and prolific neutrophil degranulation[151,490]. Secondary bacterial infections are an important complication of COVID-19, particularly in hospitalised patients. In the International Severe Acute Respiratory and Emerging Infections Consortium (ISARIC) WHO Clinical Characterisation Protocol UK (CCP-UK) study, 1107/48902 (22.6%) of hospitalised patients (enrolled 06/02/2020-08/06/2020) had a secondary bacterial infection, with *S. aureus*, *Haemophilus influenzae* and *Enterobacteriaceae* the most common causative species in respiratory co-infections and secondary respiratory infections. 85·2% patients in the ISARIC CCP-UK study received antimicrobials at some stage in their hospital admission[491]. Many patients with severe COVID-19 are hypoxic and many moderate to severe hospitalised patients will receive oxygen therapy[492,493]. Importantly, increased concentrations of neutrophil-derived proteases in the blood and lungs of people with COVID-19 have been

associated with disease severity and mortality[494]. Both BE and COVID-19 are thus disease settings where bacteria including *S. aureus,* will encounter neutrophilic inflammation, hypoxia and antimicrobial therapy.

Due to the evidence of the role of neutrophils in COVID-19 a multi-centre double-blinded, phase III, clinical trial of brensocatib was instigated[260]. Brensocatib is an oral competitive inhibitor of dipeptidyl peptidase-1 (DPP-1) which is required to activate neutrophil serine proteases (such as elastase, cathepsin G, proteinase-3) during neutrophil maturation in the bone marrow. Treatment with brensocatib resulted in reduced neutrophil serine protease activity in blood[495], and in a clinical trial in bronchiectasis, brensocatib reduced neutrophil elastase release and increased the time to disease exacerbation, thereby reducing the need for antibiotic intervention[496]. During and after the initial COVID-19 lockdown I assessed neutrophil function in patients enrolled on the trial (STOP-COVID19[260]) in Sheffield and Dundee. In total 406 patients (214 placebo; 192 brensocatib) were recruited to STOP-COVID19 (20 patient in Sheffield, 132 in Dundee) between 05/06/2020- 25/01/2021. It was hypothesised that "DPP1 inhibition would improve outcomes in hospitalized patients with COVID-19 by reducing neutrophil serine proteases in the airway"[260].

Like many important antibiotics (including β-lactams and glycopeptides targeting the cell wall and tetracyclines, aminoglycosides, macrolide and oxazidiones targeting protein synthesis), many antimicrobial proteins from neutrophil granules predominantly kill bacteria by attacking the cell wall, cell membrane or protein synthesis (section 1.2.2.2), with different targets in Gram-negative and Gram-positive bacteria. Elastase (a neutrophil serine protease (NSP)) kills predominantly Gram-negative bacteria, targeting the integrity of the cell membrane and hence causing bacterial lysis[107,108]. Cathepsin G is also a NSP but mainly kills Gram-positive bacteria, including *S. aureus*, with some activity against the Gram-negatives *P. aeruginosa* and *E. coli*. Cathepsin G causes bacterial death through inhibition of protein synthesis[111,112]. BPI is another potent antimicrobial protein active against Gram -egative bacteria. BPI kills by binding to LPS and degrading phospholipids and peptidoglycans, thereby inducing lesions in the cell membrane[96,97]. In addition, a range of small antimicrobial peptides are secreted by neutrophils. These antimicrobial peptides include HNP-1 (defensin) which can kill both Gram-negative and Gram-positive bacteria. Like elastase, HNP-1 causes cell death by permeabilising

the membrane leading to cell lysis[93,497]. The antimicrobial peptide LL-37 is an amphipathic α-helical peptide which inserts into the cell membrane and forms pores[498]. This leads to damage, depolarisation and cell lysis of both Gram negative and positive bacteria[94,367]. There is some evidence in the literature of an interaction between sensitivity to neutrophil antimicrobial proteins and antibiotic resistance. For example, penicillin resistance in *Neisseria gonorrhoeae* caused by mutations in *penA* correlates with increased bacterial susceptibly to cathepsin G[499]; polymyxin-B resistance in *Salmonella enterica* serovar Typhimurium conferred resistance against BPI[500]; colistin resistance in *Klebsiella pneumoniae* correlated with resistance against LL-37, although this was not linked to a difference to survival in vivo[501].

Considering the prevalence of neutrophil proteins at sites of infections, the overlapping targets between antimicrobial proteins and antibiotics (section 1.3.1), plus previous evidence of an interaction between resistance to neutrophil proteins and antimicrobial resistance, I wished to investigate the interactions between bacterial killing by neutrophil antimicrobial proteins and antibiotic resistance. To do this, I selected antimicrobial proteins prevalent in infections, tested the antimicrobial activity of number of relevant recombinant neutrophil proteins against *S. aureus* and, finally, studied the antimicrobial resistant clones from chapter 4 for any change in susceptibility to the antimicrobial peptide LL-37.

7.2 Hypothesis and aims

In this chapter I have tested the following research hypothesis:

Neutrophil antimicrobial proteins will suppress *S. aureus* growth, and this effect will be impacted by antimicrobial resistance.

The specific aims of this section were:

- Identify relevant neutrophil-derived antimicrobial proteins present at infection sites including blood and sputum
- Measure the antimicrobial activity of candidate recombinant antimicrobial proteins against *S. aureus*
- Determine if antimicrobial resistance, developed by evolution in the presence of antibiotics, can influence the killing of *S. aureus* by LL-37

7.3 Results

7.3.1 Sputum analysis confirms local neutrophil activation and degranulation in chronic lung disease

Whilst on placement with Prof. James Chalmers (University of Dundee), to identify neutrophil-derived proteins to which bacteria are exposed during lung infections in vivo, I analysed the protein signature of 95 sputum samples from 55 subjects. These patients had a range of underlying respiratory diseases (21 bronchiectasis without CF, 19 COPD, 15 cystic fibrosis), and n=15 had underlying NTM infections[261]. The most frequently isolated non-NTM bacterial pathogens were *H. influenzae, P. aeruginosa, S. aureus* and *S. pneumoniae*. Sample collection plus mass spectrometry had already been carried out (Dr Jeffrey TJ Huang, Alun K Barton, Dr Holly R Keir, Dr Huw Ellis, Prof. William Cookson, Prof. Miriam Moffatt, Prof. Michael Loebinger and Prof. James D Chalmers). As part of this analysis, I interrogated the interaction between bacterial pathogens (non-NTM or NTM coinfections) and sputum proteomic profile[261]. I also compared the sputum proteomic profile from patients with *P. aeruginosa* infections compared to those with Gram-positive (predominantly *S. pneumoniae* and *S. aureus*) and other Gram-negative (predominantly *H. influenzae*) bacterial infections (Figure 7-1A, B) independent of underlying NTM infections (with (n=15) or without NTM infections (n=40)). From the principal component (PCA) analysis, the greatest divergence in proteomic profile was between participants with no identified bacterial infections and patients with *P. aeruginosa* infections (Figure 7-1A). I therefore compared the sputum protein concentrations between the participants with no co-infection (n=22) and *P. aeruginosa* infection (n=10) groups to characterise differentially expressed proteins. There were 47 proteins significantly up-regulated in the sputum from participants with *P. aeruginosa* infection compared to no bacterial infection (Figure 7-1C, full list of significantly changed proteins in appendix 1). The significantly upregulated proteins in the *P. aeruginosa* group were largely neutrophil-derived, including S100A9/A8 (a cytoplasmic protein), azurocidin, MPO and neutrophil elastase. CAMP, the precursor for LL-37, was higher in the sputum in participants with *P. aeruginosa* infections but this did not reach significance (CAMP: p= 0.256, log2FC= -0.102). There was no significant difference in any of the sputum proteins from the participants with *P. aeruginosa* infections (n=10) when comparing proteomes of patients with *P. aeruginosa* infections plus

CF (n=6) or bronchiectasis (n=4) suggesting the CFTR mutation is less important than the infecting pathogen in this setting. These data align with previous studies showing a strong neutrophil-related signature associated with chronic respiratory diseases and *P. aeruginosa* infections[487]. Unfortunately, there were too few participants (n=3) with chronic *S. aureus* infection to allow me to interrogate their sputum neutrophil proteomic profile individually or in comparison with other groups. However, many participants with *P. aeruginosa* infections have a mixed infection, including 20-50% of participants with CF co-colonised with *S. aureus*[284]. Therefore, *S. aureus* in this setting will be exposed to similar proteins which are a product of neutrophilic inflammation in vivo.

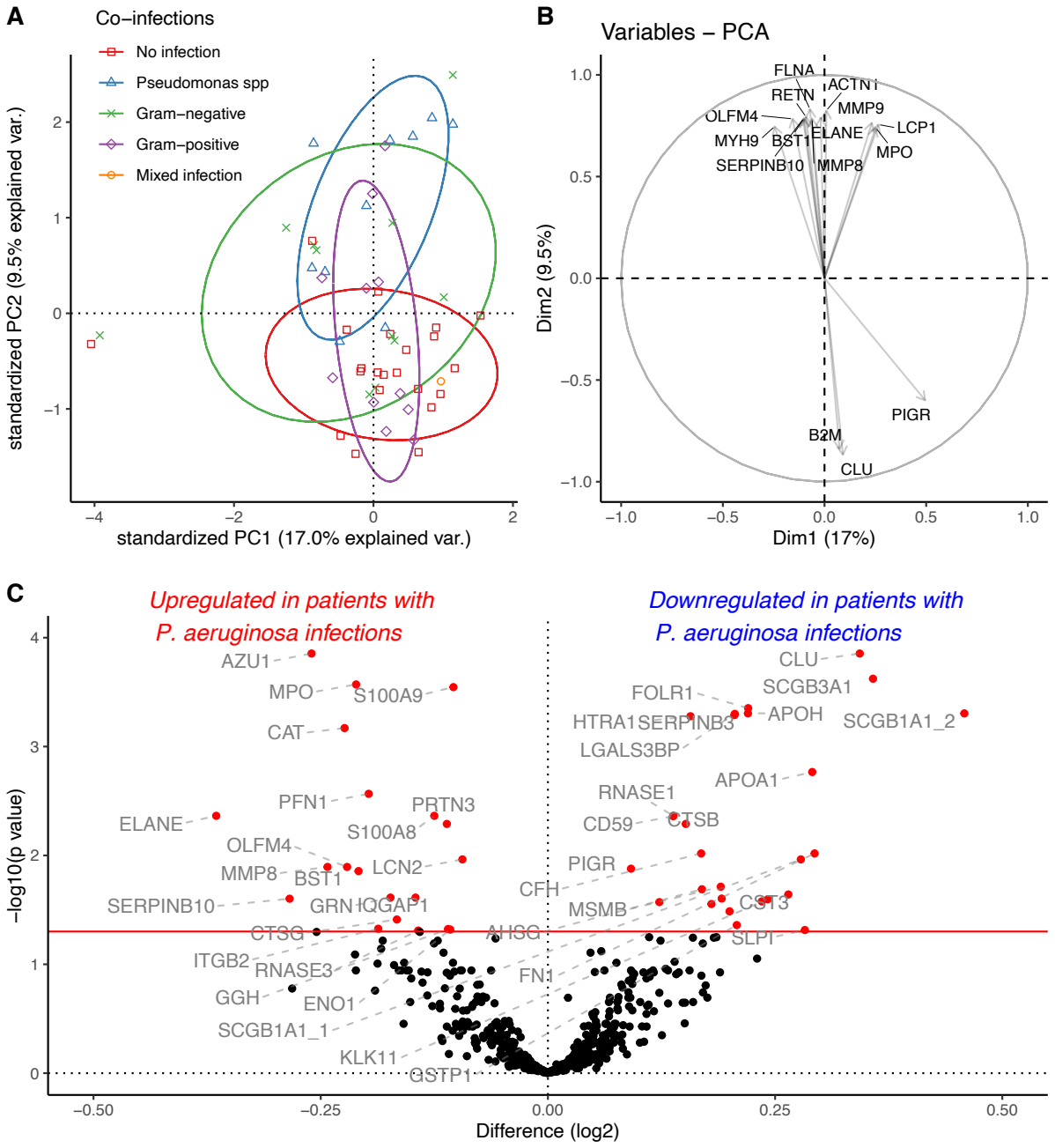

Figure 7-1: Neutrophil-derived proteins are abundant in sputum, many are increased in* P. aeruginosa *infection

Proteomic analysis of 693 proteins of sputum from participants with CF (n=15), BE (n=21) or COPD (19) with (n=15) or without NTM infections (n=40) to compare the impact of non-NTM coinfections on proteomic profile. Liquid chromatography-tandem mass spectrometry to identify the proteins and quantify their abundance in sputum from participants undertaken by other investigators. 1st visit samples were used from all participants if multiple visits were carried out. A) Principal component analysis of proteins comparing presence of non-NTM co-infections, red square=no co-infection, blue

triangles=Pseudomonas spp, green crosses=Gram-negative, purple diamonds=Gram-positive, orange circles=mixed co-infection. Ellipses represent core area for each group with 68% CI. B) Top 15 proteins contributing to principal components 1 and 2 used from the reductional analysis in plot A. C) Volcano plots of mean log_2 fold change in protein abundance in sputum between no co-infection (n=22) vs. Pseudomonas co-infection (n=10) groups. p-values show T-test between 2 infection groups with Benjamini & Hochberg correction. Significantly upregulated proteins (p<0.05) are represented in red. Full list of upregulated proteins in appendix 1. Full proteomic analysis in[261].

7.3.2 Neutrophil degranulation is increased in COVID-19 but is unaffected by brensocatib

STOP-COVID19 was a randomized, double-blind, placebo-controlled trial of the DPP-1 inhibitor brensocatib which reduces the activity of NSPs. The STOP-COVID19 study showed brensocatib did not improve day 29 clinical status of hospitalised patients with COVID-19 and was in fact associated with increased mortality (mortality over 28 days was 11% in the placebo group and 15% in the brensocatib group[260]). I was involved in a sub study of the trial which took place in Sheffield, and at Dundee while I was on placement for 4 months. Along with the laboratory teams at both sites (Sheffield: Dr Rebecca Dowey and Helena Turton; Dundee: Dr Holly R Keir, Dr Merete B Long, Yan Hui Giam, Thomas Pembridge, Lilia Delgado, Amy Gilmour and Chloe Hughes) I processed research samples and carried out functional assays on neutrophils from patients recruited in the trial at day 1, days 7 and 14 if still in hospital, and day 28. Assisted by Dr Rebecca Dowey, I set up these assays in the CatIII laboratory in Sheffield. I was directly involved in the processing and neutrophil functional assays from approximately 60 patient samples in Dundee and 20 patient samples in Sheffield.

A number of assays were undertaken (including measuring NETosis, phagocytosis and 5 surface markers) but the relevant work to this thesis is the quantification of neutrophil surface expression of the degranulation marker CD63 by flow cytometry. CD63 is a tetraspanin and a surface marker for degranulation of azurophilic neutrophil granules[502,503]. CD63 levels fell significantly over the 28 days (Figure 7-2, day Pr(>F)= 0.00032) and were unaffected by brensocatib treatment versus placebo (Figure 7-2, treatment Pr(>F)= 0.223). These data suggest high levels of degranulation in patients with acute COVID-19 (day 1) which diminished over time and was unaffected by NSP inhibition. Systemic neutrophil activation is thus associated with the release of neutrophil-derived granule proteins in the circulation. Elastase activity in patient peripheral blood, measured by other members of the study group, was significantly lower in the brensocatib group compared to the placebo group ($p<0.0001$[260]) showing the on-target effect of brensocatib during the study.

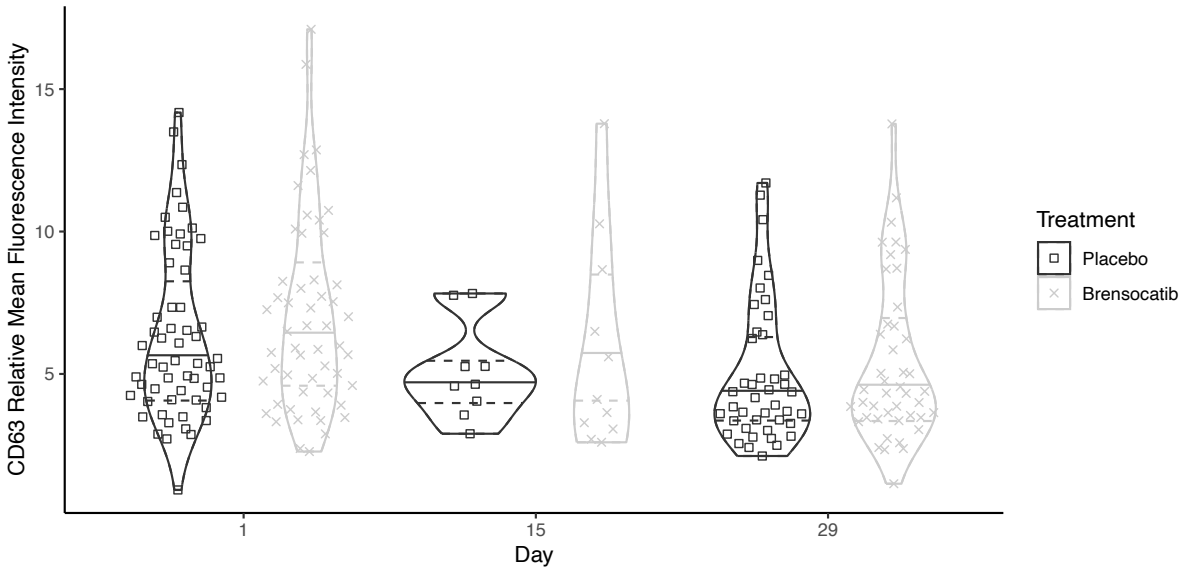

Figure 7-2: CD63 expression decreases from initial high level during COVID-19 infections.

Assay of neutrophils isolated from patients with COVID-19 in the STOP-COVID19 trial in the placebo (black boxes) or brensocatib (grey crosses) arm at day 1, (day 15 for patients remaining hospitalised patients only), and day 29. Neutrophil CD63 expression was analysed through flow cytometry, with neutrophils gated by forward and side scatter, and single cells identified by comparing forward scatted signal area (FCS-A) and signal height (FCS-H) and selecting cells with a linear relationship between the 2 parameters (section 3.2.12.11). Relative fluorescence of neutrophils labelled with CD63 PE antibody for 30 mins normalised to unlabelled cells. Day 1: placebo, n=57, brensocatib, n=51; Day 15, placebo, n=9, brensocatib, n=11; Day 28, placebo, n=43, brensocatib, n=44. Fluorescence represents geometric mean. Statistical analysis by ANOVA with Satterthwaite's method of linear mixed effect model: treatment, Pr(>F)= 0.223; day, Pr(>F)= 0.00032. Violin plot shows data distribution with lines at the 25/50/75 percentile.

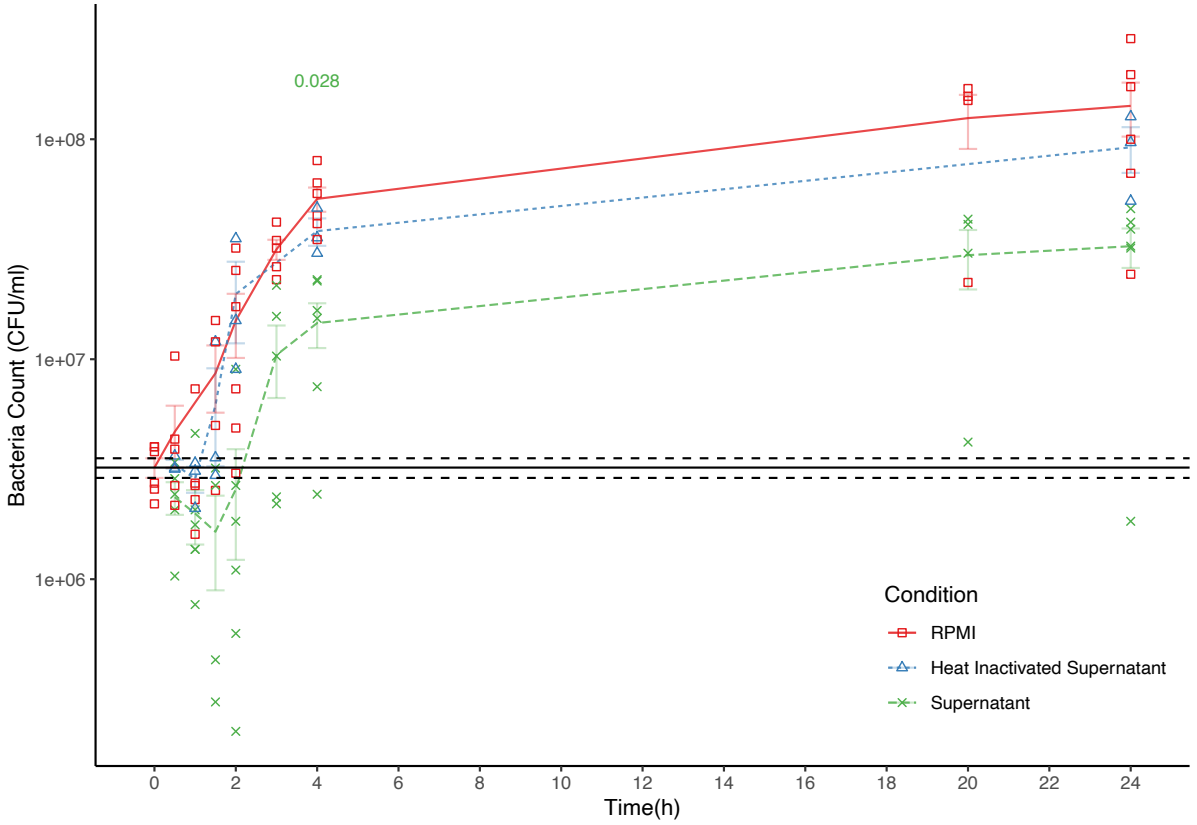

Figure 7-3: Neutrophil supernatants may reduce* S. aureus *growth

Plasma-Percoll density gradient neutrophils (isolated without additional washing steps) were incubated in RPMI (with no serum) for 1 h at 37°C, and the neutrophils were removed by centrifugation. Growth of SH1000 in the resulting supernatant was measured over 24 h incubation (green crosses), compared with growth in identical supernatants following heat inactivation at 95°C for 10 mins (blue triangles) or RPMI alone as control (red squares). MOI 1:5 neutrophil (used to generate supernatant): S. aureus. Initial S. aureus counts are shown (solid black line) +/- SE (black dashed lines). Bacteria were incubated with neutrophil supernatants for time points shown, before plating samples after serial dilution to determine bacteria numbers. n= 2-6 independent donors carried out in triplicate. Error bars are mean +/- SE. Statistical analysis by Kruskal-Wallis rank sum test with Wilcoxon rank sum post-hoc testing and Benjamini-Hochberg correction; comparison to RPMI groups for supernatant (green). Only significant p value is shown above the time point on the graph. There were no significant comparisons for the heat inactivated group. 3 h and 20 h for heat inactivated supernatant excluded from statistical analysis as n=2.

7.3.3 Trace amounts of plasma supress *S. aureus* growth

Neutrophil supernatants differ, with enhanced degranulation, in hypoxia compared to normoxic conditions[142]. In view of the potential for interaction between hypoxia, antimicrobial resistance and neutrophil degranulation, I aimed to explore neutrophil supernatants (ultimately aiming to explore normoxic and hypoxic supernatants) to identify bactericidal components. Neutrophils were isolated by Percoll density gradient centrifugation and incubated in RPMI 10% (heat inactivated) FBS for 4 h. Neutrophils were removed by centrifugation and the resulting supernatants were incubated with *S. aureus* to detect bacterial killing or suppression of growth. Surprisingly, supernatants from unstimulated neutrophils were able to suppress bacterial growth, with significantly lower bacterial counts at 4h compared to bacteria grown in RPMI alone (Figure 7-3: 4 h supernatant versus RPMI 4 h, p=0.028). Following heat inactivation of the neutrophil supernatants (95°C for 10 mins), suppression of *S. aureus* growth was abolished (Figure 7-3, 4 h heat inactivated supernatant versus RPMI, p=0.408), suggesting that the antimicrobial element(s) were proteins. Unstimulated neutrophils supernatants diluted 1 in 100 (but not 1 in 1000) appeared to retain bactericidal activity (Figure 7-4A), which was considered biologically implausible. Coomassie staining of undiluted neutrophil supernatants isolated following a 1 h incubation in RPMI (Figure 7-4B) demonstrated a large range of proteins were present; these were felt to be far more abundant than expected from unstimulated neutrophil supernatants and seemed to overlap with those present in serum (1% FBS, Figure 7-4B). The source of many of these proteins and potentially the bactericidal activity was thus suspected to be trace amounts of platelet poor plasma (PPP), which is used during the neutrophil isolation process. I undertook additional washing of neutrophils twice in PPP-free media at the end of the isolation and initially assessed the protein content of the wash eluates (Coomassie staining the eluates following polyacrylamide gel electrophoresis, Figure 7-5A). The initial washes from each of 3 donors had substantial protein content, likely derived from contaminating serum, with minimal protein in the second wash. I then assessed the ability of the 'wash' eluates to kill *S. aureus*. Eluate of additional 'wash 1' of neutrophils possessed antistaphylococcal activity, although this was only seen after incubation for 24 h (Figure 7-5B, 24 h, p=0.029). In contrast wash 2 from the neutrophil isolation showed no significant anti-staphylococcal activity versus the media control at 2 or 24 h (Figure 7-5C, 24 h, p=0.89). Preliminary work of lysates of

washed neutrophils showed some potential to recover antimicrobial proteins, but supernatants no longer killed bacteria (data not shown as only n=1). Unfortunately, this avenue of research was stopped by COVID-19 lockdown and subsequent restrictions. When neutrophil preparation from healthy volunteers could be resumed, we found many donors (most of whom had experienced COVID-19) still had activated neutrophils that were difficult to isolate by density gradient centrifugation as they stuck to red blood cells and could not be removed cleanly. The above work and a plan to fractionate active supernatants were not further pursued due to these issues.

Due to the ongoing challenges due to COVID-19 associated with isolating fresh neutrophils antimicrobial products, I decided to select recombinant proteins with known antimicrobial activity to study the interaction between antimicrobial resistance and neutrophil products.

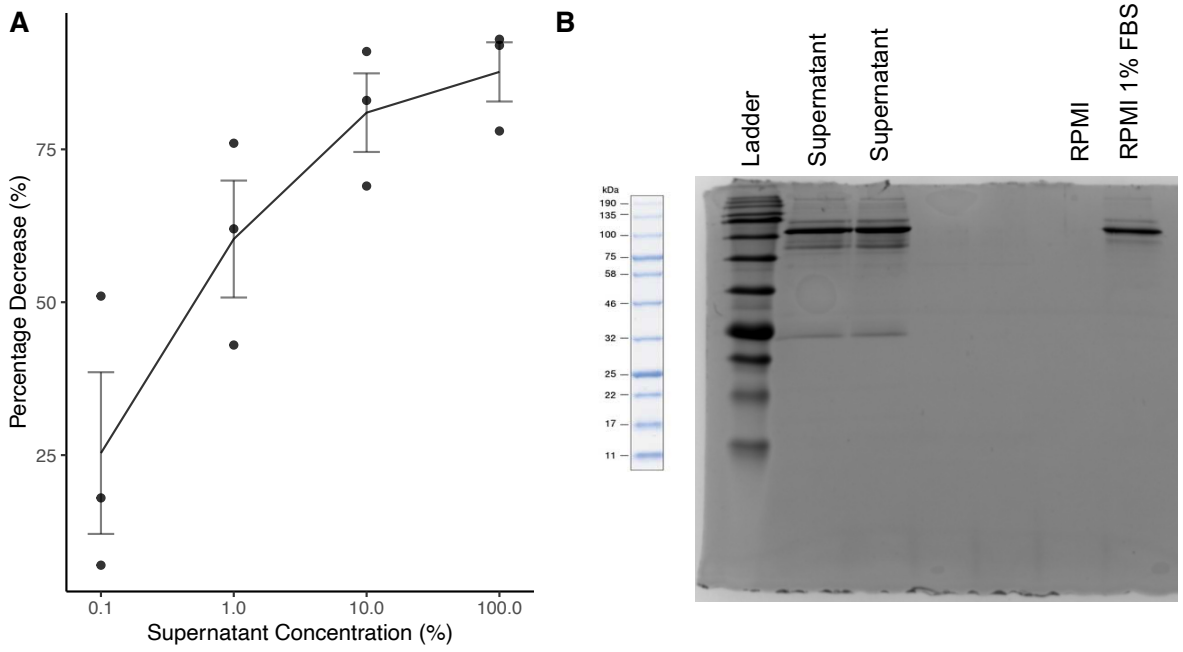

Figure 7-4: The apparent bactericidal activity of neutrophil supernatants is resistant to dilution and may reflect contamination

Supernatants from plasma-Percoll density gradient neutrophils (2.5 million neutrophils/ml no additional wash steps) underwent serial dilution prior to assessment for bactericidal activity, and the protein content of undiluted supernatants from n=1 donors were assessed for protein content compared to 1% fetal bovine serum (FBS). A) Neutrophils (5 million) were incubated at 37°C for 1 h in RPMI 10% (heat inactivated) FBS and the resulting supernatants (neutrophils removed by centrifugation) were diluted as indicated prior to incubation with S. aureus SH1000, MOI 1:5 neutrophil (used to generate supernatant): S. aureus, for 24 h. Surviving bacteria quantified by dilution and plating. n=3 independent donors. Error bars show mean +/-SE. B) Neutrophil were incubated in RPMI for 1 h at a concentration of 2.5 million neutrophils/ml. Supernatants were removed by centrifugation. 20 µl of sample was denatured in Laemelli buffer followed by polyacrylamide gel electrophoresis on a 15% SDS polyacrylamide gel and stained using Coomassie blue. Negative control of RPMI only positive control of RPMI plus 1% FBS shown. n=1, Samples were run in duplicate.

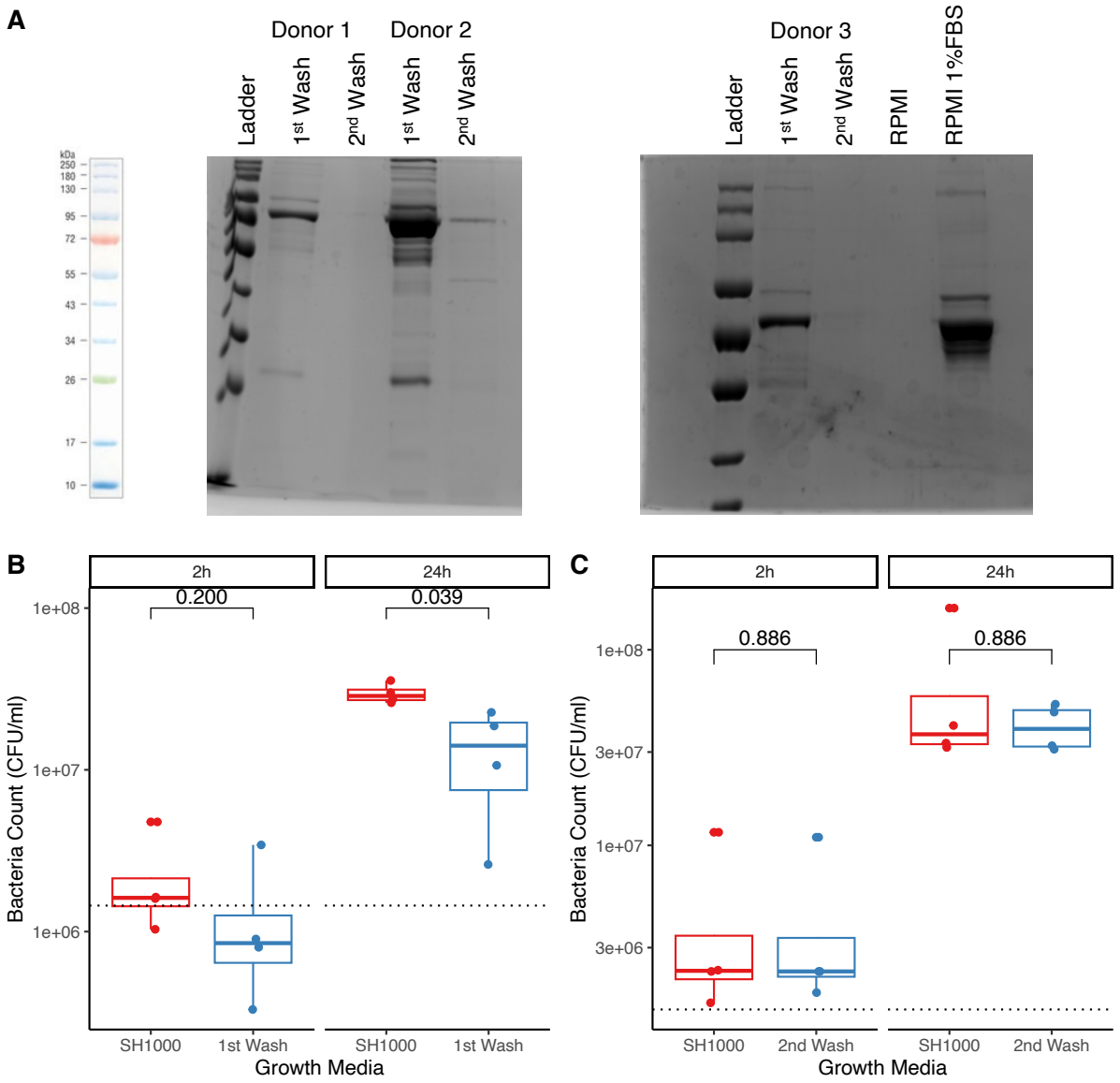

Figure 7-5: Antimicrobial activity of neutrophil supernatants is likely due to PPP contamination

A) Eluates from neutrophil isolation with initial (1st wash) extra wash in HBSS or 1st plus extra 2nd wash in RPMI. 20 µl of sample was denatured in Laemelli buffer followed by polyacrylamide gel electrophoresis and stained using Coomassie blue. Donor 40 and 202 on 15% resolving gel, donor 192 on 10% resolving gel. Negative control of RPMI and 1%FBS positive control shown for donor 3, in error these controls were on a different gel for donor 1 and 2. B, C) S. aureus SH1000 growth in eluate from neutrophil prep washes or equivalent media at 2 h and 24 h at 5% CO_2, 37°C. Mean 0 h bacterial counts shown (black dashed line). n=4 carried out in triplicate. Statistical analysis by Wilcox-rank sum compared to SH1000 in control media as indicated. Box and whisker plots present median, 25/75% quantile (upper and lower hinge), smallest/largest observation ≤ upper/lower hinge +/- 1.5 inter quantile range (whiskers).

7.3.4 LL-37 has antimicrobial activity against *S. aureus* in vitro

The choice of these proteins/peptides was informed by the published literature (section 1.2.2.2[93,96,97,107,108,111,112,497,498]), by my results depicted in Figure 7-1, and also from unpublished neutrophil proteomics data[490] from the STOP-COVID19 study. Proteins/peptides with a range of targets were also selected, and whilst the focus was on those that would plausibly kill *S. aureus*, those thought to predominantly kill Gram-negative organisms were not excluded if otherwise biologically relevant. A commercial source of adequate amounts of highly pure recombinant protein was also essential. Based on these criteria, the proteins selected were: BPI, cathepsin G, elastase, HNP-1 and LL-37. The antistaphylococcal activity of these proteins was tested by incubating an increasing concentration of each protein with *S. aureus* SH1000 for 4 h. 4 h was used due to previous studies showing antibacterial activity of cathepsin G at 2-4 h[111], elastase at 4 h[107], plus the significant decrease in bacterial counts at 4h when bacteria were incubated with neutrophil supernatants (Figure 7-4). Growth of *S. aureus* SH1000 in each of the 5 recombinant neutrophil proteins at a range of concentrations was compared to that in BSA prepared in identical solutes, as a protein control. The data from all 5 recombinant proteins was not normally distributed, hence non-parametric analysis was performed. As only n=3 experiments were performed, using non-parametric statistics I would be unlikely to detect a significant difference between bacterial numbers following incubation in neutrophil proteins, and indeed this was the case (Figure 7-6). However, there was no visible decrease in bacterial numbers following incubation in BPI, cathepsin G or elastase compared to incubation in the BSA control (Figure 7-6A-C), although high concentrations of protein seemed to inhibit growth non-specifically. For *S. aureus* incubated with HNP-1 there was no clear concentration dependent decrease in bacterial numbers compared to BSA, although a trend to reduced growth was observed at 10 µg/ml only (Figure 7-6D). In contrast, LL-37 appeared to reduce *S. aureus* numbers in a concentration-dependent manor, compared to the BSA control (Figure 7-6E, 10 ng/ml, p=0.2, 100 ng/ml, p=0.2, 1 µg/ml, p=0.2, 10 µg/ml, p=0.2). As noted, these results were not statistically significant with n=3 replicates, however the ability of LL-37 to kill *S. aureus* was subsequently confirmed (see later, Figure 7-9B and Figure 7-10A).

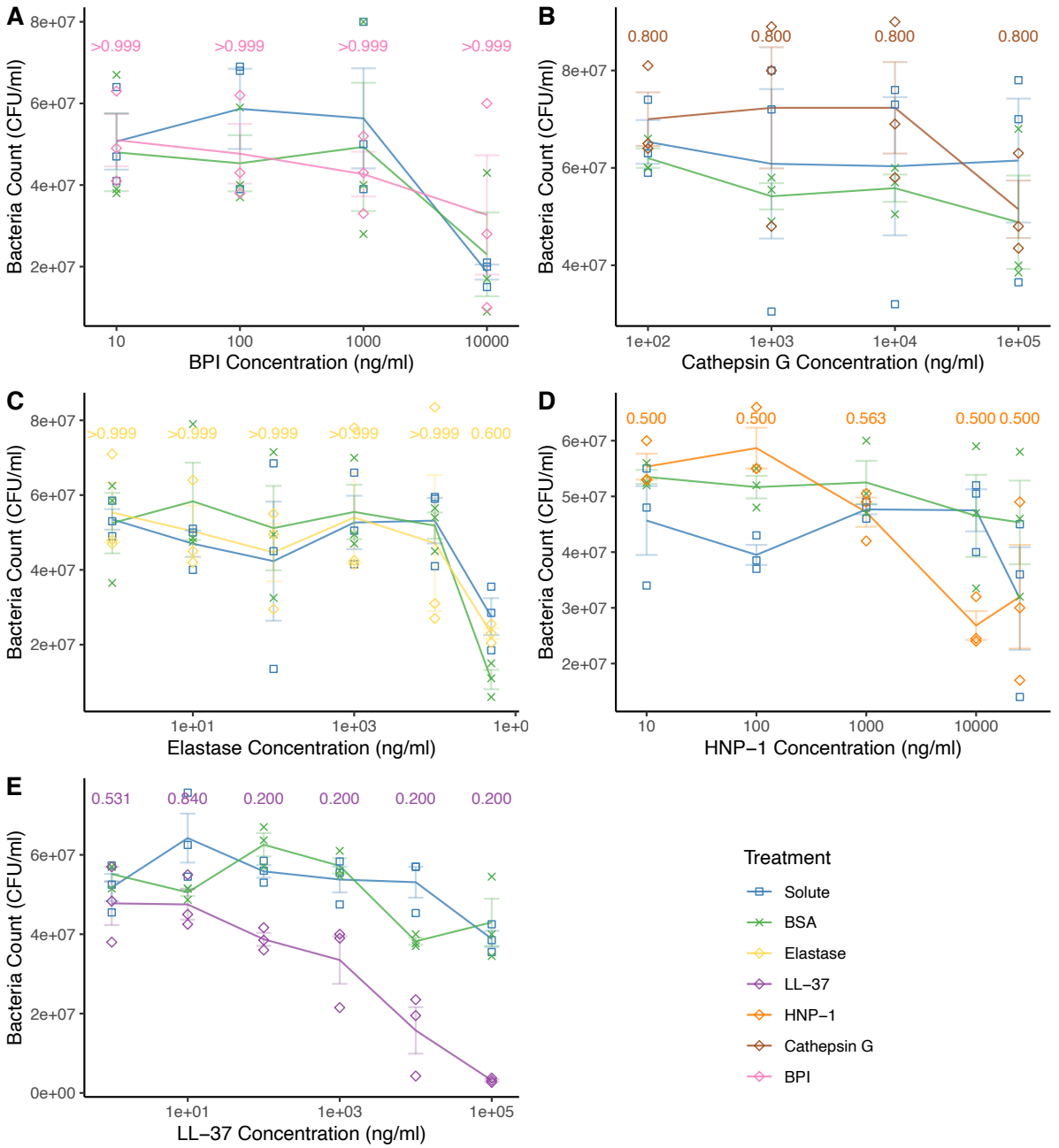

***Figure 7-6: Neutrophil-derived protein concentration response curves for activity against* S. aureus**

SH1000 counts were quantified by serial dilution and plating following 4 h exposure to neutrophil proteins (diamonds) at concentrations indicated on individual plots for A) BPI=pink, B) Cathepsin G= brown, C) Elastase=yellow, D) HNP-1=orange, E) LL-37=purple, all compared to corresponding solute only for each protein (blue squares) or BSA at matched concentrations and in the same solute as the protein (green crosses). Static incubation at in 5% CO_2, 37°C. Error bars represent mean +/- SE of n=3. Statistical analysis by of protein versus. BSA control, by Wilcoxon-rank sum with Benjamini-Hochberg correction, p values shown above each individual data point.

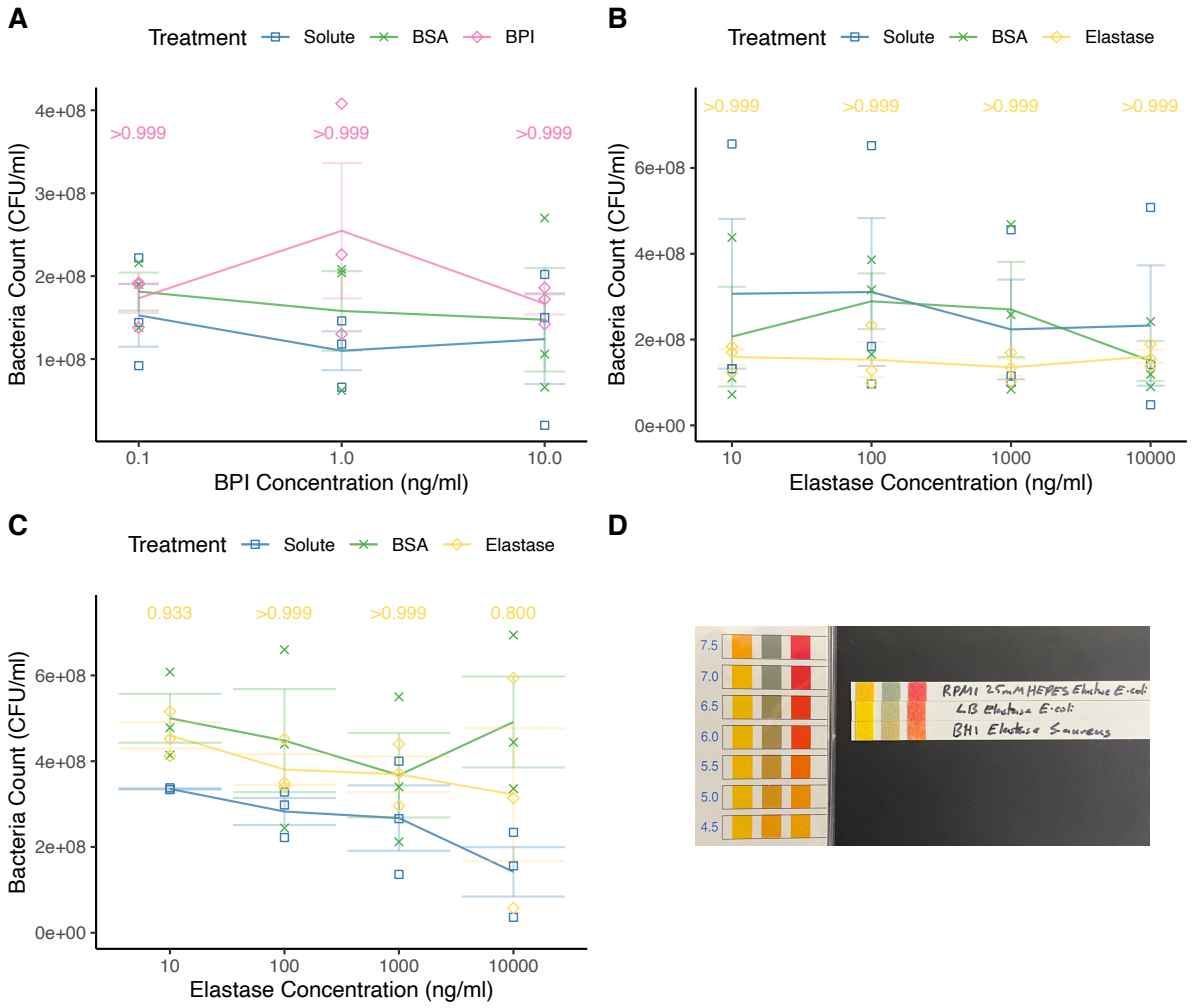

Figure 7-7: Recombinant BPI or Elastase do not restrict* E. coli *growth

E. coli *counts were quantified by serial dilution and plating following 4 h in 5% CO_2, 37°C and exposure to neutrophil proteins (diamonds) at concentrations shown for A) BPI=pink, B, C) Elastase=yellow. Incubations undertaken in A, B) LB broth or C) RPMI 10 mM HEPES. Static incubation at in 5% CO_2, 37°C. Error bars represent mean +/- SE of n=3. Statistical analysis by of protein vs. BSA control, by Wilcoxon-rank sum with Benjamini-Hochberg correction, p values shown above individual data points. D) pH of 10 µg/ml elastase in a range of media for* E. coli *and* S. aureus*. Approximate values are:* E. coli *RPMI 25 mM HEPES≈pH 7.5;* E. coli *LB broth≈pH 6,* S. aureus *BHI broth ≈pH 5.5.*

BPI and elastase are both reported to have mostly Gram-negative targets[97,108] and hence it was not implausible that they would not suppress *S. aureus* growth. However, given their biological importance and prominence in the setting of sputum of patients with chronic lung diseases (Figure 7-1C) and COVID-19, I wished to confirm the activity of the elastase and BPI recombinant proteins by testing their ability to suppress the growth of *E. coli*. Very surprisingly, neither BPI nor elastase caused a significant decrease in *E. coli* numbers compared to the BSA control at any of the concentrations measured (Figure 7-7A BPI: 0.1 ng/ml, p>0.999; 1 ng/ml, p>0.999, 10 ng/ml, p>0.999) (Figure 7-7B Elastase: 10 ng/ml, p>0.999; 100 ng/ml, p>0.999, 1 μg/ml, p>0.999, 10 μg/ml, p>0.999). Elastase was also tested for its ability to kill *E. coli* in RPMI 10% HEPES to see if the lack of activity was due to pH, but again there was no suppression of growth (Figure 7-7C, D, 10 ng/ml, p=0.933; 100n g/ml, p>0.999, 1 μg/ml, p>0.999, 10 μg/ml, p>0.800). These indicate either the recombinant BPI and elastase were not active, or the experimental conditions were not suitable for these proteins. They were not further explored.

There were signs of a likely concentration dependent response for suppression of *S. aureus* growth by LL-37 (concentration range 10 ng/ml-10 μg/ml, Figure 7-6E). Data for HNP-1 suggested possible suppression of growth at 10 μg/ml, although without a clear concentration dependent response (Figure 7-6D). Both peptides were further investigated. As ultimately I wished to explore possible interactions between peptide-mediated killing of *S. aureus* and antibiotic resistance, the 6 'control' clones which were evolved under no antibiotic selection for 20 transfers from chapter 4 (see overview flow chart, Figure 7-8) were used as further test strains. The control clones from chapter 4 were exposed to 10 μg/ml LL-37 or 10 μg/ml HNP-1 over 24 h, with quantification of bacteria at time points shown in Figure 7-9. There was no significant impact on *S. aureus* growth seen by incubating SH1000 with HNP-1 compared to BSA at any of the time points tested (2 h, p=0.412; 4 h, p=0.936; 8 h, p=0.936; Figure 7-9A). In contrast, there was significant suppression of *S. aureus* growth by LL-37 compared to BSA at 4 h and 8 h (4 h, p=0.010; 8 h, p=0.007; Figure 7-9B). At 4 h bacterial counts were below 0 h counts indicative of killing. By 24 h, bacterial counts in the presence of LL-37 did not differ from control BSA. All SH1000 clones were fully susceptible to gentamicin (positive control) as expected.

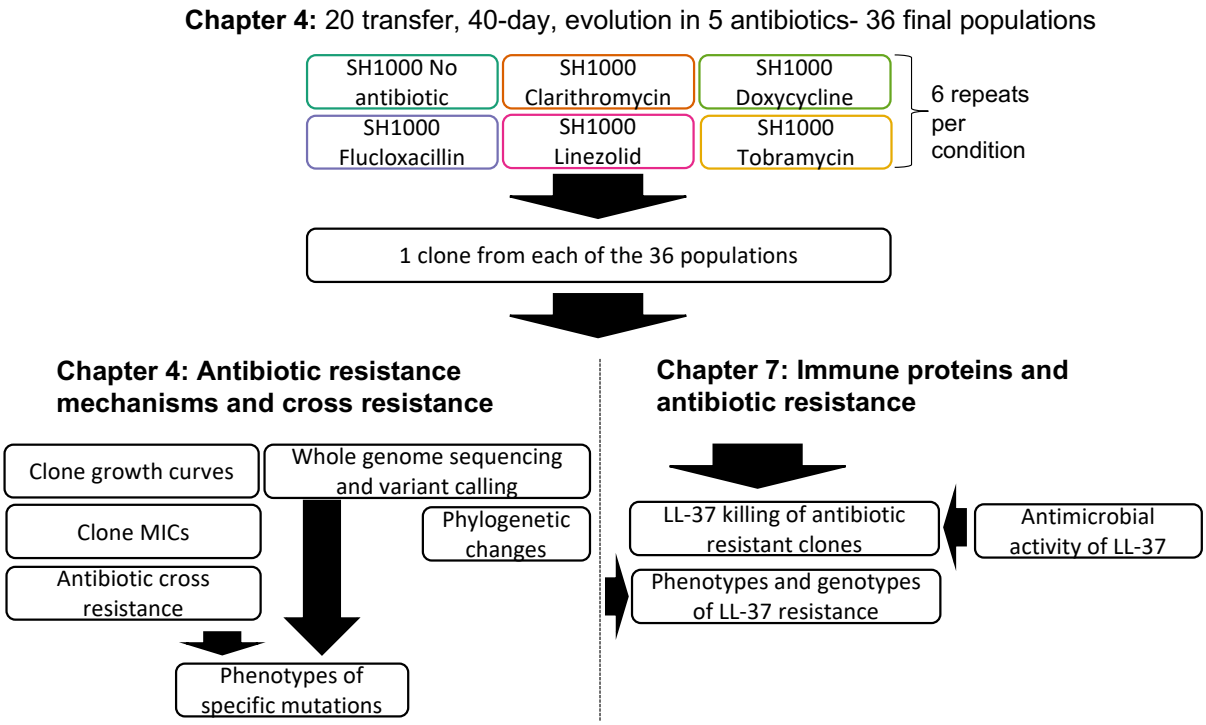

Figure 7-8: Overview of analysis on clones evolved in antibiotics in chapter 4 and 7

Flowchart of analysis of clones following 20 transfer evolution as described in full in Chapter 4. 6 experimental lines of SH1000 were evolved on an antibiotic gradient of: clarithromycin, doxycycline, flucloxacillin, linezolid and tobramycin plus a no antibiotic control. In chapter 4 the evolved clone MICs in all antibiotics and growth curves were measured, and whole genome sequence analysis carried out. For the work in this chapter, one clone from each experimental line evolved in each of the 6 conditions (36 clones) was taken forward to examine their sensitivity to killing by LL-37.

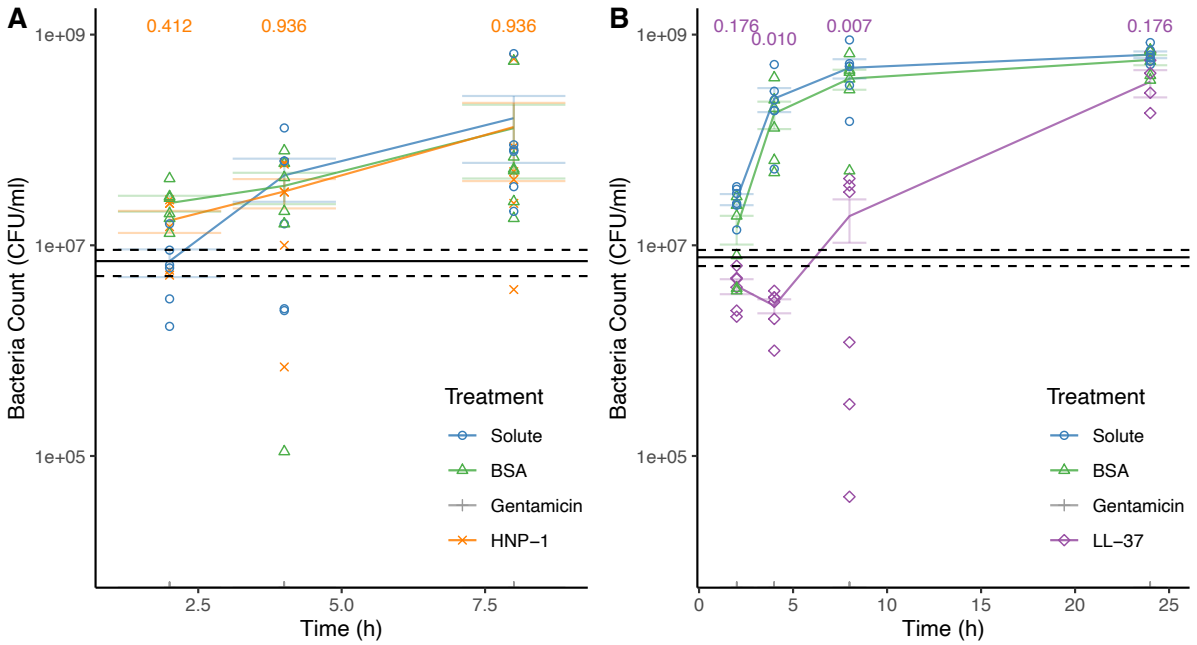

***Figure 7-9: Antimicrobial peptide LL-37 but not HNP-1 can kill* S. aureus**

SH1000 counts were quantified by serial dilution and plating following exposure to 10 µg/ml HNP-1 (orange cross) or 10 µg/ml LL-37 (purple diamond) compared to corresponding solute (H_2O), for each protein (blue circle), 10 µg/ml BSA in H_2O (green triangle) or 50 µg/ml gentamicin (grey plus). n=6 were clones 1-6 from transfer 20, antibiotic free selection of SH1000 in chapter 4. Measurements were taken at time points shown. Incubations carried out in BHI broth in static 96 well plates at 37℃, 5% CO_2. Black line= mean bacterial counts at 0 h, dashed line +/- SE. Error bars represent mean +/- SE. Statistical analysis of protein vs. BSA control, by Wilcoxon-rank sum with Benjamini-Hochberg correction.

7.3.5 Resistance to clarithromycin, tobramycin and linezolid reduces *S. aureus* killing by LL-37

Using the conditions for LL-37 killing as optimised above, I next explored if there is an interaction between the development of antimicrobial resistance and killing of *S. aureus* by LL-37. Clones which had been selected for antibiotic resistance against clarithromycin, doxycycline, flucloxacillin, linezolid or tobramycin (Chapter 4) were tested for sensitivity to LL-37 compared to their ancestor, SH1000. Exposure to LL-37 caused a significant decrease in bacterial numbers compared to BSA for the ancestor SH1000 ($p=0.014$, Figure 7-10A), likewise clones evolved with no antibiotics ($p=0.014$, Figure 7-10B), with doxycycline ($p=0.014$, Figure 7-10C), and with flucloxacillin ($p=0.014$, Figure 7-10D). The clones evolved in doxycycline and flucloxacillin had only developed low levels of antibiotic resistance compared to SH1000 (Chapter 4, fold increase in MIC: doxycycline, 2-4; flucloxacillin, 4-16). In contrast, no significant decrease in bacterial number was seen on exposure to LL-37 for clones evolved in clarithromycin ($p=0.362$, Figure 7-10E), linezolid ($p=0.252$, Figure 7-10F) or tobramycin ($p=0.205$, Figure 7-10G). The clones evolved in clarithromycin and tobramycin had developed high-level antibiotic resistance compared to their ancestor (Chapter 4, fold increase: clarithromycin, 16-4096; tobramycin, 8-256). Whilst these data might suggest an interaction between high level antibiotic resistance and decreased killing of *S. aureus* by LL-37, clones evolved in linezolid had developed lower grade antibiotic resistance compared to SH1000 (Chapter 4, fold increase: linezolid, 2-16).

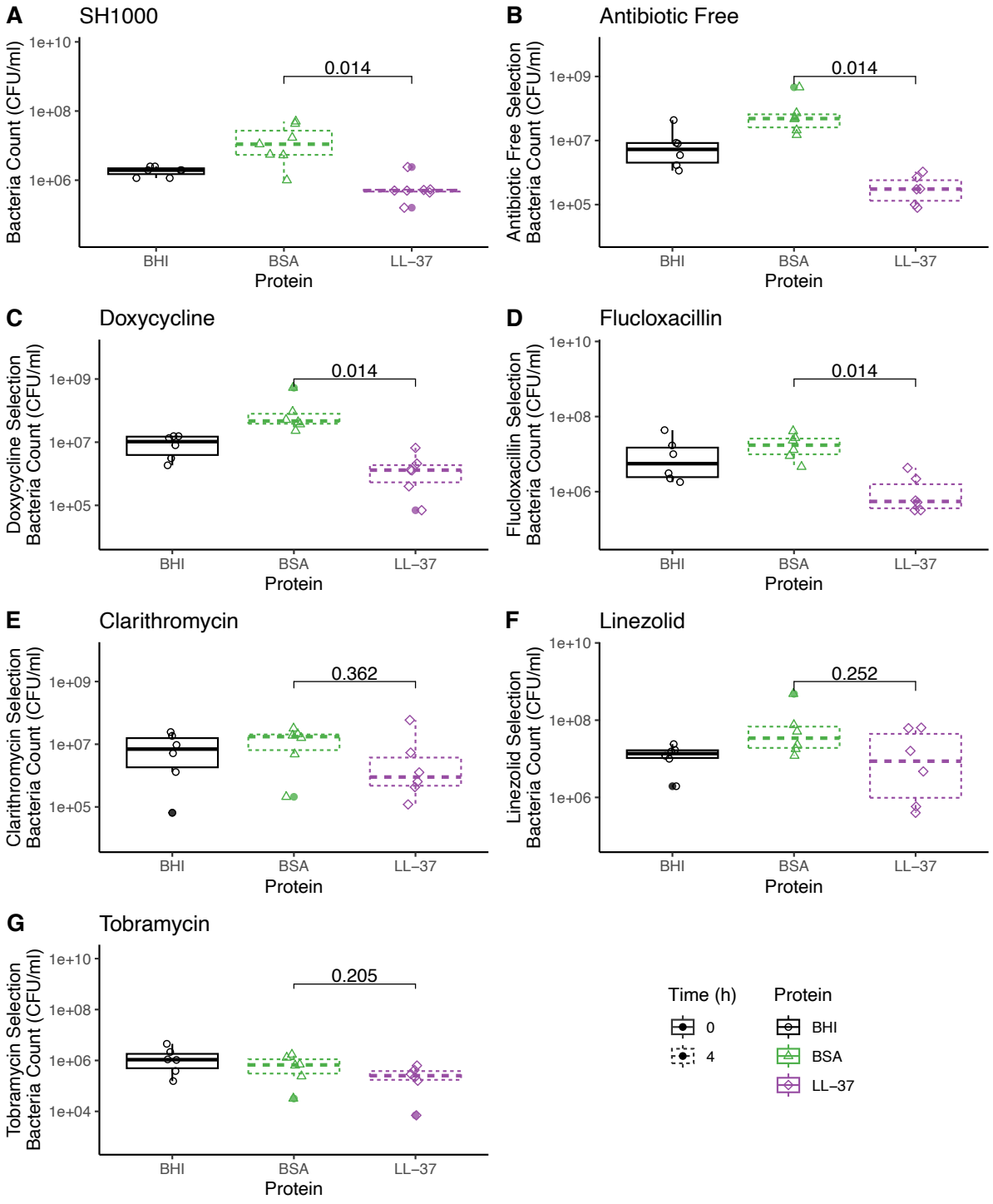

***Figure 7-10: Antibiotic resistance to tobramycin, clarithromycin and linezolid is associated with decreased killing of* S. aureus by LL-37**

Sensitivity of the clones evolved in antibiotics (chapter 4) was assessed to LL-37. A) SH1000 ancestor, clones evolved in: B) no antibiotic, C) doxycycline, D) flucloxacillin, E) clarithromycin, F) linezolid, G) tobramycin. Bacterial counts quantified by serial dilution and plating following 4 h (dashed lines)

exposure to 10 µg/ml LL-37 (purple diamond) or 10 µg/ml BSA (green triangle). 0h counts as BHI black solid lines and circles. Cultures carried out in BHI broth in static 96 well plates at 37℃, 5% CO_2. n=6 clones studied per evolution condition. Error bars represent mean +/- SE. Statistical analysis of Protein vs. BSA Control, by Wilcoxon-rank sum with Benjamini-Hochberg correction. Box and whisker plots present median, 25/75% quantile (upper and lower hinge), smallest/ largest observation ≤ upper/lower hinge +/- 1.5 inter quantile range (whiskers).

To better understand the changes in sensitivity of clones evolved in antibiotics to LL-37 the growth characteristics and genetic variants of clones evolved in antibiotics compared to their ancestor SH1000 (as measured in chapter 4), were correlated with their sensitivity to LL-37. Final bacterial counts of clones evolved in antibiotics following exposure to LL-37 for 4h were normalised to the BSA control. Normalisation of the LL-37 suppression data was particularly important for clones evolved in tobramycin, which had lower starting bacterial counts. There was a poor correlation between suppression of bacterial growth by LL-37 and bacterial growth rates in antibiotic free media for clones evolved in no antibiotics (R^2=0.16, Figure 7-11A). Small colony variants (SCV) characteristically have lower rates of metabolism and deficient electron transfer chains[504], and have previously been associated with resistance to antimicrobial peptides[505]. SCVs were observed following the evolution of SH1000 for at least 1 of the 6 clones evolved in clarithromycin, doxycycline and linezolid, and for all clones evolved in flucloxacillin and tobramycin (Figure 7-11B). There is a trend towards clones evolved in antibiotics with a SCV phenotype having decreased sensitivity to LL-37, although did not achieve significance (p=0.079, Figure 7-11B). There was no significant change in sensitivity to LL-37 based on any genetic changes in the clones evolved in antibiotics, including CplX variants (p=0.76, Figure 7-11C) which has previously been reported to interact with LL-37 resistance in *Bacillus anthracis*[367].

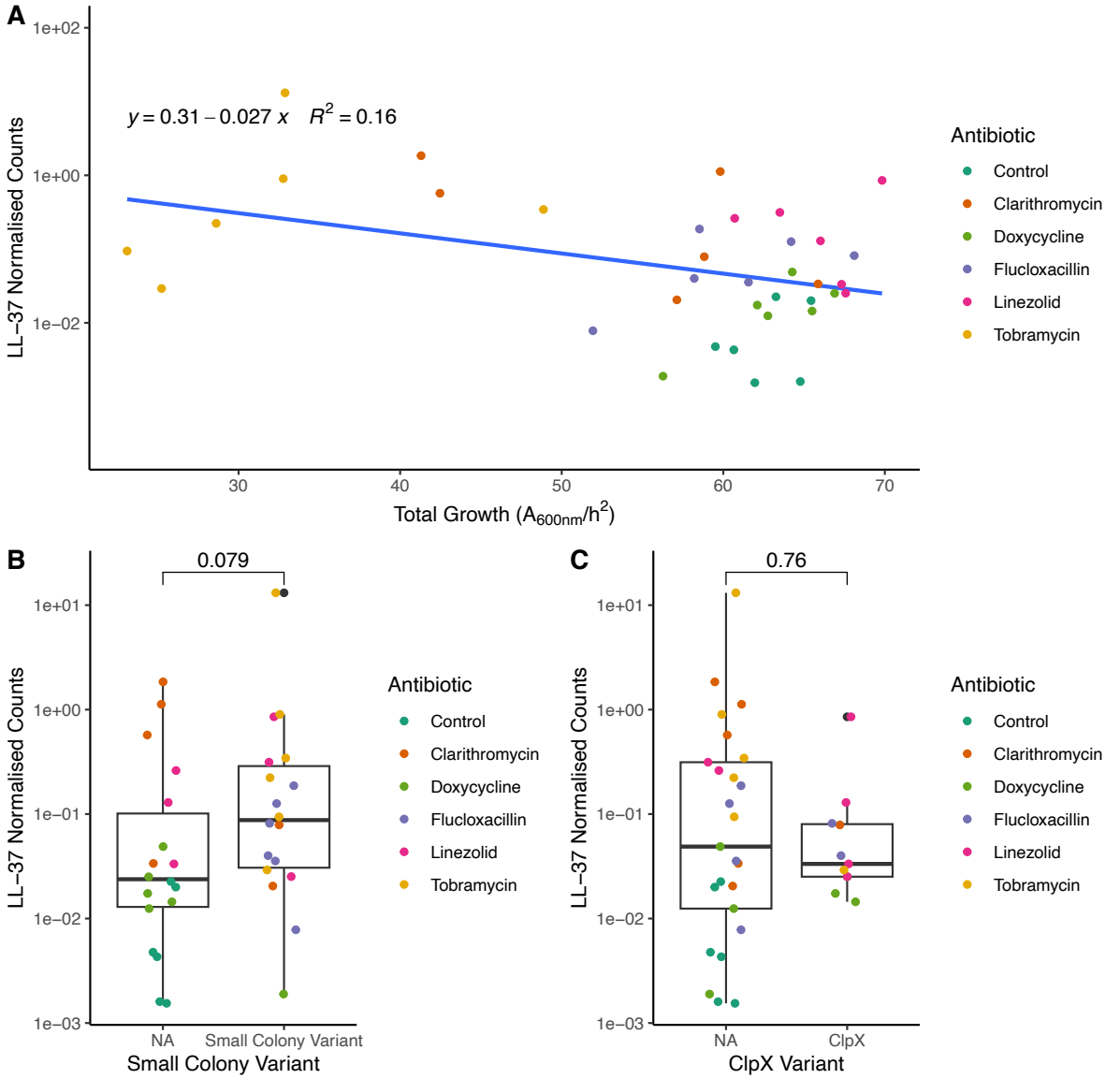

Figure 7-11: There is no clear phenotype or genotype associated with LL-37 resistance

Genotypes and phenotypes determined in chapter 4 of clones following antibiotic selection in no antibiotic (control), clarithromycin, doxycycline, flucloxacillin, linezolid or tobramycin, compared to sensitivity to LL-37. Bacterial counts of clones following 4h exposure to 10 µg/ml LL-37 normalised to 10 µg/ml BSA. Incubations carried out in BHI broth in static 96 well plates at 37℃, 5% CO_2. A) Integral total 48 h growth curves of 100µl of clone overnight cultures diluted to a starting density of A_{600nm}=0.05 at 37°C, 120 rpm, n=36; B) clones with (n=18) or without (n=18) small colony variant phenotypes. C) clones with (n=11) or without mutations (n=25) in ATP-dependent protease ATP-binding subunit ClpX. Statistical analysis by A) linear model, B, C) Wilcoxon-rank sum. Box and whisker plots present median, 25/75% quantile (upper and lower hinge), smallest/ largest observation ≤ upper/lower hinge +/- 1.5 inter quantile range (whiskers).

7.4 Discussion

In the work outlined in this chapter, I have investigated a range of immune products, some of which have anti-staphylococcal activity, and looked for interactions with antibiotic resistance. Proteomic analysis of sputum samples from 55 patients with chronic lung diseases show a strong neutrophilic signature associated with *P. aeruginosa* infections, supporting the abundance of neutrophils and their propensity to release proteins (by degranulation, NETosis or necrosis) in this inflammatory setting. Likewise, I found evidence of neutrophil degranulation (CD63 surface expression) in the systemic circulation during infection with SarsCoV2, although this was not affected by the study drug brensocatib. Trace levels of platelet poor plasma had a distinct antimicrobial activity against *S. aureus*, as did LL-37. In contrast, there was no apparent anti-staphylococcal activity for neutrophil-derived granule proteins BPI, cathepsin G, elastase, and HNP-1; however LL-37 killed *S. aureus* in a concentration-dependent fashion. Finally, I have shown that development of high-level antimicrobial resistance against clarithromycin and tobramycin, as well as more modest resistance to linezolid, is associated with in a reduction in the bactericidal activity of LL-37.

In the setting of chronic lung disease, *P. aeruginosa* respiratory infection is strongly associated with neutrophilic inflammation, consistent with the signature obtained from proteomic analysis of sputum both herein and elsewhere. *P. aeruginosa* can cause persistent, difficult-to-treat infections in immuno-compromised patients, particularly when biofilms develop[506]. Previously, Sibila et al.[507] have shown that symptoms of patients with BE are strongly linked to bacterial load, and neutrophilic inflammation when bacterial loads were greater than 10^7 CFU/g was associated with increased exacerbations, inflammation and elastase activity[507]. In patients with BE and *P. aeruginosa* infections successful treatment with intravenous antibiotics was associated with a reduction in neutrophilic inflammation and associated proteins[487]. The proteomic analysis presented here, including patients with CF, BE, COPD, supports these studies showing *P. aeruginosa* infections increase neutrophilic inflammation and release of neutrophil-derived proteins into the airways[261].

In my analysis of the sputum proteome, proteins upregulated in patients with *P. aeruginosa* infections included the NSPs elastase and cathepsin G as well as a strong signal from other

antimicrobial proteins such as S100A9 and azurocidin. S100A8/A9 is constitutively expressed in neutrophils but is cytoplasmic rather than granule-associated, acting as a Ca^{2+} sensor with a role in cytoskeleton rearrangement and arachidonic acid metabolism. During inflammation, S100A8/A9 is released and may modulate the inflammatory response by stimulating leukocyte recruitment and inducing cytokine secretion[508]. As it is not a granule-protein, and is expressed by a large number of different cell types, I did not study it further. Azurocidin (also known as CAP37 or heparin-binding protein) is present in secretory vesicles as well as azurophilic granules and is hence readily released on minimal stimulation, perhaps explaining its abundance in patient sputum (Figure 7-1C). However, azurocidin has pleiotropic effects and is regarded as an 'alarmin', activating the endothelium[509], and recruiting[510] and activating monocytes[511]. Azurocidin has been reported to opsonise *S. aureus* rather than kill this organism directly[117] hence again it did not seem a promising candidate to take forwards in this study. Another top 'hit' in my proteomic study, MPO is an azurophilic granule protein which interacts at the phagosome with the ROS generated by the neutrophil NAPDH oxidase to generate hypohalous acids; in view of its indirect effects, it was not deemed suitable for further study in my in vitro system. Of course, all of these neutrophil products may be relevant to exerting evolutionary pressure in an infection in vivo. I did consider evolving bacteria by serial passage through neutrophils, selecting 'persister' organisms from each cycle, however only very small numbers survive each encounter (Figure 6-14, Natalia Hajdamowicz, PhD graduate from Prof Condliffe's laboratory, personal communication) and the experiment was felt to be too time-consuming to undertake at this stage of my PhD studies.

One emerging therapy to treat neutrophilic inflammation is brensocatib, which has recently been shown to reduce exacerbations in patients with BE in a phase II trial[496]. It was based on the rationale of treating neutrophilic inflammation and neutrophil extracellular trap (NET) formation that brensocatib entered phase III clinical trials (STOP-COVID19) for patients with COVID19. However, there was increased mortality in patients taking brensocatib, who also had significantly fewer ventilation- and oxygen-free days compared to the placebo group[260]. Brensocatib is likely to have been working on target, with reduced circulating elastase activity in patients taking brensocatib versus the placebo. These data challenge the extent neutrophilic inflammation and neutrophil NETs[152,512,513] are driving disease pathology in COVID-19. Of note the majority of the increased mortality in the brensocatib group occurred

later in the course of disease and was associated with respiratory failure, potentially indicating a positive role for serine proteases in inflammation resolution or an anti-fibrotic action ([260] and Prof James Chalmers University of Dundee, personal communication).

Herein I found that CD63 levels (azurophilic granule degranulation marker) were increased in the setting of acute SarsCoV2 infection but did not differ between patients treated with brensocatib (NSPs inhibited) compared to the placebo group. I detected an increase in CD63 expression on neutrophils at day 1 of the study compared to day 28, suggesting increased azurophilic degranulation in acute COVID-19 infections. These data are supported by an exploratory proteomic study of a subset of the STOP-COVID patients[490], showing increased expression of 1,748 neutrophil protein in patients with severe COVID-19 compared to the non-infected control group. Some of these proteins upregulated in the most severe patients were associated with metabolic changes in neutrophils associated with hypoxia[490], linking the results to my findings in Chapters 5 and 6. Stratifying our data by disease severity could show whether severity correlates with enhanced CD63 expression or other parameters of neutrophil function, however at the time of writing this thesis I did not have access to the patients' clinical data.

There were no changes in secondary bacterial infection between the placebo and brensocatib groups in the STOP-COVID19 trial[260] suggesting patients did not have a major change in susceptibility to bacterial infections, however, overall numbers of patients with bacterial secondary infections were very low. I found evidence of impaired neutrophil phagocytosis of heat-inactivated *E. coli* (again unaffected by brensocatib treatment) early in SarsCoV2 infection (data not shown) but did not assess killing of *S. aureus* or other bacteria, as it was not part of the trial protocol. To confirm neutrophil killing was unimpaired by brensocatib, neutrophil killing assays and live phagocytosis assay would have needed to be performed on neutrophils isolated from patients in both the placebo and brensocatib group. It was not possible to include these additional assays in STOP-COVID19 due to short timeframe available to optimise assays for inclusion in the trial, however, I did optimise and include live *S. aureus* and *P. aeruginosa* killing and phagocytosis assays in the STAR-COVID19 trial (a randomised, double-blind, placebo-controlled trial of SFX-01, which activates the anti-inflammatory

transcription factor Nrf2). This study is still ongoing and so the data could not be included here (data is not un-blinded).

The antimicrobial activity found to be attributable to trace PPP contamination from the neutrophil isolation highlights the potency of antimicrobial proteins which form part of our innate immune defences. In additional investigations, I found potent antimicrobial activity using up to 1/100 dilution of unstimulated neutrophil supernatants from 'unwashed' neutrophils. Coomassie staining of proteins in the PPP-contaminated neutrophil supernatants revealed a large range of proteins, making the antibacterial activity seen likely a co-operative response of multiple proteins. Plasma has previously been associated with high antimicrobial activity. The identity of which elements from PPP exert antimicrobial activity are poorly delineated. Plasma, platelet-derived factors including α-granule contents, complement and activity of the coagulation cascade are all likely contributors[72,514,515]. I inactivated the supernatant components at 95°C, of note a temperature of 56°C has been used to selectively inactivate complement[516] which could be used to further identify the components responsible for the antibacterial activity. The antimicrobial activity of plasma is essential to protect against infections in wounds, although most studies investigating this do not deplete platelets, for example work by Çetinkaya et al.[517]. One of the abundant proteins in plasma is hCAP-18, the pro-form of LL-37, which has a measured plasma concentration of 1.18μg/ml, with the majority predicted to be neutrophil derived[518]. The concentration of LL-37 will also likely be higher within an infection site, where neutrophils are very abundant. Herein I have shown LL-37 has antimicrobial activity against *S. aureus* and speculate it is contributing to the antimicrobial activity I detected with PPP contamination. In support of this theory, Douglas et al.[519] identified that expression of the *S. aureus tcaA* gene (which encodes a membrane bound protein TcaA) sensitised the bacteria to factors found in human serum including antimicrobial peptides HNP and LL-37. TcaA expression was enhanced on exposure to serum, and the authors speculated that this represents an evolutionary adaption to limit the ability of *S. aureus* to invade the bloodstream, since bloodstream infection is high likely to kill the host and hence is a 'dead-end' for the bacteria.

I did not see consistent antimicrobial activity associated with cathepsin G, HNP-1, elastase and BPI against *S. aureus*. Elastase and BPI are known to have Gram negative targets, so lack

of antimicrobial activity against *S. aureus* is not implausible. However, cathepsin G and HNP-1 reportedly target Gram positive bacteria and had no detectable effect, and elastase and BPI also remained inactive against the Gram-negative *E. coli*[97,108]. Factors relevant to this lack of activity could include differences in media, pH, NaCl concentrations, and incubation conditions between studies[111,497,520,521]. It is also possible that the commercially sourced recombinant proteins were not correctly folded and lacked sufficient biological activity. As noted above, expression of staphylococcal TcaA sensitised *S. aureus* to HNP-1 as well as to LL-37[519]. Notably, members of our group have previously shown antimicrobial activity of HNP-1 against the Gram-positive pathogen *Streptococcus pneumoniae* measured in cation-adjusted (0.4–0.5 mM Mg^{2+} plus 0.5–0.6 mM Ca^{2+}) Mueller-Hinton broth[522]. I used the BHI media to match the media used in the evolution of the antibiotic resistance clones and the MIC measurements of these clones in Chapter 4 and it is possible that this did not support optimal HNP activity. Another potential reason for the inactivity of these proteins is that due to the COVID-19 pandemic, they were stored (in the recommended manufactures conditions) for almost a year before being used, and hence could have lost activity during this time; however they were not freeze-thawed during this time. Given more time I would have optimised the media used for testing the antimicrobial activity of the recombinant neutrophil proteins using different media and salt concentrations, plus carried out activity assays on the NSPs to confirm activity.

I found the antimicrobial activity of LL-37 was reduced in clones which had been evolved high-level clarithromycin and tobramycin resistance plus low-level linezolid resistance (Figure 7-10). Previously, studies have shown some clinical strains of *S. aureus* (including MSSA, MRSA and VRSA isolates) lack sensitivity to LL-37, although LL-37 activity against laboratory *S. aureus* strains was not confirmed in this setting[523,524]. Interestingly, one of these studies showed a synergistic effect of LL-37 and vancomycin on 2 clinical isolates[524]. Both these studies[523,524] used the LL-37 MIC cut off, whereas I studied a change in sensitivity to LL-37 at a lower concentration based on the concentration response curve I generated (Figure 7-6E). Habets et al.[522] carried out a more comprehensive assessment of the impact of LL-37 on the growth of 15 *Streptococcus pneumoniae* clinical isolates, and found a large variation in relative growth between strains; this variation was not linked to pneumococcal capsular serotype, with genetic differences between clones proposed to be important in the different strains

susceptibility to LL-37. Interestingly, *S. pneumoniae* isolates associated with carriage, rather than invasive infection, had higher levels of resistance to LL-37 an HNP-1. This could reflect the fact that isolates associated with carriage are exposed to the immune system for a longer duration allowing them to adapt to the immune environment[522]. My work adds to this evidence, showing genetic variation driven by selection in antibiotics, can influence susceptibility to LL-37. Had time allowed it would have been of interest to explore this in other *S. aureus* strains including clinical isolates.

Previous studies have suggested a possible link between antibiotic resistance and changes in sensitivity to serum and LL-37. LL-37 is a major antimicrobial constituent of serum and has been studied in association with serum resistance in multiple studies. Ledger et al.[525] found that serum-adapted *S. aureus* were less sensitive to killing by daptomycin, vancomycin and gentamycin compared to clones pre-treated in TSB (tryptic soy broth) media. In this study LL-37 was found to be the major serum component which induced tolerance to daptomycin, in part by activating the GraRS two-component system and altering the phospholipid composition of the cell wall in *S. aureus*[525]. Another study by Douglas et al.[519] found, as noted above, that deletion of the membrane protein TcaA (*tcaA* gene) is associated with increased in serum resistance for *S. aureus*; of note here TcaA is also associated with resistance to teicoplanin (glycopeptide antibiotic). The USA300 LAC JE2 transposon mutant for *tcaA* was less sensitive to LL-37 compared to WT USA300 LAC JE2[519] and was also less sensitive to vancomycin. Interestingly in clinical isolates, polymorphisms in the *tcaA* gene were associated with reduced killing by LL-37 and by vancomycin.

ClpX has previously been shown to be important for resistance to LL-37, and the antibiotics nisin and daptomycin in *B. anthracis*[367]. As described in Chapter 4, 18/36 clones evolved in antibiotics (represented in all classes of antibiotics studied) had variants in ClpX (Figure 4-17D), however there was no association with ClpX variants and sensitivity to LL-37 (Figure 7-11). Despite the fact that I used isolates that had been fully sequenced, I was unable to identify specific genes associated with resistance to LL-37 and antibiotic resistance. As noted in Chapter 4, the mutations in the clones resistant to clarithromycin and linezolid were largely centred on ribosomal proteins (Figures 4-10 and 4-11), with one tobramycin-evolved clone likewise having a mutation in a ribosomal subunit (but with more mutations in Elongation

Factor G, Figure 4-12). By screening the USA300 LAC JE2[254] Nebraska Transposon Mutant Library for resistance to LL-37, Golla et al. identified 24 resistance-associate genes with a wide variety of functions[526]. Many of these were linked to adhesion and biofilm formation, and although ribosomal genes were not specifically represented, 6 of the mutations were classed as affecting 'biosynthesis and metabolism'. It is thus possible that reduced biosynthetic activity associated with some ribosomal mutations might link antimicrobial resistance and sensitivity to LL-37. I could potentially use gene knockouts from the Nebraska transposon mutant library, focussing on genes associated with resistance to the clarithromycin, linezolid and tobramycin to see if they change *S. aureus* sensitivity to LL-37. However, the genetic changes in my clones evolved in antibiotics have not been characterised and are unlikely to equate to whole gene knock out of specific individual genes; additionally the majority have multiple genetic variants compared to their ancestor likely contributing to the observed antibiotic resistance and resistance to LL-37, hence looking at individual gene knockouts might not fully recapitulate the biological complexity of resistance to LL-37.

In addition to genetic changes in clones resistant to clarithromycin, linezolid and tobramycin, there were changes in the bacterial growth for clones evolved in tobramycin and the SCV phenotype for at least 1 clone evolved in each antibiotic. Whilst there was no clear correlation between growth rate of *S. aureus* evolved in antibiotics and sensitivity to LL-37 (Figure 7-11A), clones with SCVs show a non-significant trend towards decreased sensitivity to LL-37 (Figure 7-11B). Previously, LL-37 has been shown to be less efficient at killing *S. aureus* clinical isolates with a SCV phenotype compared to wild-type *S. aureus*[505]. The combination of SCV development and antibiotic resistance genes will be different depending on which antibiotic clones were evolved against. Looking at clones evolved in each antibiotic independent of clones evolved in other antibiotics could help disentangle the association between antibiotic resistance and resistance to killing by LL-37.

Overall, this work adds to the literature linking *S. aureus* antimicrobial resistance to sensitivity to the important antimicrobial peptide LL-37. LL-37 is produced by innate immune cells including neutrophils, but also by mucosal cells such as keratinocytes. Thus in addition to the immune-mediated antibacterial effects I have been studying this may have relevance to common mucosal infections for example of the skin[527].

8 Overall Discussion

8.1 Overview

Antimicrobial resistance (AMR) is a major global threat and understanding the drivers of AMR is key to combatting its evolution. Much of our understanding of the development of antibiotic resistance in *S. aureus* comes from studies in laboratory conditions[191,318,327,341], which do not resemble the harsh environmental conditions at sites of infections. During infections such as a staphylococcal abscess[57,62,63], *S. aureus* is exposed to adverse conditions including hypoxia, proteins and peptides derived from degranulating neutrophils, and antibiotics. My project was to explore how these factors drive *S. aureus* mutations and antimicrobial resistance.

In this thesis I have shown *S. aureus* undergoes mutational events at different rates when exposed to 5 different anti-staphylococcal antibiotics (with the highest rate driven by flucloxacillin). Much of the resistance was at low level with only minor increase in the relevant antibiotic MICs, but clones evolved in clarithromycin and tobramycin were more likely to develop higher level resistance associated with ribosomal mutations or mutations in elongation factor G (Chapter 4). When investigating the impact of hypoxia on antimicrobial resistance, I unexpectedly identified a fitness cost of carrying a chromosomal tetracycline resistance gene (*tetL*, SH1000_TetR) in hypoxia, but not normoxia (Chapter 5). Populations chronically exposed to tetracyclines developed increased tetracycline resistance and grew better in antibiotics, but were less well adapted for hypoxic growth in the antibiotic-free setting, suggesting that such adaptations are context-specific (Chapter 5). Mutations in 30S ribosomal protein S10, rluD-like protein and *tetL* duplication were associated with the increased tetracycline resistance, with mutations in DNA gyrase B associated with increased bacterial fitness in hypoxia without antibiotics (Chapter 6). Finally, I found high level clarithromycin and tobramycin resistance, and moderate linezolid resistance, was associated with decreased killing of *S. aureus* by the immune peptide LL-37 (Chapter 7).

8.2 Failure of antibiotic treatment of *S. aureus* infection

Whilst AMR due to genetic modification is regarded as a global threat, it is important to remember that other factors may limit the ability of antibiotics to cure *S. aureus* infections, including sub-optimal dosing and poor compliance. Infection niches such as the abscess cavity or the formation of biofilms have been suggested to limit antibiotic access to the infecting organisms; however, several antibiotics have been shown to penetrate such niches and biofilms effectively[528,529]. Adverse conditions such as nutrient deprivation and hypoxia present in such niches or in biofilms promote the emergence small colony variants (SCVs), tolerance, and so-caller 'persister' cells. SCVs are adapted to survive in hostile environments, exhibiting characteristics such as AMR, increased adhesive capacity and biofilm formation, and downregulation of virulence factors such as haemolysins (recently reviewed in[530]). SCV formation is complicated and incompletely understood but is associated with mutations in genes regulating metabolic pathways such as fatty acid and thymidine biosynthesis, and TCSs such as Agr and SigB also promote SCV[530]. Whilst I identified slower bacterial growth in some settings, for example following tobramycin exposure, it was not linked to the SCV phenotype (Figure 4-6C), nor were SCVs associated with evolution in hypoxia (Figure 5-7) or change in sensitivity to LL-37 (Figure 7-11). Of note, I did not employ a system that would facilitate biofilm formation, and this would be of interest for future work.

Persister organisms are small sub-populations of bacteria including *S. aureus*[531] that exhibit pronounced AMR without any specific resistance mechanisms other than a dormant metabolic state; on reculture they exhibit restored growth and antibiotic sensitivity. Since I observed reduced growth at a population level, it is unlikely that persisters underpin this phenotype, although this was not specifically explored. Of note, the intracellular environment may promote the persister phenotype and enable dissemination; it would be of interest to undertake serial passage of *S. aureus* through neutrophils exposed to antibiotics (including a hypoxic treatment arm, which may limit cellular microbicidal mechanisms) and explore the emergence of AMR. This would be technically challenging with a significant risk of the bacterial populations being completely killed at each passage, and hence was not undertaken during the course of this PhD. In contrast to persistence which affects only a sub-population of bacteria, the closely related phenomenon of tolerance is a population-level effect allowing

the bacterial population to survive a transient antibiotic treatment several times above the minimum inhibitory concentration (MIC) without a clear resistance mechanism and without an increase in the MIC. Like persistence, tolerance may reflect a phenotypic adaptation to stress condition, but can also be conferred by mutations in genes involved in metabolism or stress regulation[532]. Importantly, mutations associated with tolerance and persistence may promote the selection of resistance mutations[533].

Although I found evidence for these phenotypic changes in my experimental system (for example, clones evolved in flucloxacillin had SCV phenotype, irrespective of the nature of the mutations they encompassed), I have focused in particular on the mutational consequences of evolution under conditions of stress (antibiotics and hypoxia).

8.3 Discussion of results

8.3.1 Development of antibiotic resistance

Fluctuation assays identify mutations that occur spontaneously in antibiotic-free conditions, with higher mutation rates potentially implicating loci associated with resistance and demonstrating the ease with which bacteria acquire antibiotic resistance. In Chapter 4 (Table 4-2), I found the highest spontaneous mutation rate was against flucloxacillin, with much lower mutation rates seen in clarithromycin and tobramycin. No spontaneous mutants were found against doxycycline and linezolid. These mutation rates suggest there are a higher number of non-essential genetic loci which can confer resistance against flucloxacillin than the other antibiotics. *S. aureus* evolved in flucloxacillin were also found to have a higher number of point mutations compared to clones evolved in other antibiotics (Chapter 4, Figure 4-14). The flucloxacillin-resistant clones, both from fluctuation assays and from evolution in flucloxacillin, had relatively low-level gains in antibiotic resistance (Figure 4-2, fluctuation assays, 0.0625-0.1875 µg/ml increase in MIC; Figure 4-14, flucloxacillin gradient, 0.375-1.875 µg/ml increase in MIC). Across the human body there is spatial variation in antibiotic concentrations[386]. *S. aureus* also replicates, and acquires mutations in commensal, antibiotic free settings, such as the nasal cavity[534]. My results imply that in the absence of antibiotics as well as in the setting of sub-therapeutic flucloxacillin concentrations, the likelihood of mutations conferring resistance is high, and the low fitness cost of the identified mutations

suggests these mutations can readily become fixed in the population. Survival in a low antibiotic concentration can facilitate high level resistance especially in combination with a horizontally acquired element[199]. There was a low mutation rate in fluctuation assays for clarithromycin and tobramycin, and no spontaneous mutants were identified against doxycycline and linezolid (Table 4-2) indicating *S. aureus* is less likely to acquire spontaneous mutations conferring resistance to these antibiotics in the absence of treatment.

S. aureus which carried an introduced antibiotic resistance gene (*tetL*) evolved higher levels of resistance against tetracycline and its derivative doxycycline. The resistance acquired was more than the antibiotic concentration in the evolution experiment (Chapter 5, Figure 5-9, evolution tetracycline concentration 30 μg/ml, evolved TET MICs 128-256 μg/ml, evolution doxycycline concentration 2 μg/ml, evolved DOX MICs 8-64 μg/ml). These MICs are in the range of high level antibiotic resistance seen in clinical isolates carrying tetracycline resistance genes including *tetK* (tetracycline MICs: 32-128 μg/ml) and *tetM* (tetracycline MICs: 16-128 μg/ml)[440], emphasising the potential clinical relevance of my results.

My findings also support previous evolution studies showing the acquisition of a low-level resistance determinant is the first step in the development of high-level resistance[199,204,423]. In fluctuation assays, clones evolved in doxycycline did not develop significant increases in doxycycline resistance (Chapter 4). In contrast, in Chapter 5 (Figure 5-9), SH1000 already carrying the *tetL* resistance gene (which enhances the efflux of tetracycline) increased doxycycline resistance from their baseline by 6-62 μg/ml on evolution in doxycycline. 4 out of 47 SH1000_TetR clones evolved in antibiotic (doxycycline or tetracycline) had mutations in 30S ribosomal protein S10, which is known to be associated with tetracycline resistance in *S. aureus* (Chapter 6, Figure 6-6)[448]. In contrast, SH1000 without the *tetL* insert evolved on a doxycycline gradient did not develop mutations in 30S ribosomal protein S10 (Chapter 4). These observations support previous studies showing mutations conferring resistance to doxycycline are slow to develop[191], with mutations in *Vibrio cholerae,* including 30S ribosomal protein S10, taking ~210 days of 12 h transfers to develop resistance[324]. These results suggest tetracycline/doxycycline resistance through 30S ribosomal proteins S10 requires additional mutations elsewhere in the chromosome (such as the introduction of an efflux pump) to become established.

Through whole genome sequencing of clones evolved in antibiotics, I identified mutations which are already known to confer antibiotic resistance, including clarithromycin resistance mutations in the 50S ribosomal subunit (L4, L22 or L32)[355-357], tobramycin resistance mutations in 50S ribosomal subunit L10[362] and elongation factor G[308,326], and linezolid resistance conferred by mutations in 50S ribosomal protein L3 and 23S ribosomal RNA[360,361]. The identification of mutations in known resistance genes validates these models as selecting for relevant mutations. Additionally, I found mutations rluD-like protein (chapter 6) were strongly associated with tetracycline resistance, with one of the mutations (Ala29Thr) previously reported in a clinical isolate[473]. I also found tetracycline resistance to be strongly associated with duplication of the resistance gene *tetL* (Figure 6-8, 15/24 clones evolved in tetracyclines), and resistance gene duplications have also been identified in clinical isolates, albeit at low frequency[471,472]. In one clone evolved in flucloxacillin, 2 variants were found in a hypothetical protein SAOUHSC_00826 also identified in a clinical MRSA strain (KUH140331)[365]. Some novel mutations were also identified in my experiments. Variants in the 30S ribosomal protein S21 was associated with linezolid resistance (Figure 4-11; 4/6 clones), which has not previously been associated with linezolid resistance as far as I can ascertain. One clarithromycin resistant clone only had one mutation in PBP-2 and no other mutations in their chromosome (Figure 4-10), which could be causing resistance by altering clarithromycin penetration of the cell wall. There were many other observed mutations which could not be clearly linked to the evolution conditions and have not been reported in clinical isolates, likely due to the fact that the experimental system used is too simplistic to fully recapitulate mutations in true clinical settings.

In line with previous studies mainly conducted with *E. coli*[286,287,339] but also *S. aureus*[191], I found low level cross resistance could develop in *S. aureus* evolved in certain classes of antibiotics (Figure 4-18). The antibiotic combinations I employed have not been used in similar experiments previously. Low-level cross resistance was observed between clarithromycin and linezolid, with increased linezolid resistance overall for all clones selected in clarithromycin, and multiple clones developing slightly increased clarithromycin resistance following selection in doxycycline, flucloxacillin or linezolid. Whilst macrolides, linezolid and doxycycline target ribosomal subunits/protein, there is no shared target with flucloxacillin to easily explain the observed cross-resistance. Previously, aminoglycoside have been found to

have few cross resistance interactions[286], however in contrast I found *S. aureus* following doxycycline selection did not become doxycycline resistant but half of the doxycycline-exposed clones developed cross resistance to tobramycin, although this was not recipricated. Thus exposure to antibiotics can influence the emergence of cross resistance across classes of antibiotics, even if it does not cause resistance to the antibiotic inciting cross-resistance. This phenomenon may help to explain why the use of antibiotic 'cycling' to reduce antibiotic resistance can have limited success[191,409,535].

8.3.2 Fitness cost of resistance

The fitness cost associated with resistance determinants is an important factor in determining whether they are maintained within a bacterial population, with genes with high cost expected to be outcompeted in vivo particularly once the antibiotic is withdrawn[536]. However, the ability to limit antibiotic resistance by limiting/optimising antibiotic prescribing appears to only be successful for certain resistance-drug pair[537], supporting the view that complex factors maintain antibiotic resistance in bacterial communities, with the potential for compensatory mutations to enable the perpetuation of AMR[538].

I found a significant fitness cost of carrying the chromosomal tetracycline resistance gene *tetL* in hypoxia but not normoxia (Figure 5-1). When SH1000_TetR was evolved in hypoxia but without antibiotics for 30 days, the resistance gene was maintained in each of the 6 experimental lines. Hypoxia-evolved SH1000_TetR had increased fitness in hypoxia through chromosomal mutations. The bacterial DNA gyrase is a tetramer comprising two gyrase A and two gyrase B subunits that induce negative supercoiling to protect bacterial DNA[461]. Mutations in DNA gyrase B were strongly associated with evolution in hypoxia (Figure 6-6 and 6-12). Ala439Ser mutation in DNA gyrase B was shown to be directly associated with increased fitness in hypoxia, with gains in fitness reduced by the presence of tetracycline (Figure 6-12). Precisely how the Ala439Ser mutation affects fitness in hypoxia is unclear. Modelling suggests the potential for introduction of new hydrogen bonds, which could stabilise the variant, impacting positively on its ability to process substrates. However, it is also possible the mutation is destabilising, which could either increase or decrease reaction rates depending on what part of the mechanistic pathway the amino acid is involved in e.g. if

product release is limiting in the wild type, destabilising the bound product state could accelerate the reaction. To fully understand the impact of the mutation I would need to express, purify and characterise the mutant and wild type proteins and the time constraints of my PhD did not permit this. It is of interest that the DNA gyrase A is the main target of the quinolone antimicrobials such as ciprofloxacin, and it is regarded as an important target for the development of novel antimicrobials including for *S. aureus*[539]. Whilst the focus has largely been on the DNA gyrase A subunit, it is of interest that in vitro evolution of *E. coli* in ciprofloxacin resulted in the emergence of *gyrB* mutants with a persister (dormant) phenotype in two out of three evolution lines[540]; the mutants could survive in ciprofloxacin but showed no significant MIC increase. Of note, the DNA gyrase B mutations that resulted from hypoxic evolution of *S. aureus* did not affect normoxic growth, antimicrobial resistance including to ciprofloxacin (data not shown), or ability to persist in neutrophils.

These findings are in keeping with other studies which have shown that the fitness cost of antibiotic resistance can be reduced by compensatory mutations[441,541]. Compensatory mutations can explain how such "costly" resistance genes are maintained in a population. When antibiotics were present during evolution (tetracycline or doxycycline), *S. aureus* evolved high level antibiotic resistance, but was not able to adapt to hypoxia to the same extent as *S. aureus* evolved in an antibiotic free setting (Figures 5-8, 5-10, 6-4), showing a trade-off between high level resistance and adaptation to hypoxia. If this adaptation were to be recapitulated in vivo, a hypoxia-evolved *S. aureus* would be expected to outcompete a highly resistant clone in an antibiotic free setting, such as in a commensal *S. aureus* population colonising the nasal cavity. Additional work, including in vivo models, would be needed to test this. Of note, Dr Tom Darton in the Department of Infection, Immunity and Cardiovascular Sciences, is setting up models of *S. aureus* human challenge that could be used to investigate these effects in the future (Dr Tom Darton, personal communication to Prof Alison Condliffe).

Another resistance trait which conferred a high cost in an antibiotic free setting was tobramycin resistance. Following evolution in tobramycin, *S. aureus* had decreased growth compared to *S. aureus* evolved in no antibiotics, clarithromycin, doxycycline, flucloxacillin and linezolid that persisted in antibiotic free settings (Figure 4-5). Mutations in elongation factor G were found in 5/6 of these tobramycin-evolved clones. Mutations in elongation factor G

have previously been shown to cause resistance to fusidic acid by slowing tRNA translocation, ribosomal recycling, and reducing bacterial growth[542]. All clones evolved in flucloxacillin had SCV characteristics (Figure 7-11B), associated with slow growth, aminoglycoside resistance and persistence during infections[504,543,544]. Therefore, the resistance is likely due to the reduced growth and switch to SCV lifestyle, rather than specific mutations.

8.3.3 Neutrophil proteins

Neutrophil degranulation is known to contribute to the pathogenesis of a range of inflammatory diseases including rheumatoid arthritis[82], COPD[142], and ARDS[150]. The release of certain neutrophil proteins by degranulation of some neutrophil proteins is upregulated in hypoxia[89]. In line with previous findings[487,507], I found several neutrophil proteins (including elastase, cathepsin G, s100A9 and azurocidin) were upregulated in sputum from participants with chronic *P. aeruginosa* infections in the context of COPD, CF or BE[261] (Figure 7-1). In hospitalised patients with COVID-19 the neutrophil degranulation surface marker, CD63, was upregulated at day 1 compared to day 28, indicating increased degranulation in patient with acute infections (Figure 7-2). Increased neutrophil degranulation in patients with acute COVID-19 has also been found in proteomic studies[490]. These data support treating neutrophilic inflammation to reduce the burden of disease. Whilst inhibiting neutrophils will increase risk of infection, neutrophil-targeting drugs have been used successfully in certain settings; for example colchicine (which inhibits microtubule assembly and hence impairs neutrophil recruitment, as well as having other anti-inflammatory effects) is used to treat neutrophilic inflammation driving the manifestations of gout[545], Familial Mediterranean Fever[546] and the neutrophilic dermatosis known as Sweet's syndrome[547]. Colchicine has generated interest as a potential treatment for COVID-19, however there is limited evidence to date. Patients with pre-existing gout and COVID-19 (12% of whom were taking colchicine long-term) had poor outcomes with a frequent need for ventilatory support and a high mortality[548], perhaps in part related to co-morbidities. In contrast in a small placebo-controlled study of colchicine in COVID-19 hospitalized patients, there was no difference in mortality but a small decrease in length of stay was noted[549]. It is thought that the elevated levels of neutrophil serine proteases elastase, proteinase 3, and cathepsin G present in sputum (and hence in the airways) drive adverse outcomes in bronchiectasis. Since inhibiting

dipeptidyl peptidase-1 (which activates neutrophil serine proteases) with brensocatib improved clinical outcomes in bronchiectasis[496], it was of major interest to explore the efficacy of this drug in COVID-19. In keeping with literature suggesting COVID-19 is associated with enhanced neutrophil degranulation, I found that acute infection with SarsCoV2 was associated with increased neutrophil surface expression of the degranulation marker CD63 (Figure 7-2). Disappointingly, brensocatib was associated with a small but significant increase in mortality in COVID-19, predominantly at later time points after hospital discharge**[260]** and associated with later respiratory failure rather than infection. The reasons for this are not understood but we speculate that neutrophils serine proteases are required for repair of scarred or fibrotic tissue in the lungs. It is possible brensocatib could be more effective against the more recent omicron variant as recent studies have suggested it is more reliant than previous variants (alpha, beta and delta) on the NSPs for spike cleavage and cell entry than TMPRSS2[145-147]. These important findings emphasise the need for caution in extending the use of neutrophil-targeting drugs to different conditions.

Of the neutrophil proteins abundant at sites of infections, many are known to have antimicrobial activity including elastase[107,108], cathepsin G[111,112], BPI[96,97], HNP-1[93,497] and LL-37[498]. The antimicrobial peptide LL-37 is abundant in plasma[518] and will be at sites of infection[550]. Serum has been reported to induce tolerance of *S. aureus* to daptomycin and this was found at least in part due to LL-37 by triggering the staphylococcal GraRS two-component system[525]. In Chapter 7 (Figure 7-10), I found decreased killing by LL-37 of *S. aureus* which had evolved high-level clarithromycin and tobramycin resistance or moderate linezolid resistance, but not *S. aureus* which had evolved in doxycycline or flucloxacillin. In contrast to the findings of Ledger et al.[525] I did not find a clear link between LL-37 resistance and decreased growth or the SCV phenotype (Figure 7-11). Unfortunately, I was not able to explore the impact of daptomycin in this system, as daptomycin appeared to have no bactericidal effect above that of its solute. My findings have potential clinical implications, as LL-37 was found to be effective in killing clinical strains of *S. aureus*, indeed more effectively than conventional antibiotics[551], and LL-37 was found to be effective at killing *S. aureus* biofilms adherent to a titanium plate (recapitulating a joint implant), leading to suggestions that LL-37 might be used to treat prosthetic joint infections[552]. Since such infections are treated with multiple antibiotics for lengthy periods, my results suggest the evolution of AMR to some agents may

limit the efficacy of LL-37 in some situations. LL-37 and other AMPs have been further proposed as the structural basis for the development of new antibiotics and anti-biofilm agents[553,554]. It is not clear if the resistance that evolved to LL-37 in association with AMR would also occur with these novel agents.

8.4 Study limitations

In this thesis I have modelled the in vitro evolution of *S. aureus* in hypoxia and antibiotics, however, the model I have used is still relatively simple and more factors need to be included to represent the factors *S. aureus* faces in vivo. There are multiple characteristics of infection sites which I have not incorporated. For example, I carried out experiments in nutrient rich media, as the rate of evolution is dependent on replication, however, during infections nutrients are limited activating the bacterial stringent response which is known to influence antibiotic resistance[555-557]. This may explain why I did not find a major role for tolerance or SCVs in the majority of cases. Other compounding factors at sites of infections include bacterial co-infections, biofilm formation and immune cells[62,230,284]. Conditions at true infection sites will vary according to the precise site of the infection, including different levels of hypoxia across the human body[16,58], which is not seen in a 96 well plate exposed to just 1 level of hypoxia. All these factors will be influencing bacteria in vivo, although creating a model incorporating all of these would prevent the individual factor causing changes in antibiotic resistance to be identified.

Although I did not explore the ability of plasma to drive *S. aureus* pathogenicity and AMR, I found potent antimicrobial activity from trace platelet poor plasma, which might suggest this exerts an evolutionary pressure (Figure 7-4). Bacterial adaptation to the plasma protein fibrinogen has previously been associated with biofilm formation and resistance to neutrophil phagocytosis[558]. As noted, I found that the evolution of resistance to some antimicrobial agents influenced killing of *S. aureus* by LL-37 (Figure 7-10), which is abundant in plasma[518]. I also found increasing concentrations of antimicrobial proteins from neutrophils in sputum from patients with *P. aeruginosa* infections (Figure 7-1). I did not have the patient samples to study antimicrobial proteins in *S. aureus* infections which would have been of considerable

relevance. A more representative model of the evolution of antibiotic resistance for *S. aureus* in infections might incorporate antimicrobial proteins in a hypoxic setting.

SH1000 is an established model organism for studying *S. aureus* as it has been studied extensively[559,560]. However, it is a laboratory adapted strain which is not as pathogenic as many clinical isolates[408]. SH1000 is also methicillin sensitive and MRSA strains are a major burden of antibiotic resistance in *S. aureus*. Therefore, other strains of *S. aureus* need to be studied, including the evolution of clinical isolates. When considering bacterial strains, those including plasmids and horizontal elements should ideally also be incorporated. Horizontal gene transfer was not the focus of my PhD, although the human body is not a closed system and *S. aureus* will encounter horizontal elements[561], so these will need to be considered in future work.

Whilst I studied the impact of evolution in adverse conditions at the population level, my genetic studies were limited to a small number of clones from such populations, chosen at random by selecting the clones closest to a pre-made mark. The small number of clones sequenced (limited by the costs of sequencing and the volume of data generated) means that an unknown number of potentially important genetic changes were not detected in my study. The observation that multiple clones evolved in specific conditions developed mutations in the same genes in parallel does give credence to the relevance of the detected mutations but does not exclude important resistance determinants being missed. Higher throughput methodologies would be required to undertake a more comprehensive assessment.

8.5 Future work

From this work hypoxia and neutrophil proteins appear to interact with the evolution of *S. aureus.* Further study could aid in better understanding the mechanisms of these interactions and the potential impact on infection.

8.5.1 Genetics

Whole genome sequencing is a good starting point to identify mutations in evolved clones which are linked to antibiotic resistance. However, I have limited data showing the mechanisms of resistance. Examples include (but are not limited to) mutations in GntR

accessory regulator gene linked to adaptation to hypoxia (Figure 6-6), rluD-like protein associated with increased tetracycline resistant for SH1000_TetR (Figure 6-9), and mutations in 30S ribosomal protein S21 associated with linezolid resistance (Figure 4-11). To confirm if these genes are driving the observed increases in resistance, one option for non-essential genes would be to employ deletion mutations such as those available from the Nebraska transposon mutant library[254]. However, as we outlined in Chapter 6 with the rluD-like mutant, any transposon mutants should be transduced into the same background as where the mutations were found (SH1000), and the transposon insertion site confirmed. Any mutants should then be complemented with the genes expressed on a plasmid to confirm the transposon mutant is driving any effects. To confirm specific mutations, and mutations in essential genes, mutations could be recreated in *S. aureus* by site directed mutagenesis[562] in both the SH1000 background, and also in other backgrounds, such as USA300_LAC_JE2, to see if the impact of any mutations is restricted or widespread.

I have hypothesised there are compensatory mutations that develop in the evolution of *S. aureus* in hypoxia and antibiotics. To confirm that the mutations are likely compensatory, the order of gene acquisition should be established by sampling clones which were archived over the evolution period[249] (every 5 transfers) to confirm the 'compensatory' mutations occur after the mutations conferring resistance. Furthermore, clones with and without apparent compensatory mutations need to have their growth, antibiotic resistance and fitness compared to assess the contribution of sequential genetic changes.

One of the advantages of carrying out these experiments in *S. aureus* SH1000 is that the closely related genome, NCTC 8325, is comparatively well understood[559]. However, half of the genes in NCTC 8325 have not in fact been characterised[563]. In 6 clones evolved in flucloxacillin, mutations were identified in 11 hypothetical (uncharacterised) proteins (Figure 4-14), and mutations in such hypothetical proteins were frequently seen in other setting also. I hypothesise many adaptations to hypoxia and antibiotics are influenced by these hypothetical proteins. However, to confirm this, these mutations would firstly need to be re-expressed in a background with no other mutations by site directed mutagenesis, with characterisation of their growth in hypoxia or antibiotics as appropriate. However, this alone will not be conclusive, as these mutations could be co-dependent on additional mutations

which occurred in these clones, hence a number of mutations might need to be introduced in parallel. A large amount of work is required to characterise hypothetical proteins, including: sequence and structural homology, structural modelling, modelling the active site, predicting protein-protein interactions, and cellular location and stability[563]. Following such in silico work, proteins can be recombinantly expressed and their interactions and functions studied, by methods that include structural analyses (cryoEM, x-ray crystallography)[564], protein DNA interactions (chromatin immune-precipitation technique ChIP seq)[565] and protein activity assessed according to the nature of the target mutation.

Mutations alone do not capture the full interactions leading to adaptation to antibiotics and hypoxia. RNA sequencing (RNA-seq) could be used to identify changes in gene expression in *S. aureus* following evolution in antibiotics or hypoxia[204,566,567]. This would allow better study of the known pathways such as the two component systems and stringent response, and is unbiased and can therefore detect previously unknown mediators. RNA-seq experiments could also be carried out on clones with point mutations in non-coding regions, to see if the upstream and downstream gene expression has been influenced. This would be useful in evaluating the non-coding mutations in SH1000_TetR evolved clones between *lytM* and *malK* (Figure 6-6), and in delineating bacterial response on a transcriptomic level to the *tetL* gene duplications following evolution of SH1000_TetR in tetracyclines (Figure 6-8). On a smaller scale, to confirm *tetL* duplications do increase *tetL* expression RT-qPCR (reverse transcription, quantitative PCR) of *tetL*, could measure *tetL* expression. It is unclear the cause of the fitness cost of *tetL* in hypoxia (Figure 5-1), and this could also be investigated further with transcriptional analysis; however such data might be challenging to interpret due to the large number of genes which will be influenced by hypoxia[44].

8.5.2 Host-pathogen interaction

I had initially intended to further explore the anti-staphylococcal activity of serum using column fractionation, to show whether the majority of this activity resides in complement of the antimicrobial peptides; this was not pursued because of the time lost during the COVID-19 pandemic but would still be of interest. To better understand how the change in sensitivity to the antimicrobial peptide LL-37 seen in clones evolved in clarithromycin, linezolid and

tobramycin might affect bacterial killing, ex-vivo neutrophil intracellular survival assay (as illustrated in Figure 6-14) could show if there is a change in neutrophil killing of *S. aureus* evolved in different antibiotics; LL-37 and other antimicrobial peptides are discharged into the bacterial phagosome and may help kill the contained bacteria. Neutrophil killing of antibiotic resistant *S. aureus* would be best measured in hypoxia, as this is a more physiological condition, and due to the increase importance of antimicrobial proteins in antimicrobial killing in hypoxia[89,91]. Dual RNA-seq[568,569] could be carried out, on *S. aureus* and neutrophils, to find the transcriptome associated with survival from neutrophil killing, such as the difference in killing *S. aureus* with hypoxic or normoxic mid-log cultures (Figure 6-14), and find any changes in the neutrophil response to different antibiotic resistant bacteria.

8.5.3 Animal models

As noted, the complexity of an in vivo infection cannot be recapitulated in vitro and to validate hypotheses generated in vitro, it is ultimately important to explore key findings of clinical relevance in cellular, tissue or animal models. Cell culture, prosthetic surface and skin explants are all potentially relevant but again do not truly mimic the complexity of infections. Models of *S. aureus* infection have been developed in mice (reviewed in[570]) and models of skin or bone infection might be used either to recapitulate the evolution experiments in vivo, or to test the pathogenicity of the genetic variants I have found. It would be important in such experiments to determine the level of hypoxia in the relevant tissue, but it is worth noting that even moderate systemic hypoxia converted a mild staphylococcal skin model in mice to a lethal challenge due to leukocyte re-programming[571]. Such experiments should thus be carefully planned and undertaken only where there is good in vitro evidence and biological relevance.

8.6 Concluding summary

Bacterial pathogens encounter various challenges at the site of infection, including exposure to antibiotic treatments and physiological stresses such as hypoxia[62,225,418]. I have shown: exposure to antibiotics drives mutations at different rates depending on the antibiotic (Chapter 4); selecting for antibiotic resistance causes low level cross-resistance between antibiotics of different classes (Chapter 4); tetracycline resistance in hypoxia causes a fitness

cost not seen in normoxia (Chapter 5); evolution of high level tetracycline resistance in SH1000_TetR is at the cost of adaptation to hypoxia in antibiotic free conditions (Chapter 5, 6); neutrophil antimicrobial proteins are abundant in infections (Chapter 7) and finally, development of clarithromycin, linezolid and tobramycin resistance reduces the efficacy of *S. aureus* killing by the antimicrobial peptide LL-37 (Chapter 4, 7). Together, these support the hypothesis that the harsh environment *S. aureus* encounters during infections is driving mutations to enhance survival, with exposure to these conditions likely altering the longer-term evolutionary trajectory of antibiotic resistant lineages. Further studies are required to establish the in vivo relevance of these findings.

9 References

1. Tong SYC, Davis JS, Eichenberger E, Holland TL, Fowler VG. *Staphylococcus aureus* Infections: Epidemiology, Pathophysiology, Clinical Manifestations, and Management. *Clin Microbiol Rev.* Vol 282015:603-661.

2. Foster TJ. Antibiotic resistance in *Staphylococcus aureus*. Current status and future prospects. *FEMS Microbiol Rev.* 2017;41(3):430-449.

3. Chambers HF, DeLeo FR. Waves of Resistance: *Staphylococcus aureus* in the Antibiotic Era. *Nature reviews. Microbiology.* 2009;7(9):629-641.

4. Antimicrobial Resistance Collaborators. Global burden of bacterial antimicrobial resistance in 2019: a systematic analysis. *Lancet (London, England).* 2022.

5. Kourtis AP, Hatfield K, Baggs J, et al. Vital Signs: Epidemiology and Recent Trends in Methicillin-Resistant and in Methicillin-Susceptible *Staphylococcus aureus* Bloodstream Infections - United States. *MMWR Morb Mortal Wkly Rep.* 2019;68(9):214-219.

6. Ahmed AO, van Belkum A, Fahal AH, et al. Nasal carriage of *Staphylococcus aureus* and epidemiology of surgical-site infections in a Sudanese university hospital. *Journal of clinical microbiology.* 1998;36(12):3614-3618.

7. van Belkum A, Verkaik Nelianne J, de Vogel Corné P, et al. Reclassification of *Staphylococcus aureus* Nasal Carriage Types. *The Journal of Infectious Diseases.* 2009;199(12):1820-1826.

8. Weidenmaier C, Goerke C, Wolz C. *Staphylococcus aureus* determinants for nasal colonization. *Trends in microbiology.* 2012;20(5):243-250.

9. Kluytmans J, van Belkum A, Verbrugh H. Nasal carriage of *Staphylococcus aureus*: epidemiology, underlying mechanisms, and associated risks. *Clinical microbiology reviews.* 1997;10(3):505-520.

10. von Eiff C, Becker K, Machka K, Stammer H, Peters G. Nasal carriage as a source of *Staphylococcus aureus* bacteremia. Study Group. *The New England journal of medicine.* 2001;344(1):11-16.

11. Stegeman CA, Tervaert JW, Sluiter WJ, Manson WL, de Jong PE, Kallenberg CG. Association of chronic nasal carriage of *Staphylococcus aureus* and higher relapse rates in Wegener granulomatosis. *Annals of internal medicine.* 1994;120(1):12-17.

12. Klevens RM, Morrison MA, Nadle J, et al. Invasive methicillin-resistant *Staphylococcus aureus* infections in the United States. *Jama.* 2007;298(15):1763-1771.

13. Kollef MH, Shorr A, Tabak YP, Gupta V, Liu LZ, Johannes RS. Epidemiology and outcomes of health-care-associated pneumonia: results from a large US database of culture-positive pneumonia. *Chest.* 2005;128(6):3854-3862.

14. Duerden B, Fry C, Johnson AP, Wilcox MH. The Control of Methicillin-Resistant *Staphylococcus aureus* Blood Stream Infections in England. *Open Forum Infect Dis.* 2015;2(2):ofv035.

15. Cheung GYC, Bae JS, Otto M. Pathogenicity and virulence of *Staphylococcus aureus. Virulence.* 2021;12(1):547-569.

16. Hajdamowicz NH, Hull RC, Foster SJ, Condliffe AM. The Impact of Hypoxia on the Host-Pathogen Interaction between Neutrophils and *Staphylococcus aureus*. *Int J Mol Sci.* 2019;20(22).

17. Echániz-Aviles G, Velazquez-Meza ME, Rodríguez-Arvizu B, Carnalla-Barajas MN, Noguerón AS. Detection of capsular genotypes of methicillin-resistant *Staphylococcus aureus* and clonal distribution of the *cap5* and *cap8* genes in clinical isolates. *Arch Microbiol.* 2022;204(3):186.

18. Cocchiaro JL, Gomez MI, Risley A, Solinga R, Sordelli DO, Lee JC. Molecular characterization of the capsule locus from non-typeable *Staphylococcus aureus*. *Molecular microbiology.* 2006;59(3):948-960.

19. Lei MG, Lee CY. Regulation of Staphylococcal Capsule by *sarZ* is SigA-Dependent. *Journal of bacteriology.* 2022;204(8):e0015222.

20. Jenul C, Horswill AR. Regulation of *Staphylococcus aureus* Virulence. *Microbiol Spectr.* 2019;7(2).

21. Yarwood JM, Schlievert PM. Quorum sensing in *Staphylococcus* infections. *J Clin Invest.* Vol 1122003:1620-1625.

22. Ji G, Beavis RC, Novick RP. Cell density control of staphylococcal virulence mediated by an octapeptide pheromone. *Proceedings of the National Academy of Sciences of the United States of America.* 1995;92(26):12055-12059.

23. Benito Y, Kolb FA, Romby P, Lina G, Etienne J, Vandenesch F. Probing the structure of RNAIII, the Staphylococcus aureus *agr* regulatory RNA, and identification of the RNA domain involved in repression of protein A expression. *RNA.* 2000;6(5):668-679.

24. Pang YY, Schwartz J, Thoendel M, Ackermann LW, Horswill AR, Nauseef WM. *agr*-Dependent Interactions of *Staphylococcus aureus* USA300 with Human Polymorphonuclear Neutrophils. *Journal of Innate Immunity.* 2018;2(6):546-559.

25. Voyich JM, Braughton KR, Sturdevant DE, et al. Insights into mechanisms used by *Staphylococcus aureus* to avoid destruction by human neutrophils. *J Immunol.* 2005;175(6):3907-3919.

26. Moldovan A, Fraunholz MJ. In or out: Phagosomal escape of *Staphylococcus aureus*. *Cellular microbiology.* 2018:e12997.

27. Leliefeld PHC, Pillay J, Vrisekoop N, et al. Differential antibacterial control by neutrophil subsets. *Blood Adv.* Vol 22018:1344-1355.

28. O'Riordan K, Lee JC. *Staphylococcus aureus* Capsular Polysaccharides. *Clin Microbiol Rev.* Vol 172004:218-234.

29. Falugi F, Kim HK, Missiakas DM, Schneewind O. Role of Protein A in the Evasion of Host Adaptive Immune Responses by *Staphylococcus aureus*. *mBio.* Vol 42013.

30. Higgins J, Loughman A, van Kessel KP, van Strijp JA, Foster TJ. Clumping factor A of *Staphylococcus aureus* inhibits phagocytosis by human polymorphonuclear leucocytes. *FEMS microbiology letters.* 2006;258(2):290-296.

31. Lacey KA, Geoghegan JA, McLoughlin RM. The Role of *Staphylococcus aureus* Virulence Factors in Skin Infection and Their Potential as Vaccine Antigens. *Pathogens.* Vol 52016.

32. Rooijakkers SH, Milder FJ, Bardoel BW, Ruyken M, van Strijp JA, Gros P. Staphylococcal complement inhibitor: structure and active sites. *Journal of immunology (Baltimore, Md. : 1950).* 2007;179(5):2989-2998.

33. Laarman AJ, Ruyken M, Malone CL, van Strijp JA, Horswill AR, Rooijakkers SH. *Staphylococcus aureus* metalloprotease aureolysin cleaves complement C3 to mediate immune evasion. *Journal of immunology (Baltimore, Md. : 1950).* 2011;186(11):6445-6453.

34. Genestier AL, Michallet MC, Prévost G, et al. *Staphylococcus aureus* Panton-Valentine leukocidin directly targets mitochondria and induces Bax-independent apoptosis of human neutrophils. *J Clin Invest.* Vol 1152005:3117-3127.

35. Peschel A, Otto M. Phenol-soluble modulins and staphylococcal infection. *Nature reviews. Microbiology.* 2013;11(10):667-673.

36. de Haas CJC, Veldkamp KE, Peschel A, et al. Chemotaxis inhibitory protein of *Staphylococcus aureus*, a bacterial antiinflammatory agent. *The Journal of experimental medicine.* 2004;199(5):687-695.

37. Guerra FE, Borgogna TR, Patel DM, Sward EW, Voyich JM. Epic Immune Battles of History: Neutrophils vs. Staphylococcus aureus. *Frontiers in cellular and infection microbiology.* 2017;7:286-286.

38. Woehl JL, Stapels DA, Garcia BL, et al. The Extracellular Adherence Protein from *Staphylococcus aureus* Inhibits the Classical and Lectin Pathways of Complement by Blocking Formation of the C3 Pro-Convertase. *Journal of immunology (Baltimore, Md. : 1950).* 2014;193(12):6161-6171.

39. Fraser JD, Proft T. The bacterial superantigen and superantigen-like proteins. *Immunological reviews.* 2008;225:226-243.

40. Bera A, Herbert S, Jakob A, Vollmer W, Gotz F. Why are pathogenic staphylococci so lysozyme resistant? The peptidoglycan O-acetyltransferase OatA is the major determinant for lysozyme resistance of Staphylococcus aureus. *Molecular microbiology.* 2005;55(3):778-787.

41. Kanafani H, Martin SE. Catalase and superoxide dismutase activities in virulent and nonvirulent *Staphylococcus aureus* isolates. *J Clin Microbiol.* 1985;21(4):607-610.

42. Clements MO, Watson SP, Foster SJ. Characterization of the Major Superoxide Dismutase of *Staphylococcus aureus* and Its Role in Starvation Survival, Stress Resistance, and Pathogenicity. *J Bacteriol.* Vol 1811999:3898-3903.

43. Clauditz A, Resch A, Wieland KP, Peschel A, Götz F. Staphyloxanthin Plays a Role in the Fitness of *Staphylococcus aureus* and Its Ability To Cope with Oxidative Stress. *Infect Immun.* Vol 742006:4950-4953.

44. Kinkel TL, Roux CM, Dunman PM, Fang FC, Gilmore MS. The *Staphylococcus aureus srrAB* Two-Component System Promotes Resistance to Nitrosative Stress and Hypoxia. 2013.

45. Cramton SE, Ulrich M, Götz F, Döring G. Anaerobic Conditions Induce Expression of Polysaccharide Intercellular Adhesin in Staphylococcus aureus and Staphylococcus epidermidis. *Infect Immun.* Vol 692001:4079-4085.

46. Brinkmann V, Reichard U, Goosmann C, et al. Neutrophil extracellular traps kill bacteria. *Science.* 2004;303(5663):1532-1535.

47. Rigby KM, DeLeo FR. Neutrophils in innate host defense against *Staphylococcus aureus* infections. *Seminars in immunopathology.* 2012;34(2):237-259.

48. Fraunholz M, Sinha B. Intracellular staphylococcus aureus: Live-in and let die. *Front Cell Infect Microbiol.* 2012;2.

49. Gresham HD, Lowrance JH, Caver TE, Wilson BS, Cheung AL, Lindberg FP. Survival of *Staphylococcus aureus* inside neutrophils contributes to infection. *J Immunol.* 2000;164(7):3713-3722.

50. Prajsnar TK, Serba JJ, Dekker BM, et al. The autophagic response to *Staphylococcus aureus* provides an intracellular niche in neutrophils. *Autophagy.* 2021;17(4):888-902.

51. Hajdamowicz NH. Hypoxia and Reactive Oxygen Species Modulate the Interaction Between Human Neutrophils and *Staphylococcus aureus* [PhD Thesis], University of Sheffield; 2021.

52. Arya R, Princy SA. An insight into pleiotropic regulators Agr and Sar: molecular probes paving the new way for antivirulent therapy. *Future microbiology.* 2013;8(10):1339-1353.

53. Arnold DE, Heimall JR. A Review of Chronic Granulomatous Disease. *Advances in therapy.* 2017;34(12):2543-2557.

54. Winkelstein JA, Marino MC, Johnston RB, Jr., et al. Chronic granulomatous disease. Report on a national registry of 368 patients. *Medicine.* 2000;79(3):155-169.

55. Talan DA, Krishnadasan A, Gorwitz RJ, et al. Comparison of *Staphylococcus aureus* from skin and soft-tissue infections in US emergency department patients, 2004 and 2008. *Clinical infectious diseases : an official publication of the Infectious Diseases Society of America.* 2011;53(2):144-149.

56. Kobayashi SD, Malachowa N, DeLeo FR. Pathogenesis of *Staphylococcus aureus* abscesses. *The American journal of pathology.* 2015;185(6):1518-1527.

57. Nizet V, Johnson RS. Interdependence of hypoxic and innate immune responses. *Nat Rev Immunol.* 2009;9(9):609-617.

58. Carreau A, Hafny-Rahbi BE, Matejuk A, Grillon C, Kieda C. Why is the partial oxygen pressure of human tissues a crucial parameter? Small molecules and hypoxia. *J Cell Mol Med.* 2011;15(6):1239-1253.

59. Sitkovsky M, Lukashev D. Regulation of immune cells by local-tissue oxygen tension: HIF1 alpha and adenosine receptors. *Nat Rev Immunol.* 2005;5(9):712-721.

60. Huber A, Dorn A, Witzmann A, Cervos-Navarro J. Microthrombi formation after severe head trauma. *International journal of legal medicine.* 1993;106(3):152-155.

61. Campbell EL, Bruyninckx WJ, Kelly CJ, et al. Transmigrating neutrophils shape the mucosal microenvironment through localized oxygen depletion to influence resolution of inflammation. *Immunity.* 2014;40(1):66-77.

62. Hofstee MI, Riool M, Terjajevs I, et al. Three-Dimensional In Vitro *Staphylococcus aureus* Abscess Communities Display Antibiotic Tolerance and Protection from Neutrophil Clearance. *Infect Immun.* 2020;88(11).

63. Cheng AG, DeDent AC, Schneewind O, Missiakas D. A play in four acts: *Staphylococcus aureus* abscess formation. *Trends in microbiology.* 2011;19(5):225-232.

64. Lone AG, Atci E, Renslow R, et al. *Staphylococcus aureus* Induces Hypoxia and Cellular Damage in Porcine Dermal Explants. *Infect Immun.* Vol 832015:2531-2541.

65. Long DR, Wolter DJ, Lee M, et al. Polyclonality, Shared Strains, and Convergent Evolution in Chronic Cystic Fibrosis *Staphylococcus aureus* Airway Infection. *Am J Respir Crit Care Med.* 2021;203(9):1127-1137.

66. Masters EA, Trombetta RP, de Mesy Bentley KL, et al. Evolving concepts in bone infection: redefining "biofilm", "acute vs. chronic osteomyelitis", "the immune proteome" and "local antibiotic therapy". *Bone Res.* 2019;7:20.

67. Lavigne JP, Hosny M, Dunyach-Remy C, et al. Long-Term Intrahost Evolution of *Staphylococcus aureus* Among Diabetic Patients With Foot Infections. *Front Microbiol.* 2021;12:741406.

68. Jubrail J, Morris P, Bewley MA, et al. Inability to sustain intraphagolysosomal killing of *Staphylococcus aureus* predisposes to bacterial persistence in macrophages. *Cellular microbiology.* 2016;18(1):80-96.

69. Uebele J, Stein C, Nguyen MT, et al. Antigen delivery to dendritic cells shapes human CD4+ and CD8+ T cell memory responses to *Staphylococcus aureus. PLoS pathogens.* 2017;13(5):e1006387.

70. Wu X, Xu F. Dendritic cells during *Staphylococcus aureus* infection: subsets and roles. *J Transl Med.* Vol 122014.

71. Lee LY, Hook M, Haviland D, et al. Inhibition of complement activation by a secreted *Staphylococcus aureus* protein. *J Infect Dis.* 2004;190(3):571-579.

72. Drago L, Bortolin M, Vassena C, Romanò CL, Taschieri S, Del Fabbro M. Plasma components and platelet activation are essential for the antimicrobial properties of autologous platelet-rich plasma: an in vitro study. *PLoS One.* 2014;9(9):e107813.

73. Benjamin RJ, McLaughlin LS. Plasma components: properties, differences, and uses. *Transfusion.* 2012;52 Suppl 1:9s-19s.

74. Yeaman MR. Platelets: at the nexus of antimicrobial defence. *Nature reviews. Microbiology.* 2014;12(6):426-437.

75. Heesterbeek DAC, Angelier ML, Harrison RA, Rooijakkers SHM. Complement and Bacterial Infections: From Molecular Mechanisms to Therapeutic Applications. *J Innate Immun.* 2018;10(5-6):455-464.

76. Athens JW, Haab OP, Raab SO, et al. Leukokinetic studies. IV. The total blood, circulating and marginal granulocyte pools and the granulocyte turnover rate in normal subjects. *The Journal of clinical investigation.* 1961;40(6):989-995.

77. Lahoz-Beneytez J, Elemans M, Zhang Y, et al. Human neutrophil kinetics: modeling of stable isotope labeling data supports short blood neutrophil half-lives. *Blood.* 2016;127(26):3431-3438.

78. Muller WA. Getting Leukocytes to the Site of Inflammation. *Vet Pathol.* 2013;50(1):7-22.

79. Yoo SK, Starnes TW, Deng Q, Huttenlocher A. Lyn is a redox sensor that mediates leukocyte wound attraction in vivo. *Nature.* 2011;480(7375):109-112.

80. Kobayashi Y. The role of chemokines in neutrophil biology. *Frontiers in bioscience : a journal and virtual library.* 2008;13:2400-2407.

81. de Oliveira S, Rosowski EE, Huttenlocher A. Neutrophil migration in infection and wound repair: going forward in reverse. *Nat Rev Immunol.* 2016;16(6):378-391.

82. Wright HL, Moots RJ, Bucknall RC, Edwards SW. Neutrophil function in inflammation and inflammatory diseases. *Rheumatology (Oxford).* 2010;49(9):1618-1631.

83. Faurschou M, Borregaard N. Neutrophil granules and secretory vesicles in inflammation. *Microbes and infection.* 2003;5(14):1317-1327.

84. Kyme P, Thoennissen NH, Tseng CW, et al. C/EBPε mediates nicotinamide-enhanced clearance of *Staphylococcus aureus* in mice. *The Journal of clinical investigation.* 2012;122(9):3316-3329.

85. Gombart AF, Koeffler HP. Neutrophil specific granule deficiency and mutations in the gene encoding transcription factor C/EBP(epsilon). *Curr Opin Hematol.* 2002;9(1):36-42.

86. Sowerby JM, Thomas DC, Clare S, et al. NBEAL2 is required for neutrophil and NK cell function and pathogen defense. *The Journal of clinical investigation.* 2017;127(9):3521-3526.

87. Clawson CC, Repine JE, White JG. The Chediak-Higashi Syndrome: Quantitation of a Deficiency in Maximal Bactericidal Capacity. *Am J Pathol.* 1979;94(3):539-547.

88. Cadwallader KA, Uddin M, Condliffe AM, et al. Effect of priming on activation and localization of phospholipase D-1 in human neutrophils. *European journal of biochemistry.* 2004;271(13):2755-2764.

89. Hoenderdos K, Lodge KM, Hirst RA, et al. Hypoxia upregulates neutrophil degranulation and potential for tissue injury. *Thorax.* 2016;71(11):1030-1038.

90. Winterbourn CC, Kettle AJ, Hampton MB. Reactive Oxygen Species and Neutrophil Function. *Annual review of biochemistry.* 2016;85:765-792.

91. McGovern NN, Cowburn AS, Porter L, et al. Hypoxia selectively inhibits respiratory burst activity and killing of *Staphylococcus aureus* in human neutrophils. *Journal of immunology (Baltimore, Md. : 1950).* 2011;186(1):453-463.

92. Lehrer R, Lichtenstein A, Ganz T. Defensins: antimicrobial and cytotoxic peptides of mammalian cells. *Annual review of immunology.* 1993;11.

93. Kobayashi SD, Malachowa N, DeLeo FR. Neutrophils and Bacterial Immune Evasion. *J Innate Immun.* 2018;10(5-6):432-441.

94. Turner J, Cho Y, Dinh NN, Waring AJ, Lehrer RI. Activities of LL-37, a cathelin-associated antimicrobial peptide of human neutrophils. *Antimicrob Agents Chemother.* 1998;42(9):2206-2214.

95. Gabay JE, Scott RW, Campanelli D, et al. Antibiotic proteins of human polymorphonuclear leukocytes. *Proceedings of the National Academy of Sciences of the United States of America.* 1989;86(14):5610-5614.

96. Weiss J, Franson C, Schmeidler K, Elsbach P. Reversible Envelope Effects During and After Killing of *Escherichia coli* W by a Highly-Purified Rabbit Polymorpho-Nuclear Leukocyte Fraction. *Biochimica et biophysica acta.* 1976;436(1).

97. Schultz H, Weiss JP. The bactericidal/permeability-increasing protein (BPI) in infection and inflammatory disease. *Clin Chim Acta.* 2007;384(1-2):12-23.

98. Zackular J, Chazin W, Skaar E. Nutritional Immunity: S100 Proteins at the Host-Pathogen Interface. *The Journal of biological chemistry.* 2015;290(31).

99. Voganatsi A, Panyutich A, Miyasaki K, Murthy R. Mechanism of Extracellular Release of Human Neutrophil Calprotectin Complex. *Journal of leukocyte biology.* 2001;70(1).

100. Cho H, Jeong DW, Liu Q, et al. Calprotectin Increases the Activity of the *saeRS* Two Component System and Murine Mortality during Staphylococcus aureus Infections. *PLoS Pathog.* Vol 112015.

101. Legrand D. Overview of Lactoferrin as a Natural Immune Modulator. *The Journal of pediatrics.* 2016;173 Suppl.

102. Molloy A, Winterbourn C. Release of Iron From Phagocytosed *Escherichia coli* and Uptake by Neutrophil Lactoferrin. *Blood.* 1990;75(4).

103. Yamauchi K, Tomita M, Giehl TJ, Ellison RT. Antibacterial activity of lactoferrin and a pepsin-derived lactoferrin peptide fragment. *Infect Immun.* 1993;61(2):719-728.

104. Campanelli D, Detmers PA, Nathan CF, Gabay JE. Azurocidin and a homologous serine protease from neutrophils. Differential antimicrobial and proteolytic properties. *J Clin Invest.* 1990;85(3):904-915.

105. Hahn I, Klaus A, Janze A-K, et al. Cathepsin G and Neutrophil Elastase Play Critical and Nonredundant Roles in Lung-Protective Immunity against *Streptococcus pneumoniae* in Mice. 2011.

106. Belaaouaj A, McCarthy R, Baumann M, et al. Mice lacking neutrophil elastase reveal impaired host defense against gram negative bacterial sepsis. *Nat Med.* 1998;4(5):615-618.

107. Belaaouaj A, Kim KS, Shapiro SD. Degradation of outer membrane protein A in *Escherichia coli* killing by neutrophil elastase. *Science.* 2000;289(5482):1185-1188.

108. Belaaouaj A. Neutrophil elastase-mediated killing of bacteria: lessons from targeted mutagenesis. *Microbes and infection.* 2002;4(12):1259-1264.

109. Hirche TO, Gaut JP, Heinecke JW, Belaaouaj A. Myeloperoxidase plays critical roles in killing *Klebsiella pneumoniae* and inactivating neutrophil elastase: effects on host defense. *J Immunol.* 2005;174(3):1557-1565.

110. Nganje CN, Haynes SA, Qabar CM, Lent RC, Bou Ghanem EN, Shainheit MG. PepN is a non-essential, cell wall-localized protein that contributes to neutrophil elastase-mediated killing of *Streptococcus pneumoniae*. *PLoS One.* 2019;14(2):e0211632.

111. Odeberg H, Olsson I. Antibacterial activity of cationic proteins from human granulocytes. *The Journal of clinical investigation.* 1975;56(5):1118-1124.

112. Odeberg H, Olsson I. Mechanisms for the microbicidal activity of cationic proteins of human granulocytes. *Infect Immun.* 1976;14(6):1269-1275.

113. Perera NC, Schilling O, Kittel H, Back W, Kremmer E, Jenne DE. NSP4, an elastase-related protease in human neutrophils with arginine specificity. *Proceedings of the National Academy of Sciences of the United States of America.* 2012;109(16):6229-6234.

114. Perera NC, Wiesmuller KH, Larsen MT, et al. NSP4 is stored in azurophil granules and released by activated neutrophils as active endoprotease with restricted specificity. *Journal of immunology (Baltimore, Md. : 1950).* 2013;191(5):2700-2707.

115. Wilde CG, Snable JL, Griffith JE, Scott RW. Characterization of two azurphil granule proteases with active-site homology to neutrophil elastase. *The Journal of biological chemistry.* 1990;265(4):2038-2041.

116. Weiss J, Elsbach P, Olsson I, Odeberg H. Purification and characterization of a potent bactericidal and membrane active protein from the granules of human polymorphonuclear leukocytes. *The Journal of biological chemistry.* 1978;253(8):2664-2672.

117. Heinzelmann M, Platz A, Flodgaard H, Miller FN. Heparin binding protein (CAP37) is an opsonin for *Staphylococcus aureus* and increases phagocytosis in monocytes. *Inflammation.* 1998;22(5):493-507.

118. López-Boado YS, Espinola M, Bahr S, Belaaouaj A. Neutrophil Serine Proteinases Cleave Bacterial Flagellin, Abrogating Its Host Response-Inducing Activity. 2004.

119. Kim C, Gajendran N, Mittrücker HW, et al. Human α-defensins neutralize anthrax lethal toxin and protect against its fatal consequences. *Proc Natl Acad Sci U S A.* Vol 1022005:4830-4835.

120. Kim C, Slavinskaya Z, Merrill AR, Kaufmann SH. Human alpha-defensins neutralize toxins of the mono-ADP-ribosyltransferase family. *Biochem J.* 2006;399(2):225-229.

121. Cardot-Martin E, Casalegno JS, Badiou C, et al. alpha-Defensins partially protect human neutrophils against Panton-Valentine leukocidin produced by *Staphylococcus aureus*. *Lett Appl Microbiol.* 2015;61(2):158-164.

122. Overhage J, Campisano A, Bains M, Torfs EC, Rehm BH, Hancock RE. Human host defense peptide LL-37 prevents bacterial biofilm formation. *Infect Immun.* 2008;76(9):4176-4182.

123. Shafer WM, Onunka VC. Mechanism of staphylococcal resistance to non-oxidative antimicrobial action of neutrophils: importance of pH and ionic strength in determining the bactericidal action of cathepsin G. *J Gen Microbiol.* 1989;135(4):825-830.

124. Korkmaz B, Moreau T, Gauthier F. Neutrophil elastase, proteinase 3 and cathepsin G: physicochemical properties, activity and physiopathological functions. *Biochimie.* 2008;90(2):227-242.

125. McCabe D, Cukierman T, Gabay JE. Basic residues in azurocidin/HBP contribute to both heparin binding and antimicrobial activity. *The Journal of biological chemistry.* 2002;277(30):27477-27488.

126. Mannion BA, Weiss J, Elsbach P. Separation of sublethal and lethal effects of the bactericidal/permeability increasing protein on *Escherichia coli. The Journal of clinical investigation.* 1990;85(3):853-860.

127. Sorensen OE, Follin P, Johnsen AH, et al. Human cathelicidin, hCAP-18, is processed to the antimicrobial peptide LL-37 by extracellular cleavage with proteinase 3. *Blood.* 2001;97(12):3951-3959.

128. Tongaonkar P, Golji AE, Tran P, Ouellette AJ, Selsted ME. High fidelity processing and activation of the human alpha-defensin HNP1 precursor by neutrophil elastase and proteinase 3. *PLoS One.* 2012;7(3):e32469.

129. Noack B, Görgens H, Schacher B, et al. Functional Cathepsin C mutations cause different Papillon-Lefèvre syndrome phenotypes. *J Clin Periodontol.* 2008;35(4):311-316.

130. McGuire MJ, Lipsky PE, Thiele DL. Generation of active myeloid and lymphoid granule serine proteases requires processing by the granule thiol protease dipeptidyl peptidase I. *The Journal of biological chemistry.* 1993;268(4):2458-2467.

131. Sørensen OE, Clemmensen SN, Dahl SL, et al. Papillon-Lefèvre syndrome patient reveals species-dependent requirements for neutrophil defenses. *The Journal of clinical investigation.* 2014;124(10):4539-4548.

132. Nauseef WM. Proteases, neutrophils, and periodontitis: the NET effect. *J Clin Invest.* Vol 1242014:4237-4239.

133. Sanchez Klose FP, Björnsdottir H, Dahlstrand Rudin A, et al. A rare CTSC mutation in Papillon-Lefèvre Syndrome results in abolished serine protease activity and reduced NET formation but otherwise normal neutrophil function. *PLoS One.* 2021;16(12):e0261724.

134. Chacko BK, Kramer PA, Ravi S, et al. Methods for defining distinct bioenergetic profiles in platelets, lymphocytes, monocytes, and neutrophils, and the oxidative burst from human blood. *Lab Invest.* Vol 932013:690-700.

135. Berra E, Benizri E, Ginouvès A, Volmat V, Roux D, Pouysségur J. HIF prolyl-hydroxylase 2 is the key oxygen sensor setting low steady-state levels of HIF-1α in normoxia. *EMBO J.* Vol 222003:4082-4090.

136. Masson N, Ratcliffe PJ. HIF prolyl and asparaginyl hydroxylases in the biological response to intracellular O_2 levels. *Journal of cell science.* 2003;116(Pt 15):3041-3049.

137. Lodge KM, Thompson AA, Chilvers ER, Condliffe AM. Hypoxic regulation of neutrophil function and consequences for *Staphylococcus aureus* infection. *Microbes and infection.* 2017;19(3):166-176.

138. Egners A, Erdem M, Cramer T. The Response of Macrophages and Neutrophils to Hypoxia in the Context of Cancer and Other Inflammatory Diseases. *Mediators Inflamm.* 2016;2016.

139. Peyssonnaux C, Datta V, Cramer T, et al. HIF-1α expression regulates the bactericidal capacity of phagocytes. *J Clin Invest.* Vol 1152005:1806-1815.

140. Watts ER, Walmsley SR. Inflammation and Hypoxia: HIF and PHD Isoform Selectivity. *Trends in molecular medicine.* 2019;25(1):33-46.

141. Fritzenwanger M, Jung C, Goebel B, Lauten A, Figulla HR. Impact of short-term systemic hypoxia on phagocytosis, cytokine production, and transcription factor activation in peripheral blood cells. *Mediators Inflamm.* 2011;2011:429501.

142. Lodge KM, Vassallo A, Liu B, et al. Hypoxia Increases the Potential for Neutrophil-mediated Endothelial Damage in Chronic Obstructive Pulmonary Disease. *Am J Respir Crit Care Med.* 2022;205(8):903-916.

143. Völlger L, Akong-Moore K, Cox L, et al. Iron-chelating agent desferrioxamine stimulates formation of neutrophil extracellular traps (NETs) in human blood-derived neutrophils. *Biosci Rep.* 2016;36(3).

144. Mykytyn AZ, Breugem TI, Riesebosch S, et al. SARS-CoV-2 entry into human airway organoids is serine protease-mediated and facilitated by the multibasic cleavage site. *Elife.* 2021;10.

145. Hui KPY, Ho JCW, Cheung MC, et al. SARS-CoV-2 Omicron variant replication in human bronchus and lung ex vivo. *Nature.* 2022;603(7902):715-720.

146. Schilling NA, Kalbacher H, Burster T. Variation of Proteolytic Cleavage Sites towards the N-Terminal End of the S2 Subunit of the Novel SARS-CoV-2 Omicron Sublineage BA.2.12.1. *Molecules.* 2022;27(18).

147. Mustafa Z, Kalbacher H, Burster T. Occurrence of a novel cleavage site for cathepsin G adjacent to the polybasic sequence within the proteolytically sensitive activation loop of the SARS-CoV-2 Omicron variant: The amino acid substitution N679K and P681H of the spike protein. *PLoS One.* 2022;17(4):e0264723.

148. Hoffmann M, Kleine-Weber H, Schroeder S, et al. SARS-CoV-2 Cell Entry Depends on ACE2 and TMPRSS2 and Is Blocked by a Clinically Proven Protease Inhibitor. *Cell.* 2020;181(2):271-280.e278.

149. Bridges JP, Vladar EK, Huang H, Mason RJ. Respiratory epithelial cell responses to SARS-CoV-2 in COVID-19. *Thorax.* 2022;77(2):203-209.

150. Mirchandani AS, Jenkins SJ, Bain CC, et al. Hypoxia shapes the immune landscape in lung injury and promotes the persistence of inflammation. *Nat Immunol.* 2022;23(6):927-939.

151. Meizlish ML, Pine AB, Bishai JD, et al. A neutrophil activation signature predicts critical illness and mortality in COVID-19. *Blood Adv.* 2021;5(5):1164-1177.

152. Veras FP, Pontelli MC, Silva CM, et al. SARS-CoV-2-triggered neutrophil extracellular traps mediate COVID-19 pathology. *J Exp Med.* 2020;217(12).

153. Ouwendijk WJD, Raadsen MP, van Kampen JJA, et al. High Levels of Neutrophil Extracellular Traps Persist in the Lower Respiratory Tract of Critically Ill Patients With Coronavirus Disease 2019. *J Infect Dis.* 2021;223(9):1512-1521.

154. Chiang CC, Korinek M, Cheng WJ, Hwang TL. Targeting Neutrophils to Treat Acute Respiratory Distress Syndrome in Coronavirus Disease. *Front Pharmacol.* 2020;11:572009.

155. Dowey R, Cole J, Thompson AAR, et al. Enhanced neutrophil extracellular trap formation in COVID-19 is inhibited by the protein kinase C inhibitor ruboxistaurin. *ERJ Open Res.* 2022;8(2).

156. Barnes BJ, Adrover JM, Baxter-Stoltzfus A, et al. Targeting potential drivers of COVID-19: Neutrophil extracellular traps. *J Exp Med.* Vol 2172020.

157. Horby P, Lim WS, Emberson JR, et al. Dexamethasone in Hospitalized Patients with Covid-19. *The New England journal of medicine.* 2021;384(8):693-704.

158. RECOVERY Collaborative Group. Tocilizumab in patients admitted to hospital with COVID-19 (RECOVERY): a randomised, controlled, open-label, platform trial. *Lancet (London, England).* 2021;397(10285):1637-1645.

159. Hazeldine J, Lord JM. Neutrophils and COVID-19: Active Participants and Rational Therapeutic Targets. *Front Immunol.* 2021;12:680134.

160. Ackermann M, Anders HJ, Bilyy R, et al. Patients with COVID-19: in the dark-NETs of neutrophils. *Cell Death Differ.* 2021;28(11):3125-3139.

161. Davies J, Davies D. Origins and Evolution of Antibiotic Resistance. *Microbiol Mol Biol Rev.* Vol 742010:417-433.

162. EclinicalMedicine. Antimicrobial resistance: a top ten global public health threat. *eClinicalMedicine.* 2021;41.

163. Jones RN, Mendes RE, Sader HS. Ceftaroline activity against pathogens associated with complicated skin and skin structure infections: results from an international surveillance study. *The Journal of antimicrobial chemotherapy.* 2010;65 Suppl 4:iv17-31.

164. Zhanel GG, Walkty AJ, Karlowsky JA. Fidaxomicin: A novel agent for the treatment of *Clostridium difficile* infection. *Can J Infect Dis Med Microbiol.* 2015;26(6):305-312.

165. Sheng ZK, Hu F, Wang W, et al. Mechanisms of tigecycline resistance among *Klebsiella pneumoniae* clinical isolates. *Antimicrob Agents Chemother.* 2014;58(11):6982-6985.

166. Fala L. Sivextro (Tedizolid Phosphate) Approved for the Treatment of Adults with Acute Bacterial Skin and Skin-Structure Infections. *Am Health Drug Benefits.* 2015;8(Spec Feature):111-115.

167. Shaw KJ, Poppe S, Schaadt R, et al. In vitro activity of TR-700, the antibacterial moiety of the prodrug TR-701, against linezolid-resistant strains. *Antimicrob Agents Chemother.* 2008;52(12):4442-4447.

168. Kapoor G, Saigal S, Elongavan A. Action and resistance mechanisms of antibiotics: A guide for clinicians. *J Anaesthesiol Clin Pharmacol.* 2017;33(3):300-305.

169. Rayner C, Munckhof WJ. Antibiotics currently used in the treatment of infections caused by *Staphylococcus aureus*. *Intern Med J.* 2005;35 Suppl 2:S3-16.

170. Dijkmans AC, Zacarías NVO, Burggraaf J, et al. Fosfomycin: Pharmacological, Clinical and Future Perspectives. *Antibiotics (Basel).* 2017;6(4).

171. Straus SK, Hancock RE. Mode of action of the new antibiotic for Gram-positive pathogens daptomycin: comparison with cationic antimicrobial peptides and lipopeptides. *Biochim Biophys Acta.* 2006;1758(9):1215-1223.

172. Miller WR, Bayer AS, Arias CA. Mechanism of Action and Resistance to Daptomycin in *Staphylococcus aureus* and *Enterococci*. *Cold Spring Harb Perspect Med.* 2016;6(11).

173. Gleckman R, Blagg N, Joubert DW. Trimethoprim: mechanisms of action, antimicrobial activity, bacterial resistance, pharmacokinetics, adverse reactions, and therapeutic indications. *Pharmacotherapy.* 1981;1(1):14-20.

174. Yun MK, Wu Y, Li Z, et al. Catalysis and sulfa drug resistance in dihydropteroate synthase. *Science.* 2012;335(6072):1110-1114.

175. Aldred KJ, Kerns RJ, Osheroff N. Mechanism of quinolone action and resistance. *Biochemistry.* 2014;53(10):1565-1574.

176. Wehrli W, Knüsel F, Schmid K, Staehelin M. Interaction of rifamycin with bacterial RNA polymerase. *Proceedings of the National Academy of Sciences of the United States of America.* 1968;61(2):667-673.

177. Chopra I, Hawkey PM, Hinton M. Tetracyclines, molecular and clinical aspects. *The Journal of antimicrobial chemotherapy.* 1992;29(3):245-277.

178. Krause KM, Serio AW, Kane TR, Connolly LE. Aminoglycosides: An Overview. *Cold Spring Harb Perspect Med.* 2016;6(6).

179. Vázquez-Laslop N, Mankin AS. How Macrolide Antibiotics Work. *Trends Biochem Sci.* 2018;43(9):668-684.

180. Polikanov YS, Aleksashin NA, Beckert B, Wilson DN. The Mechanisms of Action of Ribosome-Targeting Peptide Antibiotics. *Front Mol Biosci.* 2018;5:48.

181. Douthwaite S. Interaction of the antibiotics clindamycin and lincomycin with Escherichia coli 23S ribosomal RNA. *Nucleic Acids Res.* 1992;20(18):4717-4720.

182. Schlünzen F, Zarivach R, Harms J, et al. Structural basis for the interaction of antibiotics with the peptidyl transferase centre in eubacteria. *Nature.* 2001;413(6858):814-821.

183. Diekema DI, Jones RN. Oxazolidinones: a review. *Drugs.* 2000;59(1):7-16.

184. Mlynarczyk-Bonikowska B, Kowalewski C, Krolak-Ulinska A, Marusza W. Molecular Mechanisms of Drug Resistance in *Staphylococcus aureus*. *Int J Mol Sci.* 2022;23(15).

185. McInnes RS, McCallum GE, Lamberte LE, van Schaik W. Horizontal transfer of antibiotic resistance genes in the human gut microbiome. *Curr Opin Microbiol.* 2020;53:35-43.

186. Johnston C, Martin B, Fichant G, Polard P, Claverys JP. Bacterial transformation: distribution, shared mechanisms and divergent control. *Nature reviews. Microbiology.* 2014;12(3):181-196.

187. Cabezón E, Ripoll-Rozada J, Peña A, de la Cruz F, Arechaga I. Towards an integrated model of bacterial conjugation. *FEMS Microbiol Rev.* 2015;39(1):81-95.

188. Tran TT, Munita JM, Arias CA. Mechanisms of drug resistance: daptomycin resistance. *Ann N Y Acad Sci.* 2015;1354:32-53.

189. Munita JM, Arias CA. Mechanisms of Antibiotic Resistance. *Microbiol Spectr.* 2016;4(2).

190. Ross JI, Eady EA, Cove JH, Cunliffe WJ. 16S rRNA mutation associated with tetracycline resistance in a gram-positive bacterium. *Antimicrob Agents Chemother.* 1998;42(7):1702-1705.

191. Rodriguez de Evgrafov M, Gumpert H, Munck C, Thomsen TT, Sommer MOA. Collateral Resistance and Sensitivity Modulate Evolution of High-Level Resistance to Drug Combination Treatment in *Staphylococcus aureus*. *Molecular Biology and Evolution.* 2015;32(5):1175-1185.

192. Roberts MC. Mechanism of Resistance for Characterized tet and otr Genes. 2021; http://faculty.washington.edu/marilynr/tetweb1.pdf. Accessed 07/09/2022.

193. Roberts MC. Tetracycline resistance determinants: mechanisms of action, regulation of expression, genetic mobility, and distribution. *FEMS Microbiol Rev.* 1996;19(1):1-24.

194. McArthur AG, Waglechner N, Nizam F, et al. The comprehensive antibiotic resistance database. *Antimicrob Agents Chemother.* 2013;57(7):3348-3357.

195. Dönhöfer A, Franckenberg S, Wickles S, Berninghausen O, Beckmann R, Wilson DN. Structural basis for TetM-mediated tetracycline resistance. *Proc Natl Acad Sci U S A.* Vol 1092012:16900-16905.

196. Warburton PJ, Amodeo N, Roberts AP. Mosaic tetracycline resistance genes encoding ribosomal protection proteins. *J Antimicrob Chemother.* Vol 712016:3333-3339.

197. Volkers G, Palm GJ, Weiss MS, Wright GD, Hinrichs W. Structural basis for a new tetracycline resistance mechanism relying on the TetX monooxygenase. *FEBS Lett.* 2011;585(7):1061-1066.

198. Saber H, Jasni AS, Jamaluddin T, Ibrahim R. A Review of Staphylococcal Cassette Chromosome mec (SCCmec) Types in Coagulase-Negative Staphylococci (CoNS) Species. *Malays J Med Sci.* 2017;24(5):7-18.

199. Bilyk BL, Panchal VV, Tinajero-Trejo M, Hobbs JK, Foster SJ. An Interplay of Multiple Positive and Negative Factors Governs Methicillin Resistance in *Staphylococcus aureus*. *Microbiol Mol Biol Rev.* 2022;86(2):e0015921.

200. Wang H, Gill CJ, Lee SH, et al. Discovery of wall teichoic acid inhibitors as potential anti-MRSA β-lactam combination agents. *Chem Biol.* 2013;20(2):272-284.

201. Lee SH, Jarantow LW, Wang H, et al. Antagonism of chemical genetic interaction networks resensitize MRSA to β-lactam antibiotics. *Chem Biol.* 2011;18(11):1379-1389.

202. Bæk KT, Gründling A, Mogensen RG, et al. β-Lactam resistance in methicillin-resistant *Staphylococcus aureus* USA300 is increased by inactivation of the ClpXP protease. *Antimicrob Agents Chemother.* 2014;58(8):4593-4603.

203. Mwangi MM, Kim C, Chung M, et al. Whole-genome sequencing reveals a link between β-lactam resistance and synthetases of the alarmone (p)ppGpp in *Staphylococcus aureus*. *Microb Drug Resist.* 2013;19(3):153-159.

204. Panchal VV, Griffiths C, Mosaei H, et al. Evolving MRSA: High-level β-lactam resistance in *Staphylococcus aureus* is associated with RNA Polymerase alterations and fine tuning of gene expression. *PLoS pathogens.* 2020;16(7):e1008672.

205. Kim C, Mwangi M, Chung M, Milheiriço C, de Lencastre H, Tomasz A. The mechanism of heterogeneous beta-lactam resistance in MRSA: key role of the stringent stress response. *PLoS One.* 2013;8(12):e82814.

206. Wright GD. Antibiotic Adjuvants: Rescuing Antibiotics from Resistance. *Trends in microbiology.* 2016;24(11):862-871.

207. Bush K, Bradford PA. β-Lactams and β-Lactamase Inhibitors: An Overview. *Cold Spring Harb Perspect Med.* 2016;6(8).

208. Senior K. FDA approves first drug in new class of antibiotics. *Lancet.* Vol 355. England2000:1523.

209. Sauermann R, Rothenburger M, Graninger W, Joukhadar C. Daptomycin: a review 4 years after first approval. *Pharmacology.* 2008;81(2):79-91.

210. Mitcheltree MJ, Pisipati A, Syroegin EA, et al. A synthetic antibiotic class overcoming bacterial multidrug resistance. *Nature.* 2021;599(7885):507-512.

211. Brodiazhenko T, Turnbull KJ, Wu KJY, et al. Synthetic oxepanoprolinamide iboxamycin is active against *Listeria monocytogenes* despite the intrinsic resistance mediated by VgaL/Lmo0919 ABCF ATPase. *JAC Antimicrob Resist.* 2022;4(3):dlac061.

212. Rodvold KA. Clinical pharmacokinetics of clarithromycin. *Clin Pharmacokinet.* 1999;37(5):385-398.

213. Nguyen F, Starosta AL, Arenz S, Sohmen D, Dönhöfer A, Wilson DN. Tetracycline antibiotics and resistance mechanisms. *Biol Chem.* 2014;395(5):559-575.

214. Sum PE, Lee VJ, Testa RT, et al. Glycylcyclines. 1. A new generation of potent antibacterial agents through modification of 9-aminotetracyclines. *J Med Chem.* 1994;37(1):184-188.

215. Neu HC. beta-Lactam antibiotics: structural relationships affecting in vitro activity and pharmacologic properties. *Rev Infect Dis.* 1986;8 Suppl 3:S237-259.

216. Neu HC. Tobramycin: an overview. *J Infect Dis.* 1976;134 Suppl:S3-19.

217. Bleul L, Francois P, Wolz C. Two-Component Systems of *S. aureus*: Signaling and Sensing Mechanisms. *Genes (Basel).* 2021;13(1).

218. Fitzgerald JR. Evolution of *Staphylococcus aureus* during human colonization and infection. *Infection, genetics and evolution : journal of molecular epidemiology and evolutionary genetics in infectious diseases.* 2014;21:542-547.

219. Johannessen M, Sollid JE, Hanssen AM. Host- and microbe determinants that may influence the success of *S. aureus* colonization. *Front Cell Infect Microbiol.* 2012;2.

220. Masalha M, Borovok I, Schreiber R, Aharonowitz Y, Cohen G. Analysis of Transcription of the *Staphylococcus aureus* Aerobic Class Ib and Anaerobic Class III Ribonucleotide Reductase Genes in Response to Oxygen. *J Bacteriol.* Vol 1832001:7260-7272.

221. Geiger T, Goerke C, Mainiero M, Kraus D, Wolz C. The virulence regulator Sae of *Staphylococcus aureus*: promoter activities and response to phagocytosis-related signals. *Journal of bacteriology.* 2008;190(10):3419-3428.

222. Liu Q, Yeo WS, Bae T. The SaeRS Two-Component System of *Staphylococcus aureus*. *Genes (Basel).* 2016;7(10).

223. Wieneke MK, Dach F, Neumann C, et al. Association of Diverse *Staphylococcus aureus* Populations with *Pseudomonas aeruginosa* Coinfection and Inflammation in Cystic Fibrosis Airway Infection. *mSphere.* 2021;6(3):e0035821.

224. Montgomery ST, Mall MA, Kicic A, Stick SM. Hypoxia and sterile inflammation in cystic fibrosis airways: mechanisms and potential therapies. 2017.

225. Gangell C, Gard S, Douglas T, et al. Inflammatory responses to individual microorganisms in the lungs of children with cystic fibrosis. *Clinical infectious diseases : an official publication of the Infectious Diseases Society of America.* 2011;53(5):425-432.

226. Limoli DH, Yang J, Khansaheb MK, et al. *Staphylococcus aureus* and *Pseudomonas aeruginosa* co-infection is associated with cystic fibrosis-related diabetes and poor clinical outcomes. *European journal of clinical microbiology & infectious diseases : official publication of the European Society of Clinical Microbiology.* 2016;35(6):947-953.

227. Tuchscherr L, Kreis CA, Hoerr V, et al. *Staphylococcus aureus* develops increased resistance to antibiotics by forming dynamic small colony variants during chronic osteomyelitis. *The Journal of antimicrobial chemotherapy.* 2016;71(2):438-448.

228. Lattar SM, Tuchscherr LPN, Caccuri RL, et al. Capsule Expression and Genotypic Differences among *Staphylococcus aureus* Isolates from Patients with Chronic or Acute Osteomyelitis ▿ . *Infect Immun.* Vol 772009:1968-1975.

229. Goerke C, Gressinger M, Endler K, et al. High phenotypic diversity in infecting but not in colonizing *Staphylococcus aureus* populations. *Environmental microbiology.* 2007;9(12):3134-3142.

230. McAdam PR, Holmes A, Templeton KE, Fitzgerald JR. Adaptive evolution of *Staphylococcus aureus* during chronic endobronchial infection of a cystic fibrosis patient. *PLoS One.* 2011;6(9):e24301.

231. Yachi S, Loreau M. Biodiversity and ecosystem productivity in a fluctuating environment: the insurance hypothesis. *Proceedings of the National Academy of Sciences of the United States of America.* 1999;96(4):1463-1468.

232. McVicker G, Prajsnar TK, Williams A, et al. Clonal Expansion during *Staphylococcus aureus* Infection Dynamics Reveals the Effect of Antibiotic Intervention. *PLoS Pathog.* Vol 102014.

233. Gardete S, Tomasz A. Mechanisms of vancomycin resistance in *Staphylococcus aureus*. *J Clin Invest.* Vol 1242014:2836-2840.

234. Mwangi MM, Wu SW, Zhou Y, et al. Tracking the in vivo evolution of multidrug resistance in *Staphylococcus aureus* by whole-genome sequencing. *Proc Natl Acad Sci U S A.* Vol 1042007:9451-9456.

235. Sievert DM, Rudrik JT, Patel JB, McDonald LC, Wilkins MJ, Hageman JC. Vancomycin-resistant *Staphylococcus aureus* in the United States, 2002-2006. *Clinical infectious diseases : an official publication of the Infectious Diseases Society of America.* 2008;46(5):668-674.

236. Weigel LM, Clewell DB, Gill SR, et al. Genetic Analysis of a High-Level Vancomycin-Resistant Isolate of *Staphylococcus aureus*. 2003.

237. Jamrozy DM, Harris SR, Mohamed N, et al. Pan-genomic perspective on the evolution of the *Staphylococcus aureus* USA300 epidemic. *Microb Genom.* 2016;2(5):e000058.

238. Chen CJ, Huang YC, Shie SS. Evolution of Multi-Resistance to Vancomycin, Daptomycin, and Linezolid in Methicillin-Resistant *Staphylococcus aureus* Causing Persistent Bacteremia. *Front Microbiol.* 2020;11:1414.

239. Aiba Y, Katayama Y, Hishinuma T, Murakami-Kuroda H, Cui L, Hiramatsu K. Mutation of RNA polymerase β-subunit gene promotes heterogeneous-to-homogeneous conversion of β-lactam resistance in methicillin-resistant *Staphylococcus aureus*. *Antimicrob Agents Chemother.* 2013;57(10):4861-4871.

240. Villanueva M, Jousselin A, Baek KT, et al. Rifampin Resistance rpoB Alleles or Multicopy Thioredoxin/Thioredoxin Reductase Suppresses the Lethality of Disruption of the Global Stress Regulator *spx* in *Staphylococcus aureus*. *Journal of bacteriology.* 2016;198(19):2719-2731.

241. Thitiananpakorn K, Aiba Y, Tan X-E, et al. Association of *mprF* mutations with cross-resistance to daptomycin and vancomycin in methicillin-resistant *Staphylococcus aureus* (MRSA). *Scientific Reports.* 2020;10(1):16107.

242. Andrä J, Goldmann T, Ernst CM, Peschel A, Gutsmann T. Multiple peptide resistance factor (MprF)-mediated Resistance of *Staphylococcus aureus* against antimicrobial peptides coincides with a modulated peptide interaction with artificial membranes comprising lysyl-phosphatidylglycerol. *The Journal of biological chemistry.* 2011;286(21):18692-18700.

243. Kim S, Lieberman TD, Kishony R. Alternating antibiotic treatments constrain evolutionary paths to multidrug resistance. *Proceedings of the National Academy of Sciences of the United States of America.* 2014;111(40):14494-14499.

244. Silva RF, Mendonça SCM, Carvalho LM, et al. Pervasive Sign Epistasis between Conjugative Plasmids and Drug-Resistance Chromosomal Mutations. *PLOS Genetics.* 2011;7(7):e1002181.

245. Hall JPJ, Wright RCT, Harrison E, et al. Plasmid fitness costs are caused by specific genetic conflicts enabling resolution by compensatory mutation. *PLoS Biol.* 2021;19(10):e3001225.

246. Levin BR, Perrot V, Walker N. Compensatory mutations, antibiotic resistance and the population genetics of adaptive evolution in bacteria. *Genetics.* 2000;154(3):985-997.

247. Björkman J, Nagaev I, Berg OG, Hughes D, Andersson DI. Effects of environment on compensatory mutations to ameliorate costs of antibiotic resistance. *Science.* 2000;287(5457):1479-1482.

248. Pacheco JO, Alvarez-Ortega C, Rico MA, Martínez JL. Metabolic Compensation of Fitness Costs Is a General Outcome for Antibiotic-Resistant *Pseudomonas aeruginosa* Mutants Overexpressing Efflux Pumps. *mBio.* 2017;8(4):e00500-00517.

249. Blount ZD, Barrick JE, Davidson CJ, Lenski RE. Genomic analysis of a key innovation in an experimental *Escherichia coli* population. *Nature.* 2012;489(7417):513-518.

250. Guerrini V, Subbian S, Santucci P, Canaan S, Gennaro ML, Pozzi G. Experimental Evolution of *Mycobacterium tuberculosis* in Human Macrophages Results in Low-Frequency Mutations Not Associated with Selective Advantage. *PLOS ONE.* 2016;11(12):e0167989.

251. Ramiro RS, Costa H, Gordo I. Macrophage adaptation leads to parallel evolution of genetically diverse *Escherichia coli* small-colony variants with increased fitness in vivo and antibiotic collateral sensitivity. *Evol Appl.* 2016;9(8):994-1004.

252. Azevedo M, Sousa A, Moura de Sousa J, Thompson JA, Proença JT, Gordo I. Trade-Offs of *Escherichia coli* Adaptation to an Intracellular Lifestyle in Macrophages. *PLoS One.* 2016;11(1):e0146123.

253. Horsburgh MJ, Aish JL, White IJ, Shaw L, Lithgow JK, Foster SJ. sigmaB modulates virulence determinant expression and stress resistance: characterization of a functional *rsbU* strain derived from *Staphylococcus aureus* 8325-4. *Journal of bacteriology.* 2002;184(19):5457-5467.

254. Fey PD, Endres JL, Yajjala VK, et al. A Genetic Resource for Rapid and Comprehensive Phenotype Screening of Nonessential *Staphylococcus aureus* Genes. *mBio.* Vol 42013.

255. Mainiero M, Goerke C, Geiger T, Gonser C, Herbert S, Wolz C. Differential Target Gene Activation by the *Staphylococcus aureus* Two-Component System saeRS. 2010.

256. Jeong H, Kim HJ, Lee SJ. Complete Genome Sequence of *Escherichia coli* Strain BL21. *Genome Announc.* 2015;3(2).

257. Krašovec R, Richards H, Gomez G, Gifford DR, Mazoyer A, Knight CG. Measuring Microbial Mutation Rates with the Fluctuation Assay. *J Vis Exp.* 2019(153).

258. Mazoyer A, Drouilhet R, Despreaux S, Ycart B. flan: An R Package for Inference on Mutation Models. *R Journal.* 2017;9(1):334-351.

259. EUCAST. Clinical breakpoints for bacteria. 2019; http://www.eucast.org/clinical_breakpoints/. Accessed 08/07/19.

260. Keir HR, Long MB, Abo-Leyah H, et al. Dipeptidyl peptidase-1 inhibition in patients hospitalised with COVID-19: a multicentre, double-blind, randomised, parallel-group, placebo-controlled trial. *The Lancet Respiratory Medicine.* 2022.

261. Hull RC, Huang JT, Barton AK, et al. Sputum Proteomics in non-Tuberculous Mycobacterial Lung Disease. *Chest.* 2021.

262. Haslett C, Guthrie LA, Kopaniak MM, Johnston RB, Henson PM. Modulation of multiple neutrophil functions by preparative methods or trace concentrations of bacterial lipopolysaccharide. *Am J Pathol.* 1985;119(1):101-110.

263. Blanter M, Cambier S, De Bondt M, et al. Method Matters: Effect of Purification Technology on Neutrophil Phenotype and Function. *Front Immunol.* 2022;13:820058.

264. Jolliffe IT, Cadima J. Principal component analysis: a review and recent developments. *Philos Trans A Math Phys Eng Sci.* 2016;374(2065):20150202.

265. Deatherage DE, Barrick JE. Identification of mutations in laboratory-evolved microbes from next-generation sequencing data using breseq. *Methods in molecular biology (Clifton, N.J.).* 2014;1151:165-188.

266. Robinson JT, Thorvaldsdóttir H, Winckler W, et al. Integrative genomics viewer. *Nature Biotechnology.* 2011;29(1):24.

267. Guérillot R, Kostoulias X, Donovan L, et al. Unstable chromosome rearrangements in Staphylococcus aureus cause phenotype switching associated with persistent

infections. *Proceedings of the National Academy of Sciences of the United States of America.* 2019;116(40):20135-20140.

268. Bankevich A, Nurk S, Antipov D, et al. SPAdes: a new genome assembly algorithm and its applications to single-cell sequencing. *J Comput Biol.* 2012;19(5):455-477.

269. Li H, Durbin R. Fast and accurate short read alignment with Burrows-Wheeler transform. *Bioinformatics.* 2009;25(14):1754-1760.

270. Altschul SF, Gish W, Miller W, Myers EW, Lipman DJ. Basic local alignment search tool. *J Mol Biol.* 1990;215(3):403-410.

271. Kelley LA, Mezulis S, Yates CM, Wass MN, Sternberg MJ. The Phyre2 web portal for protein modeling, prediction and analysis. *Nat Protoc.* 2015;10(6):845-858.

272. Berman HM, Westbrook J, Feng Z, et al. The Protein Data Bank. *Nucleic Acids Res.* 2000;28(1):235-242.

273. The PyMOL Molecular Graphics System, Version 1.2r3pre, Schrödinger, LLC.

274. Vanden Broeck A, Lotz C, Ortiz J, Lamour V. Cryo-EM structure of the complete *E. coli* DNA gyrase nucleoprotein complex. *Nat Commun.* 2019;10(1):4935.

275. Kuznetsova A, Brockhoff PB, Christensen RHB. lmerTest Package: Tests in Linear Mixed Effects Models. *Journal of Statistical Software.* 2017;82(13):1-26.

276. Reygaert WC. An overview of the antimicrobial resistance mechanisms of bacteria. *AIMS Microbiol.* 2018;4(3):482-501.

277. Gullberg E, Cao S, Berg OG, et al. Selection of resistant bacteria at very low antibiotic concentrations. *PLoS pathogens.* 2011;7(7):e1002158.

278. Lyon BR, Skurray R. Antimicrobial resistance of *Staphylococcus aureus*: genetic basis. *Microbiol Rev.* 1987;51(1):88-134.

279. Leibovici L, Shraga I, Andreassen S. How do you choose antibiotic treatment? *Bmj.* 1999;318(7198):1614-1616.

280. Roope LSJ, Buchanan J, Morrell L, et al. Why do hospital prescribers continue antibiotics when it is safe to stop? Results of a choice experiment survey. *BMC Med.* 2020;18(1):196.

281. Sabat AJ, Tinelli M, Grundmann H, et al. Daptomycin Resistant *Staphylococcus aureus* Clinical Strain With Novel Non-synonymous Mutations in the *mprF* and *vraS* Genes: A New Insight Into Daptomycin Resistance. *Frontiers in Microbiology.* 2018;9.

282. Keynan Y, Rubinstein E. *Staphylococcus aureus* bacteremia, risk factors, complications, and management. *Critical care clinics.* 2013;29(3):547-562.

283. Shteinberg M, Elborn JS. Use of inhaled tobramycin in cystic fibrosis. *Advances in therapy.* 2015;32(1):1-9.

284. Camus L, Briaud P, Vandenesch F, Moreau K. How Bacterial Adaptation to Cystic Fibrosis Environment Shapes Interactions Between *Pseudomonas aeruginosa* and *Staphylococcus aureus*. *Front Microbiol.* 2021;12:617784.

285. Davidovich C, Bashan A, Yonath A. Structural basis for cross-resistance to ribosomal PTC antibiotics. *Proceedings of the National Academy of Sciences of the United States of America.* 2008;105(52):20665-20670.

286. Lázár V, Nagy I, Spohn R, et al. Genome-wide analysis captures the determinants of the antibiotic cross-resistance interaction network. *Nature Communications.* 2014;5(1):1-12.

287. Szybalski W, Bryson V. Genetic studies on microbial cross resistance to toxic agents. I. Cross resistance of *Escherichia coli* to fifteen antibiotics. *Journal of bacteriology.* 1952;64(4):489-499.

288. Blumenthal KG, Lu N, Zhang Y, Li Y, Walensky RP, Choi HK. Risk of meticillin resistant *Staphylococcus aureus* and *Clostridium difficile* in patients with a documented penicillin allergy: population based matched cohort study. *Bmj.* 2018;361:k2400.

289. McGhee CN, Anastas CN. Widespread ocular use of topical chloramphenicol: is there justifiable concern regarding idiosyncratic aplastic anaemia? *Br J Ophthalmol.* 1996;80(2):182-184.

290. Alcock BP, Raphenya AR, Lau TTY, et al. CARD 2020: antibiotic resistome surveillance with the comprehensive antibiotic resistance database. *Nucleic Acids Res.* 2020;48(D1):D517-d525.

291. The National Institute for Health and Care Excellence. Boils, carbuncles, and staphylococcal carriage. February 2022; https://cks.nice.org.uk/topics/boils-carbuncles-staphylococcal-carriage/, 13/07/22.

292. The National Institute for Health and Care Excellence. Chronic obstructive pulmonary disease (acute exacerbation): antimicrobial prescribing NICE guideline [NG114]. 05 December 2018; https://www.nice.org.uk/guidance/ng114. Accessed 14/12/21.

293. National Institute for Health and Care Excellence. Leg ulcer infection: antimicrobial prescribing. 11 February 2020; https://www.nice.org.uk/guidance/ng152/chapter/Recommendations#choice-of-antibiotic, 13/07/22.

294. National Institute for Health and Care Excellence. Dental abscess. January 2022; https://cks.nice.org.uk/topics/dental-abscess/.

295. Schmitz FJ, Sadurski R, Kray A, et al. Prevalence of macrolide-resistance genes in *Staphylococcus aureus* and *Enterococcus faecium* isolates from 24 European university hospitals. *J Antimicrob Chemother.* 2000;45(6):891-894.

296. Fyfe C, Grossman TH, Kerstein K, Sutcliffe J. Resistance to Macrolide Antibiotics in Public Health Pathogens. *Cold Spring Harb Perspect Med.* 2016;6(10).

297. National Institute for Health and Care Excellence. Complicated skin and soft-tissue infections caused by Gram-positive bacteria. https://bnf.nice.org.uk/drugs/daptomycin/#indications-and-dose. Accessed 14/07/22.

298. Dubrac S, Msadek T. Tearing down the wall: peptidoglycan metabolism and the WalK/WalR (YycG/YycF) essential two-component system. *Adv Exp Med Biol.* 2008;631:214-228.

299. National Institute for Health and Care Excellence. Cough (acute): antimicrobial prescribing. 07 February 2019; https://www.nice.org.uk/guidance/ng120/chapter/Recommendations, 13/07/22.

300. Grossman TH. Tetracycline Antibiotics and Resistance. *Cold Spring Harb Perspect Med.* 2016;6(4):a025387.

301. National Institute for Health and Care Excellence. Diabetic foot problems: prevention and management. 11 October 2019; https://www.nice.org.uk/guidance/ng19/chapter/Recommendations, 13/07/22.

302. Worthington RJ, Melander C. Overcoming resistance to β-lactam antibiotics. *J Org Chem.* 2013;78(9):4207-4213.

303. National Institute for Health and Care Excellence. Pneumonia (hospital-acquired): antimicrobial prescribing. 16 September 2019; https://www.nice.org.uk/guidance/ng139/chapter/Recommendations#choice-of-antibiotic, 13/07/22.

304. Stefani S, Bongiorno D, Mongelli G, Campanile F. Linezolid Resistance in Staphylococci. *Pharmaceuticals (Basel).* 2010;3(7):1988-2006.

305. Meka VG, Gold HS. Antimicrobial resistance to linezolid. *Clinical infectious diseases : an official publication of the Infectious Diseases Society of America.* 2004;39(7):1010-1015.

306. National Institute for Health and Care Excellence. Cystic fibrosis: diagnosis and management. 25 October 2017; https://www.nice.org.uk/guidance/ng78/chapter/Recommendations, 13/07/22.

307. Wistrand-Yuen E, Knopp M, Hjort K, Koskiniemi S, Berg OG, Andersson DI. Evolution of high-level resistance during low-level antibiotic exposure. *Nat Commun.* 2018;9(1):1599.

308. Scribner MR, Santos-Lopez A, Marshall CW, Deitrick C, Cooper VS. Parallel Evolution of Tobramycin Resistance across Species and Environments. *mBio.* 2020;11(3).

309. Wang G, Wilson TJ, Jiang Q, Taylor DE. Spontaneous mutations that confer antibiotic resistance in *Helicobacter pylori. Antimicrob Agents Chemother.* 2001;45(3):727-733.

310. Weisblum B. Erythromycin resistance by ribosome modification. *Antimicrob Agents Chemother.* 1995;39(3):577-585.

311. Canu A, Malbruny B, Coquemont M, Davies TA, Appelbaum PC, Leclercq R. Diversity of ribosomal mutations conferring resistance to macrolides, clindamycin, streptogramin, and telithromycin in *Streptococcus pneumoniae. Antimicrob Agents Chemother.* 2002;46(1):125-131.

312. Ban N, Nissen P, Hansen J, Moore PB, Steitz TA. The complete atomic structure of the large ribosomal subunit at 2.4 A resolution. *Science.* 2000;289(5481):905-920.

313. Prunier AL, Trong HN, Tande D, Segond C, Leclercq R. Mutation of L4 ribosomal protein conferring unusual macrolide resistance in two independent clinical isolates of *Staphylococcus aureus*. *Microb Drug Resist.* 2005;11(1):18-20.

314. Malbruny B, Canu A, Bozdogan B, et al. Resistance to quinupristin-dalfopristin due to mutation of L22 ribosomal protein in *Staphylococcus aureus*. *Antimicrob Agents Chemother.* 2002;46(7):2200-2207.

315. Binh TT, Shiota S, Suzuki R, et al. Discovery of novel mutations for clarithromycin resistance in *Helicobacter pylori* by using next-generation sequencing. *The Journal of antimicrobial chemotherapy.* 2014;69(7):1796-1803.

316. Zaman S, Fitzpatrick M, Lindahl L, Zengel J. Novel mutations in ribosomal proteins L4 and L22 that confer erythromycin resistance in *Escherichia coli. Molecular microbiology.* 2007;66(4):1039-1050.

317. Flamm RK, Mendes RE, Hogan PA, Streit JM, Ross JE, Jones RN. Linezolid Surveillance Results for the United States (LEADER Surveillance Program 2014). *Antimicrob Agents Chemother.* 2016;60(4):2273-2280.

318. Zurenko GE, Yagi BH, Schaadt RD, et al. In vitro activities of U-100592 and U-100766, novel oxazolidinone antibacterial agents. *Antimicrob Agents Chemother.* 1996;40(4):839-845.

319. Sadowy E. Linezolid resistance genes and genetic elements enhancing their dissemination in enterococci and streptococci. *Plasmid.* 2018;99:89-98.

320. Pfaller MA, Mendes RE, Streit JM, Hogan PA, Flamm RK. Five-Year Summary of In Vitro Activity and Resistance Mechanisms of Linezolid against Clinically Important Gram-Positive Cocci in the United States from the LEADER Surveillance Program (2011 to 2015). *Antimicrob Agents Chemother.* 2017;61(7).

321. Copsey-Mawer S, Hughes H, Scotford S, et al. UK Bacteroides species surveillance survey: Change in antimicrobial resistance over 16 years (2000–2016). *Anaerobe.* 2021;72:102447.

322. Huber S, Knoll MA, Berktold M, et al. Genomic and Phenotypic Analysis of Linezolid-Resistant *Staphylococcus epidermidis* in a Tertiary Hospital in Innsbruck, Austria. *Microorganisms.* 2021;9(5).

323. Chopra I, Roberts M. Tetracycline antibiotics: mode of action, applications, molecular biology, and epidemiology of bacterial resistance. *Microbiol Mol Biol Rev.* 2001;65(2):232-260 ; second page, table of contents.

324. Narendrakumar L, Chandrika SK, Thomas S. Adaptive laboratory evolution of *Vibrio cholerae* to doxycycline associated with spontaneous mutation. *Int J Antimicrob Agents.* 2020;56(3):106097.

325. Yang Y, Mi J, Liang J, et al. Changes in the Carbon Metabolism of *Escherichia coli* During the Evolution of Doxycycline Resistance. *Front Microbiol.* 2019;10:2506.

326. Bolard A, Plésiat P, Jeannot K. Mutations in Gene fusA1 as a Novel Mechanism of Aminoglycoside Resistance in Clinical Strains of *Pseudomonas aeruginosa. Antimicrob Agents Chemother.* 2018;62(2).

327. Roch M, Gagetti P, Davis J, et al. Daptomycin Resistance in Clinical MRSA Strains Is Associated with a High Biological Fitness Cost. *Front Microbiol.* 2017;8:2303.

328. Friedman L, Alder JD, Silverman JA. Genetic changes that correlate with reduced susceptibility to daptomycin in *Staphylococcus aureus*. *Antimicrob Agents Chemother.* 2006;50(6):2137-2145.

329. Mishra NN, Bayer AS, Weidenmaier C, et al. Phenotypic and genotypic characterization of daptomycin-resistant methicillin-resistant Staphylococcus aureus strains: relative roles of *mprF* and *dlt* operons. *PLoS One.* 2014;9(9):e107426.

330. Howden BP, McEvoy CR, Allen DL, et al. Evolution of multidrug resistance during *Staphylococcus aureus* infection involves mutation of the essential two component regulator WalKR. *PLoS pathogens.* 2011;7(11):e1002359.

331. Cui L, Isii T, Fukuda M, et al. An RpoB mutation confers dual heteroresistance to daptomycin and vancomycin in *Staphylococcus aureus. Antimicrob Agents Chemother.* 2010;54(12):5222-5233.

332. Bæk KT, Thøgersen L, Mogenssen RG, et al. Stepwise decrease in daptomycin susceptibility in clinical *Staphylococcus aureus* isolates associated with an initial mutation in *rpoB* and a compensatory inactivation of the *clpX* gene. *Antimicrob Agents Chemother.* 2015;59(11):6983-6991.

333. El Haddad L, Hanson BM, Arias CA, et al. Emergence and Transmission of Daptomycin and Vancomycin-Resistant *Enterococci* Between Patients and Hospital Rooms. *Clinical*

infectious diseases : an official publication of the Infectious Diseases Society of America. 2021;73(12):2306-2313.

334. Menezes MNd, de Marco BA, Fiorentino FAM, Zimmermann A, Kogawa AC, Salgado HRN. Flucloxacillin: A Review of Characteristics, Properties and Analytical Methods. *Critical Reviews in Analytical Chemistry.* 2018:1-11.

335. Espedido BA, Gosbell IB. Chromosomal mutations involved in antibiotic resistance in *Staphylococcus aureus*. *Front Biosci (Schol Ed).* 2012;4(3):900-915.

336. Cazer CL, Westblade LF, Simon MS, et al. Analysis of Multidrug Resistance in *Staphylococcus aureus* with a Machine Learning-Generated Antibiogram. *Antimicrobial Agents and Chemotherapy.* 2021;65(4):e02132-02120.

337. Costa SS, Viveiros M, Amaral L, Couto I. Multidrug Efflux Pumps in *Staphylococcus aureus*: an Update. *Open Microbiol J.* 2013;7:59-71.

338. Lázár V, Pal Singh G, Spohn R, et al. Bacterial evolution of antibiotic hypersensitivity. *Molecular Systems Biology.* 2013;9(1).

339. Imamovic L, Sommer MO. Use of collateral sensitivity networks to design drug cycling protocols that avoid resistance development. *Science translational medicine.* 2013;5(204):204ra132.

340. Beckley AM, Wright ES. Identification of antibiotic pairs that evade concurrent resistance via a retrospective analysis of antimicrobial susceptibility test results. *Lancet Microbe.* 2021;2(10):e545-e554.

341. Rodriguez de Evgrafov MC, Faza M, Asimakopoulos K, Sommer MOA. Systematic Investigation of Resistance Evolution to Common Antibiotics Reveals Conserved Collateral Responses across Common Human Pathogens. *Antimicrob Agents Chemother.* 2020;65(1).

342. Lan S, Li Z, Su A, et al. Study on the mechanisms of the cross-resistance to TET, PIP, and GEN in *Staphylococcus aureus* mediated by the Rhizoma Coptidis extracts. *The Journal of Antibiotics.* 2021;74(5):330-336.

343. Nicolae Dopcea G, Dopcea I, Nanu AE, Diguţă CF, Matei F. Resistance and cross-resistance in *Staphylococcus spp.* strains following prolonged exposure to different antiseptics. *J Glob Antimicrob Resist.* 2020;21:399-404.

344. Desai SK, Kenney LJ. Switching Lifestyles Is an in vivo Adaptive Strategy of Bacterial Pathogens. *Front Cell Infect Microbiol.* 2019;9:421.

345. Sendi P, Rohrbach M, Graber P, Frei R, Ochsner PE, Zimmerli W. *Staphylococcus aureus* small colony variants in prosthetic joint infection. *Clinical infectious diseases : an official publication of the Infectious Diseases Society of America.* 2006;43(8):961-967.

346. Massey RC, Buckling A, Peacock SJ. Phenotypic switching of antibiotic resistance circumvents permanent costs in *Staphylococcus aureus*. *Curr Biol.* 2001;11(22):1810-1814.

347. Edwards AM. Phenotype switching is a natural consequence of *Staphylococcus aureus* replication. *Journal of bacteriology.* 2012;194(19):5404-5412.

348. Chuard C, Vaudaux PE, Proctor RA, Lew DP. Decreased susceptibility to antibiotic killing of a stable small colony variant of *Staphylococcus aureus* in fluid phase and on fibronectin-coated surfaces. *The Journal of antimicrobial chemotherapy.* 1997;39(5):603-608.

349. Foster PL. Methods for determining spontaneous mutation rates. *Methods Enzymol.* 2006;409:195-213.

350. Myers JA, Curtis BS, Curtis WR. Improving accuracy of cell and chromophore concentration measurements using optical density. *BMC Biophys.* 2013;6(1):4.

351. Melnyk AHW, Alex. Kassen, Rees. The fitness costs of antibiotic resistance mutations. 2014.

352. Ender M, McCallum N, Adhikari R, Berger-Bächi B. Fitness cost of *SCCmec* and methicillin resistance levels in *Staphylococcus aureus*. *Antimicrob Agents Chemother.* 2004;48(6):2295-2297.

353. Lenski RE. Experimental evolution and the dynamics of adaptation and genome evolution in microbial populations. *Isme j.* 2017;11(10):2181-2194.

354. Lizcano A, Sanchez CJ, Orihuela CJ. A role for glycosylated serine-rich repeat proteins in gram-positive bacterial pathogenesis. *Mol Oral Microbiol.* 2012;27(4):257-269.

355. Arévalo MA, Tejedor F, Polo F, Ballesta JP. Protein components of the erythromycin binding site in bacterial ribosomes. *The Journal of biological chemistry.* 1988;263(1):58-63.

356. Chittum HS, Champney WS. Ribosomal protein gene sequence changes in erythromycin-resistant mutants of *Escherichia coli. Journal of bacteriology.* 1994;176(20):6192-6198.

357. Han D, Liu Y, Li J, et al. Twenty-seven-nucleotide repeat insertion in the *rplV* gene confers specific resistance to macrolide antibiotics in *Staphylococcus aureus*. *Oncotarget.* 2018;9(40):26086-26095.

358. Tanaka Y, Tsujimura A, Fujita N, Isono S, Isono K. Cloning and analysis of an *Escherichia coli* operon containing the *rpmF* gene for ribosomal protein L32 and the gene for a 30-kilodalton protein. *Journal of bacteriology.* 1989;171(10):5707-5712.

359. Swaney SM, Aoki H, Ganoza MC, Shinabarger DL. The oxazolidinone linezolid inhibits initiation of protein synthesis in bacteria. *Antimicrob Agents Chemother.* 1998;42(12):3251-3255.

360. Hashemian SMR, Farhadi T, Ganjparvar M. Linezolid: a review of its properties, function, and use in critical care. *Drug Des Devel Ther.* 2018;12:1759-1767.

361. Long KS, Vester B. Resistance to linezolid caused by modifications at its binding site on the ribosome. *Antimicrob Agents Chemother.* 2012;56(2):603-612.

362. Yen P, Papin JA. History of antibiotic adaptation influences microbial evolutionary dynamics during subsequent treatment. *PLoS Biol.* 2017;15(8):e2001586.

363. Pinho MG, Errington J. Dispersed mode of *Staphylococcus aureus* cell wall synthesis in the absence of the division machinery. *Molecular microbiology.* 2003;50(3):871-881.

364. Ferrer-González E, Huh H, Al-Tameemi HM, Boyd JM, Lee SH, Pilch DS. Impact of FtsZ Inhibition on the Localization of the Penicillin Binding Proteins in Methicillin-Resistant Staphylococcus aureus. *Journal of bacteriology.* 2021;203(16):e0020421.

365. Hikichi M, Nagao M, Murase K, et al. Complete Genome Sequences of Eight Methicillin-Resistant *Staphylococcus aureus* Strains Isolated from Patients in Japan. *Microbiol Resour Announc.* 2019;8(47).

366. Fernández L, Breidenstein EB, Song D, Hancock RE. Role of intracellular proteases in the antibiotic resistance, motility, and biofilm formation of *Pseudomonas aeruginosa. Antimicrob Agents Chemother.* 2012;56(2):1128-1132.

367. Zou L, Evans CR, Do VD, Losefsky QP, Ngo DQ, McGillivray SM. Loss of the ClpXP Protease Leads to Decreased Resistance to Cell-Envelope Targeting Antimicrobials in Bacillus anthracis Sterne. *Front Microbiol.* 2021;12:719548.

368. Luo Y, Helmann JD. Analysis of the role of Bacillus subtilis σ(M) in β-lactam resistance reveals an essential role for c-di-AMP in peptidoglycan homeostasis. *Molecular microbiology.* 2012;83(3):623-639.

369. Zhu Y, Pham TH, Nhiep TH, et al. Cyclic-di-AMP synthesis by the diadenylate cyclase CdaA is modulated by the peptidoglycan biosynthesis enzyme GlmM in Lactococcus lactis. *Molecular microbiology.* 2016;99(6):1015-1027.

370. Gottesman S, Clark WP, de Crecy-Lagard V, Maurizi MR. ClpX, an alternative subunit for the ATP-dependent Clp protease of *Escherichia coli.* Sequence and in vivo activities. *The Journal of biological chemistry.* 1993;268(30):22618-22626.

371. Gottesman S, Maurizi MR. Regulation by proteolysis: energy-dependent proteases and their targets. *Microbiol Rev.* 1992;56(4):592-621.

372. Poirier R. Comparative study of clarithromycin and roxithromycin in the treatment of community-acquired pneumonia. *The Journal of antimicrobial chemotherapy.* 1991;27 Suppl A:109-116.

373. Rahimi F. Characterization of Resistance to Aminoglycosides in Methicillin-Resistant *Staphylococcus aureus* Strains Isolated From a Tertiary Care Hospital in Tehran, Iran. *Jundishapur J Microbiol.* 2016;9(1):e29237.

374. Ida T, Okamoto R, Shimauchi C, Okubo T, Kuga A, Inoue M. Identification of aminoglycoside-modifying enzymes by susceptibility testing: epidemiology of methicillin-resistant *Staphylococcus aureus* in Japan. *J Clin Microbiol.* 2001;39(9):3115-3121.

375. Arii K, Kawada-Matsuo M, Oogai Y, Noguchi K, Komatsuzawa H. Single mutations in BraRS confer high resistance against nisin A in *Staphylococcus aureus*. *Microbiologyopen.* 2019;8(11):e791.

376. Yao W, Xu G, Li D, et al. *Staphylococcus aureus* with an erm-mediated constitutive macrolide-lincosamide-streptogramin B resistance phenotype has reduced susceptibility to the new ketolide, solithromycin. *BMC Infect Dis.* 2019;19(1):175.

377. Baquero F. Low-level antibacterial resistance: a gateway to clinical resistance. *Drug Resist Updat.* 2001;4(2):93-105.

378. Händel N, Schuurmans JM, Feng Y, Brul S, ter Kuile BH. Interaction between mutations and regulation of gene expression during development of de novo antibiotic resistance. *Antimicrob Agents Chemother.* 2014;58(8):4371-4379.

379. Barrick JE, Yu DS, Yoon SH, et al. Genome evolution and adaptation in a long-term experiment with *Escherichia coli*. *Nature.* 2009;461(7268):1243-1247.

380. Chen W, He C, Yang H, et al. Prevalence and molecular characterization of methicillin-resistant *Staphylococcus aureus* with mupirocin, fusidic acid and/or retapamulin resistance. *BMC microbiology.* 2020;20(1):183.

381. Chen Y, Koripella RK, Sanyal S, Selmer M. *Staphylococcus aureus* elongation factor G--structure and analysis of a target for fusidic acid. *The FEBS journal.* 2010;277(18):3789-3803.

382. Goldstein F. The potential clinical impact of low-level antibiotic resistance in *Staphylococcus aureus. The Journal of antimicrobial chemotherapy.* 2007;59(1):1-4.

383. Gomez JE, Kaufmann-Malaga BB, Wivagg CN, et al. Ribosomal mutations promote the evolution of antibiotic resistance in a multidrug environment. *Elife.* 2017;6.

384. Novak R, Henriques B, Charpentier E, Normark S, Tuomanen E. Emergence of vancomycin tolerance in *Streptococcus pneumoniae*. *Nature.* 1999;399(6736):590-593.

385. Markham PN, Neyfakh AA. Inhibition of the multidrug transporter NorA prevents emergence of norfloxacin resistance in *Staphylococcus aureus. Antimicrob Agents Chemother.* 1996;40(11):2673-2674.

386. Baquero F, Negri MC. Selective compartments for resistant microorganisms in antibiotic gradients. *Bioessays.* 1997;19(8):731-736.

387. Polianciuc SI, Gurzău AE, Kiss B, Ştefan MG, Loghin F. Antibiotics in the environment: causes and consequences. *Med Pharm Rep.* 2020;93(3):231-240.

388. Toprak E, Veres A, Michel JB, Chait R, Hartl DL, Kishony R. Evolutionary paths to antibiotic resistance under dynamically sustained drug selection. *Nat Genet.* 2011;44(1):101-105.

389. Qodrati M, SeyedAlinaghi S, Dehghan Manshadi SA, Abdollahi A, Dadras O. Antimicrobial susceptibility testing of *Staphylococcus aureus* isolates from patients at a tertiary hospital in Tehran, Iran, 2018-2019. *Eur J Med Res.* 2022;27(1):152.

390. McGillivray SM, Tran DN, Ramadoss NS, et al. Pharmacological inhibition of the ClpXP protease increases bacterial susceptibility to host cathelicidin antimicrobial peptides and cell envelope-active antibiotics. *Antimicrob Agents Chemother.* 2012;56(4):1854-1861.

391. Jensen C, Bæk KT, Gallay C, et al. The ClpX chaperone controls autolytic splitting of *Staphylococcus aureus* daughter cells, but is bypassed by β-lactam antibiotics or inhibitors of WTA biosynthesis. *PLoS pathogens.* 2019;15(9):e1008044.

392. Łeski TA, Tomasz A. Role of penicillin-binding protein 2 (PBP2) in the antibiotic susceptibility and cell wall cross-linking of *Staphylococcus aureus*: evidence for the cooperative functioning of PBP2, PBP4, and PBP2A. *Journal of bacteriology.* 2005;187(5):1815-1824.

393. Sauvage E, Kerff F, Terrak M, Ayala JA, Charlier P. The penicillin-binding proteins: structure and role in peptidoglycan biosynthesis. *FEMS Microbiol Rev.* 2008;32(2):234-258.

394. Pinho MG, Filipe SR, de Lencastre H, Tomasz A. Complementation of the essential peptidoglycan transpeptidase function of penicillin-binding protein 2 (PBP2) by the drug resistance protein PBP2A in *Staphylococcus aureus*. *Journal of bacteriology.* 2001;183(22):6525-6531.

395. Hackbarth CJ, Kocagoz T, Kocagoz S, Chambers HF. Point mutations in *Staphylococcus aureus* PBP 2 gene affect penicillin-binding kinetics and are associated with resistance. *Antimicrob Agents Chemother.* 1995;39(1):103-106.

396. Kosowska K, Jacobs MR, Bajaksouzian S, Koeth L, Appelbaum PC. Alterations of penicillin-binding proteins 1A, 2X, and 2B in *Streptococcus pneumoniae* isolates for

which amoxicillin MICs are higher than penicillin MICs. *Antimicrob Agents Chemother.* 2004;48(10):4020-4022.

397. Brown MR, Collier PJ, Gilbert P. Influence of growth rate on susceptibility to antimicrobial agents: modification of the cell envelope and batch and continuous culture studies. *Antimicrob Agents Chemother.* 1990;34(9):1623-1628.

398. Greulich P, Scott M, Evans MR, Allen RJ. Growth-dependent bacterial susceptibility to ribosome-targeting antibiotics. *Mol Syst Biol.* 2015;11(3):796.

399. Long H, Miller SF, Strauss C, et al. Antibiotic treatment enhances the genome-wide mutation rate of target cells. *Proceedings of the National Academy of Sciences of the United States of America.* 2016;113(18):E2498-2505.

400. Ren L, Rahman MS, Humayun MZ. *Escherichia coli* cells exposed to streptomycin display a mutator phenotype. *Journal of bacteriology.* 1999;181(3):1043-1044.

401. Mamber SW, Kolek B, Brookshire KW, Bonner DP, Fung-Tomc J. Activity of quinolones in the Ames *Salmonella* TA102 mutagenicity test and other bacterial genotoxicity assays. *Antimicrob Agents Chemother.* 1993;37(2):213-217.

402. Händel N, Hoeksema M, Freijo Mata M, Brul S, ter Kuile BH. Effects of Stress, Reactive Oxygen Species, and the SOS Response on De Novo Acquisition of Antibiotic Resistance in *Escherichia coli. Antimicrob Agents Chemother.* 2015;60(3):1319-1327.

403. Hoeksema M, Brul S, Ter Kuile BH. Influence of Reactive Oxygen Species on De Novo Acquisition of Resistance to Bactericidal Antibiotics. *Antimicrob Agents Chemother.* 2018;62(6).

404. Kohanski MA, Dwyer DJ, Hayete B, Lawrence CA, Collins JJ. A common mechanism of cellular death induced by bactericidal antibiotics. *Cell.* 2007;130(5):797-810.

405. Martinez JL, Baquero F. Mutation frequencies and antibiotic resistance. *Antimicrob Agents Chemother.* 2000;44(7):1771-1777.

406. Zwep LB, Haakman Y, Duisters KLW, Meulman JJ, Liakopoulos A, van Hasselt JGC. Identification of antibiotic collateral sensitivity and resistance interactions in population surveillance data. *JAC-Antimicrobial Resistance.* 2021;3(4).

407. Theuretzbacher U, Gottwalt S, Beyer P, et al. Analysis of the clinical antibacterial and antituberculosis pipeline. *Lancet Infectious Diseases.* 2019;19(2):E40-E50.

408. Land AD, Hogan P, Fritz S, Levin PA. Phenotypic Variation Is Almost Entirely Independent of the Host-Pathogen Relationship in Clinical Isolates of S. aureus. *PLoS One.* 2015;10(6):e0129670.

409. van Duijn PJ, Verbrugghe W, Jorens PG, et al. The effects of antibiotic cycling and mixing on antibiotic resistance in intensive care units: a cluster-randomised crossover trial. *Lancet Infect Dis.* 2018;18(4):401-409.

410. Chua K, Laurent F, Coombs G, Grayson ML, Howden BP. Antimicrobial resistance: Not community-associated methicillin-resistant *Staphylococcus aureus* (CA-MRSA)! A clinician's guide to community MRSA - its evolving antimicrobial resistance and implications for therapy. *Clinical infectious diseases : an official publication of the Infectious Diseases Society of America.* 2011;52(1):99-114.

411. Cong Y, Yang S, Rao X. Vancomycin resistant *Staphylococcus aureus* infections: A review of case updating and clinical features. *J Adv Res.* 2020;21:169-176.

412. McGuinness WA, Malachowa N, DeLeo FR. Vancomycin Resistance in *Staphylococcus aureus*. *Yale J Biol Med.* 2017;90(2):269-281.

413. Speer BS, Shoemaker NB, Salyers AA. Bacterial resistance to tetracycline: mechanisms, transfer, and clinical significance. *Clinical microbiology reviews.* 1992;5(4):387-399.

414. Hong J, Ensom MHH, Lau TTY. What Is the Evidence for Co-trimoxazole, Clindamycin, Doxycycline, and Minocycline in the Treatment of Methicillin-Resistant *Staphylococcus aureus* (MRSA) Pneumonia? *Ann Pharmacother.* 2019;53(11):1153-1161.

415. Metlay JP, Waterer GW, Long AC, et al. Diagnosis and Treatment of Adults with Community-acquired Pneumonia. An Official Clinical Practice Guideline of the American Thoracic Society and Infectious Diseases Society of America. *Am J Respir Crit Care Med.* 2019;200(7):e45-e67.

416. The National Institute for Health and Care Excellence. Cellulitis and erysipelas: antimicrobial prescribing NICE guideline [NG141]. 27 September 2019; https://www.nice.org.uk/guidance/ng141. Accessed 14/12/21.

417. Douglas M, Moy S, Hernandez N. Impact of COVID-19 on Outpatient Antimicrobial Prescribing Patterns in New York City. *Infect Dis Clin Pract (Baltim Md).* 2021;29(6):e352-e355.

418. Baltrus DA. Exploring the costs of horizontal gene transfer. *Trends Ecol Evol.* 2013;28(8):489-495.

419. Dunai A, Spohn R, Farkas Z, et al. Rapid decline of bacterial drug-resistance in an antibiotic-free environment through phenotypic reversion. 2019.

420. Lynch M, Marinov GK. The bioenergetic costs of a gene. *Proceedings of the National Academy of Sciences of the United States of America.* 2015;112(51):15690-15695.

421. Nagaev I, Björkman J, Andersson DI, Hughes D. Biological cost and compensatory evolution in fusidic acid-resistant *Staphylococcus aureus*. *Molecular microbiology.* 2001;40(2):433-439.

422. Schrag SJ, Perrot V. Reducing antibiotic resistance. *Nature.* 1996;381(6578):120-121.

423. Maisnier-Patin S, Andersson DI. Adaptation to the deleterious effects of antimicrobial drug resistance mutations by compensatory evolution. *Res Microbiol.* 2004;155(5):360-369.

424. Björkman J, Hughes D, Andersson DI. Virulence of antibiotic-resistant *Salmonella typhimurium*. *Proceedings of the National Academy of Sciences of the United States of America.* 1998;95(7):3949-3953.

425. Dastgheyb SS, Otto M. Staphylococcal adaptation to diverse physiologic niches: an overview of transcriptomic and phenotypic changes in different biological environments. *Future microbiology.* 2015;10(12):1981-1995.

426. Guiberson ER, Weiss A, Ryan DJ, et al. Spatially Targeted Proteomics of the Host-Pathogen Interface during Staphylococcal Abscess Formation. *ACS Infect Dis.* 2021;7(1):101-113.

427. Leung AH, Hawthorn BR, Simpson AH. The Effectiveness of Local Antibiotics in Treating Chronic Osteomyelitis in a Cohort of 50 Patients with an Average of 4 Years Follow-Up. *Open Orthop J.* 2015;9:372-378.

428. Wilde AD, Snyder DJ, Putnam NE, et al. Bacterial Hypoxic Responses Revealed as Critical Determinants of the Host-Pathogen Outcome by TnSeq Analysis of *Staphylococcus aureus* Invasive Infection. *PLoS pathogens.* 2015;11(12):e1005341.

429. Worlitzsch D, Tarran R, Ulrich M, et al. Effects of reduced mucus oxygen concentration in airway *Pseudomonas* infections of cystic fibrosis patients. *J Clin Invest.* 2002;109(3):317-325.

430. Kinkel TL, Roux CM, Dunman PM, Fang FC. The *Staphylococcus aureus* SrrAB two-component system promotes resistance to nitrosative stress and hypoxia. *MBio.* 2013;4(6):e00696-00613.

431. Hall JW, Yang J, Guo H, Ji Y. The *Staphylococcus aureus* AirSR Two-Component System Mediates Reactive Oxygen Species Resistance via Transcriptional Regulation of Staphyloxanthin Production. *Infect Immun.* 2017;85(2).

432. Kloos J, Gama JA, Hegstad J, Samuelsen Ø, Johnsen PJ. Piggybacking on Niche Adaptation Improves the Maintenance of Multidrug-Resistance Plasmids. *Mol Biol Evol.* 2021;38(8):3188-3201.

433. Vagner V, Dervyn E, Ehrlich SD. A vector for systematic gene inactivation in *Bacillus subtilis*. *Microbiology (Reading, England).* 1998;144 (Pt 11):3097-3104.

434. Cooper EL, García-Lara J, Foster SJ. YsxC, an essential protein in *Staphylococcus aureus* crucial for ribosome assembly/stability. *BMC microbiology.* 2009;9:266.

435. McVicker G, Prajsnar T, Williams A, et al. Clonal Expansion during *Staphylococcus aureus* Infection Dynamics Reveals the Effect of Antibiotic Intervention. *PLoS pathogens.* 2014;10(2):e1003959.

436. Horsburgh MJ, Aish JL, White IJ, Shaw L, Lithgow JK, Foster SJ. sigmaB modulates virulence determinant expression and stress resistance: characterization of a functional *rsbU* strain derived from *Staphylococcus aureus* 8325-4. *Journal of bacteriology.* 2002;184(19):5457-5467.

437. Ferreira MT, Manso AS, Gaspar P, Pinho MG, Neves AR. Effect of oxygen on glucose metabolism: utilization of lactate in Staphylococcus aureus as revealed by in vivo NMR studies. *PLoS One.* 2013;8(3):e58277.

438. Wiser MJ, Lenski RE. A Comparison of Methods to Measure Fitness in *Escherichia coli*. *PLoS One.* 2015;10(5):e0126210.

439. Attia AS, Cassat JE, Aranmolate SO, Zimmerman LJ, Boyd KL, Skaar EP. Analysis of the *Staphylococcus aureus* abscess proteome identifies antimicrobial host proteins and bacterial stress responses at the host-pathogen interface. *Pathog Dis.* 2013;69(1):36-48.

440. Trzcinski K, Cooper BS, Hryniewicz W, Dowson CG. Expression of resistance to tetracyclines in strains of methicillin-resistant *Staphylococcus aureus*. *The Journal of antimicrobial chemotherapy.* 2000;45(6):763-770.

441. Bottery MJ, Wood AJ, Brockhurst MA. Adaptive modulation of antibiotic resistance through intragenomic coevolution. *Nature ecology & evolution.* 2017;1(9):1364-1369.

442. Wistrand-Yuen E, Knopp M, Hjort K, Koskiniemi S, Berg OG, Andersson DI. Evolution of high-level resistance during low-level antibiotic exposure. *Nature Communications.* 2018;9(1):1-12.

443. Van den Bergh B, Swings T, Fauvart M, Michiels J. Experimental Design, Population Dynamics, and Diversity in Microbial Experimental Evolution. *Microbiol Mol Biol Rev.* 2018;82(3).

444. Mahrt N, Tietze A, Künzel S, et al. Bottleneck size and selection level reproducibly impact evolution of antibiotic resistance. *Nature ecology & evolution.* 2021;5(9):1233-1242.

445. Garoff L, Pietsch F, Huseby DL, Lilja T, Brandis G, Hughes D. Population Bottlenecks Strongly Influence the Evolutionary Trajectory to Fluoroquinolone Resistance in *Escherichia coli*. *Mol Biol Evol.* 2020;37(6):1637-1646.

446. Wein T, Dagan T. The Effect of Population Bottleneck Size and Selective Regime on Genetic Diversity and Evolvability in Bacteria. *Genome Biol Evol.* 2019;11(11):3283-3290.

447. Mallia P, Webber J, Gill SK, et al. Role of airway glucose in bacterial infections in patients with chronic obstructive pulmonary disease. *J Allergy Clin Immunol.* 2018;142(3):815-823.e816.

448. Hu M, Nandi S, Davies C, Nicholas RA. High-level chromosomally mediated tetracycline resistance in *Neisseria gonorrhoeae* results from a point mutation in the *rpsJ* gene encoding ribosomal protein S10 in combination with the *mtrR* and *penB* resistance determinants. *Antimicrob Agents Chemother.* 2005;49(10):4327-4334.

449. Beabout K, Hammerstrom TG, Perez AM, et al. The ribosomal S10 protein is a general target for decreased tigecycline susceptibility. *Antimicrob Agents Chemother.* 2015;59(9):5561-5566.

450. Bouma JE, Lenski RE. Evolution of a bacteria/plasmid association. *Nature.* 1988;335(6188):351-352.

451. Pragman AA, Yarwood JM, Tripp TJ, Schlievert PM. Characterization of virulence factor regulation by SrrAB, a two-component system in *Staphylococcus aureus*. *Journal of bacteriology.* 2004;186(8):2430-2438.

452. Acker KP, Wong Fok Lung T, West E, et al. Strains of *Staphylococcus aureus* that Colonize and Infect Skin Harbor Mutations in Metabolic Genes. *iScience.* 2019;19:281-290.

453. Evans NT, Naylor PF. The systemic oxygen supply to the surface of human skin. *Respir Physiol.* 1967;3(1):21-37.

454. Jiang JH, Bhuiyan MS, Shen HH, et al. Antibiotic resistance and host immune evasion in *Staphylococcus aureus* mediated by a metabolic adaptation. *Proceedings of the National Academy of Sciences of the United States of America.* 2019;116(9):3722-3727.

455. Davies EV, James CE, Williams D, et al. Temperate phages both mediate and drive adaptive evolution in pathogen biofilms. *Proceedings of the National Academy of Sciences of the United States of America.* 2016;113(29):8266-8271.

456. Brodersen DE, Clemons WM, Jr., Carter AP, Morgan-Warren RJ, Wimberly BT, Ramakrishnan V. The structural basis for the action of the antibiotics tetracycline, pactamycin, and hygromycin B on the 30S ribosomal subunit. *Cell.* 2000;103(7):1143-1154.

457. Rahman MM, Hunter HN, Prova S, Verma V, Qamar A, Golemi-Kotra D. The *Staphylococcus aureus* Methicillin Resistance Factor FmtA Is a d-Amino Esterase That Acts on Teichoic Acids. *mBio.* 2016;7(1):e02070-02015.

458. Hamma T, Ferré-D'Amaré AR. Pseudouridine synthases. *Chem Biol.* 2006;13(11):1125-1135.

459. Renzoni A, Barras C, François P, et al. Transcriptomic and functional analysis of an autolysis-deficient, teicoplanin-resistant derivative of methicillin-resistant *Staphylococcus aureus*. *Antimicrob Agents Chemother.* 2006;50(9):3048-3061.

460. Yao Z, Li W, Lin Y, et al. Proteomic Analysis Reveals That Metabolic Flows Affect the Susceptibility of Aeromonas hydrophila to Antibiotics. *Sci Rep.* 2016;6:39413.

461. Reece RJ, Maxwell A. DNA gyrase: structure and function. *Crit Rev Biochem Mol Biol.* 1991;26(3-4):335-375.

462. Creech CB, Al-Zubeidi DN, Fritz SA. Prevention of Recurrent Staphylococcal Skin Infections. *Infect Dis Clin North Am.* 2015;29(3):429-464.

463. van der Heijden C, Duizer ML, Fleuren H, et al. Intravenous flucloxacillin treatment is associated with a high incidence of hypokalaemia. *Br J Clin Pharmacol.* 2019;85(12):2886-2890.

464. Wagner C, Sauermann R, Joukhadar C. Principles of antibiotic penetration into abscess fluid. *Pharmacology.* 2006;78(1):1-10.

465. Agwuh KN, MacGowan A. Pharmacokinetics and pharmacodynamics of the tetracyclines including glycylcyclines. *Journal of Antimicrobial Chemotherapy.* 2006;58(2):256-265.

466. Krismer B, Liebeke M, Janek D, et al. Nutrient limitation governs *Staphylococcus aureus* metabolism and niche adaptation in the human nose. *PLoS pathogens.* 2014;10(1):e1003862.

467. Lister JL, Horswill AR. *Staphylococcus aureus* biofilms: recent developments in biofilm dispersal. *Front Cell Infect Microbiol.* 2014;4:178.

468. Tuson HH, Weibel DB. Bacteria-surface interactions. *Soft Matter.* 2013;9(18):4368-4380.

469. Sandegren L, Andersson DI. Bacterial gene amplification: implications for the evolution of antibiotic resistance. *Nature reviews. Microbiology.* 2009;7(8):578-588.

470. Clewell DB, Yagi Y, Bauer B. Plasmid-determined tetracycline resistance in *Streptococcus faecalis*: evidence for gene amplification during growth in presence of tetracycline. *Proceedings of the National Academy of Sciences of the United States of America.* 1975;72(5):1720-1724.

471. Gao W, Monk IR, Tobias NJ, et al. Large tandem chromosome expansions facilitate niche adaptation during persistent infection with drug-resistant *Staphylococcus aureus*. *Microb Genom.* 2015;1(2):e000026.

472. Belikova D, Jochim A, Power J, Holden MTG, Heilbronner S. "Gene accordions" cause genotypic and phenotypic heterogeneity in clonal populations of *Staphylococcus aureus. Nat Commun.* 2020;11(1):3526.

473. Kime L, Randall CP, Banda FI, et al. Transient Silencing of Antibiotic Resistance by Mutation Represents a Significant Potential Source of Unanticipated Therapeutic Failure. *mBio.* 2019;10(5).

474. Johnston PR, Dobson AJ, Rolff J. Genomic Signatures of Experimental Adaptation to Antimicrobial Peptides in *Staphylococcus aureus.* 2016.

475. Lima WG, de Brito JCM, Cardoso VN, Fernandes SOA. In-depth characterization of antibacterial activity of melittin against *Staphylococcus aureus* and use in a model of non-surgical MRSA-infected skin wounds. *Eur J Pharm Sci.* 2021;156:105592.

476. Wang JC. Cellular roles of DNA topoisomerases: a molecular perspective. *Nature reviews. Molecular cell biology.* 2002;3(6):430-440.

477. Yamamoto N, Droffner ML. Mechanisms determining aerobic or anaerobic growth in the facultative anaerobe *Salmonella typhimurium*. *Proceedings of the National Academy of Sciences of the United States of America.* 1985;82(7):2077-2081.

478. Hsieh LS, Burger RM, Drlica K. Bacterial DNA supercoiling and [ATP]/[ADP]. Changes associated with a transition to anaerobic growth. *J Mol Biol.* 1991;219(3):443-450.

479. Peschel A, Jack RW, Otto M, et al. *Staphylococcus aureus* resistance to human defensins and evasion of neutrophil killing via the novel virulence factor MprF is based on modification of membrane lipids with l-lysine. *J Exp Med.* 2001;193(9):1067-1076.

480. Collins LV, Kristian SA, Weidenmaier C, et al. *Staphylococcus aureus* strains lacking D-alanine modifications of teichoic acids are highly susceptible to human neutrophil killing and are virulence attenuated in mice. *J Infect Dis.* 2002;186(2):214-219.

481. Chan PF, Foster SJ. Role of SarA in virulence determinant production and environmental signal transduction in *Staphylococcus aureus*. *Journal of bacteriology.* 1998;180(23):6232-6241.

482. Yoshida M, Reyes SG, Tsuda S, Horinouchi T, Furusawa C, Cronin L. Time-programmable drug dosing allows the manipulation, suppression and reversal of antibiotic drug resistance in vitro. *Nat Commun.* 2017;8:15589.

483. Sheshachalam A, Srivastava N, Mitchell T, Lacy P, Eitzen G. Granule protein processing and regulated secretion in neutrophils. *Front Immunol.* 2014;5:448.

484. Soehnlein O, Kai-Larsen Y, Frithiof R, et al. Neutrophil primary granule proteins HBP and HNP1-3 boost bacterial phagocytosis by human and murine macrophages. *The Journal of clinical investigation.* 2008;118(10):3491-3502.

485. Weiss J, Olsson I. Cellular and subcellular localization of the bactericidal/permeability-increasing protein of neutrophils. *Blood.* 1987;69(2):652-659.

486. Sengeløv H, Kjeldsen L, Borregaard N. Control of exocytosis in early neutrophil activation. *Journal of immunology (Baltimore, Md. : 1950).* 1993;150(4):1535-1543.

487. Keir HR, Shoemark A, Dicker AJ, et al. Neutrophil extracellular traps, disease severity, and antibiotic response in bronchiectasis: an international, observational, multicohort study. *Lancet Respir Med.* 2021;9(8):873-884.

488. Visser SK, Bye P, Morgan L. Management of bronchiectasis in adults. *Med J Aust.* 2018;209(4):177-183.

489. Redondo M, Keyt H, Dhar R, Chalmers JD. Global impact of bronchiectasis and cystic fibrosis. *Breathe (Sheff).* 2016;12(3):222-235.

490. Long MB, Howden AJM, Keir HR, et al. Neutrophil proteomics identifies temporal changes and hallmarks of delayed recovery in COVID19. *medRxiv.* 2022:2022.2008.2021.22279031.

491. Russell CD, Fairfield CJ, Drake TM, et al. Co-infections, secondary infections, and antimicrobial use in patients hospitalised with COVID-19 during the first pandemic wave from the ISARIC WHO CCP-UK study: a multicentre, prospective cohort study. *Lancet Microbe.* 2021;2(8):e354-e365.

492. Tobin MJ, Laghi F, Jubran A. Why COVID-19 Silent Hypoxemia Is Baffling to Physicians. *Am J Respir Crit Care Med.* 2020;202(3):356-360.

493. Dhont S, Derom E, Van Braeckel E, Depuydt P, Lambrecht BN. The pathophysiology of 'happy' hypoxemia in COVID-19. *Respir Res.* 2020;21(1):198.

494. Seren S, Derian L, Keleş I, et al. Proteinase release from activated neutrophils in mechanically ventilated patients with non-COVID-19 and COVID-19 pneumonia. *Eur Respir J.* 2021;57(4).

495. Palmér R, Mäenpää J, Jauhiainen A, et al. Dipeptidyl Peptidase 1 Inhibitor AZD7986 Induces a Sustained, Exposure-Dependent Reduction in Neutrophil Elastase Activity in Healthy Subjects. *Clin Pharmacol Ther.* 2018;104(6):1155-1164.

496. Chalmers JD, Haworth CS, Metersky ML, et al. Phase 2 Trial of the DPP-1 Inhibitor Brensocatib in Bronchiectasis. *The New England journal of medicine.* 2020;383(22):2127-2137.

497. Varkey J, Nagaraj R. Antibacterial activity of human neutrophil defensin HNP-1 analogs without cysteines. *Antimicrob Agents Chemother.* 2005;49(11):4561-4566.

498. Chromek M, Slamova Z, Bergman P, et al. The antimicrobial peptide cathelicidin protects the urinary tract against invasive bacterial infection. *Nat Med.* 2006;12(6):636-641.

499. Shafer WM, Onunka VC, Jannoun M, Huthwaite LW. Molecular mechanism for the antigonococcal action of lysosomal cathepsin G. *Molecular microbiology.* 1990;4(8):1269-1277.

500. Shafer WM, Martin LE, Spitznagel JK. Cationic antimicrobial proteins isolated from human neutrophil granulocytes in the presence of diisopropyl fluorophosphate. *Infect Immun.* 1984;45(1):29-35.

501. Al-Farsi HM, Al-Adwani S, Ahmed S, et al. Effects of the Antimicrobial Peptide LL-37 and Innate Effector Mechanisms in Colistin-Resistant Klebsiella pneumoniae With *mgrB* Insertions. *Front Microbiol.* 2019;10:2632.

502. Kuijpers TW, Tool AT, van der Schoot CE, et al. Membrane surface antigen expression on neutrophils: a reappraisal of the use of surface markers for neutrophil activation. *Blood.* 1991;78(4):1105-1111.

503. Andreu Z, Yáñez-Mó M. Tetraspanins in extracellular vesicle formation and function. *Front Immunol.* 2014;5:442.

504. Proctor RA, von Eiff C, Kahl BC, et al. Small colony variants: a pathogenic form of bacteria that facilitates persistent and recurrent infections. *Nature reviews. Microbiology.* 2006;4(4):295-305.

505. Gläser R, Becker K, von Eiff C, Meyer-Hoffert U, Harder J. Decreased susceptibility of *Staphylococcus aureus* small-colony variants toward human antimicrobial peptides. *The Journal of investigative dermatology.* 2014;134(9):2347-2350.

506. Maurice NM, Bedi B, Sadikot RT. *Pseudomonas aeruginosa* Biofilms: Host Response and Clinical Implications in Lung Infections. *Am J Respir Cell Mol Biol.* 2018;58(4):428-439.

507. Sibila O, Laserna E, Shoemark A, et al. Airway Bacterial Load and Inhaled Antibiotic Response in Bronchiectasis. *Am J Respir Crit Care Med.* 2019;200(1):33-41.

508. Wang S, Song R, Wang Z, Jing Z, Wang S, Ma J. S100A8/A9 in Inflammation. *Front Immunol.* 2018;9:1298.

509. Wedmore CV, Williams TJ. Control of vascular permeability by polymorphonuclear leukocytes in inflammation. *Nature.* 1981;289(5799):646-650.

510. Soehnlein O, Xie X, Ulbrich H, et al. Neutrophil-derived heparin-binding protein (HBP/CAP37) deposited on endothelium enhances monocyte arrest under flow conditions. *Journal of immunology (Baltimore, Md. : 1950).* 2005;174(10):6399-6405.

511. Heinzelmann M, Mercer-Jones MA, Flodgaard H, Miller FN. Heparin-binding protein (CAP37) is internalized in monocytes and increases LPS-induced monocyte activation. *Journal of immunology (Baltimore, Md. : 1950).* 1998;160(11):5530-5536.

512. Zuo Y, Yalavarthi S, Shi H, et al. Neutrophil extracellular traps in COVID-19. *JCI insight.* 2020;5(11).

513. McElvaney OJ, McEvoy NL, McElvaney OF, et al. Characterization of the Inflammatory Response to Severe COVID-19 Illness. *Am J Respir Crit Care Med.* 2020;202(6):812-821.

514. Burnouf T, Chou ML, Wu YW, Su CY, Lee LW. Antimicrobial activity of platelet (PLT)-poor plasma, PLT-rich plasma, PLT gel, and solvent/detergent-treated PLT lysate biomaterials against wound bacteria. *Transfusion.* 2013;53(1):138-146.

515. Daha MR. Role of complement in innate immunity and infections. *Crit Rev Immunol.* 2010;30(1):47-52.

516. Soltis RD, Hasz D, Morris MJ, Wilson ID. The effect of heat inactivation of serum on aggregation of immunoglobulins. *Immunology.* 1979;36(1):37-45.

517. Çetinkaya RA, Yenilmez E, Petrone P, et al. Platelet-rich plasma as an additional therapeutic option for infected wounds with multi-drug resistant bacteria: in vitro antibacterial activity study. *Eur J Trauma Emerg Surg.* 2019;45(3):555-565.

518. Sørensen O, Cowland JB, Askaa J, Borregaard N. An ELISA for hCAP-18, the cathelicidin present in human neutrophils and plasma. *J Immunol Methods.* 1997;206(1-2):53-59.

519. Douglas E, Brignoli T, Recker M, O'Brien E, McLoughlin RM, Massey RC. Self-sensitisation of *Staphylococcus aureus* to the antimicrobial factors found in human blood. *bioRxiv.* 2021:2021.2007.2019.452914.

520. Sánchez-Gómez S, Lamata M, Leiva J, et al. Comparative analysis of selected methods for the assessment of antimicrobial and membrane-permeabilizing activity: a case study for lactoferricin derived peptides. *BMC microbiology.* 2008;8:196.

521. Starkey PM, Barrett AJ. Human cathepsin G. Catalytic and immunological properties. *Biochem J.* 1976;155(2):273-278.

522. Habets MG, Rozen DE, Brockhurst MA. Variation in *Streptococcus pneumoniae* susceptibility to human antimicrobial peptides may mediate intraspecific competition. *Proc Biol Sci.* 2012;279(1743):3803-3811.

523. Geitani R, Ayoub Moubareck C, Touqui L, Karam Sarkis D. Cationic antimicrobial peptides: alternatives and/or adjuvants to antibiotics active against methicillin-resistant *Staphylococcus aureus* and multidrug-resistant *Pseudomonas aeruginosa*. *BMC microbiology.* 2019;19(1):54.

524. Shurko JF, Galega RS, Li C, Lee GC. Evaluation of LL-37 antimicrobial peptide derivatives alone and in combination with vancomycin against *S. aureus*. *J Antibiot (Tokyo).* 2018;71(11):971-974.

525. Ledger EVK, Mesnage S, Edwards AM. Human serum triggers antibiotic tolerance in *Staphylococcus aureus*. *Nat Commun.* 2022;13(1):2041.

526. Golla RM, Mishra B, Dang X, et al. Resistome of *Staphylococcus aureus* in Response to Human Cathelicidin LL-37 and Its Engineered Antimicrobial Peptides. *ACS Infect Dis.* 2020;6(7):1866-1881.

527. Braff MH, Zaiou M, Fierer J, Nizet V, Gallo RL. Keratinocyte production of cathelicidin provides direct activity against bacterial skin pathogens. *Infect Immun.* 2005;73(10):6771-6781.

528. Stewart PS, Davison WM, Steenbergen JN. Daptomycin rapidly penetrates a *Staphylococcus epidermidis* biofilm. *Antimicrob Agents Chemother.* 2009;53(8):3505-3507.

529. Darouiche RO, Dhir A, Miller AJ, Landon GC, Raad, II, Musher DM. Vancomycin penetration into biofilm covering infected prostheses and effect on bacteria. *J Infect Dis.* 1994;170(3):720-723.

530. Zhou S, Rao Y, Li J, Huang Q, Rao X. *Staphylococcus aureus* small-colony variants: Formation, infection, and treatment. *Microbiol Res.* 2022;260:127040.

531. Singh R, Ray P, Das A, Sharma M. Role of persisters and small-colony variants in antibiotic resistance of planktonic and biofilm-associated *Staphylococcus aureus*: an in vitro study. *Journal of medical microbiology.* 2009;58(Pt 8):1067-1073.

532. Chebotar IV, Emelyanova MA, Bocharova JA, Mayansky NA, Kopantseva EE, Mikhailovich VM. The classification of bacterial survival strategies in the presence of antimicrobials. *Microb Pathog.* 2021;155:104901.

533. Van den Bergh B, Michiels JE, Wenseleers T, et al. Frequency of antibiotic application drives rapid evolutionary adaptation of Escherichia coli persistence. *Nature microbiology.* 2016;1:16020.

534. Szafrańska AK, Junker V, Steglich M, Nübel U. Rapid cell division of *Staphylococcus aureus* during colonization of the human nose. *BMC Genomics.* 2019;20(1):229.

535. Bergstrom CT, Lo M, Lipsitch M. Ecological theory suggests that antimicrobial cycling will not reduce antimicrobial resistance in hospitals. *Proceedings of the National Academy of Sciences.* 2004;101(36):13285-13290.

536. Nielsen KL, Pedersen TM, Udekwu KI, et al. Fitness cost: a bacteriological explanation for the demise of the first international methicillin-resistant *Staphylococcus aureus* epidemic. *Journal of Antimicrobial Chemotherapy.* 2012;67(6):1325-1332.

537. Enne VI. Reducing antimicrobial resistance in the community by restricting prescribing: can it be done? *Journal of Antimicrobial Chemotherapy.* 2009;65(2):179-182.

538. Schrag SJ, Perrot V, Levin BR. Adaptation to the fitness costs of antibiotic resistance in *Escherichia coli*. *Proc Biol Sci.* 1997;264(1386):1287-1291.

539. Samir M, Ramadan M, Abdelrahman MH, et al. New potent ciprofloxacin-uracil conjugates as DNA gyrase and topoisomerase IV inhibitors against methicillin-resistant *Staphylococcus aureus*. *Bioorg Med Chem.* 2022;73:117004.

540. Perault A, Turlan C, Eynard N, Vallé Q, Bousquet-Mélou A, Giraud E. Repeated Exposure of *Escherichia coli* to High Ciprofloxacin Concentrations Selects *gyrB* Mutants That Show Fluoroquinolone-Specific Hyperpersistence. *Front Microbiol.* 2022;13:908296.

541. Berti AD, Theisen E, Sauer JD, et al. Penicillin Binding Protein 1 Is Important in the Compensatory Response of *Staphylococcus aureus* to Daptomycin-Induced Membrane Damage and Is a Potential Target for β-Lactam-Daptomycin Synergy. *Antimicrob Agents Chemother.* 2016;60(1):451-458.

542. Koripella RK, Chen Y, Peisker K, Koh CS, Selmer M, Sanyal S. Mechanism of elongation factor-G-mediated fusidic acid resistance and fitness compensation in *Staphylococcus aureus*. *The Journal of biological chemistry.* 2012;287(36):30257-30267.

543. Vaudaux P, Kelley WL, Lew DP. Staphylococcus aureus Small Colony Variants: Difficult to Diagnose and Difficult to Treat. *Clinical Infectious Diseases.* 2006;43(8):968-970.

544. Jonsson IM, von Eiff C, Proctor RA, Peters G, Rydén C, Tarkowski A. Virulence of a *hemB* mutant displaying the phenotype of a *Staphylococcus aureus* small colony variant in a murine model of septic arthritis. *Microb Pathog.* 2003;34(2):73-79.

545. Dalbeth N, Lauterio TJ, Wolfe HR. Mechanism of action of colchicine in the treatment of gout. *Clin Ther.* 2014;36(10):1465-1479.

546. Gunes M, Cekic S, Kilic SS. Is colchicine more effective to prevent periodic fever, aphthous stomatitis, pharyngitis and cervical adenitis episodes in Mediterranean fever gene variants? *Pediatr Int.* 2017;59(6):655-660.

547. Suehisa S, Tagami H, Inoue F, Matsumoto K, Yoshikuni K. Colchicine in the treatment of acute febrile neutrophilic dermatosis (Sweet's syndrome). *Br J Dermatol.* 1983;108(1):99-101.

548. Jatuworapruk K, Montgomery A, Gianfrancesco M, et al. Characteristics and Outcomes of People With Gout Hospitalized Due to COVID-19: Data From the COVID-19 Global Rheumatology Alliance Physician-Reported Registry. *ACR Open Rheumatol.* 2022.

549. Salehzadeh F, Pourfarzi F, Ataei S. The Impact of Colchicine on COVID-19 patients: A Clinical Trial Study. *Mediterr J Rheumatol.* 2022;33(2):232-236.

550. Dorschner RA, Pestonjamasp VK, Tamakuwala S, et al. Cutaneous injury induces the release of cathelicidin anti-microbial peptides active against group A *Streptococcus*. *The Journal of investigative dermatology.* 2001;117(1):91-97.

551. Noore J, Noore A, Li B. Cationic antimicrobial peptide LL-37 is effective against both extra- and intracellular *Staphylococcus aureus*. *Antimicrob Agents Chemother.* 2013;57(3):1283-1290.

552. Wei J, Cao X, Qian J, et al. Evaluation of antimicrobial peptide LL-37 for treatment of *Staphylococcus aureus* biofilm on titanium plate. *Medicine.* 2021;100(44):e27426.

553. Ridyard KE, Overhage J. The Potential of Human Peptide LL-37 as an Antimicrobial and Anti-Biofilm Agent. *Antibiotics (Basel).* 2021;10(6).

554. Duplantier AJ, van Hoek ML. The Human Cathelicidin Antimicrobial Peptide LL-37 as a Potential Treatment for Polymicrobial Infected Wounds. *Front Immunol.* 2013;4:143.

555. Corrigan RM, Bellows LE, Wood A, Gründling A. ppGpp negatively impacts ribosome assembly affecting growth and antimicrobial tolerance in Gram-positive bacteria. *Proceedings of the National Academy of Sciences.* 2016;113(12):E1710-E1719.

556. Hobbs JK, Boraston AB. (p)ppGpp and the Stringent Response: An Emerging Threat to Antibiotic Therapy. *ACS Infect Dis.* 2019;5(9):1505-1517.

557. Zampieri M, Enke T, Chubukov V, Ricci V, Piddock L, Sauer U. Metabolic constraints on the evolution of antibiotic resistance. *Mol Syst Biol.* 2017;13(3):917.

558. Pickering AC, Vitry P, Prystopiuk V, et al. Host-specialized fibrinogen-binding by a bacterial surface protein promotes biofilm formation and innate immune evasion. *PLoS pathogens.* 2019;15(6):e1007816.

559. O'Neill AJ. *Staphylococcus aureus* SH1000 and 8325-4: comparative genome sequences of key laboratory strains in staphylococcal research. *Lett Appl Microbiol.* 2010;51(3):358-361.

560. Bæk KT, Frees D, Renzoni A, et al. Genetic Variation in the *Staphylococcus aureus* 8325 Strain Lineage Revealed by Whole-Genome Sequencing. *PLOS ONE.* 2013;8(9):e77122.

561. Langhanki L, Berger P, Treffon J, Catania F, Kahl BC, Mellmann A. In vivo competition and horizontal gene transfer among distinct *Staphylococcus aureus* lineages as major drivers for adaptational changes during long-term persistence in humans. *BMC microbiology.* 2018;18(1):152.

562. Wu CY, Alborn WE, Jr., Flokowitsch JE, et al. Site-directed mutagenesis of the mecA gene from a methicillin-resistant strain of *Staphylococcus aureus*. *Journal of bacteriology.* 1994;176(2):443-449.

563. School K, Marklevitz J, W KS, L KH. Predictive characterization of hypothetical proteins in *Staphylococcus aureus* NCTC 8325. *Bioinformation.* 2016;12(3):209-220.

564. Wang HW, Wang JW. How cryo-electron microscopy and X-ray crystallography complement each other. *Protein Sci.* 2017;26(1):32-39.

565. Ijaq J, Chandrasekharan M, Poddar R, Bethi N, Sundararajan VS. Annotation and curation of uncharacterized proteins- challenges. *Front Genet.* 2015;6:119.

566. Poudel S, Tsunemoto H, Seif Y, et al. Revealing 29 sets of independently modulated genes in *Staphylococcus aureus*, their regulators, and role in key physiological response. *Proceedings of the National Academy of Sciences of the United States of America.* 2020;117(29):17228-17239.

567. Sastry AV, Gao Y, Szubin R, et al. The *Escherichia coli* transcriptome mostly consists of independently regulated modules. *Nat Commun.* 2019;10(1):5536.

568. Thänert R, Goldmann O, Beineke A, Medina E. Host-inherent variability influences the transcriptional response of *Staphylococcus aureus* during in vivo infection. *Nature Communications.* 2017;8(1):14268.

569. Ritchie ND, Evans TJ. Dual RNA-seq in *Streptococcus pneumoniae* Infection Reveals Compartmentalized Neutrophil Responses in Lung and Pleural Space. *mSystems.* 2019;4(4):e00216-00219.

570. Kim HK, Missiakas D, Schneewind O. Mouse models for infectious diseases caused by *Staphylococcus aureus*. *J Immunol Methods.* 2014;410:88-99.

571. Thompson AAR, Dickinson RS, Murphy F, et al. Hypoxia determines survival outcomes of bacterial infection through HIF-1alpha dependent re-programming of leukocyte metabolism. *Science immunology.* 2017;2(8):eaal2861.

572. UniProt: the universal protein knowledgebase in 2021. *Nucleic Acids Res.* 2021;49(D1):D480-d489.

10 Appendix

Appendix 1: Significantly changed proteins in sputum proteomics from participants with no bacterial co-infection vs. Pseudomonas co-infection from Figure 7-1C. p values are T-test with Benjamini & Hochberg correction. Up regulated in no co-infections compared to Pseudomonas spp co-infection. Reactome or function from Uniprot[572]

Gene Name	Up/Down regulated in no co-infection	p value	Reactome/ Function
AZU1	DOWN	0.0001	Neutrophil degranulation
CLU	UP	0.0001	Platelet degranulation, terminal pathway of complement, antimicrobial peptides, regulation of complement cascade
SCGB3A1	UP	0.0002	Secreted cytokine-like protein. Inhibits cell growth in vitro.
MPO	DOWN	0.0003	Neutrophil degranulation
S100A9	DOWN	0.0003	RHO GTPases activate NADPH oxidases, regulation of TLR by endogenous ligand, neutrophil degranulation, metal sequestration by antimicrobial proteins
FOLR1	UP	0.0004	COPII-mediated vesicle transport, cargo concentration in the ER, COPI-mediated anterograde transport
SCGB1A1	UP	0.0005	Binds phosphatidylcholine, phosphatidylinositol, polychlorinated biphenyls (PCB) and weakly progesterone, potent inhibitor of phospholipase A2
APOH	UP	0.0005	Platelet degranulation
LGALS3BP	UP	0.0005	Platelet degranulation
SERPINB3	UP	0.0005	Possible papain-like cysteine protease inhibitor, inhibitor of UV-induced apoptosis

HTRA1	UP	0.0005	Degradation of the extracellular matrix
CAT	DOWN	0.0007	Detoxification of reactive oxygen species, neutrophil degranulation, peroxisomal protein import, FOXO-mediated transcription of oxidative stress, metabolic and neuronal genes
APOA1	UP	0.0017	Cholesterol metabolism, lipid metabolism, lipid transport, steroid metabolism, sterol metabolism, regulation of insulin-like growth factor
PFN1	DOWN	0.0027	Platelet degranulation, signalling by ROBO receptors, PCP/CE pathway, RHO GTPases Activate Formins
ELANE	DOWN	0.0043	Collagen degradation, degradation of the extracellular matrix, activation of matrix metalloproteinases, neutrophil degranulation, antimicrobial peptides, regulation of complement cascade
S100A8	DOWN	0.0043	Calcium- and zinc-binding protein, role in the regulation of inflammatory processes and immune response, induce neutrophil chemotaxis and adhesion, predominantly found as calprotectin (S100A8/A9)
RNASE1	UP	0.0043	Chaperone mediated autophagy, late endosomal microautophagy
CD59	UP	0.0044	COPII-mediated vesicle transport, cargo concentration in the ER, neutrophil degranulation, COPI-mediated anterograde transport, regulation of complement cascade
PRTN3	DOWN	0.0051	Fibrin clot formation, other interleukin signalling, neutrophil degranulation, antimicrobial peptides
CTSB	UP	0.0051	Collagen degradation, trafficking and processing of endosomal TLR, assembly of collagen fibrils and other multimeric structures, MHC class II antigen presentation, neutrophil degranulation
CFH	UP	0.0096	Regulation of complement cascade
FN1	UP	0.0096	Cell adhesion, cell motility, opsonization, wound healing, and maintenance of cell shape

LCN2	DOWN	0.0109	Interleukin-4 and Interleukin-13 signalling, neutrophil degranulation, metal sequestration by antimicrobial proteins, iron uptake and transport
SCGB1A1	UP	0.0109	Binds phosphatidylcholine, phosphatidylinositol, polychlorinated biphenyls (PCB) and weakly progesterone, potent inhibitor of phospholipase A2
OLFM4	DOWN	0.0128	Neutrophil degranulation
MMP8	DOWN	0.0128	Collagen degradation, degradation of the extracellular matrix, activation of matrix metalloproteinases, neutrophil degranulation
PIGR	UP	0.0132	Neutrophil degranulation
BST1	DOWN	0.0139	Post-translational modification: synthesis of GPI-anchored proteins, nicotinate metabolism, neutrophil degranulation
MSMB	UP	0.0194	Immunoglobulin-binding factor
AHSG	UP	0.0204	Platelet degranulation, regulation of insulin-like growth factor (IGF) transport and uptake by insulin-like growth factor binding proteins (IGFBPs), neutrophil degranulation, post-translational protein phosphorylation
CST3	UP	0.0228	Regulation of insulin-like growth factor (IGF) transport and uptake by insulin-like growth factor binding proteins (IGFBPs), neutrophil degranulation, post-translational protein phosphorylation, amyloid fibre formation
IQGAP1	DOWN	0.0244	Nephrin family interactions, glucagon-like Peptide-1 (GLP1) regulates insulin secretion, RHO GTPases activate IQGAPs, MAP2K and MAPK activation, neutrophil degranulation, signalling by moderate and high kinase BRAF mutants, signalling by BRAF and RAF fusions, signalling downstream of RAS mutants, signalling by RAF1 mutants
GRN	DOWN	0.0244	Neutrophil degranulation
CTSC	UP	0.0249	COPII-mediated vesicle transport, MHC class II antigen presentation, cargo concentration in the ER, neutrophil degranulation
SERPINB10	DOWN	0.025	Neutrophil degranulation

KLK11	UP	0.0253	Serine protease
B2M	UP	0.0264	ER-Phagosome pathway, endosomal/vacuolar pathway, Nef mediated downregulation of MHC class I complex cell surface expression, immunoregulatory interactions between a lymphoid and a non-lymphoid cell, DAP12 interactions and signalling, neutrophil degranulation, interferon gamma signalling, amyloid fibre formation, antigen presentation
RARRES1	UP	0.0268	Inhibitor of the cytoplasmic carboxypeptidase AGBL2, may regulate the alpha-tubulin tyrosination cycle
SERPINF1	UP	0.0279	Neurotrophic protein
HIST1H1E HIST1H1C HIST1H1D HIST1H1A	UP	0.0326	Histone H1 complex, apoptosis induced DNA fragmentation, formation of Senescence-Associated Heterochromatin Foci (SAHF)
CTSG	DOWN	0.0388	Degradation of the extracellular matrix, activation of matrix metalloproteinases, metabolism of angiotensinogen to angiotensins, regulation of insulin-like growth factor, interleukin-1 processing, neutrophil degranulation, antimicrobial peptides, suppression of apoptosis
GSTP1	UP	0.0436	Glutathione conjugation, detoxification of reactive oxygen species, neutrophil degranulation
ITGB2	DOWN	0.0471	Toll Like Receptor 4 (TLR4) Cascade, immunoregulatory interactions between a lymphoid and a non-lymphoid cell, cell surface interactions at the vascular wall, integrin cell surface interactions, interleukin-4 and interleukin-13 signalling, neutrophil degranulation
GGH	DOWN	0.0475	Neutrophil degranulation
ENO1	DOWN	0.048	Glycolysis, gluconeogenesis, manipulation of host energy metabolism
SLPI	UP	0.0484	Neutrophil degranulation
RNASE3	DOWN	0.049	Neutrophil degranulation, antimicrobial peptide